Integrated Ocean Drilling Program
Expedition 335 Preliminary Report

Superfast Spreading Rate Crust 4

Drilling gabbro in intact ocean crust formed at a superfast spreading rate

13 April–3 June 2011

Expedition 335 Scientists

Published by
Integrated Ocean Drilling Program Management International, Inc.,
for the Integrated Ocean Drilling Program

Publisher's notes

Citation:

Expedition 335 Scientists, 2011. Superfast spreading rate crust 4: drilling gabbro in intact ocean crust formed at a superfast spreading rate. *IODP Prel. Rept.,* 335. doi:10.2204/iodp.pr.335.2011

Distribution:
Electronic copies of this series may be obtained from the Integrated Ocean Drilling Program (IODP) Scientific Publications homepage on the World Wide Web at **www.iodp.org/scientific-publications/.**

This publication was prepared by the Integrated Ocean Drilling Program U.S. Implementing Organization (IODP-USIO): Consortium for Ocean Leadership, Lamont Doherty Earth Observatory of Columbia University, and Texas A&M University, as an account of work performed under the international Integrated Ocean Drilling Program, which is managed by IODP Management International (IODP-MI), Inc. Funding for the program is provided by the following agencies:

National Science Foundation (NSF), United States

Ministry of Education, Culture, Sports, Science and Technology (MEXT), Japan

European Consortium for Ocean Research Drilling (ECORD)

Ministry of Science and Technology (MOST), People's Republic of China

Korea Institute of Geoscience and Mineral Resources (KIGAM)

Australian Research Council (ARC) and GNS Science (New Zealand), Australian/New Zealand Consortium

Ministry of Earth Sciences (MoES), India

Disclaimer

July 2011

Expedition 335 participants

Expedition 335 scientists

Damon Teagle
Co-Chief Scientist
School of Ocean and Earth Science
National Oceanography Centre
University of Southampton
European Way
Southampton SO14-3ZH
United Kingdom
dat@noc.soton.ac.uk

Benoît Ildefonse
Co-Chief Scientist
Géosciences Montpellier
CNRS—Université Montpellier II
CC 60, Place Eugène Bataillon
34095 Montpellier cedex 05
France
benoit.ildefonse@um2.fr

Peter Blum
Expedition Project Manager/Staff Scientist
United States Implementing Organization
Integrated Ocean Drilling Program
Texas A&M University
1000 Discovery Drive
College Station TX 77845-9547
USA
blum@iodp.tamu.edu

Gilles Guérin
Logging Staff Scientist
Borehole Research Group
Lamont-Doherty Earth Observatory
Columbia University
PO Box 1000, 61 Route 9W
Palisades NY 10964
USA
guerin@ldeo.columbia.edu

Natalia Zakharova
Logging Staff Scientist
Borehole Research Group
Lamont-Doherty Earth Observatory
Columbia University
PO Box 1000, 61 Route 9W
Palisades NY 10964
USA
nzakh@ldeo.columbia.edu

Natsue Abe
Igneous Petrologist
Deep Sea Research Department
Japan Agency for Marine-Earth Science and Technology
2-15 Natsushima-cho, Yokosuka
Kanagawa 237-0061
Japan
abenatsu@jamstec.go.jp

Bénédicte Abily
Petrologist
Laboratoire de Dynamique Terrestre et Planétaire
Observatoire Midi-Pyrenees
Université Paul Sabatier
14 Avenue Edouard Belin
31400 Toulouse
France
benedicte.abily@gmail.com

Yoshiko Adachi
Igneous Petrologist
Center for Transdisciplinary Research
Niigata University
2-8050 Ikarashi, Nishi-ku
Niigata 950-2181
Japan
adachiy@geo.sc.niigata-u.ac.jp

Jeffrey C. Alt
Alteration Petrologist
Department of Geological Sciences
University of Michigan
2534 CC Little Building
1100 N. University
Ann Arbor MI 48109-1063
USA
jalt@umich.edu

Ryo Anma
Structural Geologist
Graduate School of Life and Environmental Sciences
University of Tsukuba
Tennodai 1-1-1, Tsukuba
Ibaraki 305-8572
Japan
ranma@sakura.cc.tsukuba.ac.jp

Graham Baines
Physical Properties Specialist
Earth and Environmental Sciences
University of Adelaide
Mawson Building
Adelaide VIC 5005
Australia
Graham.baines@adelaide.edu.au

Jeremy Deans
Structural Geologist
Department of Geosciences
Texas Tech University
125 Science Building
Lubbock TX 79409
USA
jeremy.deans@ttu.edu

Henry J.B. Dick
Igneous Petrologist
Department of Geology and Geophysics
Woods Hole Oceanographic Institution
MS #8, McLean Laboratory
Woods Hole MA 02543-1539
USA
hdick@whoi.edu

Daisuke Endo
Structural Geologist
Earth Evolution Sciences
University of Tsukuba
Tennodai 1-1-1, Tsukuba
Ibaraki 305-8572
Japan
endora@geol.tsukuba.ac.jp

Eric C. Ferre
Structural Geologist
Department of Geology
Southern Illinois University at Carbondale
1259 Lincoln Drive
Carbondale IL 62901
USA
eferre@geo.siu.edu

Lydéric France
Alteration Petrologist
Centre de Recherches Pétrographiques
et Géochimiques (UPR 9046)
CNRS
54501
France
lydextrem@yahoo.fr

Marguerite M. Godard
Inorganic Geochemist
Géosciences Montpellier
CNRS—Université Montpellier II
CC 60, Place Eugène Bataillon
34095 Montpellier cedex 05
France
marguerite.godard@um2.fr

Michelle Harris
Alteration Petrologist
National Oceanography Centre
University of Southampton
European Way
Southampton SO14 3ZH
United Kingdom
michelle.harris@noc.soton.ac.uk

Yoon-Mi Kim
Paleomagnetist
School of Earth and Environmental Sciences
Seoul National University
Sillim9-dong, Gwank-gu
Seoul 151-747
Republic of Korea
gykim@kigam.re.kr

Juergen H. Koepke
Igneous Petrologist
Institut fuer Mineralogie
University of Hannover
Callinstrasse 3
30167 Hannover
Germany
koepke@mineralogie.uni-hannover.de

Mark D. Kurz
Inorganic Geochemist
Department of Marine Chemistry and
Geochemistry
Woods Hole Oceanographic Institution
320 Woods Hole Road
MS 25
Woods Hole MA 02543
USA
mkurz@whoi.edu

C. Johan Lissenberg
Igneous Petrologist
School of Earth and Ocean Sciences
Cardiff University
Main Building, Park Place
Cardiff CF10 3YE
United Kingdom
lissenbergcj@cardiff.ac.uk

Sumio Miyashita
Igneous Petrologist
Department of Geology
Niigata University
2-8050 Ikarashi, Ikarashi
Niigata 950-2181
Japan
miyashit@geo.sc.niigata-u.ac.jp

Antony Morris
Paleomagnetist
School of Geography
Earth & Environmental Sciences
University of Plymouth
Drake Circus
Plymouth PL4 8AA
United Kingdom
amorris@plymouth.ac.uk

Ryo Oizumi
Igneous Petrologist
Department of Earth Sciences
Yamagata University
1-4-12 Kojirakawa-machi
Yamagata 990-8560
Japan
halfway55232@msn.com

Betchaida D. Payot
Igneous Petrologist
Department of Earth Sciences
Kanazawa University
Kakuma-machi
Kanazawa 920-1192
Japan
saeko_00@yahoo.com

Marie Python
Igneous Petrologist
Department of Earth and Planetary Sciences
Hokkaido University
North 10, West 8
Sapporo 060-0810
Japan
marie@mail.sci.hokudai.ac.jp

Parijat Roy
Inorganic Geochemist
Geochemistry Division
National Geophysical Research Institute (NGRI)
Uppal Road
Hyderabad 500 006
India
parijatroy@yahoo.co.in

Jessica L. Till
Paleomagnetist/Structural Geologist
Department of Geology and Geophysics
University of Minnesota, Minneapolis
310 Pillsbury Drive SE
Minneapolis MN 55455
USA
jesstill@gmail.com

Masako Tominaga
Physical Properties Specialist
Department of Geology and Geophysics
Woods Hole Oceanographic Institution
Clark 24 1B
MS 22
Woods Hole MA 02543
USA
mtominaga@whoi.edu

Douglas S. Wilson
Geophysicist
Department of Earth Sciences
University of California, Santa Barbara
1006 Webb Hall
Santa Barbara CA 93106-9630
USA
dwilson@geol.ucsb.edu

Education and outreach

Sarah McNaboe
Outreach Officer
315 Broadway, Unit 1
Newport, RI 02840
USA
smcnaboe@gmail.com

Sarah Saunders
Outreach Officer
Consortium for Ocean Leadership
1201 New York Ave NW, Fourth Floor
Washington DC 20005
USA
ssaunders@oceanleadership.org

Technical support

Grant Banta
Marine Computer Specialist

Heather Barnes
X-ray Laboratory

Christopher Bennight
Chemistry Laboratory

Michael Bertoli
Chemistry Laboratory

Timothy Blaisdell
Applications Developer

Chad Broyles
Curatorial Specialist

Etienne Claassen
Marine Instrumentation Specialist

Trevor Cobine
Paleomagnetism Laboratory

William Crawford
Imaging Specialist

Edgar "Sandy" Dillard
Downhole Tools/Thin Section Laboratory

David Fackler
Applications Developer

Tim Fulton
Publications Specialist

Thomas Gorgas
Core Laboratory

Ronald Grout
Operations Superintendent

Michael Hodge
Marine Computer Specialist

Jan Jurie Kotze
Marine Instrumentation Specialist

Mike Meiring
Marine Engineering Specialist

William Mills
Laboratory Officer

Erik Moortgat
Underway Geophysics Laboratory

Chieh Peng
Assistant Laboratory Officer

Kerry Swain
Logging Engineer

Yulia Vasilyeva
Physical Properties

Abstract

The Superfast Spreading Crust campaign, echoing long-standing ocean lithosphere community endeavors, was designed to help us understand the formation, architecture, and evolution of ocean crust formed at fast spreading rates. Integrated Ocean Drilling Program (IODP) Expedition 335, "Superfast Spreading Rate Crust 4" (13 April–3 June 2011), was the fourth scientific drilling cruise of the Superfast Spreading Crust campaign to Ocean Drilling Program (ODP) Hole 1256D. The expedition aimed to deepen this basement reference site several hundred meters into the gabbroic rocks of intact lower oceanic crust to address the following fundamental scientific questions:

- Does the lower crust form by subsidence of a crystal mush from a high-level magma chamber (gabbro glacier), by intrusion of sills throughout the lower crust, or by some other mechanism? How does melt percolate through the lower crust, and what are the reactions and chemical evolution of magmas during migration?
- Is the plutonic crust cooled by conduction or hydrothermal circulation? What are the role and extent of deeply penetrating seawater-derived hydrothermal fluids in cooling the lower crust and the chemical exchanges between the ocean crust and the oceans?
- What are the relationships among the geological, geochemical, and geophysical structure of the crust and, in particular, the nature of the seismic Layer 2–3 transition?
- What is the magnetic contribution of the lower crust to marine magnetic anomalies?

Hole 1256D is located on 15 Ma crust in the eastern equatorial Pacific Ocean (6°44.163′N, 91°56.061′W). Oceanic crust that formed at a superfast spreading rate (>200 mm/y) was specifically targeted to exploit the observed relationship between spreading rate and depth to axial low-velocity zones, thought to be magma chambers, seismically imaged at active mid-ocean ridges. This was a deliberate strategy to reduce the drilling distance to gabbroic rocks because thick sequences of lavas and dikes have proved difficult to penetrate in the past. Previous cruises to ODP Site 1256 (ODP Leg 206; IODP Expedition 309/312) have achieved their leg- and expedition-specific objectives but not the overarching strategic goals of the Superfast Spreading Crust campaign to understand magmatic accretion at fast-spreading ocean ridges. However, the three previous cruises achieved the first complete sampling of intact upper oceanic crust and successfully drilled through ~800 m of erupted lavas and thin (~345 m)

sheeted dike complex and sampled gabbros at ~1157 meters subbasement. The lowermost 100 m of the hole is a complex dike–plutonic transition zone and comprises two gabbro lenses intruded into very strongly contact metamorphosed, granoblastically recrystallized sheeted dikes.

During Expedition 335, we reentered Hole 1256D more than 5 years after our last visit and encountered and overcame a number of significant engineering challenges, each unique but of natures not unexpected in a deep, uncased marine borehole into igneous rocks. The patient, persistent efforts of the rig floor teams cleared a major obstruction at 920 meters below seafloor (mbsf) that initially prevented reentry into the hole to its full depth (1507 mbsf). The 920–960 mbsf interval was then cemented to stabilize the borehole wall. A short phase of coring deepened Hole 1256D ~13 m before the C-9 hard formation coring bit failed and was ground to a smooth stump. A progressive, logical course of action was then undertaken to clear the bottom of the hole of metal junk from the failed coring bit, open up a short interval of undergauge hole, and remove a very large amount of drilling cuttings from the hole. This was successfully completed, and the hole is open to its full depth (1521.6 mbsf). The hole-cleaning phase was followed by wireline caliper and temperature measurements of the complete hole to assist with cementing operations to stabilize the lowermost 10 m of the hole and the problematic interval at 910–940 mbsf. These remedial efforts should facilitate reentry and coring on a future return to Hole 1256D.

In addition to the few cores drilled, the junk baskets deployed during the successive fishing runs to the bottom of the hole recovered a unique collection of samples, including large cobbles (as large as 5 kg), angular rubble, and fine cuttings of principally strongly to completely recrystallized granoblastic basalt with minor gabbroic rocks and evolved plutonic rocks. The large blocks exhibit intrusive, structural, and textural relationships, along with overprinting and crosscutting hydrothermal alteration and metamorphic paragenetic sequences that hitherto have not been observed because of the small diameter of drill cores and the very low recovery of the granoblastic dikes cored so far. The high extent of metamorphic recrystallization exhibited by the granoblastic basalt, combined with operational factors, provides strong evidence that most of this material comes from the lowermost reaches of Hole 1256D (~1495 to ~1522 mbsf). Including the ~60 m thick zone of granoblastic dikes that reside above the uppermost gabbros, the dike–gabbro transition zone at Site 1256 is >170 m thick, of which >100 m is recrystallized granoblastic basalt. When the textural and contact relationships exhibited by these samples are placed in the geological context of the Hole 1256D stratigraphy, a vision emerges of a complex, dynamic thermal boundary

layer zone. This region of the crust between the principally hydrothermal domain of the upper crust and the intrusive magmatic domain of the lower crust is one of evolving geological conditions. An intimate coupling among temporally and spatially intercalated magmatic, hydrothermal, partial melting, intrusive, metamorphic, and retrograde processes is recorded in the recovered samples.

Expedition 335 left Hole 1256D after making only a very modest advance, and we have yet to recover the samples of cumulate gabbros required to test models of ocean ridge magmatic accretion and the intensity of hydrothermal cooling at depth. However, a remarkable sample suite of granoblastic basalt with minor gabbros, some of which intrude previously recrystallized dikes, was recovered and provides a detailed picture of a rarely sampled critical interval of the oceanic crust. Most importantly, the hole has been stabilized, cleared to its full depth, and is ready for deepening in the near future.

Background and geological setting

Drilling a deep hole through intact ocean crust formed at a fast spreading rate has been one of the prime motivations for scientific ocean drilling since its inception (Teagle and Ildefonse, 2011). Fast-spreading ocean crust is targeted because geological and geophysical observations indicate that long distances of the ridge crests behave relatively uniformly. Consequently, we should be able to extrapolate the findings from a few deep penetrations to describe a significant portion of the Earth's surface (~30%). Only through the recovery of a significant section of cumulate gabbro underlying the dikes and erupted lavas will we be able to test competing models of magmatic accretion at fast-spreading mid-ocean ridges and evaluate the impact of these processes on the wider Earth system.

Integrated Ocean Drilling Program (IODP) Expedition 335 (13 April–3 June 2011) is the fourth scientific drilling cruise of the Superfast Spreading Crust campaign (Ocean Drilling Program [ODP] Proposal 522Full-2; D.S. Wilson et al., unpubl. data) to ODP Hole 1256D (6°44.163′N, 91°56.061′W) to deepen this ocean crust reference penetration a significant distance into cumulate gabbros. Hole 1256D is located on 15 Ma crust in the eastern equatorial Pacific Ocean in oceanic basement that formed during a sustained episode of superfast ocean ridge spreading (>200 mm/y) (Wilson, 1996) (Figs. **F1, F2**). Ocean crust formed at a superfast spreading rate was deliberately targeted because there is strong evidence from mid-ocean-ridge seismic experiments that

gabbros occur at shallower depths in intact ocean crust with higher spreading rates. Consequently, the often difficult-to-drill upper ocean crust should be relatively thin. Expedition 335 follows ODP Leg 206 in 2002 and IODP Expedition 309/312 in 2005 (Wilson, Teagle, Acton, et al., 2003; Teagle, Alt, Umino, Miyashita, Banerjee, Wilson, et al., 2006), which prepared the first scientific borehole for deep drilling by installing a large reentry cone secured with almost 270 m of 16 inch casing through the 250 m thick sedimentary overburden and cemented into the uppermost basement (Fig. **F2**). Hole 1256D was then deepened through an ~810 m thick sequence of lavas and a thin (~346 m) sheeted dike complex, the lower 60 m of which is strongly contact metamorphosed to granoblastic textures. The first gabbroic rocks were encountered at 1407 meters below seafloor (mbsf), where the hole entered a complex dike–gabbro transition zone that includes two 20 to 50 m thick gabbro lenses intruded into granoblastic dikes. As of the end of Expedition 312, Hole 1256D had a total depth of 1507.1 mbsf and was open to its full depth. Hole 1256D is poised at a depth where, with a few hundred meters of penetration, cumulate gabbros should be recovered for the first time from in situ lower ocean crust. These will reveal hitherto unavailable fundamental observations regarding the processes that form new crust at the mid-ocean ridges and the chemical exchanges between the crust, oceans, and mantle.

The scientific justifications for deep drilling of fast-spreading ocean crust will be further explored in the Expedition reports section of the Expedition 335 volume. The specific tests of ocean crust accretion models planned for Expedition 335 are described below.

Rationale for the Superfast Spreading Crust campaign and location of Site 1256

The key to proposing the Superfast Spreading Crust campaign (Leg 206 and Expeditions 309/312 and 335) was to identify a style of crustal accretion where the extrusive lavas and dikes overlying the gabbros are predicted to be relatively thin, thus increasing the likelihood of penetrating through the complete upper crustal section in the fewest drilling days (ODP Proposal 522Full-2; D.S. Wilson et al., unpubl. data). Drilling lavas and dikes has proved problematic in past scientific ocean drilling, resulting in poor hole conditions, slow penetration rates, and low core recovery (Figs. **F3, F4**). The recognition that crust formed at a relatively fast spreading rate is a compelling target for deep drilling follows the observation that there is an inverse relationship between the depth to axial low-velocity zones imaged by seismic experiments, interpreted to be melt lenses, and spreading rate (Purdy et al., 1992) (Fig. **F5**). Since the

Purdy et al. (1992) compilation, careful velocity analysis, summarized by Hooft et al. (1996), has refined the conversion from traveltime to depth, and data from additional sites have been collected (Carbotte et al., 1997). The fastest rate spreading centers surveyed with modern multichannel seismic reflection, ~140 mm/y full rate at 14°–18°S on the East Pacific Rise (EPR), show reflectors, interpreted as the axial melt lens, at depths from 940 to 1260 mbsf (Detrick et al., 1993; Kent et al., 1994; Hooft et al., 1994, 1996). At 9°–16°N on the EPR where spreading rates are 80–110 mm/y, depths to the melt reflector are mostly 1350–1650 mbsf, where well determined (Kent et al., 1994; Hooft et al., 1996; Carbotte et al., 1997). The implication from reflection seismic studies of axial low-velocity zones is that crust formed at superfast spreading rates (>200 mm/y) should have a thin dike section and cumulate gabbros should occur at relatively shallow depths.

The theoretical basis for expecting an inverse relation between spreading rate and melt lens depth is fairly straightforward if one considers a gabbro glacier style of crustal formation (e.g., Henstock et al., 1993; Phipps Morgan and Chen, 1993; Quick and Denlinger, 1993). The latent heat released in crystallizing the gabbroic crust must be conducted through the lid of the melt lens to the base of the axial hydrothermal system, which then advects the heat to the ocean. The temperature contrast across the lid is governed by the properties of magma (1100°–1200°C) and thermodynamic properties of seawater (350°–450°C where circulating in large volumes) and will vary only slightly with spreading rate and ridge depth (e.g., Jupp and Schultz, 2000). The heat flux through the lid per unit ridge length will therefore be proportional to the width of the lens and inversely proportional to the lid thickness. For reasons that are not understood, seismic observations show uniform width of the melt lens, independent of spreading rate. With width and temperature contrast not varying, the extra heat supplied by more magma at faster spreading rates must be conducted through a thinner lid (dike layer) to maintain steady state (see Phipps Morgan and Chen [1993] for a more complete discussion). This analysis leads to the prediction that to reach cumulate gabbros in normal oceanic crust with minimal drilling, it is therefore best to target crust formed at the fastest possible spreading rates (Wilson et al., 2006).

A setting similar to the modern well-surveyed area at 14°–18°S could be expected to reach gabbro at a depth of ~1400 m, based on 1100 m to the axial magma chamber reflector and subsequent burial by an additional 300 m of extrusives (Kent et al., 1994). At faster rates, depths could be hundreds of meters shallower. In contrast, seismic velocity inversions at the axes of the Juan de Fuca Ridge and Valu Fa Ridge, Lau

Basin, are at depths of ~3 km (Purdy et al., 1992), at intermediate spreading rates comparable to Deep Sea Drilling Project (DSDP)/ODP Site 504.

Superfast spreading rate crust in the eastern equatorial Pacific Ocean

The identification of magnetic anomalies formed at the southern end of the Pacific/Cocos plate boundary led to the recognition of crust formed at full spreading rates of ~200–220 mm/y from ~20 to 11 Ma (Wilson, 1996) (Fig. **F1**), 30% to 40% faster than the fastest modern spreading rate. This episode of superfast spreading ended with a reorganization of plate motions at 10–11 Ma. The southern limit of crust formed at the superfast rates is the trace of the Cocos-Nazca-Pacific triple junction, as Nazca-Pacific and Cocos-Nazca spreading rates were not as fast. The older age limit of this spreading episode is hard to determine with the limited mapping and poor magnetic geometry of the Pacific plate, but it is at least 18 Ma. The northern limit of this province is entirely gradational, with rates dropping to ~150 mm/y somewhat north of the Clipperton Fracture Zone.

The estimated depth to an axial melt lens for ocean crust formed at such a superfast spreading rate is ~800–1000 m. The anticipated depth to the gabbros for Site 1256 is ~1100–1300 m, allowing for a reasonable thickness (~300 m) of near-axial lava flows (e.g., Hooft et al., 1996) (Table **T1;** see **"Headline results from previous drilling at Site 1256: ODP Leg 206 and IODP Expedition 309/312"**), making this region a compelling target for deep drilling to help us understand crustal accretion processes at mid-ocean ridges.

Geological setting of Site 1256

Site 1256 lies in 3635 m of water in the Guatemala Basin (6°44.2′N; 91°56.1′W) on Cocos plate crust formed at ~15 Ma on the eastern flank of the EPR (Fig. **F1**). The depth of the site is close to that predicted from bathymetry models of plate cooling (e.g., Parsons and Sclater, 1977). The site sits astride the magnetic Anomaly 5Bn–5Br transition in magnetic polarity and is centered in the zone that accreted at a superfast spreading rate (~200–220 mm/y full rate) (Wilson, 1996). The site lies ~1150 km east of the present crest of the EPR and ~530 km north of the Cocos-Nazca spreading center. The trace of the Cocos-Nazca-Pacific triple junction passes ~100 km to the southeast, with the elevated bathymetry of the Cocos Ridge recording the trail of the Galapagos plume, farther to the southeast (~500 km). The site formed on a ridge segment at least 400 km in length, ~100 km north of the ridge-ridge-ridge triple junction between the Cocos, Pacific, and Nazca plates (Fig. **F6**). This location was formed near

the Equator within the equatorial high-productivity zone and initially endured high sedimentation rates (>30 m/m.y.) (e.g., Farrell et al., 1995; Wilson, Teagle, Acton, et al., 2003). Sediment thickness in the region is between 200 and 300 m and is 250 m at Site 1256 (Wilson, Teagle, Acton, et al., 2003).

The Guatemala Basin has relatively subdued bathymetry, and the immediate surroundings of Site 1256 (~300 km) are relatively unblemished by major seamount chains or large tectonic features high enough to penetrate the sediment cover (~200–300 m). Site 1256 was one of a number of sites approved by the ODP Site Survey panel (as Site GUATB-03C) (Fig. **F7**) for operations during Leg 206, and this specific location was selected from the regions surveyed to take advantage of faster upper crustal velocities, which correctly predicted the presence of massive basalt flows, and to avoid thrust faults that occur elsewhere in the region. The details of the 1999 *Maurice Ewing* site survey cruise operations are documented in Wilson, Teagle, Acton, et al. (2003) and Wilson et al. (2003).

Site 1256 has a seismic structure reminiscent of typical Pacific off-axis seafloor (Fig. **F8**). Upper Layer 2 velocities are 4.5–5 km/s, and the Layer 2–3 transition is between ~1200 and 1500 m subbasement (msb) (Fig. **F9**). The total crustal thickness at Site 1256 is estimated at ~5–5.5 km.

Site 1256 sits atop a region of smooth seafloor and basement topography (<10 m relief) (Fig. **F7**). Northeast of Site 1256 (15–20 km), a trail of ~500 m high circular seamounts rises a few hundred meters above the sediment blanket. Using the site survey multichannel seismic data (Wilson et al., 2003), we have constructed a geological sketch map of the uppermost basement in the GUATB-03 survey region (Fig. **F10**). Elsewhere in the region, the top of basement shows a number of offsets along northwest-striking normal faults, and an abyssal hill relief of as much as 100 m is apparent in the southwest part of the area. Relief to the northeast is lower and less organized. In the northeastern sector of the GUATB-03 region, there is evidence for a basement thrust fault with a strike approximately orthogonal to the regional fabric (Wilson et al., 2003; Hallenborg et al., 2003). This feature dips gently to the northwest (~15°) and is clearly discernible to a depth of ~1.3 km on seismic Line EW9903-28 (Wilson et al., 2003), but the feature is less pronounced on seismic Line EW9903-27, indicating that the offset on the thrust decreases to the southwest.

Additional processing (A.J. Harding, unpubl. data) of ocean bottom hydrophone (OBH) recordings indicates discernible variation in the average seismic velocity

(~4.54–4.88 km/s) of the uppermost (~100 m) basement and regional coherence in velocity variations (Fig. **F10A**). Two principal features are apparent: a 5 to 10 km wide zone of relatively high upper basement velocities (>4.82 km/s) that can be traced ~20 km to the edge of data coverage southeast of Site 1256, and a relatively low velocity (4.66–4.54 km/s) bull's-eye centered around the crossing point of seismic Lines EW9903-21 and EW9903-25.

The uppermost basement at Site 1256 is capped by a massive lava flow >74 m thick (Fig. **F2**). This flow is relatively unfractured, with shipboard physical property measurements on discrete samples indicating V_P > 5.5 km/s (Wilson, Teagle, Acton, et al., 2003). As such, it is likely that the area of relatively high uppermost basement seismic velocities represents the extent of the massive flow penetrated during Leg 206 in Holes 1256C and 1256D. Assuming an average thickness of 40 m, this would conservatively suggest an eruption volume in excess of 3 km^3, plausibly >10 km^3. This is extremely large when compared to the size of mid-ocean-ridge axial low-velocity zones that are thought to be high-level melt lenses, which typically have volumes ~0.05–0.15 km^3 per kilometer of ridge axis and generally appear to be only partially molten (Singh et al., 1998).

Sheet flows (<3 m thick) and massive flows (>3 m) make up most of the lava stratigraphy at Site 1256 (Fig. **F2**) (Teagle, Alt, Umino, Miyashita, Banerjee, Wilson, et al., 2006), and such lava morphologies have been shown to dominate crust formed at fast spreading rates, away from segment tips (e.g., White et al., 2000, 2002). Subordinate pillow lavas are present in Hole 1256D (e.g., Tominaga et al., 2009), and because of the large number of fractures and pillow interstices, seismic velocities in these units are generally lower than more massive lava flows. We speculate that the bull's-eye of relatively low seismic velocities is a thick pile of dominantly pillowed lava flows.

At 15 Ma, Site 1256 is significantly older than Hole 504B (~6.9 Ma), and lower temperatures are predicted at mid-levels in the crust (~115°C at 1500 msb), so high borehole temperatures should not become an issue until a significant thickness of gabbros is penetrated (Fig. **F11**). Heat flow (~113 mW/m^2 in Hole 1256C) is close to that predicted from cooling plate models, indicating minimal active hydrothermal circulation, as was confirmed by diffusive pore water profiles in the Site 1256 sedimentary overburden (Wilson, Teagle, Acton, et al., 2003).

The only serious drawback to the GUATB-03/Site 1256 area as a crustal reference section for fast spreading rates is its low original latitude. This means that the determi-

nation of magnetic polarity from azimuthally unoriented core samples is nearly impossible. In addition, the nearly north–south ridge orientation makes the magnetic inclination insensitive to structural tilting. Magnetic logging with either the General Purpose Inclinometry Tool (GPIT) fluxgates that form part of the Formation MicroScanner/Dipole Sonic Imager (FMS-sonic) tool string (or a separate magnetic tool with gyroscopic orientation) should be adequate for polarity determination and reorientation of recovered cores to the geographic reference frame.

Headline results from previous drilling at Site 1256: ODP Leg 206 and IODP Expedition 309/312

Hole 1256D in the eastern equatorial Pacific Ocean is the first basement borehole prepared with the infrastructure desirable for drilling a moderately deep hole into the oceanic crust (~1.5–2 km). Following preliminary coring to document the sedimentary overburden at Site 1256, operations during Leg 206 installed in Hole 1256D a reentry cone supported by 20 inch casing and large-diameter (16 inch) casing all the way through the sediment cover and cemented 19 m into basement (Wilson, Teagle, Acton, et al., 2003). Armoring the sediment/basement boundary reduces erosion of the borehole walls at this weak point and assists in clearing drill cuttings from the hole. The cone and casing facilitate multiple reentries and help maintain hole stability. The large-diameter casing was deployed to protect against the situation where one or two more casing strings (13⅜ and 10 ¾ inch) would be needed to stabilize the uppermost ~100 m of oceanic basement during the initiation of Hole 1256D. It also allows the possibility that future expeditions could insert further casing into the hole to isolate unstable portions of the very uppermost basement or improve the borehole hydrodynamics for clearing cuttings from the hole (see **"Operations"**). Because of the occurrence of a very thick massive lava flow at the top of basement, casing was not necessary for securing the uppermost portion of the hole.

The volcanic sequences at Site 1256 comprise a sequence of massive flows and thinner sheet flows with subordinate pillow basalt, hyaloclastite, and breccia (Fig. **F12**). The uppermost crust at Site 1256 comprises a ~100 m thick sequence of lava dominated by a single massive lava flow >75 m thick, requiring at least this much seafloor relief to pond the lava. On modern fast-spreading ridges, such topography does not normally develop until 5–10 km from the axis (Macdonald et al., 1996). Although this lava flow cooled off-axis it may have originated at the ridge axis before flowing on to the ridge flanks, as is observed for very large lava flows on the modern ocean floor (Macdonald et al., 1989). The lava sequence immediately below includes sheet and

massive flows and minor pillow flows. Subvertical, elongate flow-top fractures filled with quenched glass and hyaloclastite in these lavas indicate flow lobe inflation requiring cooling on a subhorizontal surface off-axis (Umino et al., 2000). From this shipboard evidence, a total thickness of 284 m of lava that flowed and cooled off-axis was estimated (Table **T1**). Sheet flows and massive lava flows erupted at the ridge axis make up the remaining extrusive section to 1004 mbsf, before a lithologic transition is marked by subvertical intrusive contacts and mineralized breccia. This contrasts slightly with the volcanic stratigraphy for Hole 1256D developed from analysis of wireline geophysical imaging (Tominaga et al., 2009; Tominaga and Umino, 2010) that suggests <50% of the lava drilled crystallized within 1000 m of the axis but that the majority of the lava pile had formed within 3000 m of the ridge crest.

Rocks throughout pilot Hole 1256C and the uppermost parts of Hole 1256D exhibit dark gray background alteration where the rocks are slightly to moderately altered, olivine is replaced, and pore spaces are filled by saponite and minor pyrite as the result of low-temperature seawater interaction at relatively low cumulative seawater/rock ratios. Vein-related alteration is manifest as different-colored alteration halos along veins. Black halos contain celadonite and have been interpreted to result from the presence of upwelling distal low-temperature hydrothermal fluids enriched in iron, silica, and alkalis (Edmond et al., 1979; see summary in Alt and Teagle, 1999). The iron oxyhydroxide–rich brown mixed halos are later features that formed by circulation of oxidizing seawater. The brown halos have a similar origin and formed along fractures that were not bordered by previously formed black halos. This vein-related alteration occurs irregularly throughout Hole 1256D below the massive Unit 1 (lava pond) but is concentrated in zones of greater permeability and, consequently, increased fluid flow. The appearance of albite and saponite partially replacing plagioclase below 625 mbsf indicates a change in alteration conditions. This change may result in part because of slightly higher temperatures at depth as the lava/dike boundary is approached or from interaction with more evolved fluid compositions (e.g., decreased K/Na and elevated silica). Black, brown, and mixed halos are absent in lowermost lavas (>900 mbsf), and dark gray background alteration related to abundant saponite and pyrite is ubiquitous. Vertical vein sets become more common below ~900 mbsf.

When compared with other basement sites (e.g., DSDP/ODP Sites 417 and 418 and Holes 504B and 896A), Hole 1256D contains a much smaller number of brown, mixed, and black alteration halos (Wilson, Teagle, Acton, et al., 2003; Alt, 2004). The abundance of carbonate veins in Hole 1256D is also lower than at many other sites

(Coggon et al., 2010). Site 1256 is, however, quite similar to ODP Site 801, also in crust generated at a fast-spreading ridge, albeit 170 m.y. ago (Alt and Teagle, 2003). One important feature is the lack of any oxidation gradient with depth in Hole 1256D, in contrast to the stepwise disappearance of iron oxyhydroxide and celadonite in Hole 504B and the general downhole decrease in seawater effects at Sites 417 and 418 (Wilson, Teagle, Acton, et al., 2003; Alt, 2004). In contrast, alteration appears to have been concentrated into different zones that may be related to the architecture of the basement, such as lava morphology, distribution of breccia and fracturing, and the influence of these on porosity and permeability.

Below 1061 mbsf, subvertical intrusive contacts are numerous, indicating the start of a relatively thin, ~350 m thick sheeted dike complex dominated by massive basalt. Some basalts have doleritic textures, and many are crosscut by subvertical dikes with common strongly brecciated and mineralized chilled margins. There is no evidence from core or geophysical wireline logs for significant tilting of the dikes, consistent with subhorizontal seismic reflectors in the lower extrusive rocks that are continuous for several kilometers across the site (Hallenborg et al., 2003). Measurements of dike orientations by wireline imaging are in close agreement with direct measurements on recovered cores and indicate that the dikes at Site 1256 are slightly tilted away from the paleospreading axis (dip/dip direction = 79° ± 8°/053 ± 23°) (Tominaga et al., 2009).

The secondary mineralogy of the rocks indicates a stepwise increase in alteration grade downhole from in the lavas to the dikes, with low-temperature phases (<150°C phyllosilicates and iron oxyhydroxides) in the lavas giving way to dikes partially altered to chlorite and other greenschist facies minerals (at temperatures greater than ~250°C) (Fig. **F12**) (Alt et al., 2010). Within the dikes, alteration intensity and grade increase downward, with actinolite more abundant than chlorite below 1300 mbsf and hornblende present below 1350 mbsf, indicating temperatures approaching ~400°C (Alt et al., 2010). The dikes have significantly lower porosity (mostly 0.5%–2%) and higher *P*-wave velocities and thermal conductivity than the lavas. Porosity decreases and *P*-wave velocity increases with depth in the dikes.

In the bottommost ~60 m of the sheeted dikes (1348–1407 mbsf), basalts are partially to completely recrystallized to distinctive granoblastic textures characterized by granular secondary clinopyroxene and lesser orthopyroxene resulting from contact metamorphism by underlying gabbroic intrusions (Figs. **F12, F13**). Textural changes in oxide minerals indicate that the zone of metamorphic recrystallization may extend

for >90 m above the upper contact with the first gabbro interval. There is unequivocal evidence for hydrothermal alteration before and after the formation of the granoblastic textures and potentially small, irregular patches of partial melting (Koepke et al., 2008; France et al., 2009; Alt et al., 2010). Simple thermal calculations suggest that the two gabbro bodies so far intersected in Hole 1256D have insufficient thermal mass to be responsible for a 60 to 90 m thick high-temperature (600°–900°C) metamorphic halo if the intrusions are simple subhorizontal bodies (Koepke et al., 2008; Coggon et al., 2008). This feature requires either a much more substantial intrusion nearby or significant topography on the dike/gabbro boundary.

Aside from the granoblastic contact metamorphic assemblages in the basal dikes, hydrothermal mineralogy and inferred alteration temperatures of the lower dikes in Hole 1256D are generally similar to those in the lower dikes of Hole 504B (as high as ~400°C). The fact that the dike section at Site 1256 is much thinner than the one at Site 504 (~350 versus ~1000 m), however, indicates a much steeper hydrothermal temperature gradient at Site 1256 (~0.5°C/m versus 0.16°C/m in Hole 504B).

Gabbro and trondjhemite intrusions into sheeted dikes at 1407 mbsf mark the top of the plutonic section (Figs. **F12, F13**). Two major bodies of gabbro were penetrated beneath this contact, with the 52 m thick upper gabbro (Gabbro 1) separated from the 24 m thick lower gabbro (Gabbro 2) by a 24 m screen of granoblastic basalts (Dike screen 1). The textures and rock types observed in Hole 1256D are reminiscent of varitextured gabbros thought to represent a frozen melt lens between the sheeted dike complex and above the cumulate rocks in many ophiolites (e.g., MacLeod and Yaouancq, 2000; France et al., 2009).

Gabbro 1 is mineralogically and texturally heterogeneous, comprising gabbros, oxide gabbros, quartz-rich oxide diorites, and small trondjhemite dikelets. Oxide abundance decreases irregularly downhole, and olivine is present in significant amounts only in the lower part of Gabbro 1. These rocks are moderately to highly altered by hydrothermal fluids to actinolite, hornblende, secondary plagioclase, epidote, chlorite, prehnite, and laumontite.

The intervening Dike screen 1 is interpreted as an interval of sheeted dikes captured between the two intrusions of gabbros. Dike screen 1 consists of fine-grained metabasalt similar to the granoblastic dikes overlying Gabbro 1. Dike screen 1 is cut by a number of small quartz gabbro and tonalite dikelets of variable thickness (1–10 cm), grain size, and composition.

Gabbro 2 comprises gabbro, oxide gabbro, and subordinate orthopyroxene-bearing gabbro and trondjhemite that are similarly altered to Gabbro 1 and has clear intrusive contacts with the overlying granoblastic Dike screen 1. Partially resorbed stoped dike clasts are entrained within both the upper and lower margins of Gabbro 2 (Fig. **F13G**). Gabbro 2 is characterized by an absence of fresh olivine, high but variable orthopyroxene contents (5%–25%), and considerable local heterogeneity. Oxide abundance generally diminishes downhole. The predominant rock type is orthopyroxene-bearing gabbro with gabbronorite in the marginal units. The lowermost rock recovered from Hole 1256D during Expedition 312 was a highly altered actinolite-bearing basaltic dike that lacks granoblastic textures; hence, it is interpreted to be a late dike that postdates the intrusion of the lower gabbro.

Relative to other well-studied upper ocean crust sections (e.g., Karson, 2002), Site 1256 shows a thick lava sequence and a thin dike sequence. Steady-state thermal models require that the conductive lid separating magma from rapidly circulating seawater thins as spreading rate increases, indicating that the thin dike sequence is a direct consequence of the high spreading rate. A thick flow sequence with many massive individual flows and few pillow lavas is a reasonable consequence of short vertical transport distance from the magma chamber and is similar to observations from the mid-segments of the fastest spreading ridges in the modern ocean (White et al., 2002). This is in direct contrast to spreading models developed from observations of tectonically disrupted fast-spread crust exposed in Hess Deep (Karson et al., 2002) that suggest regions of high magma supply should have thin lavas and thick dikes. Similarly, there is little evidence for tilting (at most a few degrees) in Hole 1256D and no evidence for significant faulting. In contrast, the upper crust exposed at Hess Deep shows significant faulting and rotation within the dike complex (Karson et al., 2002), indicating that observations from that tectonic window may be site specific and not widely applicable to intact ocean crust. The massive lava flow at the top of the Site 1256 basement indicates that faults with ~50–100 m throws must exist relatively near to the ridge axis even in superfast spreading rate crust to provide the necessary relief to pond of the lava. At fast-spreading ridges, such relief is typically developed ~5 to 10 km from the axis.

Marine seismologists have long been dividing the ocean crust into seismic layers: Layer 1 comprises low-velocity sediments (V_P < 3 km/s); Layer 2 has low velocity and a high velocity gradient, with V_P typically ranging from ~3.5 to ~6.7 km/s; whereas Layer 3 has high velocity and a low velocity gradient (V_P ranges from 6.7 to 7.1 km/s). There is a widespread perception that Layer 3 is equivalent to gabbro,

even though Hole 504B has penetrated Layer 3 but not gabbro (Alt et al., 1996; Detrick et al., 1994). From regional seismic refraction data, the transition from seismic Layer 2 to Layer 3 at Site 1256 occurs at ~1450–1750 mbsf (1200–1500 msb) (Wilson et al., 2003) (Figs. **F9, F12**). Shipboard determinations of seismic velocities of discrete samples are in close agreement with in situ measurements by wireline tools to ~1320 mbsf, above the granoblastic dikes interval; below that depth, velocities are significantly lower than the sonic log, and the gabbro velocities range between ~5.3 and 6.4 km/s (Swift et al., 2008). Contrary to expectation, porosity increases and *P*-wave velocities decrease stepwise downward from the lowermost dikes into the uppermost gabbro in Hole 1256D, as the result of the contact metamorphism of the granoblastic dikes and the strong hydrothermal alteration of the uppermost gabbros (Fig. **F12**). Porosity and velocity then increase downhole in the gabbro but are still <6.5 km/s. Similar trends for porosity and velocity were observed in postcruise laboratory measurements at ambient pressure, albeit on a small suite of samples (Violay et al., 2010). However, the compressional velocities on these samples were generally ~800 m/s higher in the gabbroic section, with V_P averaging ~6.4 km/s from the middle part of gabbro to the bottom of Gabbro 2. This difference may arise from the incomplete saturation of the samples during shipboard measurements. Wireline velocity measurements end at the top of gabbro, but we interpret the gabbro intervals as within Layer 2 because a smoothed extrapolation of the downhole velocities will either have velocities <6.5 km/s, still characteristic of Layer 2, or will have an exceptionally high gradient to higher velocities, also characteristic of Layer 2. Encountering gabbro at a depth clearly within Layer 2 reinforces previous inferences that factors including porosity and alteration (Detrick et al., 1994; Alt et al., 1996; Carlson, 2010) are more important than rock type or grain size in controlling the location of the Layer 2–3 transition. The position of the dike/gabbro boundary therefore appears to have little control over the seismic velocity structure of the crust (Alt et al., 1996; Detrick et al., 1994). Unfortunately, because the transition from Layer 2 to Layer 3 most likely lies beneath Hole 1256D, we cannot yet determine what controls this transition at Site 1256.

Summary of whole-rock igneous geochemistry from Site 1256

Flows and dikes from Hole 1256D show a wide range of magmatic fractionation, from fairly primitive to evolved (Figs. **F12, F14**). Shallower than 600 mbsf, magma compositions are bimodal, with relatively evolved thick flows and more primitive thin flows. The lava pond includes rocks with the highest incompatible element compositions (Zr, TiO_2, Y, and V) and lowest compatible element concentration (Cr and Ni), sug-

gesting that it is more evolved than other basalt from Site 1256 (Fig. **F15**). The initial division (based on Leg 206 lavas only) into high Zr-TiO_2, low Zr-TiO_2, and high Zr disappears with more data from Expedition 309/312. Rare samples from the lava pond fall off the dominant Y versus Zr and TiO_2 versus Zr trends, suggesting possible minor variation in source compositions.

There are subtle variations in the basalt chemistry downhole, with a number of step changes or reversals of fractionation trends possibly indicating cycles of fractionation, replenishment, and, perhaps, assimilation (e.g., at ~600, 750, 908, and 1125 mbsf). Downhole geochemical compositions within the dike section are variable and do not define trends. Primary and evolved compositions are closely juxtaposed, as would be expected for vertically intruded magmas. The range of major element compositions in the dikes is similar to that of the overlying rocks, and the average composition of the dikes is indistinguishable from the average composition of the lavas (Figs. **F12, F14**).

The gabbros have highly variable bulk compositions. The uppermost gabbros have geochemical characteristics similar to the overlying dikes with mid-ocean-ridge basalt (MORB) chemistries (MgO ~7–8 wt%; Zr ~47–65 ppm). Conversely, deeper in Gabbro 2 the rocks are significantly less fractionated and there are general downhole trends of increasing MgO, CaO, and Ni and decreasing FeO, Zr, and Y. The uppermost rocks of Gabbro 2 are fractionated with MgO contents of 6.1 wt%, but lower in the sequence MgO reaches 9.3 wt%. Decreasing concentrations of FeO and TiO_2 downhole suggest that Gabbro 2 is fractionated similarly to Gabbro 1. The intrusive nature of both gabbro bodies and the chemical variations within them suggest that they intruded into the base of the sheeted dikes and underwent minor internal fractionation in situ resulting in the observed general geochemical stratification. Partially resorbed xenoliths of granoblastic dikes within Gabbro 2 indicate that stoping of the intruded dikes may have contaminated the gabbro compositions.

There are linear trends between MgO versus TiO_2, FeO, CaO, Na_2O, and Zr, most likely resulting from fractional crystallization of a gabbro, with the fractionating assemblage consisting of clinopyroxene and plagioclase, as expected for relatively evolved basaltic magmas. The predicted composition of the cumulate gabbros generated during this fractional crystallization is very different from that of the gabbros drilled so far. Simple mass balance calculations indicate that the average basalt has lost >30% of its original liquid mass as solid gabbro, implying the presence of at least 300 m of cu-

mulate gabbro in the crust below the present base of the hole (Teagle, Alt, Umino, Miyashita, Banerjee, Wilson, et al., 2006).

The gabbro compositions span a range similar to the flows and dikes but are on average more primitive, with higher MgO and lower FeO, albeit still within the range of EPR basalts (Figs. **F14, F15**). Even though it is less fractionated, the average gabbro composition is evolved relative to candidates for primary magma in equilibrium with mantle olivine. Possible primary mantle melt compositions should have Mg# of 70–78 and MgO of 9–14 wt%. All flows and dikes and most gabbros are too evolved to be candidates for primary magma. Therefore, the residue removed from primary magma to produce the observed gabbro and basalt compositions must occur below the present base of Hole 1256D.

The compositional ranges of fresh lava and dike samples correspond to typical values for MORB for most major elements and many trace elements (Su and Langmuir, 2003) and are similar to those observed for the northern EPR (Fig. **F15**). A few incompatible elements, including Na and Zr, have lower concentrations than observed for the modern EPR lavas, but the generally substantial overlap of compositions indicates similar process operated at the superfast spreading ridge that formed Site 1256 and the modern EPR. When trace elements are compared to EPR MORB, they are within one standard deviation of average, albeit on the relatively trace element–depleted side of MORB. For example, compared with first-order mid-ocean-ridge segments along the EPR, basalts from Site 1256 have low Zr/TiO_2 and Zr/Y. Although there is overlap among the segments and a large scatter in the data for each segment, Zr/TiO_2 and Zr/Y appear to decrease with increasing spreading rate (Teagle, Alt, Umino, Miyashita, Banerjee, Wilson, et al., 2006). The origin of this relationship remains unclear. Spreading rate may affect the extents of magma fractionation or partial melting of the mantle, or it may instead reflect regional scale mantle heterogeneity. To decrease trace element ratios to this extent would require ~30% more melting at the superfast ridge, but this appears unlikely because of normal crustal thickness (~5.5 km) at Site 1256 (Park et al., 2008).

The simplest model for mid-ocean-ridge magma plumbing is that the melt lens imaged by multichannel seismic (MCS) experiments is the magma chamber where crystal-rich residues are separated from the evolved lavas that reach the seafloor (Fig. **F16**). Hole 1256D gabbros are texturally and compositionally similar to varitextured gabbros at the base of the sheeted dike complex in Oman interpreted to be axial melt lenses (MacLeod and Yaouancq, 2000; France et al., 2009). If the gabbro bodies so far

encountered in Hole 1256D were intruded on-axis, and if they extended roughly horizontally for at least hundreds of meters, at 52 and 24 m thick they would have dimensions appropriate for axial low-velocity zones imaged by MCS experiments at intermediate to fast-spreading ridges (Singh et al., 1998). However, these bodies could not have been the site of primary magmatic fractionation. Chilled margins against the underlying dike screens precludes segregating a crystal residue that subsides to form the lower crust as in the gabbro glacier model, and its overall fractionated composition requires that crystals have been segregated elsewhere. This implies that sills or other bodies containing cumulate materials must exist deeper in the crust and/or below the crust/mantle boundary, consistent with recent models based on lower crustal sections of ophiolites (e.g., Boudier et al., 1996; Kelemen et al., 1997; MacLeod and Yaouancq, 2000) and some marine geophysical experiments (Crawford and Webb, 2002; Dunn et al., 2001; Garmany, 1989; Nedimovic et al., 2005; Canales et al., 2009). However, the gabbro glacier mode of accretion or a combination of the gabbro glacier and sheeted sills models cannot yet be rejected, as fractionated gabbros in the dike–gabbro transition zone are not unexpected, and the predicted region of cumulate rocks could still exist just below the present maximum depth of Hole 1256D. Deepening Hole 1256D by as little as a few hundred meters would provide the critical samples that enable answering this outstanding basic question.

Scientific objectives

To date, the Superfast Spreading Crust campaign has accomplished the significant initial operational objective of drilling a section of intact upper ocean crust down into gabbros (Wilson et al., 2006; Teagle, Alt, Umino, Miyashita, Banerjee, Wilson, et al., 2006). This is a major scientific and engineering achievement, but with only ~100 m penetration into a complicated dike/gabbro boundary transition zone, many scientific objectives of the Superfast Spreading Crust campaign remain unfulfilled (ODP Proposal 522Full-2; D.S. Wilson et al., unpubl. data). Before we outline specific objectives for Expedition 335 operations in Hole 1256D, it is informative to predict what might be encountered with deeper drilling at this site.

Rocks expected with deeper drilling

With deeper drilling, Hole 1256D will explore unknown territory, and hence we must use geological analogs to predict what rocks underlie the current base of Hole 1256D. Field mapping from the lower crust of the Oman ophiolite (e.g., Kelemen and Aha-

ronov, 1998; MacLeod and Yaouancq, 2000; Nicolas and Boudier, 1991; Nicolas et al., 2000) and submersible studies and shallow drilling of EPR crust at Hess Deep (e.g., Francheteau et al., 1992; Gillis, 1995; Karson et al., 1992, 2002; Natland and Dick, 1996) may be useful in this respect. However, because of the difficulties of detailed mapping and sampling using submersibles and remotely operated vehicles (ROVs) and the lack of deep drilling of the dike/gabbro boundary in Hess Deep, the well-exposed outcrops in Oman arguably provide the best available guide to the upper plutonic section of fast-spreading ocean crust (Fig. **F16**). Detailed geological mapping from the dike/gabbro boundary down toward the harzburgites of the mantle (MacLeod and Yaouancq, 2000) in Wadi Abyad, Oman, provides one of the most useful templates of what might be encountered with deeper drilling in Hole 1256D (see also Pallister and Hopson, 1981; Nicolas et al., 1996).

Similar to Hole 1256D, the rocks directly underlying the sheeted dikes complex in Wadi Abyad are varitextured gabbros and microgabbros with subordinate ferrobasalts. The varitextured gabbros are ~150 m thick and show extreme variability in texture, grain size, and chemical composition at centimeter to meter scale and are petrographically very similar to the gabbroic rocks described so far from Hole 1256D. The Oman varitextured gabbros also display a wide range of compositions from those similar to cumulate gabbros to compositions more fractionated than the overlying dikes and lavas (e.g., Mg# 38–82). An average composition weighted according to outcrop abundance indicates that this horizon (Mg# ~65) (MacLeod and Yaouancq, 2000) is a pooled basaltic liquid sourced from deeper in the crust (Kelemen and Aharonov, 1998; MacLeod and Yaouancq, 2000; Sinton and Detrick, 1992) similar to the gabbros recovered from Hole 1256D.

The varitextured gabbros grade over a few meters into ~650 m of foliated gabbros with steeply dipping, prominent magmatic foliations oriented subparallel to the strike of the overlying sheeted dikes. These rocks show only weak modal variations. These foliated gabbros pass down into layered gabbros that make up the bulk of the plutonic section in Oman. These layered gabbros exhibit Moho-parallel modal layering defined by variations in the proportion of olivine, clinopyroxene, and plagioclase. Both the foliated and layered gabbros have “cumulate” compositions with high bulk Mg# (>75). Very low P_2O_5 concentrations (<0.02 wt%) indicate low (<5%) proportions of trapped intercumulus liquids. Similar but less detailed observations are recorded from Hess Deep (Francheteau et al., 1992; Gillis, 1995).

With a few hundred meters of drilling below the section of Hole 1256D drilled during Expedition 312, we anticipate breaching the current dike–gabbro transition zone, followed by penetration through a narrow (100–200 m) zone dominated by varitextured gabbros (Fig. F16). Beneath these rocks we anticipate drilling into cumulate rocks, perhaps with strong subvertical magmatic foliations and only weak modal layering. Modally layered gabbros with subhorizontal cumulate mineral layers are predicted to occur within 1000 m of the current bottom of Hole 1256D.

Questions addressed by deepening Hole 1256D

Specific scientific questions that will be addressed by deepening Hole 1256D a significant distance into cumulate gabbros during Expedition 335 and possible future expeditions are

- What is the major mechanism of magmatic accretion in crust formed at fast spreading rates? Is the lower crust formed by gabbro glaciers or sheeted sills or by some mixed or unknown mechanism?
- How is heat extracted from the lower oceanic crust?
- What is the geological significance of the seismic Layer 2/3 boundary at Site 1256?
- What is the magnetic contribution of the gabbro layer? Can the magnetic polarity structure of the lower crust be used to constrain cooling rates?

1. Is the lower crust formed by gabbro glaciers or sheeted sills?

There are two principal models for the accretion of the lower crust at fast-spreading mid-ocean ridges (Fig. F17); the "Gabbro Glacier" model (Henstock et al., 1993; Phipps Morgan and Chen, 1993) and accretion by "Sheeted Sills" (e.g., Boudier et al., 1996; Kelemen et al., 1997; Korenaga and Kelemen, 1997; MacLeod and Yaouancq, 2000). Gabbro glacier models postulate that the entire lower crust is formed by ductile flow of solid material downward and outward from a single, shallow axial magma chamber. In contrast, sheeted sill models are based on the crystallization of gabbro throughout the lower axial crust, with, for the end-member model, negligible downward flow of solid material (Kelemen et al., 1997).

High-level mafic cumulate rocks that balance the fractionated compositions of the dikes and lavas are a predicted consequence of both the gabbro glacier and sheeted sills modes of accretion, and cumulates should occur within a few hundred meters of the dike/gabbro boundary. Sampling the cumulate section through drilling will allow us to test the relative importance of these end-member mechanisms of crustal accre-

tion. A gabbro glacier mode of crustal accretion will result in specific chemical and structural consequences for the lower oceanic crust that will be observable in drill core (Figs. **F16, F17**). One would predict that (1) the upper plutonics and the lower crust have similar compositions and (2) that there will be increasing amounts of strain and subsolidus deformation in rocks with depth in the ocean crust.

Test 1.1: Gabbro glacier models predict no variation in cumulate composition (e.g., Mg#) with depth.

If all solidification of the lower crust takes place in the shallow melt lens, then there should be no vertical variation in the composition of the cumulates (e.g., Mg# of mafic phases). However, if the stacked sills model is correct, then we should see a gradual increase in the Mg# of the mafic phases with increasing depth in the section or a random vertical repartition of variable Mg# values. Studies of high-level plutonic rocks in Oman do show chemical trends with depth over a scale of kilometers (e.g., MacLeod and Yaouancq, 2000; S. Miyashita, pers. comm., 2005), although small-scale (meters) chemical layering at the very base of the Oman crust is not well correlated with depth (Korenaga and Kelemen, 1998). Chemical layering in cumulate rocks should put constraints on melt migration and the size of magma lenses. Studies of cyclic variations in mineral trace element concentrations in Oman suggest the size of melt lenses is on the order of meters to hundreds of meters (Browning, 1984; Korenaga and Kelemen, 1997). Modeling the effects of melt flow through porous media such as a chemically layered crystal mush indicates that trace element correlations should be obliterated by melt-crystal reaction in hundreds to thousands of years (Korenaga and Kelemen, 1998). In Oman, chemical layering is well correlated for different elements and minerals, suggesting that the upwelling of melt through a crystal mush at the ridge axis cannot have occurred (Korenaga and Kelemen, 1998). These careful petrological tests have not been applied to rocks sampled from in situ ocean crust. The presence or absence of geochemical trends in whole rock and mineral chemistry will place important boundaries on mechanisms of melt migration and magma emplacement in the lower oceanic crust.

Test 1.2: Gabbro glacier models predict increasing strain with depth.

Formation of the lower crust from a single, high-level melt lens requires very large increases in strain with depth in the crust (Henstock et al., 1993; Phipps Morgan and Chen, 1993) that will manifest as stronger shape and lattice fabrics. Such high strains have not been reported from rocks sampled in Hess Deep, but to date textural and structural measurements to estimate the extent of strain have not been employed on

rocks from intact sections of fast-spread ocean crust. Lack of evidence for increasing strain with depth would favor the multiple sills model. However, increasing strain with depth has been reported for the uppermost part of the foliated gabbro section of the Oman ophiolite (Nicolas et al., 2009), suggesting that subsidence does occur from the upper melt lens. Together with the evidence for sills, these observations may support a mixed model (Boudier et al., 1996).

2. Is the plutonic crust cooled by conduction or hydrothermal circulation?

The balance between conductive and hydrothermal cooling is key to understanding the thermal structure of the ocean crust, as well as for estimating the magnitude of hydrothermal chemical exchanges between the crust and oceans. This is because the latent heat of crystallization of gabbro is a significant fraction (~⅓) of the total heat available from the cooling and crystallization of a basaltic melt. Where crystallization takes place in the crust is one of the major differences between the end-member models (Fig. **F17**). Were the gabbros, particularly cumulate gabbros, cooled by conduction or hydrothermal fluids (Manning et al., 1996; Maclennan et al., 2005)? Were hydrothermal interactions pervasive or restricted to veins, and did alteration occur at black smoker or higher temperatures (350°–800°C)? Or did most of the hydrothermal interactions occur later at subgreenschist facies conditions (e.g., prehnite and clays) some distance away from the ridge? What is the role of faults in channeling recharge and discharge fluids to and from the lower crust? How do alteration effects relate to physical properties and the seismic layering of the crust?

Simple gabbro glacier models suggest much slower rates of cooling for the lower crust (~0.02°C/y) than those required to match recent seismic tomographic models and compliance results from the EPR (Crawford and Webb, 2002; Crawford et al., 1999; Dunn et al., 2001). Multiple sills models require deep near-axis hydrothermal cooling and rapid cooling rates (~0.1°C/y); otherwise, large-scale remelting of the lower crust will occur (Chen, 2001). However, deep hydrothermal cooling may also occur in some geometries of gabbro glacier models. Although the extent of hydrothermal cooling of the lower crust must be closely linked to the mode of magmatic accretion, quantifying these rates of cooling is a separate, important, and independently achievable objective.

Test 2.1: Are cooling rates much greater than expected from conductive heat transfer in the cumulates?

Recent petrological studies of the Oman ophiolite and Hole 504B have developed techniques for estimating the cooling rates of dikes and gabbros (Coogan et al., 2005a, 2002, 2005b). The Ca in olivine geospeedometer developed and refined by Coogan and others will allow the robust estimation of vertical variations in cooling rate that are sensitive enough to identify departures from conductive cooling profiles. Li measurements of coexisiting igneous plagioclase and clinopyroxene provide an independent cooling geospeedometer (Coogan et al., 2005b).

Test 2.2: Quantify fluid evolution and fluxes through lower crust using trace elements and Sr and stable isotopic profiles.

Well-established petrologic and geochemical approaches will be used to characterize the nature and relative timing of hydrothermal exchange between seawater and the lower crust that complement the trace element cooling rate studies of magmatic minerals discussed above.

Mineral geothermometers, crosscutting vein mineral sequences coupled with trace elements and strontium, and stable isotopic measurements of whole-rock samples and mineral separates can be used to establish the chemistry of fluids reacting with the lower crust (Gregory and Taylor, 1981; Bach et al., 2004; Coggon et al., 2004; Gillis, 1995; Manning et al., 1996; Teagle et al., 1998a, 1998b). By looking at ^{87}Sr and ^{18}O profiles away from hydrothermal mineral veins, we can establish the scale of fluid channeling in the lower crust (e.g., Bickle, 1992; Teagle and Bickle, 1993). The advection of seawater-derived tracers, particularly when whole-rock and mineral data are closely coupled, have proved useful for estimating time-integrated hydrothermal fluid fluxes (Bickle and Teagle, 1992; Coogon, 2006; Gillis et al., 2005; Teagle et al., 2003).

3. What is the geological significance of the seismic Layer 2/3 boundary at Site 1256?

Understanding the seismic structure of the ocean crust requires the calibration of remotely obtained regional geophysical data against physical properties and petrological measurements of geological samples recovered from within deep ocean boreholes. Hole 504B remains the only site where the seismic Layer 2/3 boundary has been penetrated (e.g., Detrick et al., 1994). At that location, the change in seismic gradient clearly occurs within the dikes and the Layer 2/3 transition reflects changes in bulk

physical properties associated with an increased grade of hydrothermal alteration (albite + chlorite to amphibole + plagioclase). In Hole 1256D, gabbros have been recovered from crust clearly within seismic Layer 2 based on shipboard, wireline, and seismic refraction velocity measurements (Figs. **F8, F12**) (Swift et al., 2008). The depth of the Layer 2/3 boundary estimated during site survey seismic experiments at Site 1256 is between 1450 and 1750 mbsf. Drilling deeper at Site 1256 would provide a second test of the geological meaning of the seismic layering of the ocean crust, where the Layer 2–3 transition lies beneath the first appearance of gabbro.

4. What is the magnetic contribution of the gabbro layer? Can the magnetic polarity structure of the lower crust be used to constrain cooling rates?

Site 1256 was deliberately located ~5 km on the old side of the C5Cr-C5Bn magnetic reversal (Fig. **F7A**). Preliminary interpretation of the downhole magnetic field indicates that the flow and dike section has reversed polarity. Interpretation of paleomagnetic samples has been severely hampered by drilling overprint. However, the downhole magnetic field is more diagnostic than analysis of samples for determining the average in situ magnetization of a particular crustal layer. Very preliminary modeling of the downhole field intensity suggests that the flow and dike layers contribute about two-thirds of the amplitude of the marine magnetic anomalies measured at the sea surface, mostly from the thicker flow units. In addition to quantifying the contribution of gabbros to the sea-surface anomalies, magnetic measurements from a significantly deepened Hole 1256D could help determine whether the middle crust cools quickly by convection or slowly by conduction. The blocking temperature at which magnetization becomes stable over geologic time is ~400°C. The position of the site indicates that the Earth's field changed from reversed to normal polarity 50–80 k.y. after most dikes and the lower extrusives formed. End-member models for hydrothermal circulation therefore predict very different observations of the polarity structure of the middle and lower crust. Models for deep, young hydrothermal circulation (e.g., Maclennan et al., 2005) predict that reversed polarity should continue to near the base of the crust. In contrast, models with young hydrothermal circulation largely restricted to the more porous upper crust (e.g., Henstock et al., 1993) predict that normal polarity should be encountered within a few hundred meters of the base of high-volume circulation, potentially within the penetration of an additional single drilling expedition.

Operations

Drilling strategy for Hole 1256D

Leg 206 and Expedition 309/312 made significant progress in recovering an intact section of the upper oceanic crust through the erupted lavas and sheeted dikes and into the uppermost gabbros. Average rates of recovery and penetration are summarized in Figure **F18** and Table **T2.** The inverse relationship between spreading rate and depth to axial melt lenses has been confirmed, supporting the strategy of drilling in crust formed at a superfast spreading rate to achieve the first upper crustal penetration. However, fundamental questions regarding the formation of ocean crust remain. The principal goal of Expedition 335's return to Hole 1256D was to deepen the hole sufficiently into plutonic rocks (a few hundred meters) to obtain definitive answers to long-standing questions about the structure and composition of the oceanic crust and about mechanisms of crustal accretion (these ideas are developed in greater detail in **"Background and geological setting"**).

Operational planning for Expedition 335 was informed by three principal sources:

1. The Operations teams experiences during Leg 206 and Expedition 309/312 to Hole 1256D and previous deep basement coring by scientific ocean drilling;
2. Aspects of the IODP Operations Review Task Force Meeting "Expeditions 309/312 Superfast Spreading Rate Crust" (ORTF-3 [**www.iodp.org/ortf/**], June 2006); and
3. A US Implementing Organization (USIO) position paper, "Operational requirements for returning to Hole 1256D" (September 2006).

The recommendations of the Expedition 309/312 Review Task Force indicate an understanding of the nonstandard requirements of deep basement drilling and echo the suggestions made by the Co-Chief Scientists of those expeditions. Three recommendations pertinent to operations during Expedition 335 were

1. To investigate alternate scheduling strategies (e.g., at-sea crew changes, lengthening standard expedition durations to *maximize* on-site time for deep drilling objectives; ORTF-309/312-03),
2. To investigate and prioritize avenues for enhancing coring/drilling capability (particularly of hard formations) for deep-drilling programs (ORTF-309/312-11), and

3. To build on the experiences of Phase 1 expeditions and actively explore future applications of drilling muds (particularly those with heavy lifting capability) for riserless hole cleaning and stabilization (ORTF-309/312-12).

Unfortunately, there has been only modest progress on these recommendations in the 5 years since the ORTF-309/312 meeting, with a half-length expedition initially scheduled by the Science Advisory Structure for the return to Hole 1256D and an absence of new drilling and coring options for hard formations and hole cleaning.

The IODP Science Planning Committee requested in 2006 (SPC Consensus 0603-19) that the USIO identify the operational requirements for further drilling in Hole 1256D. Texas A&M University (TAMU) engineers from the USIO presented their operational plan to an audience of scientists and independent drilling engineers at the Mission Moho Workshop (Portland, Oregon, 7–9 Sept 2006) for technical review. There was consensus support for the plan proposed.

The USIO considered four deepening scenarios:

1. Resume rotary core barrel (RCB) coring in Hole 1256D using large-volume (100–150 bbl) high-viscosity mud sweeps combined with frequent bit trips,
2. Enlarge the hole to 18½ inches to isolate the out-of-gauge section using 13⅜ inch casing,
3. Forego 13⅜ inch casing and enlarge the hole to 14¾ inches to isolate the out-of-gauge section using 10¾ inch casing, and
4. Offset and start a new hole following the casing strategy employed during Leg 206.

Two key points were noted by the USIO and independent engineers at the Mission Moho Workshop:

1. Hole 1256D is in excellent condition, and remedial engineering operations such as reaming and casing are premature.
2. Neither the offshore industry nor scientific ocean drilling operators have ever attempted to open up an existing deep basement hole to any significant depth (hundreds of meters) in basalt and insert casing.

Regardless of the casing strategy proposed (2 or 3), attempting to open any portion of Hole 1256D to accommodate casing would require significant new hardware, numerous pipe trips, and extend over several expeditions. Such operations would require

unproven technology and would be extremely challenging with substantial risk of irreparable damage to Hole 1256D without any further coring or recovery. The USIO and independent experts felt that approaches 2 and 3 are not viable options and recommended that they were not considered further.

The preferred USIO strategy was 1—resuming RCB coring with frequent large-volume high-viscosity mud sweeps (ORTF-309/312-12). During Expedition 309/312, large-volume mud sweeps were effective at clearing cuttings from the hole. However, because of the end of Phase I operations, mud stock depletion precluded the vigorous implementation of this approach throughout the whole of Expedition 312. The refitted *JOIDES Resolution* should be equipped to handle the necessary supplies to maintain an aggressive mud program. Following the recommendations of the IODP Expedition 309/312 Operations Review Task Force, the *JOIDES Resolution* was stocked with at least 60 T of sepiolite and attapulgite for use during Expedition 335.

Assuming reasonable hole conditions and an average rate of penetration (ROP) comparable to previous coring in this hole, TAMU engineers estimated that this approach should deepen Hole 1256D ~350 m with 39 days on site (Teagle et al., 2010). The engineering and design lessons learned from a few hundred meters deeper penetration of intact ocean crust would be invaluable in planning and exploiting future deep penetration targets.

Further deepening of Hole 1256D using large mud sweeps is the only strategy that begins with coring, is the most likely to return samples from deeper in the hole, and has the largest possibility of building on the tremendous success of previous deepening operations on Expedition 309/312 that employed proven drilling techniques.

Before conditioning the hole for further deepening, an attempt would be made to acquire an equilibrium temperature profile and recover a water sample before the thermal structure of the crust is perturbed by cleaning and drilling operations (see next section). We would reenter the hole with a tricone drilling bit on a bit release and slowly descend past the zone around 900 mbsf that caused an obstruction during Expedition 312. If the hole was clear, we would withdraw the pipe, drop the bit, and reenter to below the rat hole to allow logging with the triple combo, including the Modular Temperature Tool (MTT). If the wireline conditions were suitably benign, we would attempt to take a borehole water sample from near the bottom of the hole using the water-sampling temperature probe (WSTP).

Expedition 335 operations

Port call

All Expedition 335 scientists transferred from their hotel in San Jose, Costa Rica, to Puntarenas, Costa Rica, and moved onto the vessel on Thursday, 14 April 2011, except for one whose travel was delayed by 3 days. The morning of Friday, 15 April, the Co-Chief Scientists engaged in a press conference at the Marine Biology Station of the Universidad National Costa Rica, located near the vessel. Regional visitors toured the ship in the afternoon. The final science party member arrived on board on Saturday, 16 April.

Transit

The last line was released on 17 April 2011 at 0420 h, and the vessel began transit to Site 1256 (6°44.2′N, 91°56.1′W) at 0430 h. The 478 nmi voyage to Hole 1256D was accomplished at an average speed of 10.6 kt. The vessel was positioned on the established coordinates of the hole at 0115 h on 19 April. The water depth established during Leg 206 was 3645.4 meters below rig floor (mbrf). The final depth of the hole at the end of Expedition 312, when it was last visited in December 2005, was 1507.1 mbsf. Below is a narrative of the operations conducted in Hole 1256D from this time (Table **T3**).

Opening Hole 1256D (19–23 April)

Run 1

Hole 1256D was reentered with a hard formation Smith 9⅞ inch F9 tricone bit (Fig. **F19A**) affixed to a mechanical bit release (MBR) and four-stand bottom-hole assembly (BHA). The initial objective was to test the openness of the hole to 1100 mbsf without circulation or rotation so that, if clear, an equilibrium temperature profile could be run to 1350 mbsf using the MTT logging suite. This would have been followed by a borehole water/microbiology sampling run using the WSTP according to plan (Teagle et al., 2010).

The drill string was lowered to ~920 mbsf, where it encountered a ledge precluding the planned wireline operations. This interval had impeded smooth transit of the drill string during Expedition 312. The wireline caliper, FMS, and Ultrasonic Borehole Imager (UBI) logs from that expedition indicate an eroded zone from ~920 to 935 mbsf (see **"Observations of highly out-of-gauge interval (920–960 mbsf)"** for more detail). Starting at 2330 h on 19 April 2011, and for 32 h until 0600 h on 21 April, the

drillers attempted to work past the obstruction without success, and the drill string was recovered.

Run 2

A more aggressive Reed 9⅞ inch tricone bit (International Association of Drilling Contractors [IADC] Type 517) (Fig. **F19B**), usually employed in softer formations, was mounted along with a tandem set of junk basket subs, and Hole 1256D was reentered for the second time at 0105 h on 22 April 2011. Drilling on the bridge at ~922 mbsf resumed at 0445 h and continued to 2100 h (16.3 h) without discernible progress. The drill string was recovered, with the bit clearing the rotary table at 0605 h on 23 April. The contents of the junk baskets were examined and found to contain angular coarse sandy basaltic chips along with a few small (2–3 cm) subrounded basaltic pebbles, consistent with the rocks cored when this interval was first drilled during Expedition 309. After discussing options with the on-board scientific leadership, it was decided that placing a cement plug at and above the bridge could possibly stabilize the zone and allow us to advance past the obstruction.

Cementing and reopening Hole 1256D (23 April–3 May)

Run 3

A cementing assembly was made up of the used Reed 9⅞ inch tricone bit without jets and two stands of drill collars. Hole 1256D was reentered for the third time at 1520 h on 23 April 2011. After the driller tagged the bridge with the bit at 922 mbsf, the circulating head was made up to the drill string and tested to 1500 psi. Five bbl of 16 ppg (pounds per US gallon; specific gravity ~ 1.9) blended cement was pumped into the hole and chased with a column of seawater equal to the volume of the drill string. The drill pipe was then pulled back to 807 mbsf, where an additional seawater flush consisting of three drill string volumes was pumped through the system. After rigging down the cementing equipment, the drill pipe was recovered, with the bit clearing the rotary table at 0515 h on 24 April.

Run 4

The Reed bit was replaced with a new 9⅞ inch tricone bit (Atlas HP61), and the drill string was deployed to 1596 mbrf. Hole 1256D was reentered for the fourth time at 1655 h on 24 April 2011 to test the result of the cementing operation. The bit tagged the bridge at 922.0 mbsf, indicting that the 5 bbl of cement deployed earlier was not sufficient to fill the cavity above the obstruction. The driller's effort to wash and ream

past the ledge met with high erratic torque and was given up after 1 h. The drill string was tripped to the surface, with the bit clearing the rotary table at 0615 h on 25 April.

Run 5

The cementing assembly was deployed for the second time, with the bit entering the reentry cone for the fifth time at 1445 h on 25 April 2011. The bit was placed at 922 mbsf, and this time 50 bbl of 15 ppg cement was pumped into the hole. The bit was recovered at 0345 h on 26 April.

Run 6

A drilling assembly with an Atlas tricone bit was redeployed, and at 1520 h on 26 April 2011, Hole 1256D was reentered for the sixth time during this expedition. The top of the cement plug was tagged at 882 mbsf. The 40 m cement plug was drilled out at an average ROP of 10.7 m/h. At 2230 h on 26 April, washing and reaming the hole at ~920 mbsf resumed, and it continued until 0600 h on 28 April with no apparent progress. The driller worked stuck pipe for 1 h during this time interval. The drill string was recovered to change the bit, which had accumulated 33.3 h of work. The used bit (Fig. **F19C**) was found to be in gauge and exhibited little wear on the cones and bit body. The two junk baskets were emptied (Fig. **F19D**) and contained basaltic cuttings ranging from fine angular sand to small pebbles. Rare small (as large as centimeter-scale) chunks of cement were also recovered. The quantity of material was noticeably less than that from the previous junk basket deployment (Run 2).

Run 7

A new hard formation Smith Q7JS (IADC code 735) tricone bit (Fig. **F19E**) was picked up and deployed with the drilling assembly. The nozzles were reduced to 14/32 inches from the usual 16/32 inches to increase the downhole hydraulic horsepower. The junk baskets were not added to the BHA to reduce the risk of downhole hardware failure. The bit entered the reentry cone for the seventh time of the expedition at 0135 h on 29 April 2011. Washing and reaming resumed, and perseverance was finally rewarded when the bit passed through the obstruction at 922 mbsf shortly before midnight on 29 April. The pipe got stuck for 2 h at 1162 mbsf. The total depth achieved during Expedition 312 (1507.1 mbsf) was reached at 0915 h on 1 May. A total of 6 m of hard fill was encountered at the bottom of the hole, which was ground and removed before the bore was flushed with a 100 bbl high-viscosity mud sweep. The wiper trip to 890 mbsf was without incident. A pill of 60 bbl of heavy mud was spotted across the zone

extending from 920 to 960 mbsf to keep the formation from bridging over the open hole prior to retrieving the pipe trip to the surface.

Run 8

The cementing assembly was deployed for the third time of the expedition with the bit entering the reentry cone for the eighth time at 1300 h on 2 May 2011. The bit was placed below the unstable zone at 960.5 mbsf, and 65 bbl of 15 ppg cement was pumped into the hole. The intent of this operation was to fill and stabilize the washed out and apparently unstable portion of the hole below 922 mbsf (see **"Observations of highly out-of-gauge interval (920–960 mbsf)"**). This region was not accessible prior to drilling through the ledge. The drill string was flushed with a large volume of seawater prior to withdrawal from the hole. The drill string was tripped to the surface, and the BHA was recovered by 0315 h on 3 May.

Coring (3–7 May)

Run 9

An RCB coring assembly made up with a Rock Bit International (RBI) C-9 hard formation coring bit, 11 controlled length drill collars, a tapered drill collar, six joints of 5½ inch drill pipe, and associated subs was deployed at 0630 h on 3 May 2011. The bit reentered the cone for the ninth reentry of the expedition at 1235 h. Thought was given to penetrating the cement plug with a center bit, but it was decided that coring the cement would be more efficient and keep the annulus cleaner. The driller tagged the cement at 924 mbsf and began coring at 1745 h on 3 May (ghost cores 335-1256D-G1 through G6) (Table **T4**). At 1330 h on 4 May, the cement plug was penetrated and the remaining portion of the hole was washed (wash core 7W) (Table **T4**) and reamed to bottom by the early morning of 5 May. Rotary coring in Hole 1256D began at 0145 h on 5 May, which was exactly 16.0 days after arriving on station. Rotary coring advanced from 1507.1 to 1520.2 mbsf (Cores 335-1256D-235R through 238R) (Table **T4**) by 1200 h on 6 May, using nonmagnetic core barrels without liners to reduce jamming and increase recovery. Coring was difficult with occasional erratically high torque. Overpull of as much as 60,000 lb was frequently needed to keep the drill string free. When the last 2 m of advance required nearly 12 h, the core barrel was recovered and found to contain only three pebbles. Initially, it was thought that the bit throat might be jammed, which is not uncommon in hard rock coring. However, examination of the core catcher sub located at the bottom of the core barrel showed evidence of grinding and abrasion damage, indicating a serious mechanical problem at the bit (Fig. **F19F**).

The drill string was recovered, with the bit clearing the rotary table at 0545 h. The bit was totally unrecognizable (Fig. **F19G, F19H**). The body of the bit was honed to a smooth profile at the bottom and on the sides, earning it the name "Stumpy." The bit was missing all four cones, four legs, and core guides. The bit spiral stabilizer blades and embedded tungsten carbide inserts were also absent. The severity of the damage indicated that the bit had continued to rotate hours after experiencing failure, likely as long as 10 h, based on changes in penetration rates. This spectacular failure was masked by the difficult drilling conditions >5 km beneath the hull.

Cleaning, milling, and reaming (7–26 May)

Run 10

Before coring could resume, the metal hardware debris, "junk," had to be removed from the bottom of the hole. The first attempt at retrieving the junk was made with a fishing assembly including a Bowen 9 inch fishing magnet (Fig. **F19I, F19K**) coupled to a tandem set of junk baskets. This assembly was run in with two stands of drill collars, reentering Hole 1256D for the tenth time at 1815 h on 7 May 2011. The fishing assembly was run in without incident to 1295 mbsf, where it contacted a ledge. The top drive was picked up, and the assembly was advanced to within 73 m of the bottom (~1434 mbsf), where circulation was lost. All attempts at unblocking the flow path by varying the pump strokes and running pressures as high as 2500 psi with 20 strokes per minute were unable to clear the blockage. Because it would be reckless to attempt to advance any further down the hole without circulation, the drill string was recovered. The magnet, both junk baskets, and the bit sub were packed with sand-sized basaltic cuttings mixed with metal shavings and some cement cuttings (Fig. **F19J**). This material apparently worked past the float valve during periods of low fluid flow and circulation breaks while making pipe connections. The consensus was that the lower section of the hole needed to be cleaned out to within a couple of meters of the wreckage before a mill or magnet could be effective.

Run 11

The next fishing attempt was made with a used Atlas tricone bit (IADC type 517), a tandem set of external junk baskets (EXJB), and three stands of drill collars. The fishing assembly reentered Hole 1256D at 0315 h on 9 May 2011. The hole was washed, reamed, and heavily flushed with large-volume, high-viscosity mud sweeps. Special attention was given to reaming and washing the ledges found at 1356 mbsf, from 1459 to 1478 mbsf, and at 1520 mbsf. The bit cleared the seafloor at 0605 h and the rotary table at 1130 h on 10 May. The surface of the reentry cone was flushed prior to

withdrawal from the hole. The two EXJBs were found to contain material ranging from fine gravel to cobble-size rocks (Fig. **F19L, F19M**).

Run 12

The next fishing attempt was made with a 9¾ inch Bowen full-flow reverse circulation junk basket (RCJB) (Fig. **F19N, F19O**). The principle of reverse circulation increases the chance of recovery of bit cones, tong pins, hammers, and similar debris. The circulating fluid is jetted outward and downward against the full circumference of the hole, where it is deflected and directs loose objects into the long hollow barrel of the basket. The unit is activated by dropping a stainless steel ball from the surface (Fig. **F19S**) and does not utilize a float shoe. The RCJB with a Type B mill was made up to a single EXJB and a six–drill collar BHA and deployed at 1300 h on 10 May 2011. The assembly reentered Hole 1256D at 2330 h. After the slow circulating parameters were obtained and the hole was flushed with a 100 bbl high-viscosity sweep, the stainless steel activation ball was dropped into the open pipe and the tool lowered to within 1 m of the bottom (~1516 mbsf). Because of the high pump rates and resulting standpipe pressure employed, the landing of the ball in the RCJB was not immediately obvious. The tool was worked for 30 min before the drill string was recovered. On the surface, all five 8¼ inch drill collars were found to be filled with fine hole cuttings weighing on the order of a few hundred kilograms (Fig. **F19P**). Coarser gravel was also found in the lower part of the BHA in the head sub, crossover subs, and bit subs. The RCJB basket (Fig. **F19Q, F19R**) contained an array of granoblastic dike rocks with 20 weighing >100 g. One specimen was 20 cm × 10 cm × 10 cm and weighed 4.5 kg. The total weight of all rocks in the basket was estimated at ~20 kg. The large rocks were assumed to be covering whatever remains of the bit cones, bit legs, and core guides at the bottom of the hole.

Run 13

The second deployment of the Bowen RCJB was made with a Type A mill shoe and reentered Hole 1256D at 1335 h on 12 May 2011. The tool was run in the hole to 1385 mbsf, where the top drive was picked up. The assembly was carefully advanced with rotation and circulation and tagged a hard ledge at 1518 mbsf but was unable to advance past this depth. The steel ball was dropped, but activation of reverse circulation was obscured by pump pressure as high as 3000 psi at 50 spm. The drill string was recovered, with the RCJB clearing the top of the cone at 0340 h on 13 May. Once on the surface, the BHA was again found filled with fine cuttings with a volume compa-

rable to the previous run (Fig. F19T). The RCJB basket contained two rocks with a total weight of 4.5 kg. The RCJB was cleaned, dressed, and laid down.

Run 14

The forth fishing attempt was made with a 9½ inch Homco flow-through junk basket (FTJB) (Fig. F19U). The FTJB does not employ reverse circulation and has a deeper throat than the RCJB. The FTJB is also deployed with a float shoe that reduces the potential for inadvertent filling of the inside of the BHA with cuttings. The fishing assembly entered the reentry cone at 2315 h on 13 May 2011 and was run in to 1521 mbsf by 0815 h. The driller slowly worked the tool on bottom for 30 min before pulling back. Mud flushes totaling 300 bbl were circulated during this process. The drill string cleared the seafloor at 1345 h and was recovered by 2015 h on 14 May. The FTJB contained two rocks of granoblastic dike origin that weighed a combined 3.2 kg. Of the two sets of junk catcher fingers, the lower set was completely devoid of fingers (Fig. F19V). Although the FTJB completed the trip to the bottom of the hole, only a fraction of the material snared by the tool was apparently captured.

Run 15

After reviewing the available options, it was decided that the best way to proceed was to reenter the hole with a hard-formation tricone drilling assembly and attempt to grind away the ~2 m of hard fill presumably overlying the metal debris of the failed core bit. Once the hard fill was removed, the metal debris could be milled down or possibly recovered by the fishing magnet. Given the persistence of cobble-sized material near the bottom of the hole, indicated by the contents of the RCJB of Run 14, a new Smith 7JS tricone bit was picked up and fitted with 3X15 nozzles and affixed to a three-stand BHA with the goal of grinding up the remaining loose rock. The drilling assembly reentered Hole 1256D at 0730 h on 15 May 2011. Hard contact was made at 1518.8 mbsf. From 1415 h on 15 May until 0615 on 16 May the hole was washed and reamed from 1518.5 to 1521.1 mbsf and flushed with 460 bbl of high-viscosity mud sweeps. (Note: the precision of these depths is ±1 m, as high tides at Site 1256 precluded accurate determination of the bit depth.) The bit was tripped to the surface after 14.5 rotating hours to ascertain the condition of the bit and assess the progress. The bit cleared the seafloor at 1015 h and the rotary table at 1545 h on 16 May. The cones exhibited virtually no wear except for a chipped insert on the gauge cutter. The bearings were tight with some apparent shirttail wear and minor junk damage present on the bit body (Fig. F19Y). These were characteristics of a bit that had done very little actual drilling. When the bit diameter was measured, it was found to be under gauge

by 7/16 inches (Fig. **F19W**). Apparently the bit had been literally squeezed into a smaller diameter hole (<10 inches in diameter). The conclusion was that the bottom ~3 m of the hole was considerably undersized and would have to be reamed to full gauge before fishing could resume. One of the EXJBs was significantly damaged (Fig. **F19X**).

Run 16

The sixth tricone bit used during the expedition was selected based less on cutting structure and more on the amount of armor on the legs, because that would be the area that would receive most of the wear during reaming. A Smith FH3VPS 9⅞ inch tricone was made up to a three-stand BHA without external junk baskets. The bit reentered Hole 1256D for the sixteenth time of the expedition at 0245 h on 17 May 2011. By 0815 h, washing and reaming operations began. The undergauge section of the hole ranging from 1516.5 to 1519.7 mbsf was reamed for 15 rotating hours and flushed with a total of 260 bbl of high-viscosity sepiolite sweeps. The bit was pulled clear of the seafloor at 0340 h on 18 May and recovered at 0900 h. The tricone bit was found to be in gauge. Although the tricone was missing six teeth on the middle row of one cone, it was in reasonably good condition (Fig. **F19Z, F19AA**). The missing teeth suggested that cone contact might have been made with debris at the bottom of the hole. During the reaming, care was taken to avoid penetrating below 1520 mbsf to prevent metal to metal contact with the RCB bit wreckage and avoid potentially leaving more junk in the hole.

Run 17

Once the reaming was concluded, a flat-bottomed 9⅝ inch mill was made up to the three-stand BHA with a bit sub junk basket (BSJB) and deployed. The mill entered Hole 1256D at 1850 h on 18 May 2011 and initiated milling at 0130 h on 19 May. Shortly after reentering the cone for the seventeenth time during the expedition, the total length of drill pipe tripped during the cruise passed 100 miles. This milestone was acknowledged by a message of thanks to the Transocean teams from the Shipboard Science Party. Milling at a depth of ~1520–1521 mbsf progressed without incident until 1330 h. The driller frequently picked up the tool a little off bottom and decreased the pump pressure to let cuttings settle and be captured in the EXJB. This is referred to as "working the junk baskets." A total of 300 bbl of mud was circulated to flush the hole during milling. The mill cleared the seafloor at 1920 h on 19 May and was recovered by 0315 h the next morning. The trip out of the hole was suspended for 1.5 h for the sixth slipping and cutting of the drilling line. The abrasive hard surface on the face of the mill was completely worn away, and the diameter of

the tool was under gauge by 0.5 inches (Fig. F19BB). The BSJB was also found damaged (Fig. F19CC).

Run 18

The second milling tool run was made with a 9 inch flat-bottom mill (Fig. F19DD), which reentered the hole at 1415 h on 20 May 2011 for the eighteenth time. From 1945 h until 0145 h on 21 May the bottom of the hole was milled and the junk basket worked. Based on the excessive wear to the first milling tool, the rotating time for the second mill run was scaled down from 12 h to 6 h. A total of 320 bbl of sepiolite mud was circulated to keep the hole clean. The drill string was pulled free of the seafloor at 0645 h, and the second milling tool was secured on deck at 1225 h on 21 May. The milling surface was abraded clean, and some minor junk damage was noted on the side of the mill (Fig. F19FF). There was also a 3 inch, 200° circumferential grove cut into the crossover sub located just above the mill. The BSJB was unloaded and found damaged (Fig. F19EE). It contained the usual small cuttings and gravel with some small fresh cuttings of metal. This was the first suggestion that we had finally started to mill bit debris.

Run 19

The next fishing attempt was made with the third deployment of the RCJB (Fig. F19GG), together with two EXJBs and one BSJB (Fig. F19HH). This assembly reentered Hole 1256D at 2230 h, on Run 19 of the expedition. The tool was run to ~3 m off bottom and the junk baskets worked for ~10 min with pump strokes as high as 150 spm and standpipe pressure reaching 1850 psi. Following a 100 bbl mud flush, the RCJB was worked to the bottom (~1521 mbsf) with minimum rotation and very light weight on bit. The string was pulled out of the hole, clearing the seafloor at 1015 h and the rotary table at 1645 h on 22 May 2011. The RCJB was filled with congealed sepiolite in which were four large rocks with a total weight of 8.9 kg (Fig. F19II). The largest sample weighed 3.9 kg. The external junk baskets contained fine cuttings, small pebbles, and a few tiny metal fragments.

Run 20

The RCJB was rebuilt and deployed for the fourth time of the expedition along with the three junk baskets and reentered Hole 1256D at 0635 h on 23 May 2011 for the twentieth time on this expedition. The trip in was extended for 3 h while the drill crew repaired the pneumatic control lines for the high clutch in the drawworks. Following the routine of working the junk baskets and flushing the hole with 100 bbl of

sepiolite mud, the RCJB was activated and advanced to the bottom of the hole at ~1521 mbsf. The RCJB assembly was pulled free of the seafloor at 1725 h on 23 May and recovered on deck by 0215 h on 24 May. The RCJB (Fig. **F19JJ**) contained three rocks with a total weight of 5.0 kg. The angularity of the rocks indicated that they were freshly deposited with a suspected origin somewhere in the bottommost 7 m of the hole. One rock (1.4 kg) was a gabbro, suggesting that the "promised land" might be tantalizingly close. The junk basket contained the usual suspects, ranging from gravel-sized cuttings to small pebbles with a few metal filings distributed throughout.

Run 21

The fifth and last RCJB run of the expedition was deployed with the three junk baskets at 0545 h on 24 May 2011. The tool entered the reentry cone at 1115 h for the twenty-first reentry of the expedition. After working the junk baskets and circulating 100 bbl of sepiolite mud, the RCJB was activated and succeeded in reaching the bottom of the hole at ~1521 mbsf. The RCJB was retracted at 1845 h and the bottom of the hole displaced with 200 bbl of drill water for logging purposes. The RCJB cleared the seafloor at 0100 h following a 1 h interruption to replace a damaged cam roller on the dual elevator handling system. The drill string was recovered at 0700 h on 25 May. The junk baskets contained the usual collection of fine cuttings and small gravel. The RCJB contained four small rocks. The trend of the progressively smaller-sized rocks and lighter yield for each succeeding run of the RCJB indicated that the rubble pile at the bottom of the hole had been successfully removed. However, the lack of significant metal in all junk basket runs was perplexing. It was decided to delay the start of the logging program and attempt to recover any metal debris at the bottom using the fishing magnet.

Run 22

The 9 inch Bowen fishing magnet was made up along with two EXJBs and one BSJB and deployed. The fishing assembly entered Hole 1256D at 1645 h on 25 May 2011. After working the junk baskets and fishing magnet at the bottom of the hole for 30 min, another 200 bbl of drill water was pumped into the bottom of the hole. The routine 100 bbl mud sweep was omitted to save time. The fishing magnet cleared the seafloor at 0230 h on 26 May and was on deck at 0900 h. The junk baskets contained the routine assorted samples of cuttings and pebbles. The magnet contained only small filings and minor amount of metal (Fig. **F19KK**).

Logging (26–28 May)

Run 23

A lightweight logging assembly was made up comprising a 9½ inch logging bit, a landing saver sub, a controlled length drill collar, a tapered drill collar, five transition joints of 5½ inch drill pipe, and a crossover sub. The logging assembly entered the cone at 1725 h on 26 May 2011 for the twenty-third reentry of the expedition. The bit was placed at a depth of 218.9 mbsf.

The first log was the triple combo (natural gamma ray logging tool [GR]/Accelerator Porosity Sonde [APS]/Hostile Environment Litho-Density Sonde [HLDS]/High-Resolution Laterolog Array [HRLA]/GPIT), which was deployed into the pipe at 2255 h and recovered at 0700 h on 27 May. The tool successfully reached the bottom of the hole, although the caliper did not open until ~1490 mbsf. The bottom of the hole, not logged during Expedition 312, was logged using standard procedures up to ~1300 mbsf. A caliper log for the rest of the hole right up into the rat hole was measured to assist planning of cementing operations at the end of the cruise. The triple combo tool returned with three damaged bowsprings on the upper centralizer (Fig. **F19LL**), and these were replaced in preparation for the second scheduled logging run with the FMS-sonic tool.

The FMS-sonic tool string was initially deployed into the pipe at 1050 h but had to be retrieved at 1410 h when it was unable to exit the BHA into the borehole because of some mechanical obstruction at the bit. Once on the surface, one damaged bowspring of the lower centralizer was replaced in preparation for the second run. The FMS-sonic was redeployed at 1500 h and again experienced difficulty exiting the BHA. On this occasion the tool became irretrievably stuck while partially outside the pipe (Fig. **F19MM**). The Kinley crimping and cutting tool had to be utilized to sever the logging cable. The loose end of the logging cable was recovered at 0330 h and secured. The BHA with ~20 m of logging tool extending below the logging bit was carefully withdrawn from the reentry cone at 0425 h.

Coring and Cementing (28–30 May)

Run 24

After the BHA was recovered and the FMS-sonic centralizer extracted from the landing saver sub (Fig. **F19MM**), a three-stand RCB coring assembly was made up with a new Ulterra 9⅞ inch RCB bit (Fig. **F19NN**). The last activity of the expedition was to run

in with the RCB assembly and deposit cement plugs at the bottom of the hole and from 910 to 940 mbsf. Before pumping the cement, it was decided to core the bottom of the hole until the core bit debris left on 6 May stopped progress or the little time remaining expired, whichever came first.

The RCB assembly entered the reentry cone for the twenty-fourth time of the expedition at 2225 h on 28 May 2011. A fresh core barrel was deployed at 0515 h on 29 May, and by 0545 h coring resumed in Hole 1256D. The core barrel was recovered after advancing from 1520.2 to 1521.6 mbsf. The nominal recovery for the 1.4 m advance was 0.5 m (36%) and consisted of 10 large pebbles (Core 335-1256D-239R) (Table **T4**). The average ROP was 0.6 m/h. The total average recovery for the 14.5 m of coring during this expedition was 11%. There was no metal in the core barrel or signs of junk in the coring process. This, together with the absence of significant metal debris recovered by the fishing magnet during Run 22, was taken as an indication that metal debris had possibly been mostly ground during Run 9, shortly after the failure of the C9 coring bit, and that the hole is now likely clean of significant metal junk.

Time for coring had expired, and cementing operations began at noon. The first cement plug was emplaced at 1521 mbsf (15 bbl), and the second plug was placed from ~940 to 910 mbsf (60 bbl). These plugs will help stabilize the two problem regions in the hole and facilitate return to the bottom of the hole and coring on a future return to Hole 1256D. The C-9 bit used for the last run of Expedition 335 returned to the rig floor in relatively good condition and nearly in gauge (Fig. **F19OO**). A few teeth were missing (Fig. **F19PP**), the shirttails were worn, with abrasion marks (Fig. **F19QQ**), much smaller than those caused by metal junk observed during Expedition 312 (Fig. **F19RR**).

Observations of highly out-of-gauge interval (920–960 mbsf)

This section summarizes geological and wireline knowledge regarding the problematic region between 920 and 960 mbsf in Hole 1256D that impeded the progress of the drill string to the full depth of the hole on both Expeditions 312 and 335. It seems prudent to collate geological and engineering information on this trouble spot to inform future drilling operations in Hole 1256D. Figure **F20** summarizes the stratigraphy of Hole 1256D following operations during Leg 206 and Expedition 309/312. Attention is drawn to the caliper log for the hole. Throughout the lava sequences, the hole diameter is strongly out of gauge between 25 and 50 cm (10 and 20 inches) diameter, reflecting the fractured nature of the formation and continued erosion result-

ing from numerous pipe trips through the lava horizons. Although there is an out-of-gauge interval at the bottom of the transition zone (from 1050 to 1060 mbsf), as of the end of Expedition 312 the hole through the sheeted dike and uppermost plutonic complexes is close to expected gauge. The changing caliper of the borehole is well illustrated in Figure **F21**, which shows the deviation of Hole 1256D (~60 m due west at 1400 mbsf). The large caliper of the hole at the bottom of the lava sequences is clearly visible. Figure **F22** presents the series of caliper logs from 900 to 1000 mbsf successively recorded during Expeditions 309/312 and 335.

Hole blockages were encountered in Hole 1256D in the interval from ~920 to 960 mbsf during the initial reentries during both Expeditions 312 and 335, which prevented the transit of the drill string to the bottom of the hole. Difficult hole conditions were not expected during Expedition 312, which occurred only 2 months after the successful deepening of Hole 1256D to 1257 mbsf during Expedition 309. On reentering Hole 1256D, the drill string advanced without incident until resistance at 927 mbsf prevented further progress. Approximately 5 days of Expedition 312 were spent reaming and cleaning the interval from 927 to 1051 mbsf, with the region of the hole from 927 to 944 mbsf being very tight and receiving the most attention.

The initial reentry into Hole 1256D during Expedition 335 was impeded by an obstruction at ~922 mbsf. A total of 15 days were then spent clearing this obstruction, stabilizing the zone from 910 to 960 mbsf, and cleaning and reaming the hole to its full depth (1507 mbsf at the end of Expedition 312).

Expedition 309 coring operations for the interval from 900 to 980 mbsf

Coring operations between ~897 and 980 mbsf (Cores 309-1256D-97R through 111R) are briefly reviewed herein. The interval from 897.8 to 958.8 mbsf (4543.2 to 4604.2 mbrf) was drilled without incident during Expedition 309, with moderate recovery (24.3%) and a ROP of 1.15 m/h (RCB Bit 3) (Fig. **F23**). Before coring commenced with the next bit, a bottom seawater sample was taken with the WSTP. The hole was then reentered and reamed from 868.6 mbsf (4514 mbrf) to the bottom, clearing ~4 m of fill at the bottom of the hole. Coring continued without incident to 974.4 mbsf with a ROP of 1.14 m/h and good recovery (46.7%) (4619.8 mbrf), until a drop in standpipe pressure following the retrieval of Cores 309-1256D-110R and 111R alerted the drillers to major damage of the bit sub (see the Operations section in Expedition 309/312 Scientists, 2006). The only operational irregularities apparent in the coring of this interval during Expedition 309 was that two cores (309-1256D-101R and 102R) were cored as 9 m advances as opposed to ~4.8 m half-cores that had been the standard

advance since Core 309-1256D-90R. However, these longer advances were not drilled at high rates of recovery as might have occurred if these increased advances had encountered softer formations (e.g., hyaloclastite, flow-top breccia).

The rocks recovered in this interval are predominantly aphyric microcrystalline to fine-grained basalt sheet and massive flows (Fig. **F23**). Rare volcanic glass, chilled margins, breccia, and altered hyaloclastite were recovered. The lavas are only slightly altered, but there are very common 0.1 to 1 mm saponite ± pyrite veins with minor silica and chalcopyrite and rare celadonite, iron oxyhydroxides, and carbonate. Saponite veins are commonly flanked by <5 mm black halos and rarely by green-gray or brown halos. These observations are consistent with a fractured and potential fragile formation. However, the rocks recovered are not especially different from any other parts of the lava sequences. A possible interpretation of the problems encountered in this area at the beginning of Expedition 335, tentatively sketched in Figure **F24,** is that a slab of a massive lava flow surrounded by more fractured intervals detached and partially obstructed the hole, wedging the BHA against the wall. This situation would explain the strong overpull required to free the pipe when it got stuck in this interval (Table **T3**).

Wireline geophysical logs clearly identify this interval between 920 and 960 mbsf, which exhibits out-of-gauge caliper and low resistivity. Temperature measured by wireline following the conclusion of drilling operations during Expeditions 309/312 and 335 display clear negative excursions (Figs. **F11, F23**). This suggests that, within this zone, the incursion of cold drilling fluid occurs during coring and cleaning operations, and this incursion inhibits the recovery of this section back to thermal equilibrium following the conclusion of drill fluid pumping.

Principal results

Hole opening, remediation operations, and the comprehensive destruction of a C-9 hard formation coring bit resulted in a major loss of time from the coring and wireline activities planned for Expedition 335. Coring during this expedition deepened Hole 1256D only modestly, from 1507.1 to 1521.6 mbsf (Cores 335-1256D-235R through 239R), at low rates of penetration (0.9 m/h) and recovery (11%) (Table **T2;** Fig. **F25**). However, the availability of the Expedition 312 archive- and working-half sections from the lowermost granoblastic dikes and the plutonic section of Hole 1256D (Table **T5;** Fig. **F26**) allowed the detailed redescription of these cores and some discrete sam-

ple measurements during the extended first phase of hole cleaning. Further fishing and hole cleaning operations at the bottom of Hole 1256D, particularly those runs that deployed the RCJB (Runs 12, 13, 19, 20, and 21) (Table T3) brought back a unique collection of large cobbles (as heavy as 4.5 kg; e.g., 335-1256D-Run 12-RCJB-Rock-A), angular rubble, and fine cuttings of principally strongly to completely recrystallized granoblastic basalt with minor gabbroic rocks and evolved plutonic rocks (Table T6). The large blocks exhibit intrusive structural and textural relationships and overprinting and crosscutting hydrothermal alteration and metamorphic paragenetic sequences that hitherto have not been observed because of the one-dimensional nature of drill cores and the very low rates of recovery (<7%) of the granoblastic dikes during Expedition 312. Some of the rubble and ~30% of the fine cuttings recovered by fishing and cleaning operations clearly came from the lava sequences at the top of the hole on the basis of igneous textures and low-temperature alteration minerals (Mg saponite and amorphous silica). These rocks will not be described further. In contrast, the high extent of metamorphic recrystallization exhibited by the granoblastic basalts, along with operational factors (e.g., pipe movements), provide strong evidence that the granoblastic basalt, minor gabbros, and evolved plutonic rocks were sourced from the lowermost reaches of Hole 1256D (1494.9–1521.6 mbsf), most probably from below Gabbro 2. Hence, the rocks recovered during Expedition 335 represent a ~15 m interval of the upper crust–lower crust transition, occurring below the ~90 m section, recovered during Expedition 312, of two gabbroic bodies (Gabbro 1 and Gabbro 2) separated by Dike screen 1.

Igneous petrology

The interval sampled during Expedition 335 comprises predominantly fine-grained granoblastic aphyric basalt. Although all samples have granoblastic textures (Fig. F27), indicative of high-temperature metamorphism, the degree of recrystallization varies, with strongly recrystallized rocks dominant over completely recrystallized rocks. Some samples preserve dike/dike contacts, and many preserve cores of former plagioclase (micro)phenocrysts (Fig. F27), indicating that the granoblastic rocks represent a metamorphosed sheeted dike complex. This interval has been designated Dike screen 2 (Fig. F28).

Approximately half of the granoblastic basalts contain small, irregular patches (<5 cm × 3 cm), veins (~1–2 mm wide), and dikelets (<1.5 cm wide) of evolved plutonic rocks (oxide gabbro, diorite, and tonalite) (Fig. F29A, F29B). The veins are observed to be offshoots of the igneous patches, and diffuse patches are issued from the dikelets.

These two observations indicate that the igneous veins, dikelets, and patches form part of the same network, marking a single generation of intrusion of melts into the granoblastic basalts. Their magmatic textures (subhedral to euhedral shapes of several phases, along with poikilitic textures) contrast strongly with the granoblastic textures of the host rocks, demonstrating that intrusion occurred after the granoblastic recrystallization of the host rock. The ubiquitous occurrence of primary magmatic amphibole in the veins and patches suggests high water activities during their formation. Moreover, the presence of quartz, as well as accessory apatite and zircon, implies that the patches, veins, and dikelets crystallized from highly evolved melts.

A small number of gabbroic rocks was recovered (Fig. **F29C**); the rocks range in composition from disseminated oxide gabbro to orthopyroxene-bearing olivine gabbro. Expedition 335 gabbroic rocks have a more "salt and pepper," equigranular appearance and less textural variability compared to the gabbroic rocks recovered during Expedition 312 (Fig. **F19C**). Hence, although the contact relationships with the granoblastic basalts were not recovered, it is likely that at least some of the gabbroic rocks occur intercalated with the granoblastic basalt, perhaps forming small intrusions.

Overall, a picture emerges of a section of metamorphosed, granoblastic sheeted dikes that underwent small-scale intrusion by both gabbroic and evolved plutonic rocks (Fig. **F30**).

Geochemistry

Only a limited number of whole-rock geochemical analyses were undertaken during Expedition 335 (Fig. **F31**). Major and trace element and volatile concentrations were determined on three granoblastic basalts from Cores 335-1256D-235R through 238R, on one basalt lava, and on five granoblastic basalt and two gabbroic rocks recovered during junk basket runs. These samples were chosen from the least altered parts of the core and rock samples and as far as possible from hydrothermal veins and magmatic intrusions to obtain the best estimate of primary compositions.

The basalt and granoblastic dikes have mid-ocean-ridge basalt (N-MORB) compositions similar to that of the variably altered basaltic lavas, dikes, and granoblastic dikes cored in the overlying crust in Hole 1256D (e.g., Teagle, Alt, Umino, Miyashita, Banerjee, Wilson, et al., 2006). The two gabbros (olivine gabbronorite and olivine gabbro) have high loss on ignition (LOI) (~1.5–2 wt%), consistent with those samples

being more affected by hydrothermal alteration processes than the neighboring granoblastic basalts. The gabbros are also quite distinct from the granoblastic dikes with respect to major and trace element concentrations. Expedition 335 gabbro compositions are typical of gabbroic cumulate suites sampled in oceanic environments but are also similar to those of the less evolved members of Gabbro 1 previously sampled in Hole 1256D. However, they are more primitive than any analysis from the lower Gabbro 2. Expedition 335 gabbroic rocks have relatively high MgO (~12 wt%) and Ni (~300 ppm) concentrations but low concentrations of incompatible trace elements compared to granoblastic dikes (Fig. **F31**). The relatively high Mg# (70–72) and Ni concentrations of the Expedition 335 gabbros principally reflect their modal olivine contents.

One characteristic of the granoblastic basalts sampled during Expedition 335 is relatively low concentrations of Cu, Zn, Zr, and Y compared to previously sampled basaltic samples in Hole 1256D (Fig. **F31**). Compared to all granoblastic and sheeted dike analyses, the Expedition 335 granoblastic basalt yields the most depleted compositions for these elements.

The lower part of Hole 1256D, below 1340 mbsf, is characterized by strong chemical variations, with Mg# ranging from 42 to 72 and Zr from 23 to 117 ppm. These changes in composition mainly reflect the changes in rock types from the low Mg#, trace element–rich sheeted dikes and granoblastic dikes to the higher Mg# and trace element–depleted gabbroic rocks of Gabbro 1 and Gabbro 2. There is a general downhole trend of decreasing incompatible element (e.g., Zr and Y) contents in the granoblastic dikes (Fig. **F31**). At a more localized scale, the granoblastic basalt sampled within Dike screen 1 and below Gabbro 2 in Dike screen 2 defines trends of increasing Zr with depth. The lowest Zr values occur directly at the upper interface between the granoblastic basalt and the overlying gabbroic intrusion. This pattern is particularly marked at the bottom of Hole 1256D, where the most trace element–poor granoblastic basalt of Hole 1256D was sampled at 1502 mbsf, just below Gabbro 2 (Yamazaki et al., 2009). Expedition 335 samples show a near doubling of Zr contents from ~30 ppm at 1507–1512 mbsf to 58 ppm at 1518 mbsf. These downhole variations in incompatible element contents are mimicked by changes in Zr/Y, with granoblastic basalt from directly below Gabbro 2 having low Zr/Y (~1.5) compared to the sheeted dikes and granoblastic dikes above Gabbro 1 (2–3). We interpret the systematic depletion observed in the granoblastic basalt just below both Gabbro 1 and Gabbro 2 as indicative of small degrees of partial melting, probably caused by gabbroic intrusions into the partially hydrated dikes (e.g., Miyashita et al., 2007; Koepke et al., 2007, 2008). The

degree of partial melting is probably minor, as the effects on dike major element compositions are undetectable. We also observe a general decrease in Cu and Zn contents in the granoblastic basalt sampled at the bottom of Hole 1256D, consistent with mobilization of Cu and Zn by high-temperature hydrothermal alteration (>400°C). At the bottom of Hole 1256D, low base metal concentrations appear to be a signature of only the granoblastic basalt. This may imply that the intrusion of Gabbro 1 and Gabbro 2 occurred after this stage of high-temperature hydrothermal alteration, consistent with the remelting process suggested by downhole Zr/Y variations.

All granoblastic basalt recovered during Expedition 335 has trace element compositions similar to the granoblastic rocks cored directly below Gabbro 2 during Expedition 312 (>1500 mbsf). This is further strong evidence that Expedition 335 granoblastic basalt comes from the lowermost levels of Hole 1256D, probably below 1494 mbsf.

Alteration and metamorphism

Rocks recovered during Expedition 335 are mainly dark gray, fine-grained basalt that was recrystallized by contact metamorphism. They are essentially identical to the granoblastic basalt from Dike screen 1 between Gabbro 1 and Gabbro 2 cored during Expedition 312. Coarser grained plutonic material occurs as separate rock fragments or as 1 mm to 1 cm sized dikelets and veins, as well as irregular intrusions into the dike rocks.

Dike screen 2 basalt is recrystallized to granoblastic assemblages of clinopyroxene, orthopyroxene, plagioclase, magnetite, ilmenite, and rare brown hornblende and quartz, with accessory sulfide minerals (pyrrhotite, chalcopyrite, and pyrite) (Fig. **F32**). Veins of granoblastic orthopyroxene ± plagioclase ± clinopyroxene, 100–200 µm wide, are common and are likely recrystallization products of hydrothermal vein protoliths. Dike samples include a chilled intrusive dike contact and a brecciated intrusive dike margin that were hydrothermally altered and then recrystallized to granoblastic assemblages during contact metamorphism.

The granoblastic rocks typically exhibit at most only slight postcontact-metamorphism hydrothermal alteration (generally <15%), mainly to amphibole. Clinopyroxene is locally partly altered to amphibole, orthopyroxene is variably altered to amphibole and local talc and smectite, and plagioclase is locally slightly altered to

trace chlorite, actinolite, secondary plagioclase, and smectite. Fe-Ti oxides are partly altered to titanite.

The dikes are cut by common 0.1–0.5 mm thick amphibole veins, with ~1–3 mm wide amphibole-rich alteration halos. These veins cut across the intrusive dike contact, granoblastic veins, and coarser grained igneous intrusive rocks. Also present are rare later veins containing actinolite, chlorite, quartz, epidote, and prehnite.

Coarser grained rocks (olivine gabbronorite, oxide gabbro, and quartz diorite) are more highly altered, with clinopyroxene highly altered to amphibole + fine magnetite and plagioclase partly altered to secondary plagioclase, amphibole, minor chlorite, and local epidote. Olivine exhibits coronitic alteration to amphibole, talc, magnetite, pyrrhotite, smectite, and rare iron oxyhydroxides. The intruded granoblastic host rocks are commonly highly altered to amphibole for as much as 1 cm around the intrusions. These observations are consistent with evidence from Expedition 312 that these intrusive boundaries are zones of enhanced fluid flow and fluid-rock exchange.

The cores and rocks recovered during Expedition 335 sample the transition from sheeted dikes to the gabbroic section of oceanic crust. The dikes underwent hydrothermal alteration in a mid-ocean-ridge hydrothermal system at the spreading axis. The altered dikes were then intruded by the two gabbro bodies cored during Expedition 312 and other magmatic bodies near the bottom of the hole and underwent contact metamorphism at temperatures of ~900°–1000°C. The effects of prior hydrothermal alteration influenced the degree of recrystallization. Cooling and fracturing allowed further penetration of fluids and hydrothermal alteration of these rocks, with formation of amphibole veins and later retrograde minerals (actinolite, quartz, epidote, chlorite, prehnite, and late smectite and iron oxyhydroxides).

The granoblastic dikes and underlying dike screens represent the conductive boundary layer between mafic magma and the overlying hydrothermal system, and the rocks from Hole 1256D are similar to those observed in ophiolites and elsewhere in oceanic crust (e.g., Gillis and Roberts, 1999; Gillis, 2008; France et al., 2009). The granoblastic basalt sampled beneath Gabbro 2 during Expedition 335 is part of a dike screen within the transition from sheeted dikes to gabbros, consistent with the presence of a significant underlying gabbro heat source.

Structural geology

Cores from the plutonic section drilled during Expedition 312 and cores, cuttings, and cobbles recovered during Expedition 335 contain important crosscutting relationships that illustrate the intimate interplay between magmatic, metamorphic, fluid flow, and brittle deformation processes. Unfortunately, because of the lack of oriented pieces, many structural investigations could not be completed.

Several vertically oriented Expedition 312 core pieces were tentatively azimuthally reoriented based on paleomagnetic data assuming normal polarity, although this remains to be definitively demonstrated. The reoriented azimuth of the upper contact between the granoblastic dikes and Gabbro 1 and between Dike screen 1 and Gabbro 2 were (dip/dip direction) 42°/260 and 81°/255, respectively. The orientations of the preserved contacts suggest that the gabbro intrusions dip at moderate to steep angles to the west-southwest, toward the paleospreading ridge. Veins from Expedition 312 cores show a bimodal orientation distribution, with a steeply dipping maximum (60°) and a second shallowly dipping maximum (10°). Using the same reorientation technique as for the contacts, all veins dominantly strike northwest–southeast.

A variable fracture density of subhorizontal irregular fractures is thought to be drilling-induced fractures. The boundaries between gabbros and granoblastic basalts have higher fracture densities.

Gabbroic rocks from the gabbro 1 interval are mineralogically and texturally heterogeneous and commonly display lighter color, leucocratic patches that result from a multistage magmatic history, with the percolation of more evolved melt through a partially crystallized gabbroic mush (Teagle, Alt, Umino, Miyashita, Banerjee, Wilson, et al., 2006). The two-dimensional distribution of these leucocratic patches was quantified using an image analysis technique on high-resolution photographs of the archive halves cut face. The shape-preferred orientation of the patches is very weak, and there is no obvious downhole trend. The image analysis also provides an accurate estimate of the modal distribution of the leucocratic patches, which shows some systematic trends downhole, correlated to distinct trends in magnetic susceptibilities, and revealing three possible distinct petrological units. These three zones are characterized by a broad upward increase in percentage of leucocratic patches and are delimited by limits that correspond to unit boundaries defined during Expedition 312 (85/86A) and Expedition 335 (89A/89C).

Paleomagnetism

Paleomagnetic analyses during Expedition 335 focused predominantly on a detailed investigation of samples from Gabbro 1 and Gabbro 2 because of the lack of oriented core recovered during Expedition 335. New data from shipboard thermal demagnetization experiments on discrete samples prepared during the expedition were augmented by unpublished shore-based data from the interval 1406–1503 mbsf that were analyzed by shipboard paleomagnetists. In addition, new data on the anisotropy of magnetic susceptibility (AMS) were acquired and reoriented using remanence data.

Samples are dominated by a steep, near-vertical drilling-induced remanent magnetization (DIRM) that represents an average of 66% of the total remanence (Fig. **F33**). Following removal of the DIRM by low–intermediate demagnetization treatments, shallow to moderate inclination components are typically isolated above 35 mT or 540°C and are considered to represent the characteristic remanent magnetization (ChRM) of the samples. The mean inclination of these components is 31°, significantly steeper than that expected for the paleoposition of Site 1256, which restores to an equatorial paleolatitude in the Miocene (Wilson, Teagle, Acton, et al., 2003). Potential causes of this apparent steepening of inclinations include the following:

1. Contamination of ChRM components by a residual DIRM persisting to high demagnetization levels. This is, however, unlikely to account fully for the observed data because it would require near complete overlap of the coercivity/unblocking temperature spectra of grains carrying the DIRM and ChRM at high fields/temperatures, and DIRM is predominantly carried by multidomain magnetite (Allerton et al., 1995) with generally low coercivity and distributed unblocking temperatures.
2. A present-day field thermoviscous overprint. This is unlikely, given the low ambient temperatures in the section and the high unblocking temperature of ChRMs, and is discounted entirely by the presence of multicomponent remanences in some interval.
3. The presence of a persistent nondipole field at Site 1256D during the Miocene. Little is known about the geometry of the field in the Pacific at 15 Ma, but analysis of anomalous skewness of younger marine magnetic anomalies in the Galapagos region (Schneider, 1988) suggests that nondipole field components may account for at most a few degrees of inclination anomaly.
4. Tectonic tilting of the section. Tilting of ~10°–20° is compatible with the observed dip of dike margins in the sheeted dike section of Hole 1256D (Teagle, Alt,

Umino, Miyashita, Banerjee, Wilson, et al., 2006; Tominga et al., 2009) and may potentially account for ~10° of inclination steepening assuming a ridge-parallel rotation axis. Larger amounts of inclination change may be produced by rotation around nonridge-parallel axes but are difficult to reconcile with the tectonic setting of the section.

5. Deflection of remanence directions by a strong anisotropy of consistent orientation. This can result in ~10°–20° of inclination change (depending on the degree of anisotropy and its orientation relative to the remanence). It can only be quantified and assessed by analysis of the anisotropy of remanence (Potter, 2004), which will form a focus of postcruise research.

The new thermal demagnetization data reveal a previously unrecognized type of remanence structure in a sample from Gabbro 2. After removal of steep DIRM by low-temperature (liquid nitrogen) demagnetization, two well-defined intermediate and high unblocking temperature components with antipodal directions are identified (Fig. **F33**). These data represent the first multipolarity remanences seen in lower crustal rocks formed at the EPR and are similar to examples reported recently from sites along the Mid-Atlantic Ridge (Meurer and Gee, 2002; Morris et al., 2009). Sampling of the gabbroic section conducted during Expedition 335 for further shore-based analyses of these multipolarity remanences will allow their distribution and significance to be determined, potentially leading to new information on the thermal evolution of the section.

AMS tensors from discrete samples from Gabbro 1 and Gabbro 2 are shown to be randomly oriented in the core reference frame (Fig. **F34**). In the absence of independent reorientation of core pieces via analysis of FMS imagery, a basic, first-order reorientation of these data is possible by applying vertical axis rotations to AMS data to align corresponding ChRM directions to present-day north. This results in a preferred north–south alignment of AMS maximum principal axes. This is particularly apparent in data from samples with prolate (lineated) AMS fabrics and may indicate that a significant along-axis preferred mineral alignment is frozen into the gabbro section. Similar ridge-parallel magnetic lineations have been reported from the slow spreading rate Troodos ophiolite (Abelson et al., 2001) and have been interpreted to indicate along-axis migration of melt. Further detailed postcruise analyses of AMS and other forms of magnetic anisotropy (e.g., anisotropy of anhysteretic remanence) should allow this hypothesis to be tested.

Physical properties

Physical property measurements during Expedition 335 revealed that the granoblastic basalt samples generally have high magnetic susceptibility (~6200 × 10^{-5} SI on average) (Fig. **F35**), whereas gabbroic rocks have lower average magnetic susceptibility (~3000 × 10^{-5} SI) but display much larger variation. In the gabbro units, magnetic susceptibility and color reflectance data follow variations in oxide and olivine content. Natural gamma radiation shows peaks that coincide with occurrence of evolved plutonic rocks consistent with relatively high concentrations of K, U, Th, and other incompatible elements in these rocks.

A measuring technique using a seawater bath was developed that greatly improved the quality of shipboard *P*-wave velocity measurements of discrete samples. The velocities of gabbro range from 6298 to 6759 m/s, whereas measurements of granoblastic basalt range from 6610 to 6907 m/s. These relatively high velocities are consistent with the trends of downhole geophysical logs above 1400 mbsf and may indicate that the lower section of Hole 1256D is close to the seismic Layer 2/3 boundary (Fig. **F36**).

Downhole logging

Because of technical troubles, the triple combo was the only logging tool string deployed during Expedition 335. It recorded the density, porosity, gamma ray emission, and resistivity of the formation, as well as the temperature of the borehole fluid over the entire hole, reaching the maximum depth of 1520 mbsf, 80 m below the deepest logs recorded at the end of Expedition 312. In addition to measuring the properties of the gabbros and dike screens at the bottom of the hole, one of the objectives of the logging program was to record a full caliper log over the entire hole to assess the results of the previous cementing operations (Figs. **F22, F23**), to help plan the end-of-expedition cementing operations to stabilize Hole 1256D for future expeditions, and to provide information for potentially casing the uppermost part of Hole 1256D.

Logging results

The hole size (Fig. **F37**) shows that the bottom was significantly enlarged after several weeks of junk basket runs dedicated to cleaning the hole. The hole is irregular below ~1410 mbsf, and the low density and high porosity readings below this depth are a direct consequence of the hole size. The decoupling between the shallow and resistivity logs is also a consequence of the hole size. However, the deepest resistivity measurement should not be affected by hole size and indicates a decrease in resistivity

with depth starting below Gabbro 1 (~1460 mbsf) that becomes more apparent by Gabbro 2. In contrast with the increase with depth expected in the plutonic section, this suggests that the deepest section might be fractured, possibly part of a fault, which could explain some of the difficulties encountered while coring.

Hole size

Higher up in the hole, hole cleaning and cementing operations around ~920 mbsf considerably changed the shape of the hole (Fig. **F38**). Although the several days spent trying to pass this interval contributed to the enlargement above it, the cement reduced the hole size and its roughness below. Between 930 and 970 mbsf the hole is large but without asperities and should not present any difficulty for future reentries, as shown by the 15 smooth reentries following the cementing operation during Run 8.

Temperature logs

Comparison between the temperature logs recorded by the two temperature tools during Expedition 335 and the temperatures measured during previous expeditions in Hole 1256D (Fig. **F39**) shows similar trends as the borehole fluid recovers from the disturbance of the drilling operations. Several excursions to lower temperatures, in particular around 925 mbsf and 1060 mbsf, coincide with intervals with lower resistivity, indicating more permeable intervals where the formation might have been invaded by the drilling fluid and is consequently recovering more slowly from the drilling process. The kick at ~1300 mbsf that was also observed during Expedition 312 coincides with lower resistivity and is probably also associated with fluid exchange with the formation. These anomalies will be the object of numerical modeling, which in combination with other logs should provide estimates of the permeability in these intervals.

Conclusions

When the textural and contact relationships exhibited by the large rocks recovered from the junk baskets are placed in the geological context of the Hole 1256D stratigraphy, a vision emerges of a complex, dynamic thermal boundary layer zone. This region of the crust between the principally hydrothermal domain of the upper crust and the intrusive magmatic domain of the lower crust is one of evolving geological conditions. There is intimate coupling between temporally and spatially intercalated

magmatic, hydrothermal, partial melting, intrusive, metamorphic, and retrograde processes.

With only a minor depth advance in Hole 1256D, we have yet to recover samples of cumulate gabbros required to test models of ocean ridge magmatic accretion and the intensity of hydrothermal cooling at depth. Nor have we crossed the Layer 2/3 boundary at Site 1256. The total vertical thickness of granoblastic basalts is >114 m, and Dike screen 2 is now about the same thickness (so far) as Dike screen 1. High perched, isolated gabbro intrusions are uncommon in ophiolites. The energy requirements for the granoblastic recrystallization at granulite facies condition of a >114 m thick zone of sheeted dikes massively exceeds the thermal capacity of Gabbros 1 and 2 (e.g., Koepke et al., 2008; Coggon et al., 2008) if a simple subhorizontal arrangement of these layers is assumed. The enormous heat requirements for such extensive granulite facies recrystallization, the evidence for partial melting, together with the tantalizing presence of minor but not uncommon gabbroic rocks and felsic intrusive, dikelets, and veins, strongly indicates that the layer of purely plutonic rocks should be at most only a few tens of meters deeper in the hole.

Although the extensive remedial operations on Expedition 335 precluded significant deepening of Hole 1256D, significant progress was made in improving the borehole. The most problematic out-of-gauge zone at ~920–960 mbsf that caused reentry problems during Expeditions 312 and 335 has been stabilized with cement. The bottom of the hole has been cleared of rubble and junk, and there appears to be only a short, slightly undergauge zone (<1 m). Importantly, the regular, large sweeps of high-viscosity mud (as much as 200 bbl sepiolite, every ~2 h), have finally overcome and expunged the vast amount of fine cuttings recirculating in the hole, some most likely resident since Leg 206. This progress is shown by the absence of soft fill in the final ~5 reentries compared to >50 m of soft fill at the end of Expedition 312. The engineering efforts during Expedition 335 have repaired and prepared Hole 1256D for further deep drilling, following 5 years of neglect. Hole 1256D is 1500 m of hard rock coring closer to cumulate gabbros than any other options in intact ocean crust. It is once more poised to answer fundamental questions about the formation of new crust at fast-spreading mid-ocean ridges, best achieved by a timely return to the site.

Preliminary assessment

Preliminary scientific assessment

Expedition 335 was the fourth ocean cruise of the Superfast Spreading Crust campaign to drill a deep hole into intact oceanic basement and returned to Hole 1256D to deepen this scientific reference penetration a significant distance into cumulate gabbros. Cores and data recovered from the uppermost lower ocean crust and the transition down to cumulate gabbroic rocks would provide hitherto unavailable observations that will test models of the accretion and evolution of the oceanic crust.

Although previous cruises to Hole 1256D (Leg 206 and Expedition 309/312) had achieved the benchmark objective of reaching gabbro in intact ocean crust, critical scientific questions remain. These include the following:

1. Does the lower crust form by the recrystallization and subsidence of a high-level magma chamber (gabbro glacier) or crustal accretion by intrusion of sills throughout the lower crust or by some other mechanism?
2. Is the plutonic crust cooled by conduction or hydrothermal circulation?
3. What is the geological nature of Layer 3 and the Layer 2/3 boundary at Site 1256?
4. What is the magnetic contribution of the lower crust to marine magnetic anomalies?

At the end of Expedition 312 in 2005, Hole 1256D was clear to its full depth and poised to be deepened into intervals where samples that should conclusively address these questions can be obtained, possibly with only a few hundred meters of drilling.

Unfortunately, operational difficulties in Hole 1256D precluded progress toward the scientific objectives with only <15 m of advance achieved in Hole 1256D, and the hole now has a total depth of 1521.6 mbsf (1271.6 msb). The bottom of the hole remains hosted by the dike–gabbro transition zone, dominated by granoblastic basalt.

In addition to the few cores drilled, the junk baskets deployed during the successive fishing runs to the bottom of the hole recovered a unique collection of samples including large cobbles (as large as 5 kg), angular rubble, and fine cuttings of principally strongly to completely recrystallized granoblastic basalt with minor gabbroic rocks and evolved plutonic rocks. The large blocks exhibit structural and textural relationships, metamorphic paragenetic sequences, and overprinting hydrothermal altera-

tion, which hitherto have not been observed because of the narrow diameter of drill cores and the very low recovery of the granoblastic basalts cored so far.

Including the ~60 m thick zone of granoblastic dikes that reside above the uppermost gabbros, the dike–gabbro transition zone at Site 1256 is >170 m thick, of which >100 m is recrystallized granoblastic basalt. This zone records a dynamically evolving complex thermal boundary layer between the principally hydrothermal domain of the upper crust and the intrusive magmatic domain of the lower crust. An intimate coupling between temporally and spatially intercalated magmatic, hydrothermal, partial melting, intrusive, metamorphic, and retrograde processes is recorded in the samples recovered, which will be subjected to a comprehensive suite of postcruise petrologic, geochemical, and geophysical studies.

Expedition 335 left Hole 1256D after making only a very modest advance, and we have yet to recover samples of cumulate gabbros required to test models of ocean ridge magmatic accretion and the intensity of hydrothermal cooling at depth. However, the remarkable sample suite of granoblastic basalt samples, with minor gabbros intruding previously recrystallized dikes, provides a detailed picture of a rarely sampled critical interval of the oceanic crust. Most importantly, the hole has been stabilized, cleared to its full depth, and is ready for deepening in the near future.

The archive and working halves of Cores 312-1256D-202R through 234R (1372.8–1507.1 mbsf) from the lower part of the granoblastic dikes to the bottom of the hole at 1507.1 mbsf, including the plutonic section of Hole 1256D, were shipped to the *JOIDES Resolution* prior to Expedition 335. These cores were made available to the science party for the purpose of familiarization with the recovered plutonic section of Hole 1256D and to establish and test description protocols during transit to Site 1256. The scientists also developed the DESClogik configuration for the capture of plutonic rock descriptions for the first time since the introduction of the LIMS database. The long duration of operations required to open Hole 1256D to its full depth at the beginning of Expedition 335 (see **"Operations"**; ~16 days) provided sufficient time for the 335 Shipboard Science Party to completely redescribe these cores. This was considerably more time than was available to the shipboard scientists at the end of Expedition 312. Some discrete measurements (paleomagnetism and physical properties) were also performed.

A new measuring protocol using a seawater bath was developed onboard that greatly improved the quality of shipboard *P*-wave velocity measurements of discrete samples.

The velocities of gabbro range from 6298 to 6759 m/s, whereas measurements of granoblastic basalt range from 6610 to 6907 m/s, as much as ~800 m/s higher than measurements done under the standard shipboard protocols during Expedition 312 (that are often significantly lower than shore-based laboratory measurements). These high velocities are more consistent with the trends of downhole geophysical logs above 1400 mbsf and may indicate that the lower section of Hole 1256D is close to the seismic Layer 2/3 boundary.

The engineering efforts during Expedition 335 (see **"Preliminary operational assessment"**) have repaired and prepared Hole 1256D for further deep drilling, following 5 years of neglect. Hole 1256D is 1500 m of hard rock coring closer to cumulate gabbros than any other options in intact ocean crust. The already great thickness of granoblastically recrystallized dikes and the tantalizing presence of minor gabbro bodies strongly suggests that the zone of 100% plutonic rocks must be close, perhaps only a few tens of meters below the present bottom of the hole. Hole 1256D is once more poised to answer fundamental questions about the formation of new crust at fast spreading mid-ocean ridges, best achieved by a timely return to the site.

Preliminary operational assessment

The principal goal of Expedition 335's return to Hole 1256D was to deepen the hole sufficiently into plutonic rocks (a few hundred meters) to obtain definitive answers to long-standing questions about the structure and composition of the oceanic crust and about mechanisms of crustal accretion (these ideas are developed in greater detail in **"Background and geological setting"**).

Operational planning for Expedition 335 was informed by three principal sources:

1. The Operations teams' experiences during Leg 206 and Expedition 309/312 to Hole 1256D and previous deep basement coring by scientific ocean drilling;
2. Aspects of the IODP Operations Review Task Force Meeting "Expeditions 309/312 Superfast Spreading Rate Crust" (ORTF-309/312-03, June 2006); and
3. A USIO position paper, "Operational requirements for returning to Hole 1256D" (September 2006).

The recommendations of the Expedition 309/312 Review Task Force indicate an understanding of the nonstandard requirements of deep basement drilling and echo the suggestions made by the Co-Chief Scientists of those expeditions. Three recommendations pertinent to operations during Expedition 335 were

1. To investigate alternate scheduling strategies (e.g., at-sea crew changes, lengthening standard expedition durations to maximize on-site time for deep drilling objectives; ORTF-309/312-03),
2. To investigate and prioritize avenues for enhancing coring/drilling capability (particularly of hard formations) for deep-drilling programs (ORTF-309/312-11), and
3. To build on the experiences of Phase 1 expeditions and actively explore future applications of drilling muds (particularly those with heavy lifting capability) for riserless hole cleaning and stabilization (ORTF-309/312-12).

Unfortunately, there has been only modest progress on these recommendations in the 5 years since the ORTF-309/312 meeting, with a half-length expedition initially scheduled by the Science Advisory Structure for the return to Hole 1256D and an absence of new drilling and coring options for hard formations and hole cleaning.

The IODP Science Planning Committee requested in 2006 (SPC Consensus 0603-19) that the USIO identify the operational requirements for further drilling in Hole 1256D. TAMU engineers from the USIO presented their operational plan to an audience of scientists and independent drilling engineers at the Mission Moho Workshop (Portland, Oregon, 7–9 Sept 2006) for technical review. There was consensus support for the plan proposed.

The USIO considered four deepening scenarios:

1. Resume RCB coring in Hole 1256D using large-volume (100–150 bbl) high-viscosity mud sweeps combined with frequent bit trips,
2. Enlarge the hole to 18½ inches to isolate the out-of-gauge section using 13⅜ inch casing,
3. Forego 13⅜ inch casing and enlarge the hole to 14¾ inches to isolate the out-of-gauge section using 10¾ inch casing, and
4. Offset and start a new hole following the casing strategy employed during Leg 206.

Two key points were noted by the USIO and independent engineers at the Mission Moho Workshop:

1. Hole 1256D is in excellent condition, and remedial engineering operations such as reaming and casing are premature.

2. Neither the offshore industry nor scientific ocean drilling operators have ever attempted to open up an existing deep basement hole to any significant depth (hundreds of meters) in basalt and insert casing.

Regardless of the casing strategy proposed (2 or 3), attempting to open any portion of Hole 1256D to accommodate casing would require significant new hardware, numerous pipe trips, and extend over several expeditions. Such operations would require unproven technology and would be extremely challenging with substantial risk of irreparable damage to Hole 1256D without any further coring or recovery. The USIO and independent experts felt that approaches 2 and 3 are not viable options and recommended that they were not considered further.

The preferred USIO strategy was 1—resuming RCB coring with frequent large-volume high-viscosity mud sweeps (ORTF-309/312-12). During Expedition 309/312, large-volume mud sweeps were effective at clearing cuttings from the hole. However, because of the end of Phase I operations, mud stock depletion precluded the vigorous implementation of this approach throughout the whole of Expedition 312. The refitted *JOIDES Resolution* should be equipped to handle the necessary supplies to maintain an aggressive mud program. Following the recommendations of the IODP Expedition 309/312 Operations Review Task Force, the *JOIDES Resolution* was stocked with at least 60 T of sepiolite and attapulgite for use during Expedition 335.

Assuming reasonable hole conditions and an average rate of penetration comparable to previous coring in this hole, TAMU engineers estimated that this approach should deepen Hole 1256D ~350 m with 39 days on site (Teagle et al., 2010). The engineering and design lessons learned from a few hundred meters deeper penetration of intact ocean crust would be invaluable in planning and exploiting future deep penetration targets.

Further deepening of Hole 1256D using large mud sweeps was the only strategy that begins with coring, was the most likely to return samples from deeper in the hole, and had the largest possibility of building on the tremendous success of previous deepening operations on Expedition 309/312 that employed proven drilling techniques.

Before conditioning the hole for further deepening, an attempt would be made to acquire an equilibrium temperature profile and recover a water sample before the thermal structure of the crust is perturbed by cleaning and drilling operations (see next section). We would reenter the hole with a tricone drilling bit on a bit release and slowly descend past the zone around 900 mbsf that caused an obstruction during Ex-

pedition 312. If the hole was clear, we would withdraw the pipe, drop the bit, and reenter to below the rat hole to allow logging with the triple combo, including the MTT temperature probe. If the wireline conditions were suitably benign, we would attempt to take a borehole water sample from near the bottom of the hole using the WSTP.

Operations

Expedition 335 operations are described in **"Operations"** and summarized in Table **T7.** The complete record of drilling in Hole 1256D and other deep basement drill holes will be documented in the Expedition reports section of the Expedition 335 volume.

Four key issues with operations in Hole 1256D have been identified:

1. The bridge at ~922 mbsf,
2. Clearing cuttings from a deep uncased hole into oceanic basement,
3. Drilling and coring very hard formations, and
4. Logging.

The bridge at 922 mbsf

On the first reentry, a bridge was encountered at ~922 mbsf that required 16 days of operations and nine reentries, including three cementing runs. Details of our best impression of the blockage are in **"Operations"** (Fig. **F24**): an inclined massive formation (e.g., base of massive flow) that squeezed the drilling bits against the borehole wall, stopping effective cutting and clearing of the blockage. Cementing and redrilling the cement above the bridge brought the hole back into gauge, restricted the lateral movement of the bit and BHA, and improved the cutting effectiveness of the tricone bit, eventually clearing the bridge and rapidly displacing lose debris in the underlying 10 to 20 m.

Once opened and cemented, this interval did not present a problem for operations. It was stabilized with 65 bbl of 14.5 ppg cement at the end of Expedition 335 operations in Hole 1256D to stop further material falling into the hole or borehole wall inflow closing this interval. In hindsight, a similar operation should have been undertaken during Expedition 312, although this may have precluded reaching the benchmark achievement of coring gabbros in intact ocean crust.

Clearing cuttings from a deep uncased hole into oceanic basement

Hole 1256D is a >1520 m deep borehole with >1250 m in uncased basement strata. Approximately 800 m of the hole penetrates through fragile and unstable volcanic formations of mixed competencies. This has led to large intervals being strongly out of gauge, a situation exacerbated by a total number of 62 reentries and pipe trips up and down the hole. The 16 inch casing string only extends ~17 m into basement, below which is a ~7 m rathole ~23 inches in diameter. The long intervals of uncased hole and the wide rathole topped by a ~280 m section of 16 inch casing greatly reduces pumping efficiencies even when using high-viscosity muds. Expedition 335 operations cleared Hole 1256D of a large amount cuttings, some of which had probably been resident in the hole since drilling during Leg 206. At the end of Expedition 335, the hole was completely clear of cuttings, as evidenced by the near complete absence of soft fill (<1 m; compare with Expedition 312, with >60 m of soft fill) and a lack of mud and suspended cuttings in the reentry cone, indicating that cuttings were being successfully swept from the hole and out onto the surrounding sedimentary blanket. Improving the hydrodynamics of Hole 1256D to enable more efficient hole clearing would greatly improve the quality of coring activities.

Drilling and coring very hard formations

Contact metamorphosed granoblastic basalts were encountered during Expedition 312 and destroyed a C-7 RCB coring bit after only 21 h of rotation. Similar rocks, although with more completely developed granoblastic textures, were encountered and resulted in the absolute destruction and grinding to a smooth featureless stump of a C-9 hard formation RCB coring bit after a maximum of 29 h (coring evidence suggests the bit failed after only 15 h of rotation). This was the first failure of a C-9 RCB bit in ocean drilling. The fine-grained, annealed texture of the granoblastic basalts makes them extremely hard with few fractures. It appears that if the hole is not absolutely clear, the stresses on these bit are such that even the smallest defect will rapidly result in equipment loss. The Expedition 309/312 Co-Chief Scientists recommended the investigation of finding ultra-hard formation drilling and coring bits. Although this recommendation was discussed by the IODP-MI Review Task Force, no progress has been made in this area. Scientific ocean drilling needs a suite of highly armored (gauge-cutters, backreamers, hard surfacing, and thick armored shirttails) drilling and coring bits for opening holes and coring in these ultra-hard intervals that can be at least 100 m thick.

Logging

A complete suite of wireline logs of Hole 1256D would have yielded important scientific and operational results. Only the triple combo logging tool was run, and it managed to get to full depth. Geophysical logs would have possibly provided caliper data to the bottom of the hole (FMS and UBI devices are at the bottom of the wireline tool string), as well as imaging of the distribution, size, and orientation of plutonic intrusions into the granoblastic dikes. Unfortunately, the FMS-sonic was not successfully deployed because it would not exit the logging bit, despite two attempts, because the fitting of new centralizer bowsprings significantly increased the external diameter of the logging tool beyond that of the logging bit sub. This necessitated the severance of the logging wireline using the Kinley crimping and cutting tool and the recovery of the logging tool lodged in the logging bit sub by tripping the pipe back to the rig floor. This precluded further logging operations.

Going forward in Hole 1256D

During the expedition, the Co-Chief Scientists built an effective relationship with the Transocean/Overseas Drilling Limited (ODL) drilling crews, and there was open and informative bilateral exchange of information. Communications with the TAMU Operations Superintendent were excellent throughout. Following the completion of site operations, the Co-Chief Scientists organized a formal meeting for an effective debrief and discussion of issues encountered during Expedition 335 while these were still fresh in everyone's mind. This meeting was attended by the Co-Chief Scientists (Teagle and Ildefonse), past Co-Chief Scientists and leading proponents (Wilson and Alt), the Expedition Project Manager/Staff Scientist (Peter Blum), the Operations Superintendent (Ron Grout), the offshore installation manager (Sam MacLelland), Core Technicians/Tool Pushers (Wayne Malone/Mark Robinson), and Driller (Craig Prosser). The meeting discussed a wide range of future options (casing, cementing, tools, coring, drilling bits, and time on site) and came up with the following comments and recommendations.

- Hole 1256D is now in good condition, clear of cuttings to its total depth. Many of the cuttings removed have probably been resident in the hole since Leg 206 (from basalt textures and alteration minerals). Hole 1256D can be deepened toward its objectives if the recommended steps below are followed.
- Cementing has proved effective at stabilizing unstable formation, but more technical advice is required on cementing options (accelerants, etc.) and operations (e.g., packers to more effectively force cement into voids).

- Casing the complete out-of-gauge section (e.g., to 1000 mbsf in Hole 1256D) of an existing open borehole is not technically feasible in oceanic basement.
- Casing through the 16 inch casing to the bottom of the rathole with 10¾ inch casing would greatly improve the hydrodynamics of the hole and enhance hole-clearing efficiencies. This operation would be reasonably straightforward and not require underreaming or other technically challenging and untested operations in hard volcanic formations.
- Return visits to Hole 1256D must be fully armed with hard/ultra-hard formation, highly armored tricone bits for hole opening and cleaning/reaming and hard/ultra-hard formation coring bits, as well as an armored suite of mills and junk baskets. The first operation upon return to Hole 1256D, before installing a 10¾ inch casing string to the bottom of the rathole, will be to reenter with an armored tricone bit, drill the cement plugs and displace the cuttings, and ream and clean the bottom of the hole before coring can resume.
- The Program should investigate the feasibility of using synthetic polymer viscosifiers ("elephant snot") for binding and lifting cuttings from the borehole open/riserless holes (as recommended at the 309/312 Review Task Force). (Note: There may be environmental concerns about the use of synthetic compounds in open/riserless holes.)
- The Program should consult with an experienced/recommended drilling engineer to evaluate the best future coring plan, including the procurement (or even design and manufacture) of ultra-hard formation drill/coring bits; fishing tools; and operations, cementing, and casing strategies.
- Transocean/ODL, with their rig floor expertise, should be directly involved in the planning of future deep drilling efforts at Hole 1256D and other deep targets drilled by the *JOIDES Resolution*.
- The Program should recognize that deep boreholes such as Holes 1256D and 504B drilled over many expeditions are as challenging endeavors as the experiments undertaken with the D/V *Chikyu* to date. Deep riserless boreholes require similar continuity of planning, management, and leadership. The Co-Chief Scientists from Expedition 335 and previous cruises to Hole 1256D have built up considerable expertise and experience relevant to the achievement of deep drilling targets, and they should be kept engaged in the planning and implementation of future operations. This, together with engaging the Transocean/ODL rig floor teams in the planning stage, will ensure the maximum use of a unique suite of experiences from previous operations in Hole 1256D.

- The Program should follow the recommendations of the IODP-MI Operations Review Task Force for Expedition 309/312 to investigate innovative cruise scheduling mechanisms to maximize time on site for the achievement of high-priority objectives that require deep drilling (e.g., back-to-back cruises and at-sea crew transfers).

Program considerations for the attainment of deep targets by scientific ocean drilling

Establishing the ideal location for drilling is only part of the challenge of successfully drilling moderately deep holes (2–3 km) to recover samples and data necessary to address long-standing primary goals of scientific ocean drilling. Experience from Holes 504B and 1256D indicates that such experiments require multiple cruises to achieve their target depths. Five hundred meters penetration per expedition is an upper limit for coring in the upper crust, with lesser advances and more frequent drilling challenges as these holes get deeper and are drilled into rocks metamorphosed at higher pressures and temperatures. Penetration and core recovery rates have been low to very low in the two sheeted dike complex sections drilled to date (Holes 504B and 1256D). However, experience to date suggests that gabbroic rocks can be cored relatively rapidly at high rates of recovery (e.g., Hole U1309D = penetration rate 2 m/h and >75% recovery), so when the dike–gabbro transition zone is breached, solid progress through the plutonic section can be anticipated.

It is very unlikely that without significant good fortune deep targets in intact ocean crust can be achieved in the current science advisory configuration. The peer-review system that has overseen the progress of both Holes 504B and 1256D has required the reevaluation of new proposals following the successful completion of each drilling increment. A system similar to the "complex drilling proposals" (CDPs) used for riser experiments should be extended to riserless targets that require multiple expeditions to achieve important scientific goals.

Such is the capriciousness of hard rock coring that scientific ocean drilling may have to consider new approaches if it is to ever successfully address some of the major science questions that remain unanswered after more than 50 years. There are unlikely to ever be "quick wins" with targets that require multiexpedition deep boreholes. Expedition 335 was initially scheduled by the IODP-MI-OTF as a short cruise (~4 weeks), despite the explicit recommendations of the postexpedition 309/312 Operational Review Task Force "to maximize on-site time for deep drilling expeditions" (Recommendation 309/312-03). Flexibility in expedition scheduling may be a low-impact means to achieve deep objectives. Back-to-back cruises to a single target could be scheduled.

This approach was successful at drilling Hole U1309D >1400 mbsf during IODP Expeditions 304 and 305. Commonly, the ship has been moved off a deep hole after the significant investment in engineering and cleaning operations that have succeeded in preparing the hole for deep drilling. For example, Expedition 312 drilled >100 m of the dike–plutonic transition zone in Hole 1256D following significant hole remediation operations but left an open clean deep hole. Five years later, most of the scheduled time during Expedition 335 was spent on hole remediation, and the hole is now cleaner than ever. There is a need for mechanisms for revising expedition schedules so that drilling can continue in deep boreholes when progress is actually being made. This would require the movement of crew, scientists, and supplies to and from the rig so that drilling and hole cleaning can continue, along with the temporary postponement of the immediately following expeditions. Clearly, this would be a major departure from the standard operating style of the *JOIDES Resolution* within ODP and IODP and a challenge to the science advisory and scheduling structure. It would require community acceptance that could be difficult to achieve. However, the present standard "1 proposal = 1 expedition" approach is not an effective process to reach targets that require multiple-expedition deep drilling. Unless the community and the drilling program are able to develop new approaches to achieving deep targets, the lack of closure on science questions that can only be addressed by deep drilling will continue to stain future renewal documents with a perceived lingering staleness due to a continued recycling of unaccomplished goals.

References

Abelson, M., Baer, G., and Agnon, A., 2001. Evidence from gabbro of the Troodos ophiolite for lateral magma transport along a slow-spreading mid-ocean ridge. *Nature (London, U. K.),* 409(6816):72–75. **doi:10.1038/35051058**

Allerton, S., Pariso, J.E., Stokking, L.B., and McClelland, E., 1995. Origin of the natural remanent magnetism of sheeted dikes in Hole 504B cored during Legs 137 and 140. *In* Erzinger, J., Becker, K., Dick, H.J.B., and Stokking, L.B. (Eds.), *Proc. ODP, Sci. Results,* 137/140: College Station, TX (Ocean Drilling Program), 263–270. **doi:10.2973/odp.proc.sr.137140.030.1995**

Alt, J.C., 2004. Alteration of the upper oceanic crust: mineralogy, chemistry, and processes. *In* Elderfield, H., and Davis, E. (Eds.), *Hydrogeology of the Oceanic Lithosphere:* New York (Cambridge Univ. Press), 456–488.

Alt, J.C., Kinoshita, H., Stokking, L.B., et al., 1993. *Proc. ODP, Init. Repts.,* 148: College Station, TX (Ocean Drilling Program). **doi:10.2973/odp.proc.ir.148.1993**

Alt, J.C., Laverne, C., Coggon, R.M., Teagle, D.A.H., Banerjee, N.R., Morgan, S., Smith-Duque, C.E., Harris, M., and Galli, L., 2010. Subsurface structure of a submarine hydrothermal system in ocean crust formed at the East Pacific Rise, ODP/IODP Site 1256. *Geochem., Geophys., Geosyst.,* 11(10):Q10010–Q10038. **doi:10.1029/2010GC003144**

Alt, J.C., Laverne, C., Vanko, D.A., Tartarotti, P., Teagle, D.A.H., Bach, W., Zuleger, E., Erzinger, J., Honnorez, J., Pezard, P.A., Becker, K., Salisbury, M.H., and Wilkens, R.H., 1996. Hydrothermal alteration of a section of upper oceanic crust in the eastern equatorial Pacific: a synthesis of results from Site 504 (DSDP Legs 69, 70, and 83, and ODP Legs 111, 137, 140, and 148.) *In* Alt, J.C., Kinoshita, H., Stokking, L.B., and Michael, P.J. (Eds.), *Proc. ODP, Sci. Results,* 148: College Station, TX (Ocean Drilling Program), 417–434. **doi:10.2973/odp.proc.sr.148.159.1996**

Alt, J.C., and Teagle, D.A.H., 1999. The uptake of carbon during alteration of ocean crust. *Geochim. Cosmochim. Acta,* 63(10):1527–1535. **doi:10.1016/S0016-7037(99)00123-4**

Alt, J.C., and Teagle, D.A.H., 2003. Hydrothermal alteration of upper oceanic crust formed at a fast-spreading ridge: mineral, chemical, and isotopic evidence from ODP Site 801. *Chem. Geol.,* 201(3–4):191–211. **doi:10.1016/S0009-2541(03)00201-8**

Bach, W., Garrido, C.J., Paulick, H., Harvey, J., and Rosner, M., 2004. Seawater-peridotite interactions: first insights from ODP Leg 209, MAR 15°N. *Geochem., Geophys., Geosyst.,* 5(9):Q09F26–Q09F47. **doi:10.1029/2004GC000744**

Bédard, J.H., Sparks, R.S.J., Renner, R., Cheadle, M.J., and Hallworth, M.A., 1988. Peridotite sills and metasomatic gabbros in the eastern layered series of the Rhum complex. *J. Geol. Soc. (London, U. K.),* 145(2):207–224. **doi:10.1144/gsjgs.145.2.0207**

Bickle, M.J., 1992. Transport mechanisms by fluid-flow in metamorphic rocks: oxygen and strontium decoupling in the Trois Seigneurs Massif: a consequence of kinetic dispersion? *Am. J. Sci.,* 292(5): 289–316. **doi:10.2475/ajs.292.5.289**

Bickle, M.J., and Teagle, D.A.H., 1992. Strontium alteration in the Troodos ophiolite: implications for fluid fluxes and geochemical transport in mid-ocean ridge hydrothermal systems. *Earth Planet. Sci. Lett.,* 113(1–2):219–237. **doi:10.1016/0012-821X(92)90221-G**

Boudier, F., Nicolas, A., and Ildefonse, B., 1996. Magma chambers in the Oman ophiolite: fed from the top and the bottom. *Earth Planet. Sci. Lett.,* 144(1–2):239–250. **doi:10.1016/0012-821X(96)00167-7**

Browning, P., 1984. Cryptic variation within the cumulate sequence of the Oman ophiolite: magma chamber depth and petrological implications. *In* Gass, I.G., Lippard, S.J., and Shelton, A.W. (Eds.), *Ophiolites and Oceanic Lithosphere*. Geol. Soc. Spec. Publ., 13(1):71–82. **doi:10.1144/GSL.SP.1984.013.01.07**

Canales, J.P., Nedimovic, M.R., Kent, G.M., Carbotte, S.M., and Detrick, R.S., 2009. Seismic reflection images of a near-axis melt sill within the lower crust at the Juan de Fuca Ridge. *Nature (London, U. K.),* 460(7251):89–93. **doi:10.1038/nature08095**

Cande, S.C., and Kent, D.V., 1995. Revised calibration of the geomagnetic polarity timescale for the Late Cretaceous and Cenozoic. *J. Geophys. Res., [Solid Earth],* 100(B4):6093–6095. **doi:10.1029/94JB03098**

Carbotte, S., Mutter, C., Mutter, J., and Ponce-Correa, G., 1997. Influence of magma supply and spreading rate on crustal magma bodies and emplacement of the extrusive layer: insights from the East Pacific Rise at lat 16°N. *Geology,* 26(5):455–458. **doi:10.1130/0091-7613(1998)026<0455:IOMSAS>2.3.CO;2**

Carlson, R.L., 2010. How crack porosity and shape control seismic velocities in the upper oceanic crust: modeling downhole logs from Holes 504B and 1256D. *Geochem., Geophys., Geosyst.,* 11(4):Q04007–Q04021. **doi:10.1029/2009GC002955**

Chen, Y.J., 2001. Thermal effects of gabbro accretion from a deeper second melt lens at the fast spreading East Pacific Rise. *J. Geophys. Res., [Solid Earth],* 106(B5):8581–8588. **doi:10.1029/2000JB900420**

Coggon, R.M., Alt, J.C., and Teagle, D.A., 2008. Thermal history of ODP Hole 1256D lower sheeted dikes: petrology, chemistry and geothermometry of the granoblastic dikes. *Eos, Trans. Am. Geophys. Union,* 89(53)(Suppl.):V44B-08. (Abstract) **http://www.agu.org/meetings/fm08/waisfm08.html**

Coggon, R.M., Teagle, D.A.H., Cooper, M.J., and Vanko, D.A., 2004. Linking basement carbonate vein compositions to porewater geochemistry across the eastern flank of the Juan de Fuca Ridge, ODP Leg 168. *Earth Planet. Sci. Lett.,* 219(1–2):111–128. **doi:10.1016/S0012-821X(03)00697-6**

Coggon, R.M., Teagle, D.A.H., Smith-Duque, C.E., Alt, J.C., and Cooper, M.J., 2010. Reconstructing past seawater Mg/Ca and Sr/Ca from mid-ocean ridge flank calcium carbonate veins. *Science,* 327(5969):1114–1117. **doi:10.1126/science.1182252**

Coogan, L.A., Hain, A., Stahl, S., and Chakraborty, S., 2005a. Experimental determination of the diffusion coefficient for calcium in olivine between 900°C and 1500°C. *Geochim. Cosmochim. Acta,* 69(14):3683–3694. **doi:10.1016/j.gca.2005.03.002**

Coogan, L.A., Howard, K.A., Gillis, K.M., Bickle, M.J., Chapman, H., Boyce, A.J., Jenkin, G.R.T., and Wilson, R.N., 2006. Chemical and thermal constraints on focused fluid flow in the lower oceanic crust. *Am. J. Sci.,* 306(6):389–427. **doi:10.2475/06.2006.01**

Coogan, L.A., Jenkin, G.R.T., and Wilson, R.N., 2002. Constraining the cooling rate of the lower oceanic crust: a new approach applied to the Oman ophiolite. *Earth Planet. Sci. Lett.,* 199(1–2):127–146. **doi:10.1016/S0012-821X(02)00554-X**

Coogan, L.A., Kasemann, S.A., and Chakraborty, S., 2005b. Rates of hydrothermal cooling of new oceanic upper crust derived from lithium geospeedometry. *Earth Planet. Sci. Lett.,* 240(2):415–424. **doi:10.1016/j.epsl.2005.09.020**

Crawford, W.C., and Webb, S.C., 2002. Variations in the distribution of magma in the lower crust and at the Moho beneath the East Pacific Rise at 9°–10°N. *Earth Planet. Sci. Lett.,* 203(1):117–130. **doi:10.1016/S0012-821X(02)00831-2**

Crawford, W.C., Webb, S.C., and Hildebrand, J.A., 1999. Constraints on melt in the lower crust and Moho at the East Pacific Rise, 9°48′N, using seafloor compliance measurements. *J. Geophys. Res., [Solid Earth],* 104(B2):2923–2939. **doi:10.1029/1998JB900087**

Detrick, R., Collins, J., Stephen, R., and Swift, S., 1994. In situ evidence for the nature of the seismic Layer 2/3 boundary in oceanic crust. *Nature (London, U. K.),* 370(6487):288–290. **doi:10.1038/370288a0**

Detrick, R.S., Harding, A.J., Kent, G.M., Orcutt, J.A., Mutter, J.C., and Buhl, P., 1993. Seismic structure of the southern East Pacific Rise. *Science,* 259(5094):499–503. **doi:10.1126/science.259.5094.499**

Dunn, R.A., Toomey, D.R., Detrick, R.S., and Wilcock, W.S.D., 2001. Continuous mantle melt supply beneath an overlapping spreading center on the East Pacific Rise. *Science,* 291(5510):1955–1958. **doi:10.1126/science.1057683**

Edmond, J.M., Measures, C., Magnum, B., Grant, B., Sclater, F.R., Collier, R., Hudson, A., Gordon, L.I., and Corliss, J.B., 1979. On the formation of metal-rich deposits at ridge crests. *Earth. Planet. Sci. Lett.,* 46(1):19–30. **doi:10.1016/0012-821X(79)90062-1**

Expedition 309/312 Scientists, 2006. Site 1256. *In* Teagle, D.A.H., Alt, J.C., Umino, S., Miyashita, S., Banerjee, N.R., Wilson, D.S., and the Expedition 309/312 Scientists. *Proc. IODP,* 309/312: Washington, DC (Integrated Ocean Drilling Program Management International, Inc.). **doi:10.2204/iodp.proc.309312.103.2006**

Farrell, J.W., Raffi, I., Janecek, T.R., Murray, D.W., Levitan, M., Dadey, K.A., Emeis, K.-C., Lyle, M., Flores, J.-A., and Hovan, S., 1995. Late Neogene sedimentation patterns in the eastern equatorial Pacific Ocean. *In* Pisias, N.G., Mayer, L.A., Janecek, T.R., Palmer-Julson, A., and van Andel, T.H. (Eds.), *Proc. ODP, Sci. Results,* 138: College Station, TX (Ocean Drilling Program), 717–756. **doi:10.2973/odp.proc.sr.138.143.1995**

France, L., Ildefonse, B., and Koepke, J., 2009. Interactions between magma and the hydrothermal system in the Oman ophiolite and in IODP Hole 1256D: fossilisation of dynamic melt lens at fast spreading ridges. *Geochem., Geophys., Geosyst.,* 10(10):Q10O19–Q10O48. **doi:10.1029/2009GC002652**

Francheteau, J., Armijo, R., Cheminée, J.L., Hekinian, R., Lonsdale, P., and Blum, N., 1992. Dyke complex of the East Pacific Rise exposed in the walls of Hess Deep and the structure of the upper oceanic crust. *Earth Planet. Sci. Lett.,* 111(1):109–121. **doi:10.1016/0012-821X(92)90173-S**

Garmany, J., 1989. Accumulations of melt at the base of young oceanic crust. *Nature (London, U. K.),* 340(6235):628–632. **doi:10.1038/340628a0**

Gillis, K.M., 1995. Controls on hydrothermal alteration in a section of fast-spreading oceanic crust. *Earth Planet. Sci. Lett.,* 134(3–4):473–489. **doi:10.1016/0012-821X(95)00137-2**

Gillis, K.M., 2008. The roof of an axial magma chamber: a hornfelsic heat exchanger. *Geology,* 36(4):299–302. **doi:10.1130/G24590A.1**

Gillis, K.M., Coogan, L.A., and Pedersen, R., 2005. Strontium isotope constraints on fluid flow in the upper oceanic crust at the East Pacific Rise. *Earth Planet. Sci. Lett.,* 232(1–2):83–94. **doi:10.1016/j.epsl.2005.01.008**

Gillis, K.M., and Roberts, M.D., 1999. Cracking at the magma-hydrothermal transition: evidence from the Troodos ophiolite, Cyprus. *Earth Planet. Sci. Lett.,* 169(3–4):227–244. **doi:10.1016/S0012-821X(99)00087-4**

Gregory, R.T., and Taylor, H.P., Jr., 1981. An oxygen isotope profile in a section of Cretaceous oceanic crust, Samail ophiolite, Oman: evidence for $\delta^{18}O$ buffering of the oceans by deep

(>5 km) seawater-hydrothermal circulation at mid-ocean ridges. *J. Geophys. Res., [Solid Earth],* 86(B4):2737–2755. **doi:10.1029/JB086iB04p02737**

Guérin, G., Goldberg, D.S., and Iturrino, G.J., 2008. Velocity and attenuation in young oceanic crust: new downhole log results from DSDP/ODP/IODP Holes 504B and 1256D. *Geochem., Geophys., Geosyst.,* 9(12):Q12014–Q12023. **doi:10.1029/2008GC002203**

Hallenborg, E., Harding, A.J., Kent, G.M., and Wilson, D.S., 2003. Seismic structure of 15 Ma oceanic crust formed at an ultrafast spreading East Pacific Rise: evidence for kilometer-scale fracturing from dipping reflectors. *J. Geophys. Res., [Solid Earth],* 108(B11):2532. **doi:10.1029/2003JB002400**

Heberling, C., Lowell, R.P., Liu, L., and Fisk, M.R., 2010. Extent of the microbial biosphere in the oceanic crust. *Geochem., Geophys., Geosyst.,* 11(8):Q08003–Q08017. **doi:10.1029/2009GC002968**

Henstock, T.J., Woods, A.W., and White, R.S., 1993. The accretion of oceanic crust by episodic sill intrusion. *J. Geophys. Res., [Solid Earth],* 98(B3):4143–4161. **doi:10.1029/92JB02661**

Hooft, E.E.E., Detrick, R.S., and Kent, G.M., 1994. Seismic structure and indicators of magma budget along the southern East Pacific Rise. *J. Geophys. Res., [Solid Earth],* 102(B12):27319–27340.

Hooft, E.E.E., Schouten, H., and Detrick, R.S., 1996. Constraining crustal emplacement processes from variation in seismic layer 2A thickness at the East pacific Rise. *Earth Planet. Sci. Lett.,* 142(3–4):289–309. **doi:10.1016/0012-821X(96)00101-X**

Jupp, T., and Schultz, A., 2000. A thermodynamic explanation for black smoker temperatures. *Nature (London, U. K.),* 403(6772):880–883. **doi:10.1038/35002552**

Karson, J.A., 2002. Geologic structure of the uppermost oceanic crust created at fast- to intermediate-rate spreading centers. *Annu. Rev. Earth Planet. Sci.,* 30:347–384. **doi:10.1146/annurev.earth.30.091201.141132**

Karson, J.A., Hurst, S.D., and Lonsdale, P., 1992. Tectonic rotations of dikes in fast-spread oceanic crust exposed near Hess Deep. *Geology,* 20(8):685–688. **doi:10.1130/0091-7613(1992)020<0685:TRODIF>2.3.CO;2**

Karson, J.A., Klein, E.M., Hurst, S.D., Lee, C.E., Rivizzigno, P.A., Curewitz, D., Morris, A.R., Miller, D.J., Varga, R.G., Christeson, G.L., Cushman, B., O'Neill, J.M., Brophy, J.G., Gillis, K.M., Stewart, M.A., and Sutton, A.L., 2002. Structure of uppermost fast-spread oceanic crust exposed at the Hess deep rift: implications for subaxial processes at the East Pacific Rise. *Geochem., Geophys., Geosyst.,* 3(1):1002. **doi:10.1029/2001GC000155**

Kelemen, P.B., and Aharonov, E., 1998. Periodic formation of magma fractures and generation of layered gabbros in the lower crust beneath oceanic spreading centers. *In* Buck, R., Delaney, P.T., Karson, J.A., and Lagabrielle, Y. (Eds.), *Faulting and Magmatism at Mid-Ocean Ridges*. Geophys. Monogr., 106:267–289.

Kelemen, P.B., Koga, K., and Shimizu, N., 1997. Geochemistry of gabbro sills in the crust-mantle transition zone of the Oman ophiolite: implications for the origin of the oceanic lower crust. *Earth Planet. Sci. Lett.,* 146(3–4):475–488. **doi:10.1016/S0012-821X(96)00235-X**

Kent, G.M., Harding, A.J., Orcutt, J.A., Detrick, R.S., Mutter, J.C., and Buhl, P., 1994. Uniform accretion of oceanic crust south of the Garrett transform at 14°15′S on the East Pacific Rise. *J. Geophys. Res., [Solid Earth],* 99(B5):9097–9116. **doi:10.1029/93JB02872**

Koepke, J., Christie, D.M., Dziony, W., Holtz, F., Lattard, D., Maclennan, J., Park, S., Scheibner, B., Yamasaki, T., and Yamazaki, S., 2008. Petrography of the dike–gabbro transition at

IDOP Site 1256 (equatorial Pacific): the evolution of the granoblastic dikes. *Geochem., Geophys., Geosyst.,* 9(7):Q07O09–Q07O37. **doi:10.1029/2008GC001939**

Koepke, J., Berndt, J., Feig, S.T., and Holtz, F., 2007. The formation of SiO_2-rich melts within the deep ocean crust by hydrous partial melting of gabbros. *Contrib. Mineral. Petrol.,* 153(1):67–84. **doi:10.1007/s00410-006-0135-y**

Korenaga, J., and Kelemen, P.B., 1997. Origin of gabbro sills in the Moho transition zone of the Oman ophiolite: implications for magma transport in the oceanic lower crust. *J. Geophys. Res., [Solid Earth],* 102(B12):27729–27749. **doi:10.1029/97JB02604**

Korenaga, J., and Kelemen, P.B., 1998. Melt migration through the oceanic lower crust: a constraint from melt percolation modeling with finite solid diffusion. *Earth Planet. Sci. Lett.,* 156(1–2):1–11. **doi:10.1016/S0012-821X(98)00004-1**

Langmuir, C.H., Bender, J.F., and Batiza, R., 1986. Petrological and tectonic segmentation of the East Pacific Rise, 5°30′N–14°30′N. *Nature (London, U. K.),* 322(6078):422–429. **doi:10.1038/322422a0**

Macdonald, K.C., Fox, P.J., Alexander, R.T., Pockalny, R., and Gente, P., 1996. Volcanic growth faults and the origin of Pacific abyssal hills. *Nature (London, U. K.),* 380(6570):125–129. **doi:10.1038/380125a0**

Macdonald, K.C., Haymon, R., and Shor, A., 1989. A 220 km² recently erupted lava field on the East Pacific Rise near lat 8°S. *Geology,* 17(3):212–216. **doi:10.1130/0091-7613(1989)017<0212:AKRELF>2.3.CO;2**

Maclennan, J., Hulme, T., and Singh, S.C., 2005. Cooling of the lower oceanic crust. *Geology,* 33(5):357–366. **doi:10.1130/G21207.1**

MacLeod, C.J., and Yaouancq, G., 2000. A fossil melt lens in the Oman ophiolite: implications for magma chamber processes at fast spreading ridges. *Earth Planet. Sci. Lett.,* 176(3–4):357–373. **doi:10.1016/S0012-821X(00)00020-0**

Manning, C.E., Weston, P.E., and Mahon, K.I., 1996. Rapid high-temperature metamorphism of East Pacific Rise gabbros from Hess Deep. *Earth Planet. Sci. Lett.,* 144(1–2):123–132. **doi:10.1016/0012-821X(96)00153-7**

Meurer, W.P., and Gee, J., 2002. Evidence for the protracted construction of slow-spread oceanic crust by small magmatic injections. *Earth Planet. Sci. Lett.,* 201(1):45–55. **doi:10.1016/S0012-821X(02)00660-X**

Miyashita, S., Adachi, Y., and Tanaka, S., 2007. Partial melting of oceanic crust: anatectitites in the gabbro–dike transition of Oman ophiolite. *Geochim. Cosmochim. Acta,* 71(15)(Suppl.):A675. (Abstract) **http://goldschmidt.info/2007/abstracts/A675.pdf**

Morris, A., Gee, J.S., Pressling, N., John, B.E., MacLeod, C.J., Grimes, C.B., and Searle, R.C., 2009. Footwall rotation in an oceanic core complex quantified using reoriented Integrated Ocean Drilling Program core samples. *Earth Planet. Sci. Lett.,* 287(1–2):217–228. **doi:10.1016/j.epsl.2009.08.007**

Müller, R.D., Sdrolias, M., Gaina, C., and Roest, W.R., 2008. Age, spreading rates, and spreading asymmetry of the world's ocean crust. *Geochem., Geophys., Geosyst.,* 9(4):Q04006–Q04024. **doi:10.1029/2007GC001743**

Natland, J.H., and Dick, H.J.B., 1996. Melt migration through high-level gabbroic cumulates of the East Pacific Rise at Hess Deep: the origin of magma lenses and the deep crustal structure of fast-spreading ridges. *In* Mével, C., Gillis, K.M., Allan, J.F., and Meyer, P.S. (Eds.), *Proc. ODP, Sci. Results,* 147: College Station, TX (Ocean Drilling Program), 21–58. **doi:10.2973/odp.proc.sr.147.002.1996**

Nedimovic, M.R., Carbotte, S.M., Harding, A.J., Detrick, R.S., Canales, J.P., Diebold, J.B., Kent, G.M., Tischer, M., and Babcock, J.M., 2005. Frozen magma lenses below the oceanic crust. *Nature (London, U. K.),* 436(7054):1149–1152. **doi:10.1038/nature03944**

Nicolas, A., and Boudier, F., 1991. Rooting of the sheeted dike complex in the Oman ophiolite. *In* Peters, T., Nicolas, A., and Coleman, R.G. (Eds.), *Ophiolite Genesis and Evolution of Oceanic Lithosphere:* Boston (Kluwer Acad.), 39–54.

Nicolas, A., Boudier, F., and France, L., 2009. Subsidence in magma chamber and the development of magmatic foliation in Oman ophiolite gabbros. *Earth Planet. Sci. Lett.,* 284(1–2):76–87. **doi:10.1016/j.epsl.2009.04.012**

Nicolas, A., Boudier, F., and Ildefonse, B., 1996. Variable crustal thickness in the Oman ophiolite: implication for oceanic crust. *J. Geophys. Res., [Solid Earth],* 101(B8):17941–17950. **doi:10.1029/96JB00195**

Nicolas, A., Boudier, F., Ildefonse, B., and Ball, E., 2000. Accretion of Oman and United Arab Emirates ophiolite—discussion of a new structural map. *Mar. Geophys. Res.,* 21(3–4):147–180. **doi:10.1023/A:1026769727917**

Pallister, J.S., and Hopson, C.A., 1981. Samail ophiolite plutonic suite: field relations, phase variation, cryptic variation and layering, and a model of a spreading ridge magma chamber. *J. Geophys. Res., [Solid Earth],* 86(B4):2593–2644. **doi:10.1029/JB086iB04p02593**

Park, S., Maclennan, J., Teagle, D., and Hauff, F., 2008. Did the Galápagos plume influence the ancient EPR?: a geochemical study of basaltic rocks from Hole 1256D. *Eos, Trans. Am. Geophys. Union,* 89(53)(Suppl.):V51F-2097. (Abstract) **http://www.agu.org/meetings/fm08/waisfm08.html**

Parsons, B., and Sclater, J.G., 1977. An analysis of the variation of ocean floor bathymetry and heat flow with age. *J. Geophys. Res., [Solid Earth],* 82:803–827. **doi:10.1029/JB082i005p00803**

Phipps Morgan, J., and Chen, Y.J., 1993. The genesis of oceanic crust: magma injection, hydrothermal circulation, and crustal flow. *J. Geophys. Res., [Solid Earth],* 98(B4):6283–6297. **doi:10.1029/92JB02650**

Potter, D.K., 2004. A comparison of anisotropy of magnetic remanence methods—a user's guide for application to palaeomagnetism and magnetic fabric studies. *In* Martín-Hernández, F., Lüneburg, C.M., Aubourg, C., and Jackson, M. (Eds.), *Magnetic Fabric: Methods and Applications*. Geol. Soc. Spec. Publ., 238(1):21–35. **doi:10.1144/GSL.SP.2004.238.01.03**

Purdy, G.M., Kong, L.S.L., Christeson, G.L., and Solomon, S.C., 1992. Relationship between spreading rate and the seismic structure of mid-ocean ridges. *Nature (London, U. K.),* 355(6363):815–817. **doi:10.1038/355815a0**

Quick, J.E., and Denlinger, R.P., 1993. Ductile deformation and the origin of layered gabbro in ophiolites. *J. Geophys. Res., [Solid Earth],* 98(B8):14015–14027. **doi:10.1029/93JB00698**

Schneider, D.A., 1988. An estimate of the long-term non-dipole field from marine magnetic anomalies. *Geophys. Res. Lett.,* 15(10):1105–1108. **doi:10.1029/GL015i010p01105**

Singh, S.C., Kent, G.M., Collier, J.S., Harding, A.J., and Orcutt, J.A., 1998. Melt to mush variations in crustal magma properties along the ridge crest at the southern East Pacific Rise. *Nature (London, U. K.),* 394(6696):874–878. **doi:10.1038/29740**

Sinton, J.M., and Detrick, R.S., 1992. Mid-ocean ridge magma chambers. *J. Geophys. Res., [Solid Earth],* 97(B1):197–216. **doi:10.1029/91JB02508**

Su, Y., and Langmuir, C.H., 2003. Global MORB chemistry compilation at segment scale [Ph.D. dissert.]. Columbia Univ., New York.

Swift, S., Reichow, M., Tikku, A., Tominaga, M., and Gilbert, L., 2008. Velocity structure of upper ocean crust at Ocean Drilling Program Site 1256. *Geochem., Geophys., Geosyst.,* 9(10):Q10O13–Q10O34. **doi:10.1029/2008GC002188**

Teagle, D., and Ildefonse, B., 2011. Journey to the mantle of the Earth. *Nature (London, U. K.),* 471(7339):437–439. **doi:10.1038/471437a**

Teagle, D.A.H., Alt, J.C., and Halliday, A.N., 1998a. Tracing the chemical evolution of fluids during hydrothermal recharge: constraints from anhydrite recovered in ODP Hole 504B. *Earth Planet. Sci. Lett.,* 155(3–4):167–182. **doi:10.1016/S0012-821X(97)00209-4**

Teagle, D.A.H., Alt, J.C. and Halliday, A.N., 1998b. Tracing the evolution of hydrothermal fluids in the upper oceanic crust: Sr-isotopic constraints from DSDP/ODP Holes 504B and 896A. *In* Harrison, K., and Mills, R.A. (Eds.), *Modern Ocean Floor Processes and the Geological Record*. Geol. Soc. Spec. Pub., 148(1):81–97. **doi:10.1144/GSL.SP.1998.148.01.06**

Teagle, D.A.H., Alt, J.C., Umino, S., Miyashita, S., Banerjee, N.R., Wilson, D.S., and Expedition 309/312 Scientists, 2006. *Proc. IODP,* 309/312: Washington, DC (Integrated Ocean Drilling Program Management International, Inc.). **doi:10.2204/iodp.proc.309312.2006**

Teagle, D.A.H., and Bickle, M.J., 1993. The transport and exchange of geochemical tracers by fluid-rock interaction: application of theory to ancient and modern ocean crust. *RIDGE Events,* 4(2):5–9.

Teagle, D.A.H., Bickle, M.J., and Alt, J.C., 2003. Recharge flux to ocean-ridge black smoker systems: a geochemical estimate from ODP Hole 504B. *Earth Planet. Sci. Lett.,* 210(1–2):81–89. **doi:10.1016/S0012-821X(03)00126-2**

Teagle, D.A.H, Ildefonse, B., and Blum, P., 2010. Superfast spreading rate crust 4. *IODP Sci. Prosp.,* 335. **doi:10.2204/iodp.sp.335.2010**

Tominaga, M., Teagle, D.A.H., Alt, J.C., and Umino, S., 2009. Determination of volcanostratigraphy of the oceanic crust formed at superfast spreading ridge: electrofacies analyses of ODP/IOPD Hole 1256D. *Geochem., Geophys., Geosyst.,* 10(1):Q01003–Q01033. **doi:10.1029/2008GC002143**

Tominaga, M., and Umino, S., 2010. Lava deposition history in ODP Hole 1256D: insights from log-based volcanostratigraphy. *Geochem., Geophys., Geosyst.,* 11(5):Q05003–Q05021. **doi:10.1029/2009GC002933**

Umino, S., Lipman, P.W., and Obata, S., 2000. Subaqueous lava flow lobes, observed on ROV *Kaiko* dives off Hawaii. *Geology,* 28(6):503–506. **doi:10.1130/0091-7613(2000)28<503:SLFLOO>2.0.CO;2**

Violay, M., Pezard, P.A., Ildefonse, B., Belghoul, A., and Laverne, C., 2010. Petrophysical properties of the root zone of sheeted dikes in the ocean crust: a case study from Hole ODP/IODP 1256D, eastern equatorial Pacific. *Tectonophysics,* 493(1–2):139–152. **doi:10.1016/j.tecto.2010.07.013**

White, S.M., Hayman, R.M., Fornari, D.J., Perfit, M.R., and Macdonald, K.C., 2002. Correlation between volcanic and tectonic segmentation of fast-spreading ridges: evidence from volcanic structures and lava flow morphology on the East Pacific Rise at 9°–10°N. *J. Geophys. Res., [Solid Earth],* 107(B8):2173. **doi:10.1029/2001JB000571**

White, S.M., Macdonald, K.C., and Haymon, R.M., 2000. Basaltic lava domes, lava lakes, and volcanic segmentation on the southern East Pacific Rise. *J. Geophys. Res., [Solid Earth],* 105(B10):23519–23536. **doi:10.1029/2000JB900248**

Wilson, D.S., 1996. Fastest known spreading on the Miocene Cocos–Pacific plate boundary. *Geophys. Res. Lett.,* 23(21):3003–3006. **doi:10.1029/96GL02893**

Wilson, D.S., Hallenborg, E., Harding, A.J., and Kent, G.M., 2003. Data report: site survey results from Cruise EW9903. *In* Wilson, D.S., Teagle, D.A.H., Acton, G.D., *Proc. ODP, Init. Repts.,* 206: College Station, TX (Ocean Drilling Program), 1–49. **doi:10.2973/odp.proc.ir.206.104.2003**

Wilson, D.S., Teagle, D.A.H., Acton, G.D., et al., 2003. *Proc. ODP, Init. Repts.,* 206: College Station, TX (Ocean Drilling Program). **doi:10.2973/odp.proc.ir.206.2003**

Wilson, D.S., Teagle, D.A.H., Alt, J.C., Banerjee, N.R., Umino, S., Miyashita, S., Acton, G.D., Anma, R., Barr, S.R., Belghoul, A., Carlut, J., Christie, D.M., Coggon, R.M., Cooper, K.M., Cordier, C., Crispini, L., Durand, S.R., Einaudi, F., Galli, L., Gao, Y., Geldmacher, J., Gilbert, L.A., Hayman, N.W., Herrero-Bervera, E., Hirano, N., Holter, S., Ingle, S., Jiang, S., Kalberkamp, U. Kerneklian, M., Koepke, J., Laverne, C., Vasquez, H.L.L., Maclennan, J., Morgan, S., Neo, N., Nichols, H.J., Park, S.-H., Reichow, M.K., Sakuyama, T., Sano, T., Sandwell, R., Scheibner, B., Smith-Duque, C.E., Swift, S.A., Tartarotti, P., Tikku, A.A., Tominaga, M., Veloso, E.A., Yamasaki, T., Yamazaki, S., and Ziegler, C., 2006. Drilling to gabbro in intact ocean crust. *Science,* 312(5776):1016–1020. **doi:10.1126/science.1126090**

Yamazaki, S., Neo, N., and Miyashita, S., 2009. Data report: whole-rock major and trace elements and mineral compositions of the sheeted dike–gabbro transition in ODP Hole 1256D. *In* Teagle, D.A.H., Alt, J.C., Umino, S., Miyashita, S., Banerjee, N.R., Wilson, D.S., and the Expedition 309/312 Scientists, *Proc. IODP,* 309/312: Washington, DC (Integrated Ocean Drilling Program Management International, Inc.). **doi:10.2204/iodp.proc.309312.203.2009**

Table T1. Predicted and actual depths to gabbros at Site 1256.

	Depth to axial low-velocity zone		100 m of off-axis lavas		300 m of off-axis lavas		450 m of off-axis lavas		575 m of off-axis lavas		Actual depth to gabbro	
	msb	mbsf	msb	mbsf	msb	mbsf	msb	mbsf	msb	mbsf	msb	mbsf
Minimum	725	975	825	1075	1025	1275	1175	1425	1300	1550	1157	1407
Maximum	1000	1250	1100	1350	1300	1550	1450	1700	1575	1825	—	—

Depths to the axial low-velocity zone estimated from the relationship with spreading rate shown in Figure **F5** (following Purdy et al., 1992, and Carbotte et al., 1997) for ocean crust spreading at 200 mm/y. The thickness of off-axis lavas estimated on textural grounds from cores recovered during Leg 206 was 284 m. Greater thicknesses of off-axis lavas have been estimated from wireline imaging logs from the occurrence of a pillow lava–rich zone between 700 and 825 mbsf in Hole 1256D (Tominaga and Umino, 2010). The actual depth where the first gabbro (Gabbro 1) was recovered was ~1407 mbsf (1157 msb). This is in excellent agreement with the observed relationship between spreading rate and depth to axial low-velocity zones and the thickness of off-axis lavas estimated from Hole 1256D. Depths in mbsf include the 250 m thick sediment cover at Site 1256. — = not available.

Table T2. Rates of recovery and rate of penetration (ROP) in Hole 1256D during Leg 206 and Expeditions 309/312 and 335.

Interval	Cored interval (m)	Average recovery (%)	Average ROP (m/h)
Leg 206 and Expedition 309/312:			
Hole 1256D (Cores 2R–234R)	1231	37	1.3
Lavas and transition zone (Cores 2R–128R)	785	41	1.5
Upper dikes (Cores 129R–191R)	287	37	0.9
Granoblastic dikes (Cores 192R–213R)	63	7	0.5
Plutonic section (Cores 214R–234R)	96	29	1.1
Gabbros (Gabbro 1: Cores 214R–224R; Gabbro 2: Cores 230R to 232R-2, 98 cm)	72	35	1.2
Dike screen 1 (granoblastic basalt)	24	11	0.9
Expedition 335:			
Dike screen 2 (granoblastic basalt) Cores 232R-2 through 239R (1507.1–1521.6 mbsf)	26.7	11	0.9
Cumulative Hole 1256D (Cores 2R–239R)	1245.5	37	1.3

Table T3. Expedition 335 operation summary. (Continued on next 12 pages.)

Operation	Start		Expedition (from departure time)				Comments
			Duration		Time (cumulative)		
	Local time (h)	Date (2011)	h	day	h	day	
In Puntarenas, Costa Rica, for port call activities.		14 Apr					Beginning of Expedition 335.
Depart Puntarenas; transit to Site 1256.	430	17 Apr	44.75	1.86	44.75	1.86	11.3 kt at 0630 h on 18 April.
On position over Hole 1256D. Pick up mouse hole, make up BHA with tricone bit and MBR. RIH drill string to 2733 mbrf while measuring and rabbiting all tubulars.	115	19 Apr	9.00	0.38	53.75	2.24	Start Run 1: Smith 9-7/8 inch F9 tricone bit.
Launch VIT.	1015	19 Apr	0.75	0.03	54.50	2.27	
RIH drill string 2733–3246 mbrf.	1100	19 Apr	1.25	0.05	55.75	2.32	
Lose VIT signal; retrieve VIT and repair cable head; redeploy VIT.	1215	19 Apr	3.25	0.14	59.00	2.46	
RIH drill string 3246–3637 mbrf.	1530	19 Apr	2.00	0.08	61.00	2.54	
Search and position vessel for reentry; reenter Hole 1256D at 1800 h.	1730	19 Apr	0.50	0.02	61.50	2.56	Reentry 1.
Continue RIH to 258.8 mbsf.	1800	19 Apr	1.25	0.05	62.75	2.61	
Recover VIT.	1915	19 Apr	0.75	0.03	63.50	2.65	
Continue RIH with 5-1/2 inch DP to 925.0 mbsf, where formation took 25,000 lb. Cancel temperature log and water sample.	2000	19 Apr	1.75	0.07	65.25	2.72	
Pull back in hole 925.0–891.9 mbsf.	2145	19 Apr	0.25	0.01	65.50	2.73	Obstruction.
Pick up 20 ft knobby and top drive.	2200	19 Apr	0.75	0.03	66.25	2.76	
RIH with top drive to 920.0 mbsf.	2245	19 Apr	0.75	0.03	67.00	2.79	
Work pipe at 920–925 mbsf, where we had hole problems during Exp. 312. Erratic torque; top drive current = 500 A.	2330	19 Apr	1.75	0.07	68.75	2.86	
Pull back 920–891.5 mbsf.	115	20 Apr	0.25	0.01	69.00	2.88	
Change out swivel packing.	130	20 Apr	1.25	0.05	70.25	2.93	
Resume washing/reaming 891.5–923.3 mbsf. Work stuck pipe 0415–0515 h when rotation lost. Unable to apply >10,000 lb WOB without stalling top drive. Circulate 600 bbl of hi-vis gel during 24 h period. Unable to penetrate deeper than 923.3 mbsf. Pump 150 bbl sweep at 923.3 mbsf. Trip drill string to change to a tricone bit with a more aggressive cutting structure.	245	20 Apr	27.25	1.14	97.50	4.06	
POOH with top drive 923.3–833.9 mbsf.	600	21 Apr	0.75	0.03	98.25	4.09	
Rack top drive.	645	21 Apr	0.50	0.02	98.75	4.11	
POOH from 833.9 mbsf and clear seafloor at 0900 h. Rack 4 stands of DC in derrick. Lay out BHA with MBR. Bit clears rotary table at 1550 h.	715	21 Apr	8.50	0.35	107.25	4.47	Clear seafloor at 0900 h. End Run 1 at 1550 h.
Make up new Reed 9-7/8 inch tricone bit, bit sub with float valve, and tandem set of boot baskets; RIH DP to 2877 mbrf.	1545	21 Apr	6.75	0.28	114.00	4.75	Start Run 2: Reed 9-7/8 inch tricone bit (IADC Type 517) plus boot baskets.
Deploy VIT.	2230	21 Apr	0.75	0.03	114.75	4.78	
Resume RIH drill string to 3638 mbrf.	2315	21 Apr	1.50	0.06	116.25	4.84	
Position vessel and reenter Hole 1256D at 0105 h.	045	22 Apr	0.50	0.02	116.75	4.86	Reentry 2.
RIH to 259.3 mbsf.	115	22 Apr	0.25	0.01	117.00	4.88	
Retrieve and recover VIT.	130	22 Apr	1.00	0.04	118.00	4.92	
Resume RIH 259.3–892.1 mbsf.	230	22 Apr	1.75	0.07	119.75	4.99	
Pick up top drive.	415	22 Apr	0.50	0.02	120.25	5.01	
Wash/ream hole from 892.1 mbsf. Attempt to pass bridge at ~920 mbsf. Pump 50 bbl hi-vis mud sweep.	445	22 Apr	1.75	0.07	122.00	5.08	
Work stuck pipe.	630	22 Apr	1.25	0.05	123.25	5.14	Stuck.
Wash/ream hole from ~920 mbsf. Circulate 100 bbl hi-vis mud sweep.	745	22 Apr	2.25	0.09	125.50	5.23	
Work stuck pipe.	1000	22 Apr	2.00	0.08	127.50	5.31	Stuck.
Wash/ream hole from ~923 mbsf. Unable to pass bridge.	1200	22 Apr	9.00	0.38	136.50	5.69	
Pull back in hole 923–863.3 mbsf.	2100	22 Apr	0.50	0.02	137.00	5.71	
Rack top drive.	2130	22 Apr	0.50	0.02	137.50	5.73	
POOH drill string and clear seafloor at 0005 h and plane of the rotary table at 0605 h.	2200	22 Apr	8.00	0.33	145.50	6.06	Clear seafloor at 0500 h. End Run 2 at 0605 h.

Table T3 (continued). (Continued on next page.)

Operation	Start		Expedition (from departure time)				Comments
			Duration		Time (cumulative)		
	Local time (h)	Date (2011)	h	day	h	day	
Lay out junk baskets and 9-7/8 inch bit. Junk baskets yielded some basaltic cuttings ranging from small gravel to rounded pebbles. Expedition 312 logs indicate a large washed-out zone at ~920–935 mbsf, which we will attempt to stabilize with a 5 bbl cement plug.	600	23 Apr	1.00	0.04	146.50	6.10	Samples Run02-EXJB. Decision to cement.
Make up cementing BHA with used Reed tricone bit without jets and 2 stands of DC. Deploy to 2676 mbrf.	700	23 Apr	6.00	0.25	152.50	6.35	Start Run 3: Reed tricone without jets.
Install VIT.	1300	23 Apr	0.50	0.02	153.00	6.37	
Resume RIH 2676–3638 mbrf.	1330	23 Apr	1.50	0.06	154.50	6.44	
Search and position vessel. Reenter Hole 1256D at 1520 h.	1500	23 Apr	0.25	0.01	154.75	6.45	Reentry 3.
RIH drill string to 262.9 mbsf.	1515	23 Apr	0.50	0.02	155.25	6.47	
POOH VIT and recover.	1545	23 Apr	1.50	0.06	156.75	6.53	
Resume RIH drill string. Tag bridge at 922 mbsf.	1715	23 Apr	1.50	0.06	158.25	6.59	
Make up circulating head and Lo-torque valves; pressure test to 1500 psi.	1845	23 Apr	0.50	0.02	158.75	6.61	
Pump 5 bbl of 16 ppg cement slurry.	1915	23 Apr	0.25	0.01	159.00	6.62	Pump cement.
Displace drill string with seawater (1× volume).	1930	23 Apr	0.50	0.02	159.50	6.65	
Lay out circulating head and pull back in hole with drill string to 806.9 mbsf.	2000	23 Apr	0.50	0.02	160.00	6.67	
Flush drill string with seawater (3× volume).	2030	23 Apr	1.25	0.05	161.25	6.72	
Lay out circulating head and POOH to 3191 mbrf. Clear top of the cone at 2320 h. Bit at rotary table at 0515 h.	2145	23 Apr	7.50	0.31	168.75	7.03	Clear seafloor at 2320 h. End Run 3 at 0515 h.
Make up new 9-7/8 inch Atlas tricone bit, inspect float, pick up 2 DC stands from derrick, and install piccolo at 199 mbrf.	515	24 Apr	1.50	0.06	170.25	7.09	Start Run 4: 9-7/8 inch tricone bit (Atlas HP61).
Service rig.	645	24 Apr	0.50	0.02	170.75	7.11	
Resume tripping drill string 199–1596 mbrf.	715	24 Apr	3.25	0.14	174.00	7.25	
Slip and cut 115 ft of drilling line.	1030	24 Apr	1.50	0.06	175.50	7.31	
Resume tripping drill string 1596–2731 mbrf.	1200	24 Apr	2.50	0.10	178.00	7.42	
Deploy VIT.	1430	24 Apr	0.50	0.02	178.50	7.44	
Continue RIH DP 2731–3636 mbrf.	1500	24 Apr	1.75	0.07	180.25	7.51	
Search and position vessel. Reenter Hole 1256D at 1655 h.	1645	24 Apr	0.25	0.01	180.50	7.52	Reentry 4.
Continue RIH drill string to 315.7 mbsf.	1700	24 Apr	0.50	0.02	181.00	7.54	
Recover VIT.	1730	24 Apr	0.75	0.03	181.75	7.57	
Continue RIH DP and tag bridge at 922 mbsf.	1815	24 Apr	1.25	0.05	183.00	7.62	
Pull back in hole to 890.6 mbsf.	1930	24 Apr	0.25	0.01	183.25	7.64	
Pick up top drive and RIH with same to 922.0 mbsf.	1945	24 Apr	1.00	0.04	184.25	7.68	
Attempt to wash/ream though bridge encountering high erratic torque; top drive max current = 650 A.	2045	24 Apr	1.00	0.04	185.25	7.72	
Pull back in hole with top drive to 890.6 mbsf.	2145	24 Apr	0.50	0.02	185.75	7.74	Decision to pump more cement.
Rack top drive.	2215	24 Apr	0.50	0.02	186.25	7.76	
POOH drill string from 890.6 to the surface. Clear seafloor at 0030 h. Bit at rotary table at 0615 h.	2245	24 Apr	7.50	0.31	193.75	8.07	Clear seafloor at 0300 h. End Run 4 at 0615 h.
Make up cementing bit (Reed type 517) without nozzles to 2 DC stands; RIH to 2661 mbrf.	615	25 Apr	6.00	0.25	199.75	8.32	Start Run 5: cementing bit (Reed type 517).
Deploy VIT.	1215	25 Apr	0.50	0.02	200.25	8.34	
Resume RIH drill string 2661–3637.8 mbrf.	1245	25 Apr	1.50	0.06	201.75	8.41	
Search and position vessel. Reenter Hole 1256D (Reentry #5) at 1445 h.	1415	25 Apr	0.50	0.02	202.25	8.43	Reentry 5.
Continue RIH drill string to 922 mbsf.	1445	25 Apr	2.50	0.10	204.75	8.53	
Install circulating head. Pressure test cement system.	1715	25 Apr	0.75	0.03	205.50	8.56	
Mix and pump 50 bbl of 15 ppg cement slurry.	1800	25 Apr	0.75	0.03	206.25	8.59	Pump cement.
Displace cement slurry with seawater.	1845	25 Apr	0.25	0.01	206.50	8.60	

Table T3 (continued). (Continued on next page.)

Operation	Start		Expedition (from departure time)				Comments
			Duration		Time (cumulative)		
	Local time (h)	Date (2011)	h	day	h	day	
Lay out circulating head and pull back in hole to 720.5 mbsf.	1900	25 Apr	0.75	0.03	207.25	8.64	
Circulate and flush drill pipe with seawater (3× drill string volume).	1945	25 Apr	1.00	0.04	208.25	8.68	
POOH drill string to surface. Clear the top of the cone at 2215 h. Bit at rotary table at 0345 h.	2045	25 Apr	7.00	0.29	215.25	8.97	Clear seafloor at 2215 h. End Run 5 at 0345 h.
Lay down Reed bit and pick up 9-7/8 inch Atlas HP61 tricone bit with tandem set of boot baskets and 2 DC stands; RIH to 200.6 mbrf.	345	26 Apr	1.75	0.07	217.00	9.04	Start Run 6: 9-7/8 inch Atlas HP61 tricone bit plus boot baskets.
Service rig: drawworks, crown, pipe stabber, traveling block, and dollies.	530	26 Apr	0.50	0.02	217.50	9.06	
Resume RIH 2676–3533 mbrf.	600	26 Apr	7.50	0.31	225.00	9.37	
Deploy VIT.	1330	26 Apr	0.50	0.02	225.50	9.40	
RIH drill string 3533–3638 mbrf.	1400	26 Apr	1.00	0.04	226.50	9.44	
Search and position vessel. Reenter Hole 1256D (Reentry #6) at 1520 h.	1500	26 Apr	0.25	0.01	226.75	9.45	Reentry 6.
Resume RIH drill string to 661.8 mbsf.	1515	26 Apr	1.75	0.07	228.50	9.52	
Recover VIT.	1700	26 Apr	0.50	0.02	229.00	9.54	
RIH drill string; make firm contact with cement at 882.0 mbsf.	1730	26 Apr	0.75	0.03	229.75	9.57	
Pick up top drive.	1815	26 Apr	0.50	0.02	230.25	9.59	
Drill out cement 882.0–922.0 mbsf. Circulate 40 bbl gel sweep at 904.6 mbsf.	1845	26 Apr	3.75	0.16	234.00	9.75	
Attempt to drill though bridge with high erratic torque. Circulate 50 bbl gel sweep at 922 mbsf. Continue to wash/ream at 922.0 mbsf. Top drive max current = 650 A.	2230	26 Apr	3.00	0.13	237.00	9.87	
Work stuck pipe at ~923 mbsf. Top drive max current = 800 A, overpull = 120,000 lb.	130	27 Apr	1.00	0.04	238.00	9.92	
Resume washing/reaming ledge at 922 mbsf with high rotary speed, high pump, and lighter WOB. We appeared to be making progress mid-morning only to lose it later in the day which may indicate that the obstruction is shifting. Circulate multiple 50 bbl hi-vis gel sweeps at 922 mbsf. Continue to wash/ream obstruction at 921.6 mbsf (tide ± 0.5 m). Circulate 100 bbl hi-vis gel sweep at 922.0 mbsf.	230	27 Apr	27.50	1.15	265.50	11.06	
Pull back with top drive 921.6–834.5 mbsf.	600	28 Apr	0.75	0.03	266.25	11.09	
Rack top drive.	645	28 Apr	0.50	0.02	266.75	11.11	
POOH from 834.5 mbsf and clear seafloor at 0850 h. Set back DC stands in the derrick and lay out junk baskets. Bit is at the rotary table at 1455 h. Lay out used bit in good condition with no appreciable shirttail wear, with all teeth intact, and exhibiting very little wear.	715	28 Apr	7.75	0.32	274.50	11.44	Clear seafloor at 0850 h. End Run 6 at 1455 h. Samples Run06-EXJB.
Make up new Smith tricone bit, bit sub with float, and 4 DC stands; RIH drill string to 2759 mbrf.	1500	28 Apr	5.75	0.24	280.25	11.68	Start Run 7: Smith tricone bit.
Slip and cut 115 ft of drilling line.	2045	28 Apr	1.50	0.06	281.75	11.74	
Install VIT.	2215	28 Apr	0.50	0.02	282.25	11.76	
Resume RIH drill string 2759–3640 mbrf. Fill DP every 10 stands.	2245	28 Apr	2.00	0.08	284.25	11.84	
Space out and position vessel to reenter Hole 1256D at 0135 h (Reentry #7).	045	29 Apr	0.75	0.03	285.00	11.88	Reentry 7.
RIH to 228.2 mbsf.	130	29 Apr	1.50	0.06	286.50	11.94	
Retrieve and recover VIT.	300	29 Apr	0.50	0.02	287.00	11.96	
Resume RIH 228.2–861.4 mbsf.	330	29 Apr	1.25	0.05	288.25	12.01	
Pick up top drive.	445	29 Apr	0.50	0.02	288.75	12.03	
RIH top drive 861.4–921.9 mbsf.	515	29 Apr	1.00	0.04	289.75	12.07	
Attempt to pass obstruction with pump and no rotation. No advance.	615	29 Apr	0.75	0.03	290.50	12.10	
Resume washing/reaming, drill though obstruction at 935.0 mbsf, and advance 921.9–941.5 mbsf. Circulate 100 bbl gel sweep at 931.0 mbsf.	700	29 Apr	17.00	0.71	307.50	12.81	Finally!

Table T3 (continued). (Continued on next page.)

Operation	Start		Expedition (from departure time)				Comments
			Duration		Time (cumulative)		
	Local time (h)	Date (2011)	h	day	h	day	
Continue washing/reaming 941.5–1143.2 mbsf. High torque and pump pressure increase of 500 psi when picking off slips at last connection. Circulate 50 bbl hi-vis gel sweeps at 988.6 and 1113.6 mbsf.	000	30 Apr	12.50	0.52	320.00	13.33	
Work back to 1114.4 mbsf and work out excess pump pressure and torque.	1230	30 Apr	1.50	0.06	321.50	13.40	
Resume washing/reaming 1143.2–1162.4 mbsf. High torque 500 psi pump pressure increase when coming off slips on last connection.	1400	30 Apr	2.50	0.10	324.00	13.50	
Work stuck pipe free.	1630	30 Apr	2.00	0.08	326.00	13.58	
Wash/ream 1162.4–1507.1 mbsf. Circulate 50 bbl hi-vis gel sweeps at 1142.6 and 1253.6 mbsf. Find 6 m of hard fill.	1830	30 Apr	14.75	0.61	340.75	14.20	Bottom of the hole.
Circulate 100 bbl hi-vis gel sweep.	915	1 May	1.25	0.05	342.00	14.25	
Pull back in hole 1507.1–1265.0 mbsf.	1030	1 May	1.75	0.07	343.75	14.32	
Set back top drive.	1215	1 May	0.50	0.02	344.25	14.34	
Pull drill string back in hole 1265.0–890.5 mbsf.	1245	1 May	2.00	0.08	346.25	14.43	
Pick up top drive.	1445	1 May	0.75	0.03	347.00	14.46	
RIH drill string and top drive to 967.3 mbsf with no drag or overpull.	1530	1 May	1.00	0.04	348.00	14.50	
Break circulation and spot 60 bbl of 10.5 ppg mud at 967 mbsf.	1630	1 May	0.50	0.02	348.50	14.52	
Pull back in hole with top drive to 861.7 mbsf.	1700	1 May	0.75	0.03	349.25	14.55	
Rack top drive.	1745	1 May	0.50	0.02	349.75	14.57	
POOH with top drive. Clear the top of the cone at 2005 h. Continue to POOH. Bit at rotary table at 0245 h.	1815	1 May	8.50	0.35	358.25	14.93	Clear seafloor at 2005 h. End Run 7 at 0245 h.
Make up cement BHA with used Reed 9-7/8 inch bit (without jets); RIH to 144 mbrf.	245	2 May	0.75	0.03	359.00	14.96	Start Run 8: cementing bit (used Reed 9-7/8 inch).
Service rig.	330	2 May	0.50	0.02	359.50	14.98	
RIH 144–2676 mbrf. Fill DP every 10 stands.	400	2 May	5.00	0.21	364.50	15.19	
Launch VIT.	900	2 May	0.75	0.03	365.25	15.22	
Resume RIH 2676–3637 mbrf.	945	2 May	3.00	0.13	368.25	15.34	
Search and position vessel. Reenter Hole 1256D at 1300 h.	1245	2 May	0.25	0.01	368.50	15.35	Reentry 8.
Resume RIH to 490.3 mbsf.	1300	2 May	1.25	0.05	369.75	15.41	
Recover VIT.	1415	2 May	0.50	0.02	370.25	15.43	
Continue RIH drill pipe to 960.5 mbsf.	1445	2 May	1.50	0.06	371.75	15.49	
Make up circulating head and pressure test same to 2000 psi.	1615	2 May	0.50	0.02	372.25	15.51	
Mix and pump 60 bbl of 15 ppg cement slurry.	1645	2 May	0.50	0.02	372.75	15.53	
Displace cement with seawater.	1715	2 May	0.50	0.02	373.25	15.55	
Lay out circulating head and pull back in hole to 605.5 mbsf.	1745	2 May	1.00	0.04	374.25	15.59	
Flush drill string with seawater (3x DP volume).	1845	2 May	1.00	0.04	375.25	15.64	
POOH drill string. Clear seafloor at 2105 h. Bit at rotary table at 0315 h.	1945	2 May	7.50	0.31	382.75	15.95	Clear seafloor at 0315 h. End Run 8 at 0315 h.
Lay out Reed tricone bit, pick up RCB assembly, and RIH to 200 mbrf. Space out RCB assembly.	315	3 May	2.75	0.11	385.50	16.06	Start Run 9: RCB assembly.
Service rig and RIS load pin transmitters.	600	3 May	0.50	0.02	386.00	16.08	
RIH DP 200–2732 mbrf.	630	3 May	4.00	0.17	390.00	16.25	
Deploy VIT.	1030	3 May	0.50	0.02	390.50	16.27	
Resume RIH 2732–3637 mbrf.	1100	3 May	1.25	0.05	391.75	16.32	
Search and position for reentry. Reenter Hole 1256D (Reentry #8) at 1235 h.	1215	3 May	0.25	0.01	392.00	16.33	Reentry 9.
RIH DP to 690.2 mbsf.	1230	3 May	1.25	0.05	393.25	16.39	
RIH DP and tag contact (ledge or top of plug) at 924.0 mbsf.	1345	3 May	1.25	0.05	394.50	16.44	
Pull back in hole 924.0–891.5 mbsf.	1500	3 May	0.25	0.01	394.75	16.45	
Pick up top drive.	1515	3 May	0.75	0.03	395.50	16.48	

Table T3 (continued). (Continued on next page.)

Operation	Start		Expedition (from departure time)				Comments
			Duration		Time (cumulative)		
	Local time (h)	Date (2011)	h	day	h	day	
Drill nonmagnetic core barrels and drop same. Establish SCR parameters.	1600	3 May	1.75	0.07	397.25	16.55	
Cut cement Cores 1G–5G (924.0–971.3 mbsf).	1745	3 May	12.25	0.51	409.50	17.06	
Pull back in hole to 833.9 mbsf.	600	4 May	0.75	0.03	410.25	17.09	
Rack top drive.	645	4 May	0.50	0.02	410.75	17.11	
Slip and cut 115 ft of drilling line.	715	4 May	1.50	0.06	412.25	17.18	
Drop wash barrel.	845	4 May	0.25	0.01	412.50	17.19	
RIH 833.9–949.1 mbsf.	900	4 May	0.50	0.02	413.00	17.21	
Pick up top drive.	930	4 May	0.50	0.02	413.50	17.23	
Continue to RIH with top drive 949.1–971.3 mbsf.	1000	4 May	0.50	0.02	414.00	17.25	
Round trip wash barrel and core 6G (971.3–980.9 mbsf).	1030	4 May	3.00	0.13	417.00	17.38	
Drop wash barrel and wash 980.9–1507.1 mbsf. Note tight hole at 1499.6–1501.1 mbsf. Pump 50 bbl hi-sweeps at 1154.6 and 1501.1 mbsf.	1330	4 May	9.25	0.39	426.25	17.76	
Circulate 50 bbl hi-vis gel sweep.	2245	4 May	1.00	0.04	427.25	17.80	
Deploy sinker bars. Round trip wash barrel at 1497.0 mbsf. Drop fresh core barrel.	2345	4 May	2.00	0.08	429.25	17.89	
RCB cores 235R–236R (1507.1–1516.5 mbsf), employing half-cores with no liners to improve recovery. All cores obtained with nonmagnetic core barrels.	145	5 May	15.25	0.64	444.50	18.52	First 335 core! 235R (7%); 236R (13%).
Attempt to core 237R (1516.5–1518.2 mbsf); max overpull = 60,000 lb, top drive max current = 800 A, WOB = 0.	1700	5 May	3.50	0.15	448.00	18.67	
RIH coring line and retrieve Core 237R (1516.5–1518.2 mbsf). Circulate 50 and 100 bbl hi-vis gel sweeps at 1518.2 mbsf.	2030	5 May	1.25	0.05	449.25	18.72	237R (empty).
Drop core barrel and attempt to core 238R (1518.2–1520.2 mbsf; tidal = ±0.8 m). Pump 50 bbl hi-vis sweep at 1520.2 mbsf. Average ROP for May 5 = 0.7 m/h.	2145	5 May	14.25	0.59	463.50	19.31	
RIH sinker bars and recover core barrel containing 20 cm roller.	1200	6 May	1.50	0.06	465.00	19.38	238R.
Drop bit deplugger. Core catcher sub was ~0.5 inch abraded, indicating downhole mechanical problem.	1330	6 May	0.50	0.02	465.50	19.40	
RIH sinker bars and recover deplugger. Lay out same. Pump 70 bbl of 10.5 ppg mud.	1400	6 May	1.25	0.05	466.75	19.45	
Rack top drive.	1515	6 May	1.50	0.06	468.25	19.51	
Pull back in hole with drill string to 58.2 mbsf.	1645	6 May	3.75	0.16	472.00	19.67	
Flush drill string with seawater to clean reentry cone of cuttings.	2030	6 May	0.50	0.02	472.50	19.69	
POOH DP to the surface. Clear seafloor at 2115 h. Clear rotary table at 0545 h. Bit body honed to a smooth profile at bottom and sides. Bit missing all 4 cones, 4 legs, and core guides. Bit spiral stabilizer blades and embedded TCI inserts absent. Bit totally unrecognizable.	2100	6 May	8.75	0.36	481.25	20.05	Clear seafloor at 2115 h. End Run 9 at 0545 h. Bit disintegrated.
Prepare and make up Bowen 9 inch fishing magnet with 2 boot baskets to 2 stands of DC; RIH to 147 mbrf.	545	7 May	3.00	0.13	484.25	20.18	Start Run 10: Bowen 9 inch fishing magnet plus two junk baskets.
Service rig.	845	7 May	0.50	0.02	484.75	20.20	
Resume RIH 147–2680 mbrf.	915	7 May	5.00	0.21	489.75	20.41	
Install VIT.	1415	7 May	0.50	0.02	490.25	20.43	
Resume RIH drill string 2680–3632 mbrf.	1445	7 May	1.75	0.07	492.00	20.50	
Search and position vessel for reentry. Observe reentry cone clouded over with mud. Attempt reentry, miss cone, and pull back. Break circulation and reenter (Reentry #10) at 1815 h.	1630	7 May	1.75	0.07	493.75	20.57	Reentry 10.
RIH drill string to 580.1 mbsf.	1815	7 May	1.25	0.05	495.00	20.63	
Recover VIT.	1930	7 May	0.50	0.02	495.50	20.65	
RIH DP 580.1–1294.6 mbsf. Contact ledge that takes 10,000 lb.	2000	7 May	2.25	0.09	497.75	20.74	

Table T3 (continued). (Continued on next page.)

Operation	Start		Expedition (from departure time)				Comments
			Duration		Time (cumulative)		
	Local time (h)	Date (2011)	h	day	h	day	
Pick up top drive.	2215	7 May	0.50	0.02	498.25	20.76	
RIH top drive 1328.7–1434.2 mbsf. Tight hole at 1328.7 mbsf takes 10,000 lb. Excessive rotary current at 20 spm. Note increase in pump pressure (2500 psi at 20 spm). Bleed off pressure at rig floor.	2245	7 May	3.00	0.13	501.25	20.89	
Pull back in hole 1434.2–1395.8 mbsf and attempt to unplug drill string with high pressure. No joy.	145	8 May	1.25	0.05	502.50	20.94	
Pull back in hole 1395.8–1242.3 mbsf with top drive.	300	8 May	1.50	0.06	504.00	21.00	
Rack top drive.	430	8 May	0.50	0.02	504.50	21.02	
Pull back in hole 1242.3–264.2 mbsf to just inside casing shoe.	500	8 May	2.00	0.08	506.50	21.10	
Attempt to circulate with circulating head. No joy.	700	8 May	0.25	0.01	506.75	21.11	
POOH from 264.2 mbsf, clear seafloor at 0755 h. Recover drill string and set back 2 stands of DC. Find 4 m of fine cuttings plugging inside of bit sub and the 2 junk baskets. Clean out same. Lay out magnet, which is at the rotary table at 1555 h.	715	8 May	8.75	0.36	515.50	21.48	Clear seafloor at 0755 h. End Run 10 at 1555 h. Bit sub and junk basket filled with cuttings. Samples Run10-DC, Run10-EXJB, and Run10-FM.
Make up Atlas tricone bit to dual set of junk baskets with 3 DC stands and deploy to 2704 mbrf.	1600	8 May	8.00	0.33	523.50	21.81	Start Run 11: Atlas tricone bit plus junk baskets.
Launch VIT.	000	9 May	1.00	0.04	524.50	21.85	
Continue RIH DP 2704–3637 mbrf. Fill every 10 stands.	100	9 May	2.00	0.08	526.50	21.94	
Space out and reenter Hole 1256D at 0315 h (Run 11).	300	9 May	0.25	0.01	526.75	21.95	Reentry 11.
Continue RIH to 461.2 mbsf.	315	9 May	1.00	0.04	527.75	21.99	
Recover VIT.	415	9 May	0.50	0.02	528.25	22.01	
Resume RIH 461.2–1356.1 mbsf where bit contacts ledge. Pull back to 1324.3 mbsf.	445	9 May	2.50	0.10	530.75	22.11	
Pick up top drive and obtain SCR parameters.	715	9 May	0.50	0.02	531.25	22.14	
Clean up ledge at 1356.1 mbsf and continue in hole to 1442.5 mbsf.	745	9 May	1.50	0.06	532.75	22.20	
Circulate 100 bbl hi-vis gel sweep at 1442.5 mbsf.	915	9 May	0.75	0.03	533.50	22.23	
RIH 1442.5–1520.3 mbsf. Clean up undergauge areas of hole with top drive max current = 500 A.	1000	9 May	1.50	0.06	535.00	22.29	
Circulate 100 bbl hi-vis gel sweep at 1520.3 mbsf.	1130	9 May	0.50	0.02	535.50	22.31	
Continue to circulate hole clean and work rathole at 1520.3 mbsf. Circulate 100 bbl hi-vis gel sweep and circulate seawater (3× volume of annulus).	1200	9 May	4.25	0.18	539.75	22.49	
Pull back in hole with top drive 1520.3–1363.0 mbsf.	1615	9 May	1.50	0.06	541.25	22.55	
RIH with top drive and tag ledge at 1473 mbsf. Work though ledge with pumps and rotation. Observe excess pump pressure and torque off slips at 1477.5 mbsf. Unable to pump. Reestablish rotation and circulation.	1745	9 May	1.75	0.07	543.00	22.62	
Work pipe 1477.5–1459.0 mbsf. Clear excess pump pressure and torque. Top drive max current = 700 A; max pump pressure = 3000 psi.	1930	9 May	0.75	0.03	543.75	22.66	
RIH with top drive and ream 1477.6–1484.6 mbsf. Continue to RIH with top drive to 1518.2 mbsf.	2015	9 May	2.50	0.10	546.25	22.76	
Pump 150 bbl gel sweep at 1518.2 mbsf.	2245	9 May	2.25	0.09	548.50	22.85	
Pull back in hole with top drive 1518.2–1324.6 mbsf.	100	10 May	1.50	0.06	550.00	22.92	
Set back top drive.	230	10 May	0.50	0.02	550.50	22.94	
Resume pulling back in hole 1324.6–78.2 mbsf.	300	10 May	2.50	0.10	553.00	23.04	
Flush top of cone with seawater.	530	10 May	0.25	0.01	553.25	23.05	
POOH drill string from 78.2 mbsf. Clear seafloor at 0605 h. Bit at rotary table at 1130 h.	545	10 May	5.75	0.24	559.00	23.29	Clear seafloor at 0605 h. End Run 11 at 1130 h.
Empty junk baskets and lay out tricone.	1130	10 May	0.75	0.03	559.75	23.32	Nice cuttings in junk baskets. Samples Run11-EXJB.

Table T3 (continued). (Continued on next page.)

Operation	Start		Expedition (from departure time)				Comments
			Duration		Time (cumulative)		
	Local time (h)	Date (2011)	h	day	h	day	
Make up Bowen reverse circulating junk basket, 1 junk basket, and 2 DC stands; RIH to 2679 mbrf.	1215	10 May	7.25	0.30	567.00	23.62	Start Run 12: Bowen reverse circulation junk basket.
Slip and cut 115 ft of drilling line.	1930	10 May	1.50	0.06	568.50	23.69	
Install VIT.	2100	10 May	0.75	0.03	569.25	23.72	
Resume RIH drill string 2679–3640 mbrf.	2145	10 May	1.50	0.06	570.75	23.78	
Search and position vessel. Reenter Hole 1256D at 2330 h (Reentry #12).	2315	10 May	0.08	0.00	570.83	23.78	Reentry 12.
RIH to 808.7 mbsf.	2320	10 May	1.67	0.07	572.50	23.85	
Recover VIT.	100	11 May	0.50	0.02	573.00	23.87	
Resume RIH 808.7–1327.5 mbsf.	130	11 May	1.00	0.04	574.00	23.92	
Pick up top drive.	230	11 May	0.50	0.02	574.50	23.94	
Obtain SCR parameters and RIH 1327.5–1517.9 mbsf.	300	11 May	3.50	0.15	578.00	24.08	
Clean hole. Circulate at 150 spm with 1600 psi. Find 2.5 m of fill.	630	11 May	2.00	0.08	580.00	24.17	
Pump 100 bbl hi-vis sweep and chase with seawater (1.5x drill string volume).	830	11 May	1.00	0.04	581.00	24.21	
Drop stainless steel ball at 0937 h and activate reverse circulation in Bowen junk basket.	930	11 May	0.50	0.02	581.50	24.23	RCJB.
Attempt to drill over junk at the bottom of the hole.	1000	11 May	0.50	0.02	582.00	24.25	
Pull back in hole 1516.1–1328.6 mbsf.	1030	11 May	1.50	0.06	583.50	24.31	
Rack top drive.	1200	11 May	0.50	0.02	584.00	24.33	
POOH 1328.6–58.9 mbrf. Clear top of cone at 1520 h.	1230	11 May	9.00	0.38	593.00	24.71	Clear seafloor at 1520 h. End Run 12 at 2200 h. Samples Run12-DC, Run12-EXJB, Run12-RCJB.
Find BHA DC up to tapered DC filled with fine cuttings (50 m) weighing several hundred kg. Individually clear each DC and provide contents to scientists. Coarser gravel found in the head, crossover, and bit subs. Empty and clean out the Bowen tool containing ~20 kg of granoblastic dike rocks.	2130	11 May	8.00	0.33	601.00	25.04	Big rock samples, no cone.
Service rig.	530	12 May	0.50	0.02	601.50	25.06	
Make up Bowen tool with single junk basket and 2 DC stands; RIH to 2678 mbrf.	600	12 May	5.50	0.23	607.00	25.29	Start Run 13: Bowen RCJB.
Launch VIT.	1130	12 May	0.50	0.02	607.50	25.31	
Resume RIH 2678–3631 mbrf.	1200	12 May	1.25	0.05	608.75	25.36	
Search and position vessel. Reenter Hole 1256D at 1335 h.	1315	12 May	0.25	0.01	609.00	25.37	Reentry 13.
RIH DP to 664.8 mbsf.	1330	12 May	1.50	0.06	610.50	25.44	
Recover VIT.	1500	12 May	0.50	0.02	611.00	25.46	
Resume RIH 664.8–1384.8 mbsf.	1530	12 May	1.50	0.06	612.50	25.52	
Pick up top drive.	1700	12 May	0.50	0.02	613.00	25.54	
RIH with top drive and rotation and circulation past a soft tag at 1465.0 mbsf and a hard tag at 1518.0 mbsf. Backflow on connections starting at 1470.0 mbsf.	1730	12 May	2.75	0.11	615.75	25.66	
Work drill string to 1518.0 mbsf and fail in an attempt to penetrate to 1520.2 mbsf with max WOB = 2000–4000 lb and 160 spm at 1600 psi. Top drive current = 200–400 A. Circulate 100 bbl hi-vis sweep. Chase same with seawater (2× drill string volume).	2015	12 May	2.00	0.08	617.75	25.74	
Drop stainless steel ball to activate reverse circulation. Unable to shear pins in tool with pump pressure as high as 3000 psi at 50 spm.	2215	12 May	0.75	0.03	618.50	25.77	
Pull back in hole with top drive to 1327.3 mbsf.	2300	12 May	1.75	0.07	620.25	25.84	
Rack top drive.	045	13 May	0.50	0.02	620.75	25.86	

Table T3 (continued). (Continued on next page.)

Operation	Start		Expedition (from departure time)				Comments
			Duration		Time (cumulative)		
	Local time (h)	Date (2011)	h	day	h	day	
POOH from 1327.3 mbsf and clear seafloor at 0340 h. Bowen junk basket at rotary table at 1100 h. Basket contains granoblastic dike rocks as large as 3.4 kg. Apparently the Bowen tool was activated by the stainless steel ball. The loss of circulation was probably due to clogged jets. Almost the entire BHA was filled with fine cuttings again.	115	13 May	9.75	0.41	630.50	26.27	Clear seafloor at 0340 h. End Run 13 at 1100 h. Samples Run13-DC, Run13-EXJB, Run13-RCJB.
Dismantle Bowen reverse circulating junk basket and clean all components and service.	1100	13 May	1.75	0.07	632.25	26.34	
Lay down Bowen tool and pick up Homco 9.75 inch flow-though junk basket with bit sub junk basket and float, 2-stand BHA, and boot basket. Lay out 1 joint of 5-1/2 inch of transition pipe. RIH to 2670 mbrf.	1245	13 May	7.75	0.32	640.00	26.67	Start Run 14: Homco 9.75 inch flow-though junk basket with bit sub junk basket and float.
Deploy VIT.	2030	13 May	0.75	0.03	640.75	26.70	
RIH DP 2670–3631 mbrf.	2115	13 May	1.75	0.07	642.50	26.77	
Search and position vessel. Reenter Hole 1256D at 2315 h (Reentry #14).	2300	13 May	0.25	0.01	642.75	26.78	Reentry 14.
RIH drill string to 512.1 mbsf.	2315	13 May	1.50	0.06	644.25	26.84	
Recover VIT.	045	14 May	2.25	0.09	646.50	26.94	
Resume RIH 512.1–1404.3 mbsf.	300	14 May	0.50	0.02	647.00	26.96	
Continue RIH 1404.3–1517.2 mbsf.	330	14 May	2.25	0.09	649.25	27.05	
Pump 100 bbl sweep and continue to work down to top of fish at 1521.0 mbsf.	545	14 May	2.50	0.10	651.75	27.16	
Attempt to recover junk/fish.	815	14 May	0.50	0.02	652.25	27.18	
Circulate 50 bbl sweep at 1520.0 mbsf.	845	14 May	1.00	0.04	653.25	27.22	
Pull back in hole with top drive 1519.2–1404.6 mbsf.	945	14 May	0.75	0.03	654.00	27.25	
Rack top drive.	1030	14 May	0.50	0.02	654.50	27.27	
POOH with drill string and clear seafloor at 1345 h. Rack back DC in derrick. Homco FTJB clears rotary at 2010 h.	1100	14 May	9.25	0.39	663.75	27.66	Clear seafloor at 1345 h. End Run 14 at 2010 h. Samples Run14-EXJB, BSJB, FTJB.
Empty FTJB of 2 rocks (combined weight = 3.2 kg). Lower set of junk catcher fingers completely torn out.	2015	14 May	0.75	0.03	664.50	27.69	
Make up new Smith hard formation 9-7/8 inch tricone bit with single junk basket to 3-stand BHA and RIH to 84 mbrf.	2100	14 May	1.25	0.05	665.75	27.74	Start Run 15: Smith hard formation 9-7/8 inch tricone bit with single junk basket.
Slip and cut 115 ft of drilling line.	2215	14 May	1.50	0.06	667.25	27.80	
RIH with 5-1/2 inch transition pipe to 132.9 mbrf.	2345	14 May	0.25	0.01	667.50	27.81	
Service rig.	000	15 May	0.50	0.02	668.00	27.83	
Resume RIH 5-1/2 inch transition pipe 133–2694 mbrf, filling every 10 stands.	030	15 May	4.50	0.19	672.50	28.02	
Deploy VIT.	500	15 May	0.50	0.02	673.00	28.04	
Resume RIH 2694–3924 mbrf. Reenter Hole 1256D (Reentry #15) at 0730 h and RIH to 278.5 mbsf	530	15 May	3.00	0.13	676.00	28.17	Reentry 15.
Recover VIT.	830	15 May	0.50	0.02	676.50	28.19	
RIH 278.5–1371.8 mbsf.	900	15 May	3.25	0.14	679.75	28.32	
Pick up top drive.	1215	15 May	0.50	0.02	680.25	28.34	
Resume RIH from 1371.8 mbsf. Tag soft fill at 1510.0 mbsf and hard tag at 1518.8 mbsf.	1245	15 May	1.50	0.06	681.75	28.41	
Pick up 30 ft knobby and work bit with light WOB at 1518.5 mbsf and then down to 1520.6 mbsf multiple times, attempting to stabilize the bottom 2–3 m of the hole. Hole packs off below 1518.0 mbsf and requires working back to bottom. Circulate multiple mud sweeps at 1520.6 mbsf (total = 400 bbl). Continue to work drill string 1518.5–1521.05 mbsf. Pump 200 bbl of sweeps. Pull drill string to inspect and change the bit.	1415	15 May	16.00	0.67	697.75	29.07	

Table T3 (continued). (Continued on next page.)

Operation	Start		Expedition (from departure time)				Comments
			Duration		Time (cumulative)		
	Local time (h)	Date (2011)	h	day	h	day	
Pull back in hole with top drive 1515.5–1410.1 mbsf.	615	16 May	1.25	0.05	699.00	29.12	
Rack top drive.	730	16 May	0.50	0.02	699.50	29.15	
POOH drill string and clear seafloor at 1015 h. Rack back 3 stands. Bit clears rotary table at 1545 h. Inspect bit and find bearings still tight with virtually no wear on teeth except for a single chipped tooth on the heel. Bit is under gauge by 0.4 inches with some shirttail wear and minor junk damage on body.	800	16 May	7.75	0.32	707.25	29.47	Clear seafloor at 1015 h. End Run 15 at 1545 h. Samples Run15-EXJB.
Clean out junk basket.	1545	16 May	0.50	0.02	707.75	29.49	
Make up new 9-7/8 inch Smith FH3VPS tricone to a 3-stand BHA; RIH to 2693 mbrf.	1615	16 May	7.75	0.32	715.50	29.81	Start Run 16: 9-7/8 inch Smith FH3VPS tricone bit.
Deploy VIT.	000	17 May	0.50	0.02	716.00	29.83	
Resume RIH 2693–3644 mbrf.	030	17 May	2.00	0.08	718.00	29.92	
Space out to reenter. Reenter Hole 1256D at 0245 h (Reentry #16).	230	17 May	0.25	0.01	718.25	29.93	Reentry 16.
Resume RIH to 507.2 mbsf. Fill pipe every 10 stands.	245	17 May	1.25	0.05	719.50	29.98	
Recover VIT.	400	17 May	0.50	0.02	720.00	30.00	
Continue RIH 507.2–1399.7 mbsf.	430	17 May	2.00	0.08	722.00	30.08	
Pick up top drive.	630	17 May	0.50	0.02	722.50	30.10	
RIH 1399.7–1516.5 mbsf.	700	17 May	1.25	0.05	723.75	30.16	
Wash/ream 1516.5–1519.7 mbsf. Circulate 60 bbl sweep at 1516.7 mbsf. Flush hole with 200 bbl mud at 1519.6 mbsf.	815	17 May	16.00	0.67	739.75	30.82	
Pull back in hole with top drive 1519.6–1399.7 mbsf.	015	18 May	0.75	0.03	740.50	30.85	
Rack top drive.	100	18 May	0.50	0.02	741.00	30.87	
POOH drill string. Clear seafloor at 0340 h. Bit at rotary table at 0900 h. Lay out used tricone bit (in gauge) and minus 6 teeth on one cone.	130	18 May	7.50	0.31	748.50	31.19	Clear seafloor at 0340 h. End Run 16 at 0900 h.
Make up 9-5/8 inch flat-bottomed mill with EXJB and 3-stand BHA and RIH to 162 mbrf.	900	18 May	1.50	0.06	750.00	31.25	Start Run 17: 9-5/8 inch flat-bottomed mill with EXJB.
Service rig.	1030	18 May	0.50	0.02	750.50	31.27	
Resume RIH 162–2695 mbrf.	1100	18 May	4.75	0.20	755.25	31.47	
Install VIT.	1545	18 May	0.50	0.02	755.75	31.49	
RIH 2695–3637 mbrf.	1615	18 May	2.50	0.10	758.25	31.59	
Search and position vessel. Reenter Hole 1256D at 1850 h.	1845	18 May	0.25	0.01	758.50	31.60	Reentry 17.
RIH drill string to 480.5 mbsf.	1900	18 May	1.25	0.05	759.75	31.66	
Recover VIT.	2015	18 May	0.50	0.02	760.25	31.68	
Resume RIH 480.5–1429.9 mbsf.	2045	18 May	2.75	0.11	763.00	31.79	
Pick up top drive.	2330	18 May	0.50	0.02	763.50	31.81	
Continue RIH with top drive 1429.9–1520.0 mbsf.	000	19 May	1.50	0.06	765.00	31.87	
Mill debris at 1520.0–1521.0 mbsf. Use junk basket pump sweeps. Pump 200 bbl sweep at 1520.0 mbsf.	130	19 May	12.00	0.50	777.00	32.37	
Circulate 100 bbl sweep and chase same with seawater (2× drill string volume).	1330	19 May	1.25	0.05	778.25	32.43	
Lay out 30 ft knobby and pull back in hole with top drive to 1429.9 mbsf.	1445	19 May	0.75	0.03	779.00	32.46	
Rack top drive.	1530	19 May	0.50	0.02	779.50	32.48	
POOH and clear seafloor at 1920 h. Offset vessel 50 m west and continue POOH to 2354 mbrf.	1600	19 May	5.50	0.23	785.00	32.71	Clear seafloor at 1920 h.
Slip and cut 115 ft of drilling line.	2130	19 May	1.50	0.06	786.50	32.77	
Resume POOH to surface. Used mill at rotary table at 0315 h.	2300	19 May	4.25	0.18	790.75	32.95	End Run 17 at 0315 h. Samples Run17-BSJB.
Lay out mill. Clean and lay out damaged junk basket. Mill heavily worn and under gauge by ~0.5 inches. Pick up new 9 inch flat mill with fresh junk basket; RIH to 162 mbrf.	315	20 May	2.25	0.09	793.00	33.04	Start Run 18: 9 inch flat mill with junk basket.

Table T3 (continued). (Continued on next page.)

Operation	Start		Expedition (from departure time)				Comments
			Duration		Time (cumulative)		
	Local time (h)	Date (2011)	h	day	h	day	
Service rig.	530	20 May	1.00	0.04	794.00	33.08	
Resume RIH 162–2694 mbrf while filling every 10 stands.	630	20 May	5.00	0.21	799.00	33.29	
Launch VIT.	1130	20 May	0.50	0.02	799.50	33.31	
Resume RIH 2694–3637 mbrf.	1200	20 May	1.75	0.07	801.25	33.39	
Search and position vessel. Reenter Hole 1256D (Reentry #18) at 1415 h.	1345	20 May	0.50	0.02	801.75	33.41	Reentry 18.
RIH drill string to 451.2 mbsf.	1415	20 May	1.25	0.05	803.00	33.46	
Recover VIT.	1530	20 May	0.50	0.02	803.50	33.48	
Resume RIH 451.2–1458.6 mbsf.	1600	20 May	2.25	0.09	805.75	33.57	
Pick up top drive.	1815	20 May	0.50	0.02	806.25	33.59	
RIH with top drive; tag fill at 1518.9 mbsf. Advance with low pump and rotary speed and tag hard fill at 1520.4 mbsf.	1845	20 May	1.00	0.04	807.25	33.64	
Mill junk and work junk basket. Pump 100 bbl sepiolite sweep; pump 120 bbl sweep at 1520.9 mbsf.	1945	20 May	6.00	0.25	813.25	33.89	
Pump 100 bbl sepiolite sweep and circulate out.	145	21 May	1.25	0.05	814.50	33.94	
Pull back in hole with top drive 1520.9–1429.8 mbsf.	300	21 May	1.00	0.04	815.50	33.98	
Rack top drive.	400	21 May	0.50	0.02	816.00	34.00	
POOH from 1520.9 mbsf and clear seafloor at 0645 h; milling tool at drill floor at 1225 h. The abrasive surface of the milling tool was eroded, with some external junk damage on the side of the tool and the crossover sub directly above the mill.	430	21 May	8.00	0.33	824.00	34.33	Clear seafloor at 0645 h.
Empty and clean out the external junk basket. In addition to the usual rock fragments and fine cuttings, some flakes of what appears to be freshly ground metal were also found.	1230	21 May	0.25	0.01	824.25	34.34	End Run 18 at 1225 h. Samples Run18-BSJB.
Make up RCJB with 3 EXJB and deploy along with a 2-stand BHA. RIH to 2670 mbrf.	1245	21 May	7.50	0.31	831.75	34.66	Start Run 19: RCJB plus 3 EXJB.
Install VIT.	2015	21 May	0.50	0.02	832.25	34.68	
RIH drill string to 3632 mbrf.	2045	21 May	1.50	0.06	833.75	34.74	
Search and position vessel. Reenter Hole 1256D (Run 19) at 2230 h.	2215	21 May	0.25	0.01	834.00	34.75	Reentry 19.
RIH DP to 599.6 mbsf.	2230	21 May	1.25	0.05	835.25	34.80	
Recover VIT.	2345	21 May	0.50	0.02	835.75	34.82	
Continue RIH 599.6–1405.7 mbsf.	015	22 May	1.25	0.05	837.00	34.87	
Pick up top drive.	130	22 May	0.50	0.02	837.50	34.90	
RIH 1405.7–1519.5 mbsf. Hard tag at 1519.5 mbsf.	200	22 May	1.25	0.05	838.75	34.95	
Work junk baskets.	315	22 May	0.50	0.02	839.25	34.97	
Pump 100 bbl sweep and chase same with seawater (2× annular volume). Continue to work junk baskets.	345	22 May	2.00	0.08	841.25	35.05	
Drop stainless steel ball in open pipe. Advance RCJB to 1520.5 mbsf with slow rotation and light WOB. Jog rotation attempting to catch debris.	545	22 May	1.25	0.05	842.50	35.10	
Pull back in hole with top drive 1520.5–1434.4 mbsf.	700	22 May	0.50	0.02	843.00	35.13	
Rack top drive.	730	22 May	0.50	0.02	843.50	35.15	
POOH with drill string and clear seafloor at 1015 h. Rack back BHA. RCJB at rotary table at 1645 h.	800	22 May	8.75	0.36	852.25	35.51	Clear seafloor at 1015 h.
Empty RCJB of congealed sepiolite and 4 large rocks (total weight = 8.9 kg; largest rock = 3.9 kg). Unload 3 EXJB of cuttings and a few small metal fragments.	1645	22 May	1.25	0.05	853.50	35.56	End Run 19 at 1645 h. Samples Run19-RCJB, BSJB, EXBJ.
Rebuild and make up RCJB and 3 EXJB with a 2-stand BHA and RIH to 1793 mbrf.	1800	22 May	6.00	0.25	859.50	35.81	Start Run 20: RCJB plus 3 EXJB.
Repair pneumatic supply lines for drawworks high clutch.	000	23 May	3.00	0.13	862.50	35.94	
Resume RIH 1793–2670 mbrf.	300	23 May	1.25	0.05	863.75	35.99	

Table T3 (continued). (Continued on next page.)

Operation	Start		Expedition (from departure time)				Comments
			Duration		Time (cumulative)		
	Local time (h)	Date (2011)	h	day	h	day	
Launch VIT.	415	23 May	0.50	0.02	864.25	36.01	
RIH 2670–3640 mbrf.	445	23 May	1.75	0.07	866.00	36.08	
Position vessel, space out, and reenter Hole 1256D at 0635 h.	630	23 May	0.25	0.01	866.25	36.09	Reentry 20.
RIH to 513.5 mbsf.	645	23 May	0.75	0.03	867.00	36.13	
Recover VIT.	730	23 May	0.50	0.02	867.50	36.15	
Resume RIH 513.5–1462.9 mbsf.	800	23 May	1.25	0.05	868.75	36.20	
Pick up top drive.	915	23 May	0.50	0.02	869.25	36.22	
Continue RIH 1462.9–1519.0 mbsf.	945	23 May	0.75	0.03	870.00	36.25	
Hard tag at 1519.5 mbsf (tide adjusted). Work external junk baskets.	1030	23 May	0.25	0.01	870.25	36.26	
Pump 100 bbl sweep followed by seawater (2× annular volume).	1045	23 May	1.75	0.07	872.00	36.33	
Drop stainless steel ball and activate RCJB. Note increase in pressure of 600 psi. Unable to pass hard tag at 1519.0 mbsf with max WOB = 7000 lb and very slow rotation.	1230	23 May	0.75	0.03	872.75	36.36	
Pull back in hole with top drive to 1462.9 mbsf.	1315	23 May	0.75	0.03	873.50	36.40	
Rack top drive.	1400	23 May	0.50	0.02	874.00	36.42	
POOH with drill string to 3042 mbrf. Clear seafloor at 1725 h.	1430	23 May	4.00	0.17	878.00	36.58	Clear seafloor at 1725 h.
Slip and cut 115 ft of drilling line.	1830	23 May	1.50	0.06	879.50	36.65	
Resume POOH from 3042 to surface. RCJB at the rotary table at 0215 h.	2000	23 May	6.25	0.26	885.75	36.91	
Lay out and empty RCJB and 3 EXJB. RCJB contained 3 rocks (total weight = 5.0 kg), one (1.4 kg) is gabbro. The angularity of the rocks indicates fresh deposition with a suspected origin somewhere in the bottommost 7 m of the hole. The external junk baskets contain gravel-sized cuttings to small pebbles.	215	24 May	2.75	0.11	888.50	37.02	End Run 20 at 0215 h. Samples Run20-RCJB, BSJB, EXJB.
Make up RCJB and 3 EXJB with 2-stand BHA; RIH to 131 mbrf.	500	24 May	0.75	0.03	889.25	37.05	Start Run 21: RCJB plus 3 EXJB.
Service rig.	545	24 May	0.50	0.02	889.75	37.07	
Continue RIH 131–2670 mbrf.	615	24 May	3.25	0.14	893.00	37.21	
Launch VIT.	930	24 May	0.50	0.02	893.50	37.23	
Resume RIH 2670–3640.0 mbrf. Reenter Hole 1256D at 1115 h (Reentry #21).	1000	24 May	1.25	0.05	894.75	37.28	Reentry 21.
Continue RIH to 340.9 mbsf.	1115	24 May	0.75	0.03	895.50	37.31	
Recover VIT.	1200	24 May	0.50	0.02	896.00	37.33	
Resume RIH 340.9–1434.4 mbsf.	1230	24 May	2.25	0.09	898.25	37.43	
Pick up top drive.	1445	24 May	0.50	0.02	898.75	37.45	
RIH with top drive and minimum pump/rotation. Tag soft fill at 1518.8 mbsf.	1515	24 May	1.00	0.04	899.75	37.49	
Wash to 1519.8 mbsf and work junk baskets.	1615	24 May	0.25	0.01	900.00	37.50	
Pump 100 bbl of sepiolite sweep mud and chase with 2× annular volume of seawater.	1630	24 May	1.50	0.06	901.50	37.56	
Drop stainless steel ball, activate RCJB, and work same.	1800	24 May	0.75	0.03	902.25	37.59	
Displace lower portion of annulus with 200 bbl of drill water in preparation for logging.	1845	24 May	0.75	0.03	903.00	37.63	
Pull back in hole with top drive to 1462.9 mbsf.	1930	24 May	0.50	0.02	903.50	37.65	
Rack top drive.	2000	24 May	0.50	0.02	904.00	37.67	
Pull back in hole with drill string to 53.2 mbsf.	2030	24 May	3.50	0.15	907.50	37.81	
Repair and replace damaged cam roller on DES.	000	25 May	1.00	0.04	908.50	37.85	
Resume POOH from 53.2 mbsf and clear seafloor at 0100 h.	100	25 May	6.00	0.25	914.50	38.10	Clear seafloor at 0100 h.
Disassemble and empty RCJB of 4 small cobbles. Empty 3 EXJBs and clean out the usual assortment of cuttings, etc.	700	25 May	1.25	0.05	915.75	38.16	End Run 21 at 0700 h. Samples Run21-RCJB, BSJB, EXJB.
Make up Bowen fishing magnet and 3 EXJB; RIH to 109.5 mbrf.	815	25 May	1.25	0.05	917.00	38.21	Start Run 22: fishing magnet plus 3 EXJB.
Service rig.	930	25 May	0.50	0.02	917.50	38.23	

Table T3 (continued). (Continued on next page.)

Operation	Start		Expedition (from departure time)				Comments
			Duration		Time (cumulative)		
	Local time (h)	Date (2011)	h	day	h	day	
Resume RIH 109.5–2612 mbrf.	1000	25 May	4.50	0.19	922.00	38.42	
Install VIT.	1430	25 May	0.50	0.02	922.50	38.44	
Continue RIH 2612–3632 mbrf.	1500	25 May	1.50	0.06	924.00	38.50	
Search and position vessel. Reenter Hole 1245D at 1645 h (Reentry #22).	1630	25 May	0.25	0.01	924.25	38.51	Reentry 22.
RIH to 427.1 mbsf.	1645	25 May	1.25	0.05	925.50	38.56	
Recover VIT.	1800	25 May	0.50	0.02	926.00	38.58	
Resume RIH 427.1–1462.6 mbsf.	1830	25 May	2.50	0.10	928.50	38.69	
Pick up top drive.	2100	25 May	0.50	0.02	929.00	38.71	
RIH with top drive; tag fill at 1519.0 mbsf.	2130	25 May	0.50	0.02	929.50	38.73	
Wash to 1520.0 mbsf. Work fishing magnet and junk baskets.	2200	25 May	0.50	0.02	930.00	38.75	
Displace lower annulus with 200 bbl of drill water.	2230	25 May	0.50	0.02	930.50	38.77	
Pull back with top drive to 1433.8 mbsf.	2300	25 May	0.75	0.03	931.25	38.80	
Rack top drive.	2345	25 May	0.50	0.02	931.75	38.82	
POOH with drill string and clear seafloor at 0230 h.	015	26 May	7.75	0.32	939.50	39.15	Clear seafloor at 0230 h.
Disassemble and empty EXJBs. Fishing magnet contained very little metal debris all of which was finely ground?!	800	26 May	1.00	0.04	940.50	39.19	End Run 22 at 0800 h. Samples Run22-FM, BSJB, EXJB.
Make up and deploy logging bit and DC and deploy same to 2923 mbrf.	900	26 May	6.50	0.27	947.00	39.46	Start Run 23: downhole measurements (logging bit).
Deploy VIT.	1530	26 May	0.50	0.02	947.50	39.48	
RIH drill string to 3638 mbrf.	1600	26 May	1.25	0.05	948.75	39.53	
Search and position vessel. Reenter Hole 1256D at 1725 h.	1715	26 May	0.25	0.01	949.00	39.54	Reentry 23.
RIH drill string to 203.3 mbsf. Pick up 2 knobbies and set EOP at 218.9 mbsf.	1730	26 May	1.25	0.05	950.25	39.59	
Recover VIT.	1845	26 May	1.25	0.05	951.50	39.65	
Rig up for logging.	2000	26 May	0.50	0.02	952.00	39.67	
Make up Log #1 (triple combo: GR/APS/HLDS/HRLA/GPIT)	2030	26 May	2.50	0.10	954.50	39.77	
Deploy Log #1 into the pipe at 2255 h. Reached the bottom of the hole at 1520.0 mbsf. Recover tool at 0700 h.	2300	26 May	8.00	0.33	962.50	40.10	
Disassemble triple combo. Make up second log (FMS-sonic). Deploy FMS-sonic into the pipe at 1050 h.	700	27 May	4.00	0.17	966.50	40.27	
Tool unable to exit pipe into hole. Recover FMS-sonic at 1410 h.	1100	27 May	3.25	0.14	969.75	40.41	
Replace damaged lower centralizer spring and redeploy FMS-sonic at 1500 h.	1415	27 May	0.75	0.03	970.50	40.44	
RIH FMS-sonic. Tool appears to jam inside BHA with lower section (~20 m) of unit extending 20 m into open hole.	1500	27 May	1.50	0.06	972.00	40.50	FMS-sonic string jammed in logging bit.
Attempt to pump tool clear without success.	1630	27 May	1.75	0.07	973.75	40.57	
Make up Kinley cutter assemblies. Drop crimper into pipe at 2135 h.	1815	27 May	4.50	0.19	978.25	40.76	
Drop hammer into pipe at 2245 h.	2245	27 May	0.50	0.02	978.75	40.78	
Assemble Kinley severing tool and drop into pipe.	2315	27 May	2.00	0.08	980.75	40.86	
Drop hammer and server logging cable.	115	28 May	0.50	0.02	981.25	40.89	
Recover and tie back logging cable.	145	28 May	1.75	0.07	983.00	40.96	
POOH with drill string to 19 mbrf. Clear seafloor at 0425 h.	330	28 May	6.00	0.25	989.00	41.21	Clear seafloor at 0425 h.
Release jammed FMS-sonic tool from landing saver sub in BHA. Tool is in good condition.	930	28 May	2.50	0.10	991.50	41.31	End Run 23 at 0930 h. No FMS-sonic, no UBI.
Make up RCB 3-stand BHA with new RCB C-9 bit. Check core barrel space out and RIH to 134 mbrf.	1200	28 May	2.00	0.08	993.50	41.40	Start Run 24: Ulterra RCB-9 bit for coring and then cementing.
Slip and cut 115 ft of drilling line (#8 of expedition).	1400	28 May	1.50	0.06	995.00	41.46	
RIH drill string to 2695 mbrf.	1530	28 May	5.00	0.21	1000.00	41.67	
Launch VIT.	2030	28 May	0.50	0.02	1000.50	41.69	

Table T3 (continued).

Operation	Start		Expedition (from departure time)				Comments
			Duration		Time (cumulative)		
	Local time (h)	Date (2011)	h	day	h	day	
RIH drill string to 3638 mbrf.	2100	28 May	1.25	0.05	1001.75	41.74	
Search and position vessel. Reenter Hole 1256D at 2225 h (Reentry #24).	2215	28 May	0.25	0.01	1002.00	41.75	Reentry 24.
RIH drill string to 1430.5 mbsf.	2230	28 May	2.75	0.11	1004.75	41.86	
Recover VIT and coat line on the way out.	115	29 May	0.75	0.03	1005.50	41.90	
Pick up top drive and obtain SCR parameters.	200	29 May	0.50	0.02	1006.00	41.92	
RIH top drive 1430.5–1520.2 mbsf.	230	29 May	1.50	0.06	1007.50	41.98	
Circulate 100 bbl sweep at 1520.0 mbsf.	400	29 May	1.25	0.05	1008.75	42.03	
Drop fresh core barrel and rotary core 239R (1520.2–1521.6 mbsf) at average ROP = 0.6 m/h. Average recovery = 36%. No indication of metal in the core barrel. No symptoms of downhole junk in the coring process. Time for coring expires. Prepare for cementing. Circulate 50 bbl sweep at 1521.6 mbsf.	515	29 May	5.00	0.21	1013.75	42.24	Core 239R.
RIH coring line to 1510.6 mbsf and coat same on retrieval.	1015	29 May	1.75	0.07	1015.50	42.31	
Rack sinker bars and dress for layup period.	1200	29 May	0.25	0.01	1015.75	42.32	
Pull back in hole with top drive to 1487.8 mbsf. Rack top drive.	1215	29 May	1.00	0.04	1016.75	42.36	
Make up circulating head and pressure test same. Position bit at 1518.6 mbsf.	1315	29 May	0.50	0.02	1017.25	42.39	
Mix and pump 15 bbl of 15 ppg cement.	1345	29 May	0.50	0.02	1017.75	42.41	Cement plug 1 (BOH).
Displace cement with seawater.	1415	29 May	0.50	0.02	1018.25	42.43	
Lay out circulating head and pull back in hole to 1372.6 mbsf.	1445	29 May	0.50	0.02	1018.75	42.45	
Flush drill string with 2× annular volumes of seawater.	1515	29 May	1.00	0.04	1019.75	42.49	
Pull back with drill string to 940.8 mbsf.	1615	29 May	1.00	0.04	1020.75	42.53	
Mix and pump 58 bbl of 15 ppg cement slurry.	1715	29 May	1.00	0.04	1021.75	42.57	Cement plug 2 (910–940 mbsf).
Displace cement with seawater.	1815	29 May	0.50	0.02	1022.25	42.59	
Pull back with drill string to 739.3 mbsf.	1845	29 May	0.75	0.03	1023.00	42.63	
Flush drill string with 2× annular volumes of seawater.	1930	29 May	0.50	0.02	1023.50	42.65	
POOH with drill string. Clear top of cone at 2135 h. Disassemble BHA and stow DC in forward tubular racks.	2000	29 May	12.00	0.50	1035.50	43.15	Clear seafloor at 2135 h. End Run 24.
Recover beacons and secure vessel for sea.	800	30 May	3.50	0.15	1039.00	43.29	
Under way to Balboa, Panama. Advance clock 1 h on 31 May (1200 h).	1130	30 May	91.50	3.81	1130.50	47.10	End of Expedition 335.

Table based on R. Grout (Operations Superintendent) daily operations reports. Time breakdown is by nearest 0.25 h. BHA = bottom-hole assembly, MBR = mechanical bit release, VIT = vibration-isolated television, RIH = run in hole, WOB = weight on bit, POOH = pull out of hole, IADC = International Association of Drilling Contractors, EXJB = external junk basket, RCB = rotary core barrel, RIS = Rig Instrumentation System, ROP = rate of penetration, TCI = tungsten carbide inserts, DC = drill collar, DP = drill pipe, SCR = slow circulating rate, RCJB = reverse circulation junk basket, TDC = tapered drill collar, FTJB = flow-through junk basket, BSJB = bit sub junk basket, DES = dual-elevator stool on the rig floor, EOP = end of pipe, GR = natural gamma ray logging tool, APS = Accelerator Porosity Sonde, HLDS = Hostile Environment Litho-Density Sonde, HRLA = High-Resolution Laterolog Array, GPIT = General Purpose Inclinometry Tool, FMS-sonic = Formation MicroScanner sonic, UBI = Ultrasonic Borehole Imager, BOH = bottom of hole.

Table T4. Expedition 335 coring summary.

Core	Top depth drilled DSF (m)	Bottom depth drilled DSF (m)	Advanced (m)	Recovered length (m)	Curated length (m)	Top depth cored CSF (m)	Bottom depth recovered (m)	Recovery (%)	Date (2011)	Local time (h)	Numbers of sections
335-U1256D-											
1G	924.0	932.9	8.9	0.12	0.12	924.0	924.12	1	3 May	2120	1
2G	932.9	942.5	9.6	0.17	0.17	932.9	933.07	2	3 May	2345	1
3G	942.5	952.1	9.6	0.08	0.08	942.5	942.58	1	4 May	0150	1
4G	952.1	961.7	9.6	0.05	0.05	952.1	952.15	1	4 May	0350	1
5G	961.7	971.3	9.6	0.03	0.03	961.7	961.73	0	4 May	0545	1
6G	971.3	980.9	9.6	0.00	0.00	971.3	971.30	0	4 May	1315	0
7W	980.9	1507.1	526.2	0.00	0.00	980.9	980.90	0	5 May	0100	1
235R	1507.1	1511.8	4.7	0.33	0.36	1507.1	1507.47	7	5 May	0815	1
236R	1511.8	1516.5	4.7	0.61	0.63	1511.8	1512.43	13	5 May	1320	1
237R	1516.5	1518.2	1.7	0.00	0.00	1516.5	1516.50	0	5 May	2135	0
238R	1518.2	1520.2	2.0	0.20	0.20	1518.2	1518.00	10	6 May	1330	1
239R	1520.2	1521.6	1.4	0.50	0.53	1520.2	1520.73	36	29 May	1015	1
Totals:			597.6	2.09	2.18						10

Excerpted from LIMS reports.

Table T5. Key parameters for Hole 1256D and preliminary subdivisions of the upper oceanic crust at Site 1256 adopted for Expedition 335.

Location: 6°44.163′N, 91°56.061′W
Water depth (m): 3634.7; 3645.4 mbrf
Sediment thickness (m): 250
Interval in Hole 1256C drilled during Leg 206: 338.5 mbsf, 88.5 msb
Casing in Hole 1256D:
  Height of reentry cone: 2.4 m
  Internal diameter of reentry cone: 3.5 m (11 ft, 5 inches)
  20 inch casing string (m): 95.12
  16 inch casing string (m) 269
Interval in Hole 1256D drilled during
  Leg 206: 752 mbsf, 502 msb; basement advance (m): 502
  Expedition 309: 1255.1 mbsf, 1005.1 msb; basement advance (m): 503
  Expedition 312: 1507.1 mbsf, 1257.1 msb; basement advance (m): 252
  Expedition 335: 1521.6 mbsf, 1271.6 msb; basement advance (m): 14.5

Major lithologic zone	Sublithology	Top of lithology	Top igneous unit	Depth (mbsf)	Criteria
Lavas	Lava pond	206-1256D-2R-1, 0 cm	1256D-1 (1256C-1 through 1256C-18)	~250	Massive ponded lava including overlying sheet flows.
	Inflated flows	206-1256D-13R-1, 0 cm	1256D-2	350.3	Massive, sheet, and pillowed flows with rare inflation features.
	Sheet and massive flows	206-1256D-43R-1, 0 cm	1256D-16	533.9	Sheet flows with subordinate massive flows.
Transition zone		309-1256D-117R-1, 85 cm	1256D-40	1004.2	Sheet flows with breccia, rare dikes, and alteration at (sub)greenschist facies conditions.
Sheeted dike complex	Upper dikes	309-1256D-129R-1, 0 cm	1256D-44a	1060.9	Massive basalt, common subvertical intrusive contacts. Elevated *P*-wave velocity and thermal conductivity.
	Granoblastic dikes	312-1256D-192R-1, 0 cm	1256D-78	1348.3	Granoblastic texture; equant grains; secondary clinopyroxene, orthopyroxene, plagioclase, hornblende, magnetite, and ilmenite.
Plutonic section	Gabbro 1	312-1256D-213R-1 (Piece 13, 52 cm)	1256D-81	1406.62	Medium-grained, generally orthopyroxene-bearing gabbroic rocks intrude overlying dikes: olivine gabbro, gabbro, and (disseminated) oxide gabbro, intruded by oxide gabbro to oxide quartz diorite.
	Dike screen 1	312-1256D-225R-1 (Piece 1, 0 cm)	1256D-90	1458.9	Fine-grained to cryptocrystalline basalt dikes. Highly altered; granoblastic texture; secondary clinopyroxene, orthopyroxene, plagioclase, magnetite, ilmenite, and hornblende.
	Gabbro 2	312-1256D-230R-1 (Piece 5, 15 cm)	1256D-91	1483.1	Plutonic rock intrudes dike screen; medium-grained disseminated oxide gabbronorite with subordinate oxide gabbro, intruded by oxide gabbro, (oxide) diorite, and oxide quartz diorite veins; all highly altered; stoped basalt.
	Dike screen 2	312-1256D-232R-2 (Piece 9, 98 cm)	1256D-94	1494.9	Fine-grained granoblastic basalt (Unit 1256D-94) may have igneous or metamorphic origin. Unrecrystallized greenschist-facies late dike (Unit 1256D-95) at 1502.6 mbsf. Strongly to completely recrystallized granoblastic basalts containing minor oxide diorite patches; subordinate quartz diorite and tonalite (Unit 1256D-96). Also includes granoblastic basalts intruded by oxide gabbro to tonalite patches, veins, and dikelets and with minor (<3%) gabbroic rocks, from the "junkyards" at ~1500–1521.6 mbsf.

Table T6. Junk basket sample summary, Hole 1256D, Expedition 335. (Continued on next page.)

Date (2011)	Local time (h)	Top depth (mbsf)	Bottom depth (mbsf)	Volume (cc)	Sample	Comments
23 Apr	0600	0	923	3000	Run02-EXJB	Basaltic cuttings (2 bags; fine gravel to rounded pebbles)
28 Apr	0715	0	923	700	Run06-EXJB	Cuttings and rock pieces (1 bag + series of pebbles)
8 May	0715	0	1434	1500	Run10-DC	Fine cuttings from bit sub in BHA
8 May	0715	0	1434	2000	Run10-EXJB	Fine cuttings
8 May	0715	0	1434	100	Run10-EXJB	Rock pieces
8 May	0715	0	1434	1500	Run10-FM	Fine metal + rock cuttings from fishing magnet
8 May	0715	0	1434	100	Run10-FM	Mud from fishing magnet
10 May	1130	1353	1520	5000	Run11-EXJB	Fine cuttings to large pieces of rock, mostly granoblastic basalt (multiple bags; various grain size), some gabbro (1 bag of rock chips)
11 May	2130	1328	1518	5000	Run12-DC	Rock material (fine cuttings) from BHA
11 May	2130	1328	1518		Run12-EXJB	Fine cuttings and pebbles (2 bags granoblastic; 1 small bag gabbro)
11 May	2130	1516	1518	5000	Run12-RCJB	Fine cuttings and pebbles (multiple bags) and large cobbles (see list below)
11 May	2130	1516	1518	1512	Run12-RCJB-Rock A	Cobble (granoblastic)
11 May	2130	1516	1518	1058	Run12-RCJB-Rock B	Cobble (granoblastic)
11 May	2130	1516	1518	454	Run12-RCJB-Rock C	Cobble (granoblastic)
11 May	2130	1516	1518	302	Run12-RCJB-Rock D	Cobble (granoblastic)
11 May	2130	1516	1518	151	Run12-RCJB-Rock E	Cobble (granoblastic)
11 May	2130	1516	1518		Run12-RCJB-Rock F	Cobble (granoblastic)
11 May	2130	1516	1518	302	Run12-RCJB-Rock G	Cobble (granoblastic)
11 May	2130	1516	1518		Run12-RCJB-Rocks H to Y	Cobble (granoblastic)
13 May	1100	270	1518	5000	Run13-DC	Large amount of fine-grained cuttings from BHA
13 May	1100	270	1518	5000	Run13-EXJB	Fine-grained cuttings
13 May	1100	270	1518	2000	Run13-RCJB	Multiple bags of fine cuttings to pebbles (mostly granoblastic rocks)
13 May	1100	270	1518		Run13-RCJB-Rock A	Cobble (granoblastic)
13 May	1100	270	1518		Run13-RCJB-Rock B	Cobble (granoblastic)
14 May	2010	1518	1520	2000	Run14-BSJB	3 bags of cuttings (various grain size, fine to gravel)
14 May	2010	1518	1520	2000	Run14-EXJB	Multiple bags of cuttings (various grain size, fine to pebbles; some gabbro chips)
14 May	2010	1518	1520		Run14-FTJB-Rock A	Cobble (granoblastic)
14 May	2010	1518	1520		Run14-FTJB-Rock B	Cobble (granoblastic)
16 May	1545	1518	1520	5000	Run15-EXJB	Multiple bags of cuttings (various grain size, fine to pebbles; granoblastic)
19 May	0315	1520	1521	2000	Run17-BSJB	7 bags of cuttings (various grain size, gravel to pebbles; granoblastic)
21 May	1230	1518	1521	5000	Run18-BSJB	4 bags of cuttings (various grain size, fine to pebbles; granoblastic); 2 small bags of leucocratic gravel
22 May	1645	1510	1520	5000	Run19-BSJB	2 bags of fine-grained cuttings
22 May	1645	1510	1520	300	Run19-EXJB1	Pebbles of basalt and granoblastic rocks, gravel
22 May	1645	1510	1520	100	Run19-EXJB2	Pebbles of basalt and granoblastic rocks, gravel
22 May	1645	1518	1521	50	Run19-RCJB	Pebbles (granoblastic + 1 gabbro)
22 May	1645	1518	1521		Run19-RCJB-Rock A	Cobble (granoblastic with diorite vein)
22 May	1645	1518	1521		Run19-RCJB-Rock B	Cobble (granoblastic)
22 May	1645	1518	1521		Run19-RCJB-Rock C	Cobble (granoblastic)
22 May	1645	1518	1521		Run19-RCJB-Rock D	Cobble (granoblastic)
24 May	0215	1510	1520	5000	Run20-BSJB	2 bags (fine to gravel-sized cuttings); 1 small bag of pebbles
24 May	0215	1510	1520	5000	Run20-EXJB1	4 bags of cuttings (various grain size, fine to pebbles; granoblastic)
24 May	0215	1510	1520	3000	Run20-EXJB2	1 bag of granoblastic pebbles; 1 bag of leucocratic pebbles
24 May	0215	1518	1521	500	Run20-RCJB	Large cobbles (see list below)
24 May	0215	1519	1519.5		Run20-RCJB-Rock A	Cobble (granoblastic)
24 May	0215	1519	1519.5		Run20-RCJB-Rock B	Cobble (granoblastic)
24 May	0215	1519	1519.5		Run20-RCJB-Rock C	Cobble (gabbro)
24 May	0215	1519	1519.5		Run20-RCJB-Rock D	Pebble (leucocratic material)
24 May	0215	1519	1519.5		Run20-RCJB-Rock E	Pebble (leucocratic material)
25 May	0700	1510	1520	2000	Run21-BSJB	3 bags of cuttings (various grain size, fine to gravel)

Table T6. (continued.)

Date (2011)	Local time (h)	Top depth (mbsf)	Bottom depth (mbsf)	Volume (cc)	Sample	Comments
25 May	0700	1510	1520	200	Run21-EXJB2	3 small bags of pebbles (granoblastic)
25 May	0700	1518	1520	200	Run21-RCJB	3 small bags of pebbles (granoblastic)
26 May	0800	1519	1520		Run22-BSJB	2 bags (fine and gravel-sized cuttings)
26 May	0800	1519	1520		Run22-EXJB	1 bag of cuttings (pebbles and chips)
26 May	0800	1519	1520		Run22-FM	Small bag of metal + fine-grained cuttings

EXJB = external junk basket, DC = drill collar, BHA = bottom hole assembly, FM = fishing magnet, RCJB = reverse circulating junk basket, BSJB = bit sub junk basket, FTJB = flow through junk basket.

Table T7. Major operational phases during Expedition 335.

Phase	Operations	Days	Reentries
1	920 mbsf: open and cement to stabilize hole (920–960 mbsf)	15.00	9
2	Core (4 cores; 8% recovery)	~2	1
3	Fish/mill junk and ream/clean hole	19	13
4	Logging	~2	1
5	Core (1 core; 35% recovery), cement to stabilize hole (BOH to 1510 mbsf, 940–910 mbsf)	~1.5	1

BOH = bottom of hole. 24 reentries and ~150 miles (~240 km) of pipe trip. 920–940 mbsf zone: stabilized (15 trips through after cementing end of Phase 1 without any trouble). Hole: clean and clear of cuttings, no metal junk left at bottom. Cone: clear. "Fieldwork" samples from ocean crust thermal boundary layer.

Figure F1. Age map of the Cocos plate and corresponding regions of the Pacific and Nazca plates. Isochrons at 5 m.y. intervals have been converted from magnetic anomaly identifications according to the timescale of Cande and Kent (1995). Selected DSDP and ODP sites that reached basement are indicated by circles. The wide spacing of the 10 to 10 m.y. isochrons to the south reflects the extremely fast (200–220 mm/y) full spreading rate. Dashed box shows location of Figure **F7A,** which shows details of magnetic anomalies near Site 1256. FZ = fracture zone.

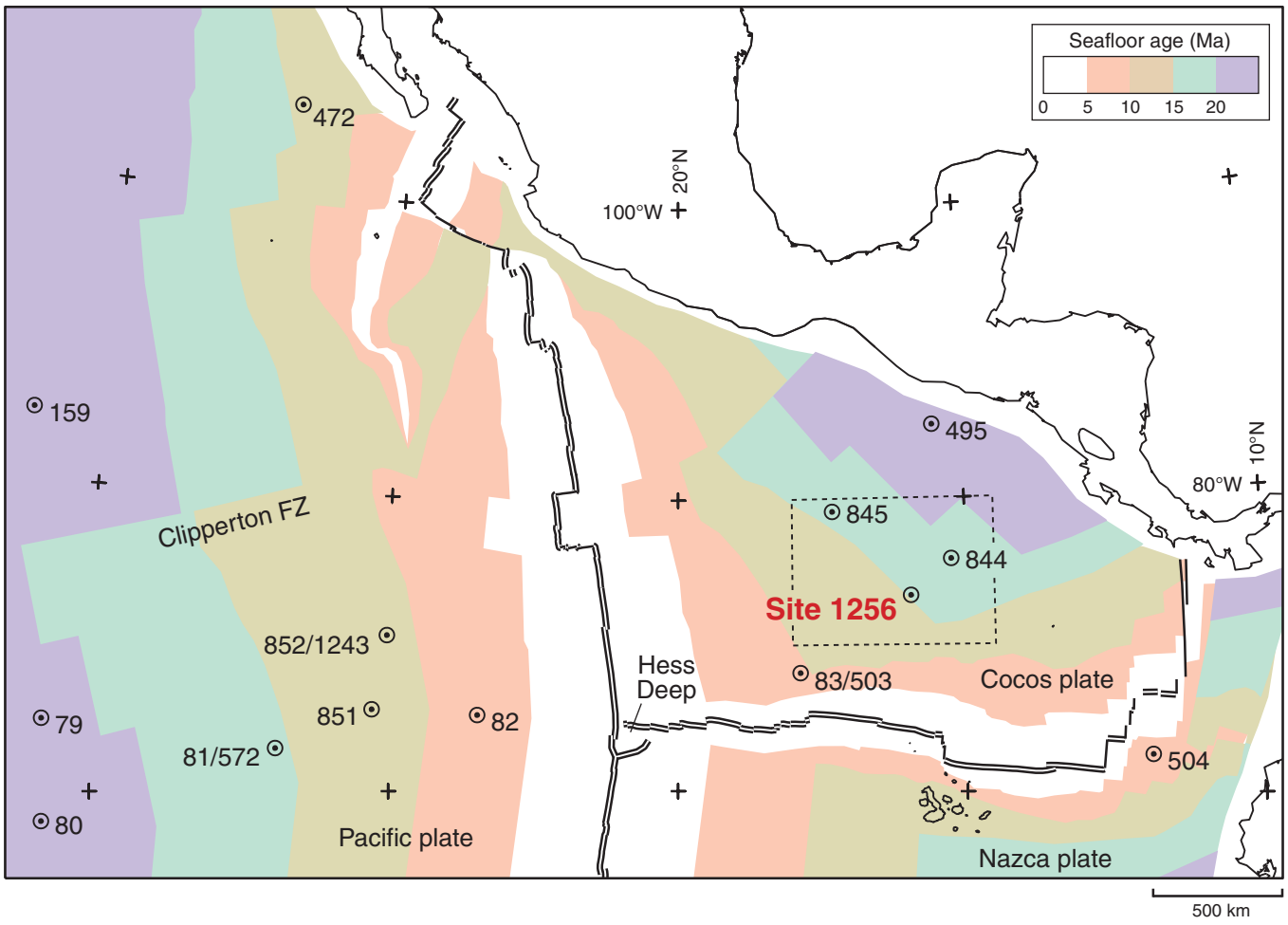

Figure F2. Simplified stratigraphy column of Hole 1256D at the end of Expedition 312, showing the major lithologic divisions of the upper oceanic crust at this site, the progress made during previous drilling cruises (Leg 206 and Expedition 309/312), and the highly variable core recovery.

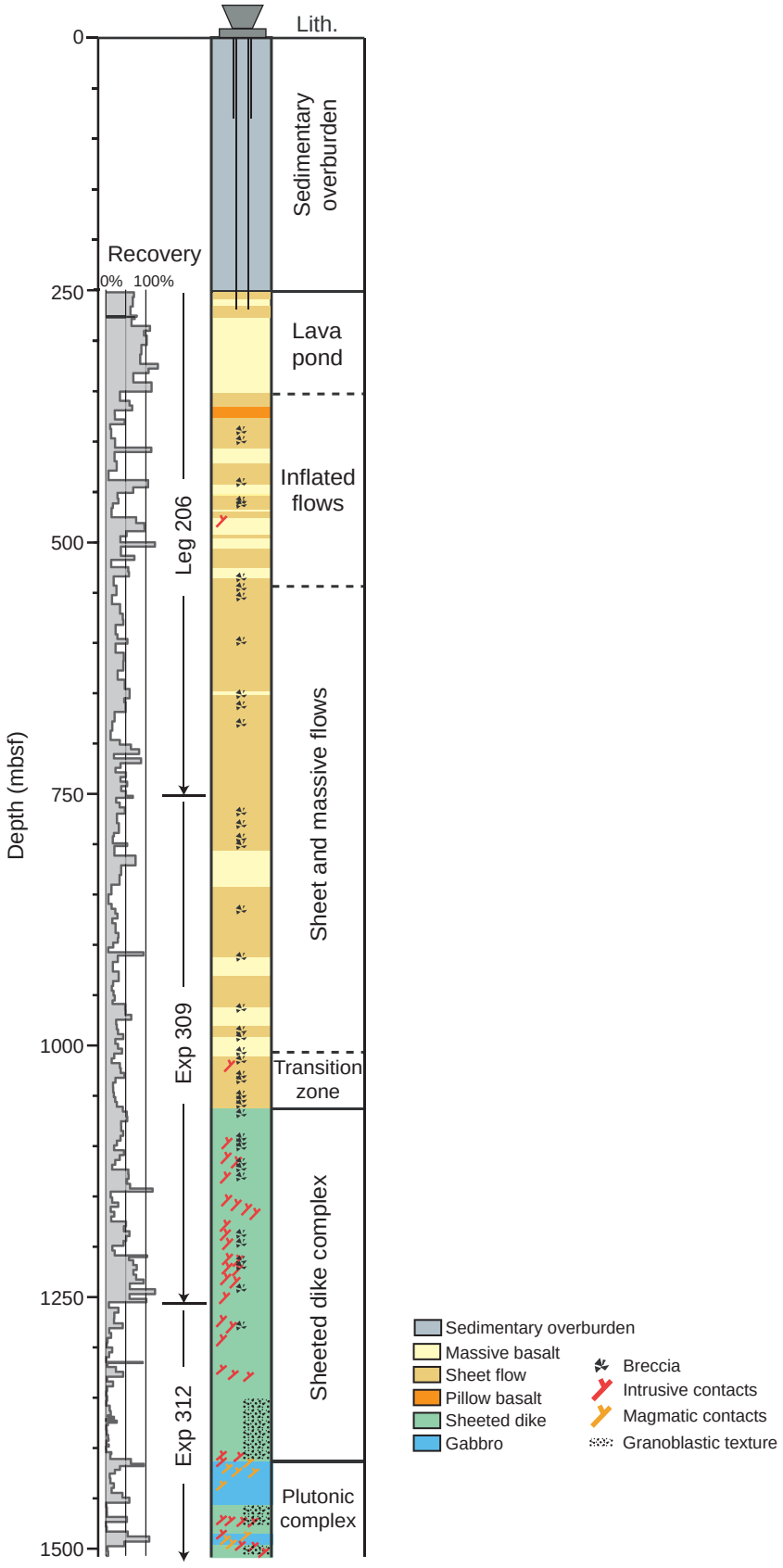

Figure F3. Map of the ocean floor age, based on age grid by Müller et al. (2008), revised version 3 (**www.earthbyte.org/**). Symbols represent DSDP, ODP, and IODP holes drilled in ocean crust >100 mbsf from 1974 to 2011. Holes deeper than 500 m in intact and rifted oceanic crust are labeled. This map does not include "hard rock" drill holes in oceanic plateaus, arc basement, hydrothermal mounds, or passive margins.

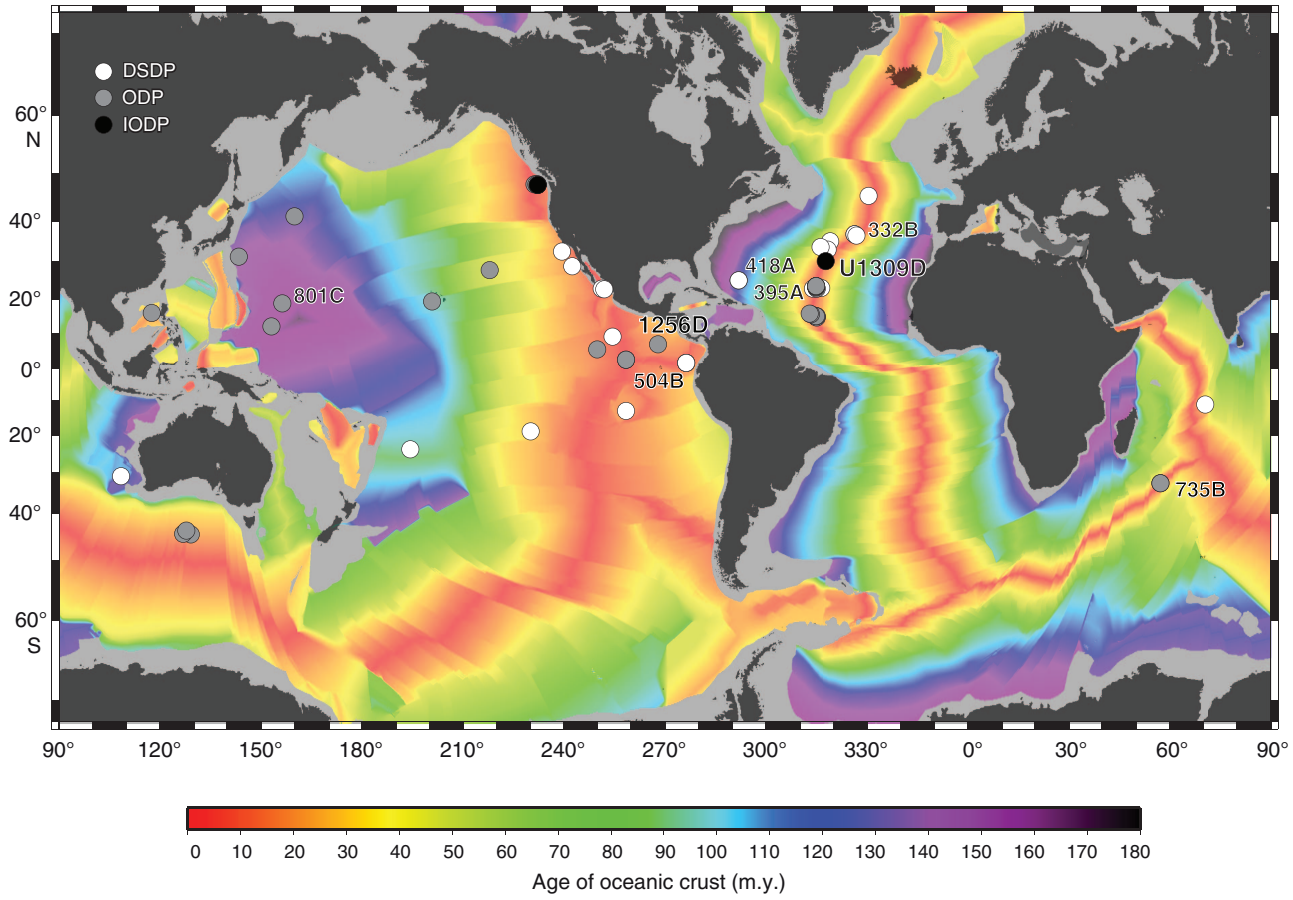

Figure F4. Compilation chart showing holes drilled >100 m in intact crust and tectonically exposed lower crust and upper mantle from 1974 to 2010 (localization in Fig. F3). For each hole are indicated the hole number and the recovery (in percent) for each lithology. This compilation does not include "hard rock" drill holes in oceanic plateaus, arc basement, hydrothermal mounds, or passive margins.

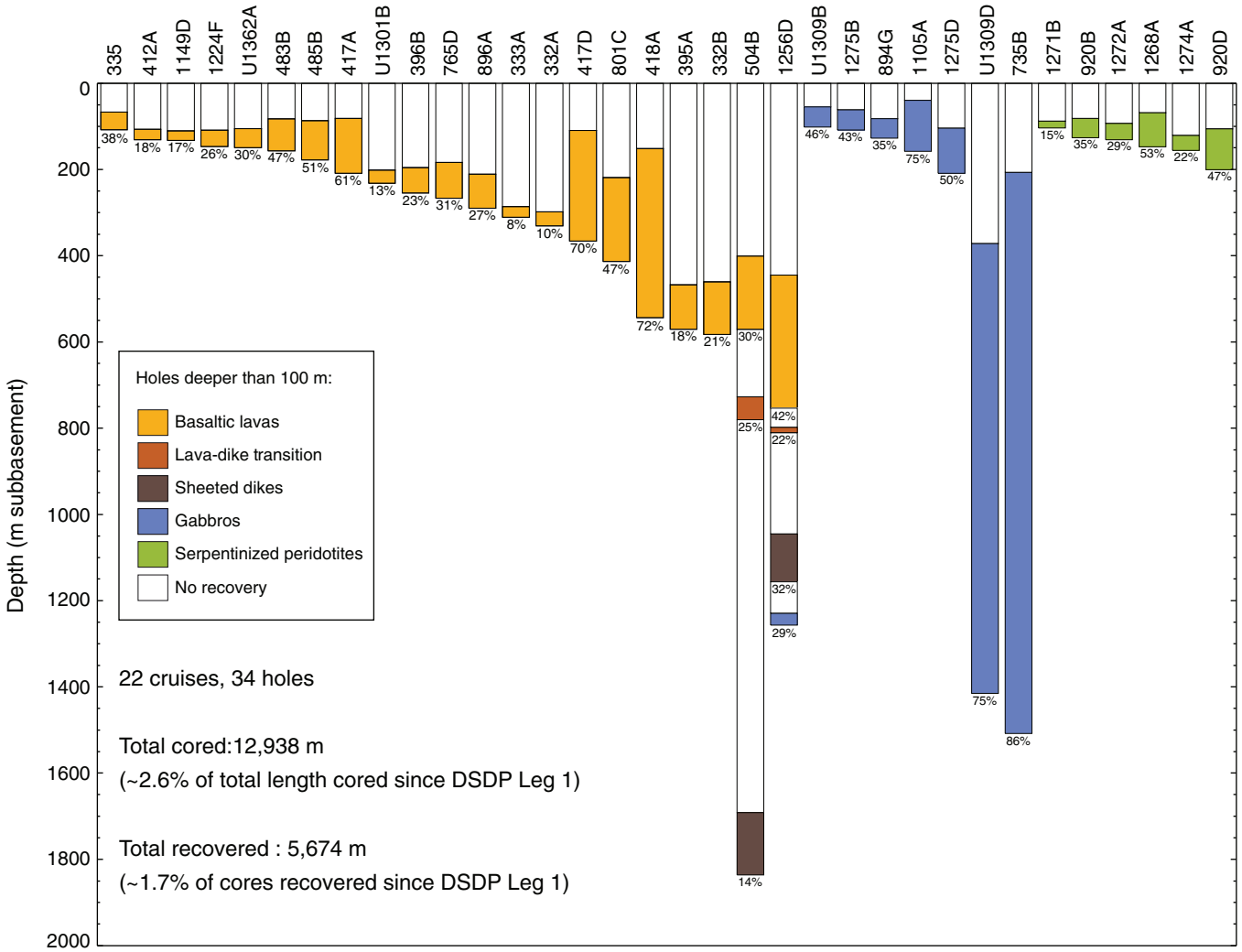

Figure F5. Depth to axial low-velocity zone plotted against spreading rate (Purdy et al., 1992; Carbotte et al., 1997). Depth versus spreading rate predictions from two models of Phipps Morgan and Chen (1993) are shown, extrapolated subjectively to 200 mm/y. Penetration to date in Holes 504B and 1256D is shown, with the depth at which gabbros were intersected indicated by the red box. Following core descriptions, a thickness of ~300 m of off-axis lava is shown for Hole 1256D and assumed for Hole 504B. EPR = East Pacific Rise, JdF = Juan de Fuca Ridge, Lau = Valu Fa Ridge in Lau Basin, CRR = Costa Rica Rift, MAR = Mid-Atlantic Ridge.

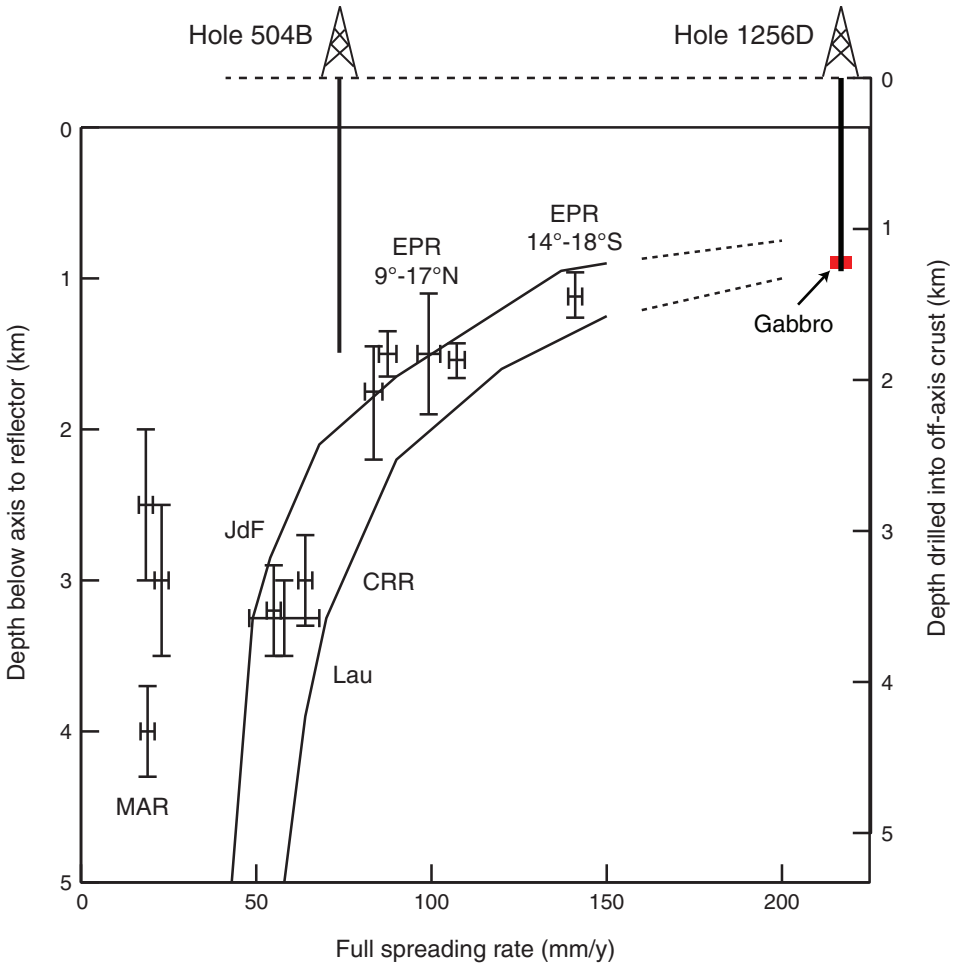

Figure F6. Reconstruction of Site 1256 and vicinity at 14 Ma, ~1 m.y. after formation of the site at the East Pacific Rise. Positions and plate velocities (arrows labeled in millimeters per year) are relative to the Antarctic plate, which is reasonably fixed relative to the spin axis and hotspots. Reconstructed positions of mapped magnetic Anomalies 5B, 5C, and 6 (ages 15–20 Ma) and other existing DSDP/ODP drill sites are shown by colored bars and circles, respectively.

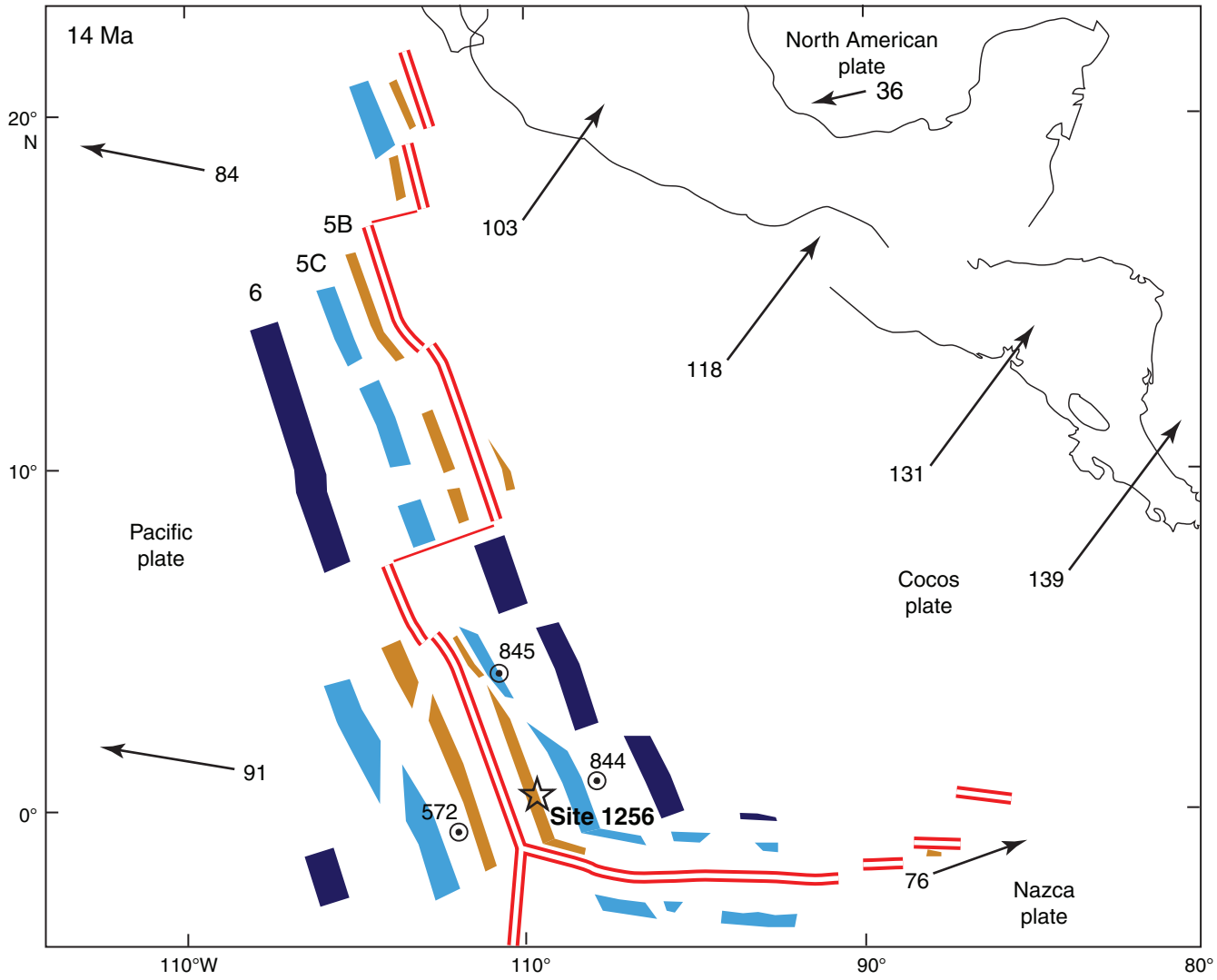

Figure F7. A. Details of isochrons inferred from magnetic anomalies near Site 1256. Shading shows normal magnetic polarity, based on digitized reversal boundaries (small circles, after Wilson, 1996). Bold line shows location of Guatemala Basin multichannel seismic (MCS) tracklines from the site survey Cruise EW9903 conducted in March–April 1999 (Wilson et al., 2003). Anomaly ages: 5A = ~12 Ma, 5B = 15 Ma, and 5D = ~17 Ma. **B.** Bathymetry and site survey track map for Site 1256 (proposed Site GUATB-03C). Abyssal hill relief of as much as 100 m is apparent in the southwest part of the area; relief to the northeast is lower and less organized. Line numbers 21–28 identify MCS lines from the site survey. OBH = ocean bottom hydrophone.

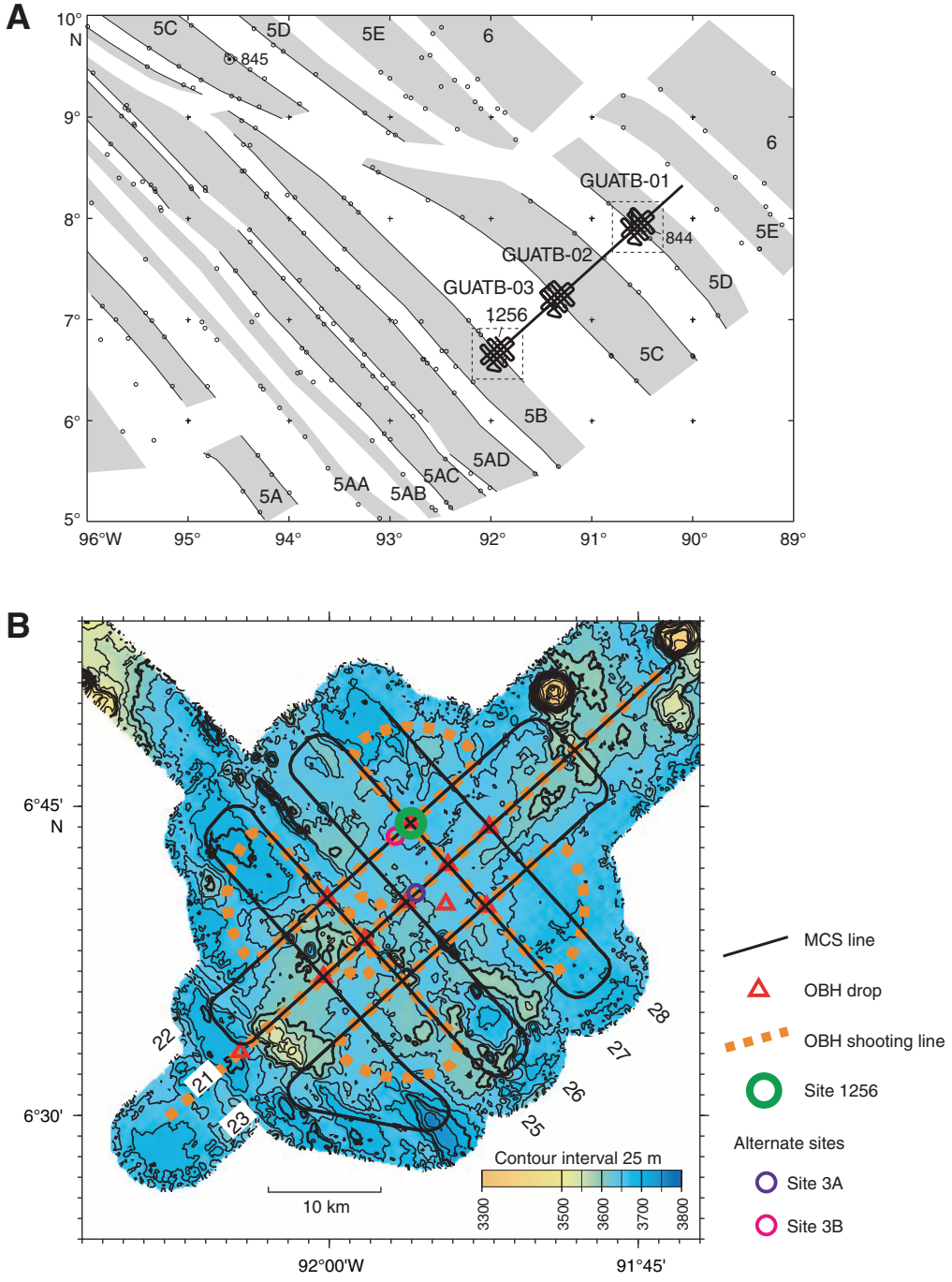

Figure F8. Site survey MCS data (Hallenborg et al., 2003) from the lines that cross at Site 1256, with penetration as of the end of Expedition 335 scaled approximately to traveltime. Horizontal reflectors in the upper basement to traveltimes of 5.5 s appear to result from contrasts between lava flow sequences, corresponding to depths of at least 800 msb.

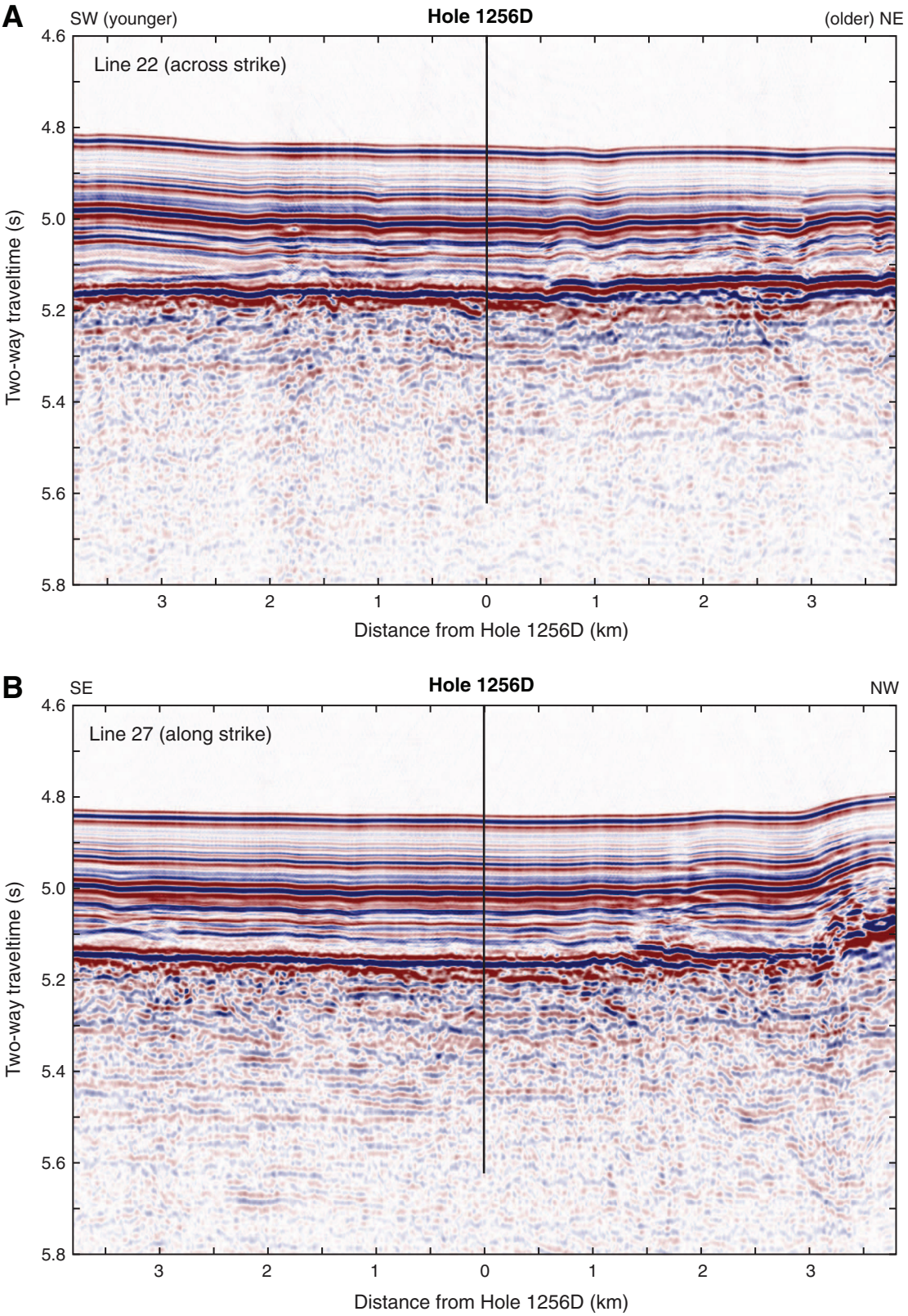

Figure F9. One-dimensional velocity model based on inversion of refraction data. At shallow depths, separate inversions were performed on northeast (NE) and southwest (SW) data subsets, with slightly faster velocities found to the northeast where abyssal hill topography is very subdued. The Layer 2/3 boundary is present in the depth range 1.2–1.5 km. The velocity model of Detrick et al. (1994) for Site 504, also based on ocean bottom hydrophone refraction data, is shown for comparison. Apparent differences are dominated by differences in the inversion techniques, but the differences at 1.3–1.7 km may be barely above uncertainty.

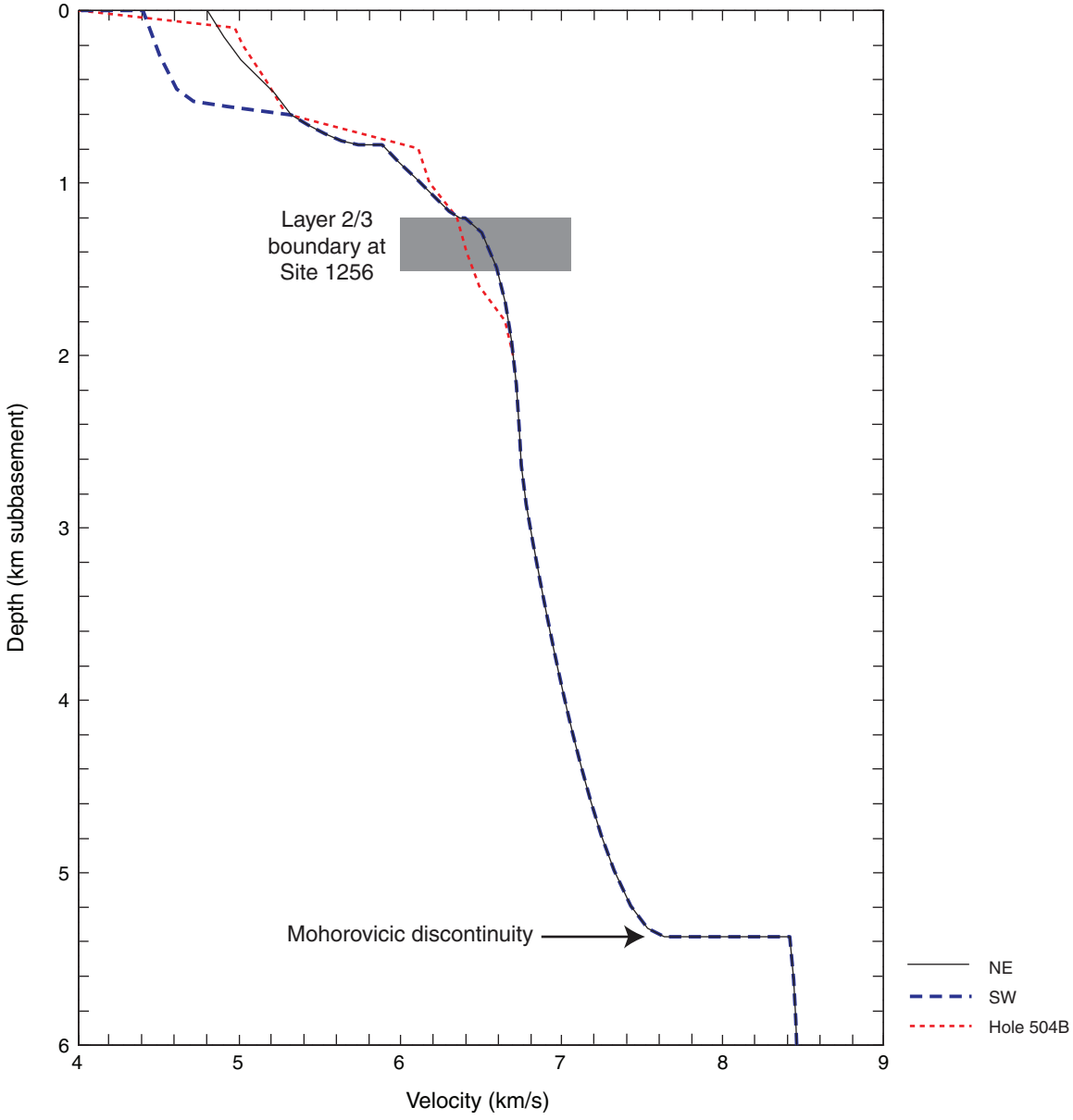

Figure F10. A. Contour map of seismic *P*-wave velocity at the top of basement, based on tomographic inversion of seismic refraction data (A.J. Harding, pers. comm., 2005). The low-velocity area west of the center may reflect pillow lavas or other porous formation. The high-velocity area extending southeast from Site 1256 may reflect the extent of the ponded lava sequence drilled at the top of Site 1256. OBH = ocean bottom hydrophone. **B.** Geological sketch map of the Site 1256 area (GUATB-03) showing bathymetry, alternate site locations, and selected top-of-basement velocity contours from A. The larger velocity contour line partially encloses velocity >4.82 km/s, which we interpret as a plausible proxy for the presence of thick ponded lava flows, as encountered at Site 1256. The smaller contour encloses velocities <4.60 km/s, possibly reflecting a greater portion of pillow lavas than elsewhere in the region. Alternate reentry Sites 3D and 3E are 0.5–1.0 km from Site 1256 and are not shown in the figure.

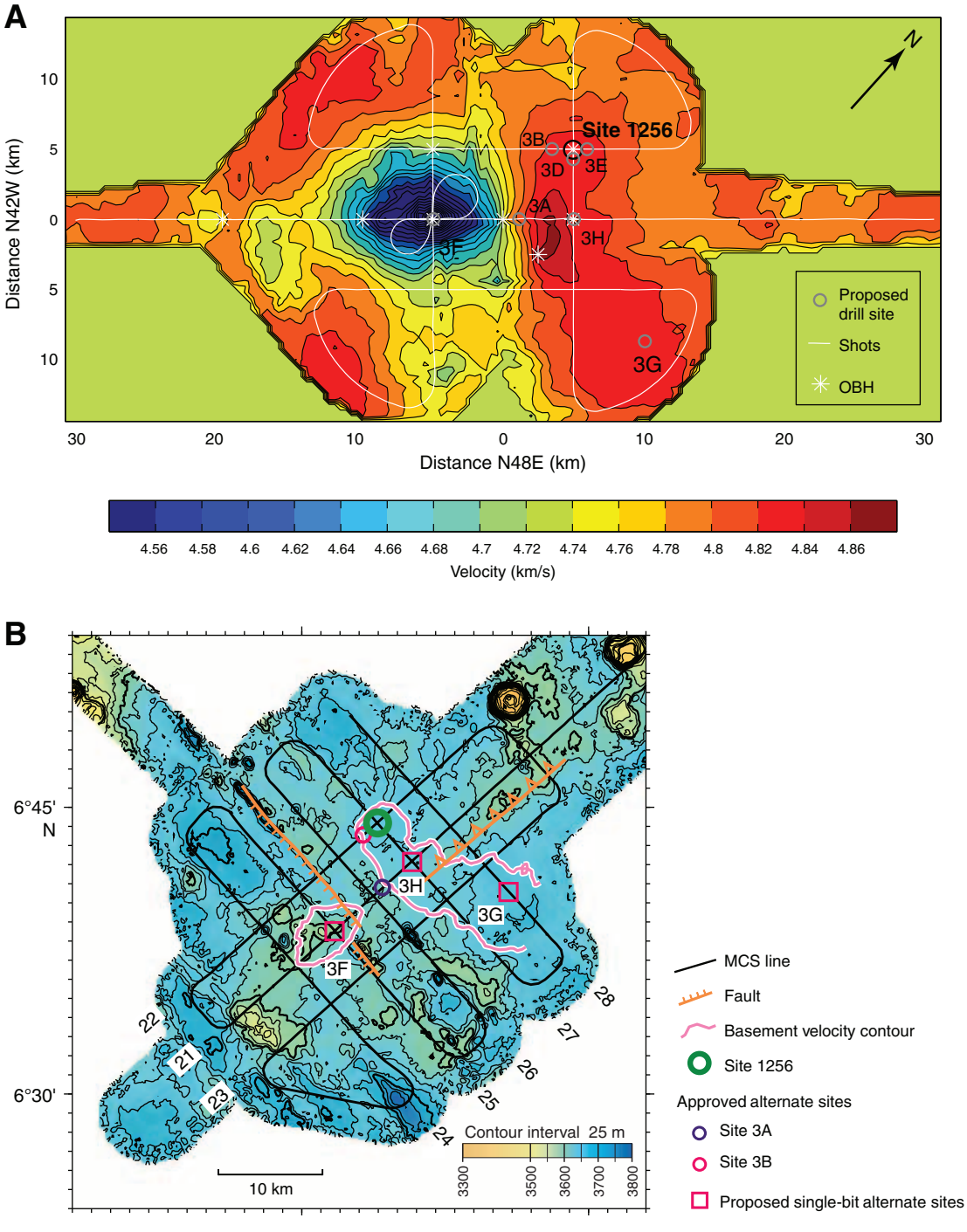

Figure F11. Measured and estimated temperatures with depth in Hole 1256D (Wilson, Teagle, Acton, et al., 2003; Teagle, Alt, Umino, Miyashita, Banerjee, Wilson, et al., 2006). Thermal profile estimated using the measured conductive heat flow and appropriate thermal conductivities for the lava, dikes, and gabbros. Thermal data for Hole 1256D is compared against the stratigraphy and equilibrium temperature log for Hole 504B located on 6.9 Ma crust south of the intermediate spreading rate Costa Rica Rift. At the depth achieved in Hole 1256D by the end of Expedition 312, that site is estimated to be ~50° cooler (~114°C) than the temperature measured at the equivalent depth in Hole 504B (~163°C). The highest temperature recorded in Hole 504B was 189°C at 1979 mbsf (Alt, Kinoshita, Stokking, et al., 1993). We highlight the 120°C isotherm, thought to be close to the limit of prokaryotic life (e.g., Heberling et al., 2010) for Holes 1256D and 504B. Hole 1256D is yet to reach this threshold, but Hole 504B is above this temperature below ~800 mbsf. TAP = Temperature/Acceleration/Pressure tool.

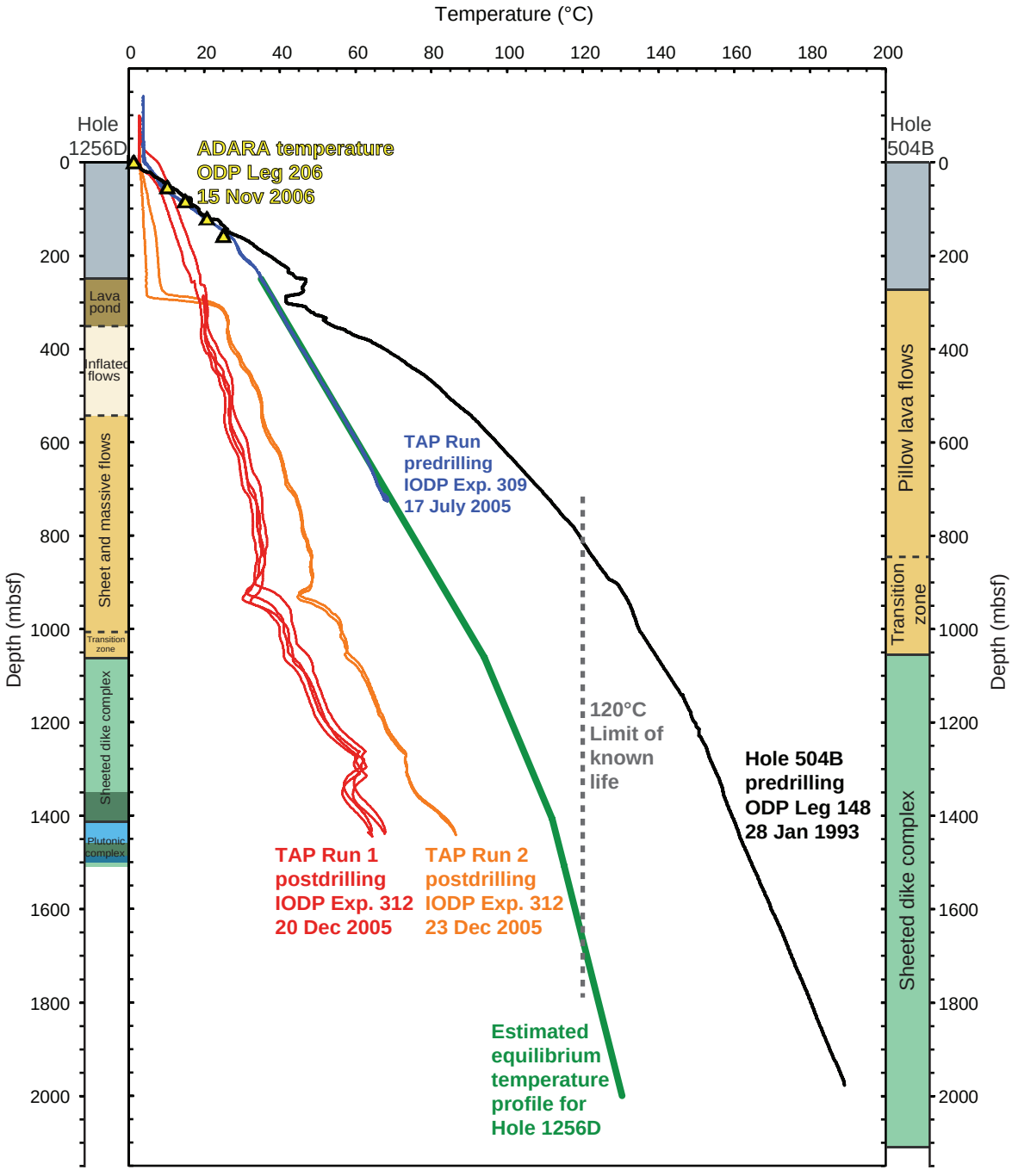

Figure F12. Summary lithostratigraphic column of the basement drilled at Site 1256 at the end of Expedition 312 showing recovery, major lithologies, downcore index alteration mineral distribution (thick lines = abundant, thin lines = rare, dashed lines = irregular; Teagle, Alt, Umino, Miyashita, Banerjee, Wilson, et al., 2006, updated by Alt et al., 2010), downcore distribution of Mg# (where Mg# = 100 × Mg/[Mg + 0.9 × Fe]) atomic ratio (symbols follow colors in the lithostratigraphic column), and seismic velocity measured on discrete samples from wireline tools (Wilson, Teagle, Acton, et al., 2003; Teagle, Alt, Umino, Miyashita, Banerjee, Wilson, et al., 2006; reprocessed data from Guérin et al., 2008) and from seismic refraction data (Wilson et al., 2003). Heavy red and orange lines show the inversion of traveltimes from Leg 206 and Expedition 312 vertical seismic profiles (VSPs), respectively (Swift et al., 2008).

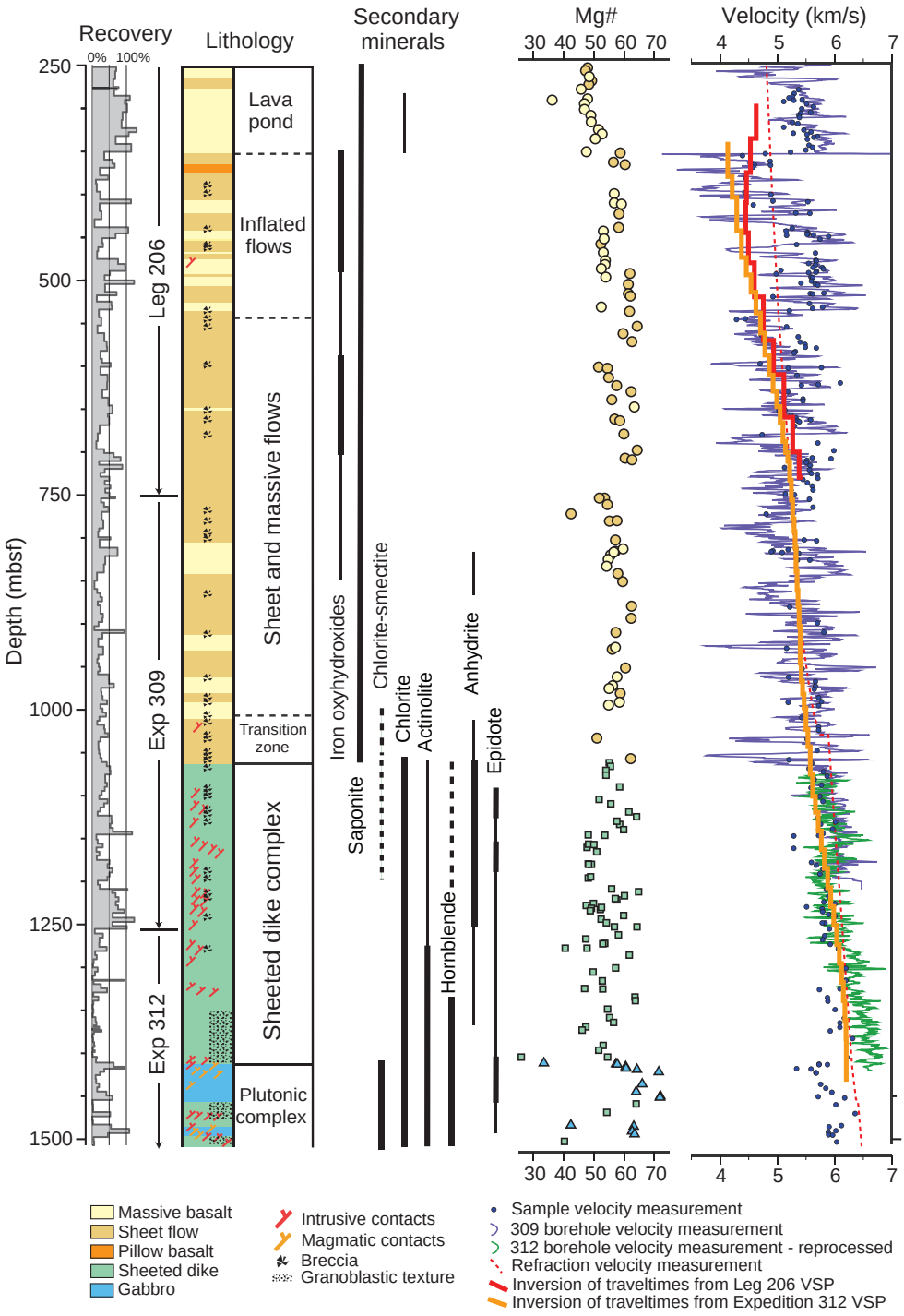

Figure F13. Plutonic section from the lower portion of Hole 1256D with representative photomicrographs of key samples. **A.** Schematic lithostratigraphy. The distribution of rock types is expanded proportionately in zones of incomplete recovery. Felsic plutonic rocks include quartz-rich oxide diorite and trondjhemite. OPX = orthopyroxene. **B.** Photomicrograph of a dike completely recrystallized to a granoblastic association of equant secondary plagioclase, clinopyroxene, magnetite, and ilmenite. Some granoblastic dikes have minor orthopyroxene. **C.** Photograph of dike/gabbro boundary. Medium-grained oxide gabbro is intruded into a granoblastically recrystallized dike along an irregular, moderately dipping contact. The gabbro is strongly hydrothermally altered. **D.** Quartz-rich oxide diorite strongly altered to actinolitic hornblende, secondary plagioclase, epidote, and chlorite. Epidote occurs in ~5 mm clots in the finer grained leucocratic portions of the rock. **E.** Disseminated oxide gabbro with patchy texture and centimeter-scale dark ophitically intergrown clinopyroxene and plagioclase patches separated by irregular, more highly altered leucocratic zones. **F.** Medium-grained strongly hydrothermally altered gabbro. The sample is cut by several chlorite + actinolite veins with light gray halos. Plagioclase is replaced by secondary plagioclase and clinopyroxene by amphibole. **G.** Clast of partially resorbed dike within gabbro. (Figure shown on next page.)

Figure F13 (continued). (Caption shown on previous page.)

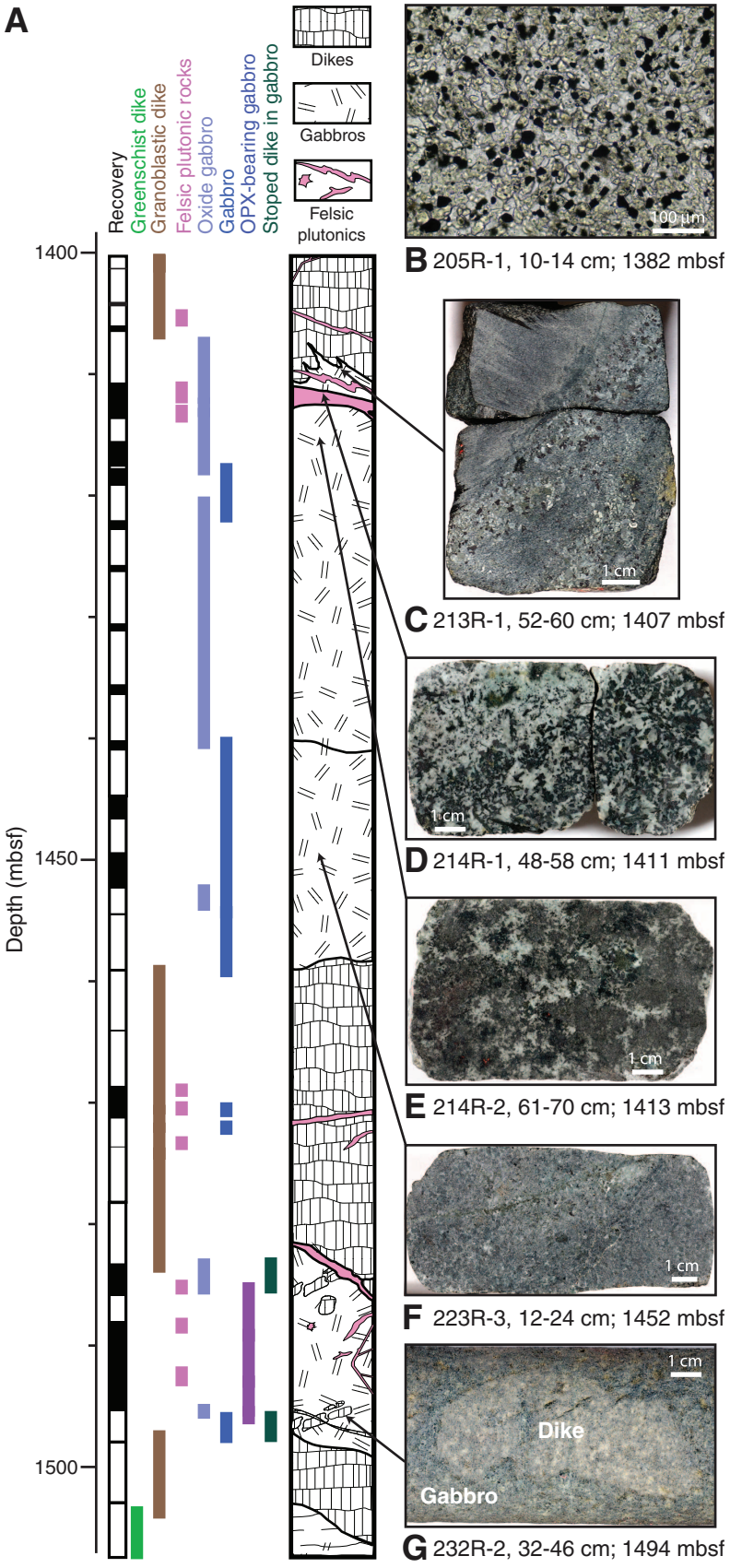

Figure F14. FeO^T (Total Fe expressed as FeO) vs. MgO for the basement at Site 1256, compared with analyses of northern East Pacific Rise (EPR) (outline, Langmuir et al., 1986). Dashed lines show constant Mg#. Possible primary mantle melt compositions should have Mg# of 70–78 and MgO of 9–14 wt%. All flows and dikes, and most gabbros, are too evolved to be candidates for primary magmas.

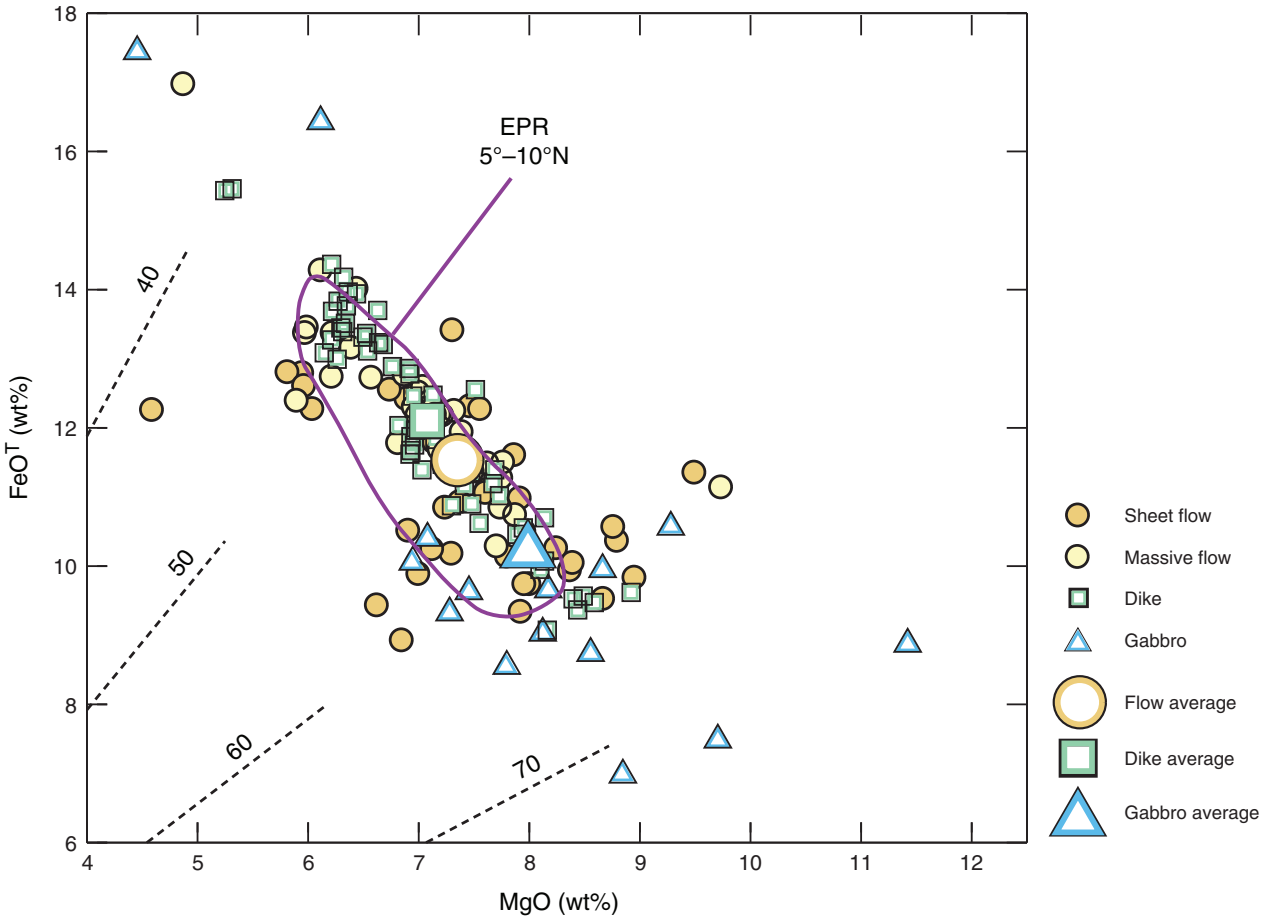

Figure F15. East Pacific Rise (EPR) mid-ocean-ridge basalt (MORB)–normalized multielement plot of the average of different lithologic subdivisions from Hole 1256D. LP = lava pond, MF = massive flow, SF = sheet flow, BD = basalt dike, G1 = Gabbro 1, G2 = Gabbro 2. EPR values of Y, Sr, Zr, and TiO_2 are taken from Su and Langmuir et al. (2003). Other elements are compiled from PETDB (**www.petdb.org/**) for basalts with MgO > 6.0 wt%.

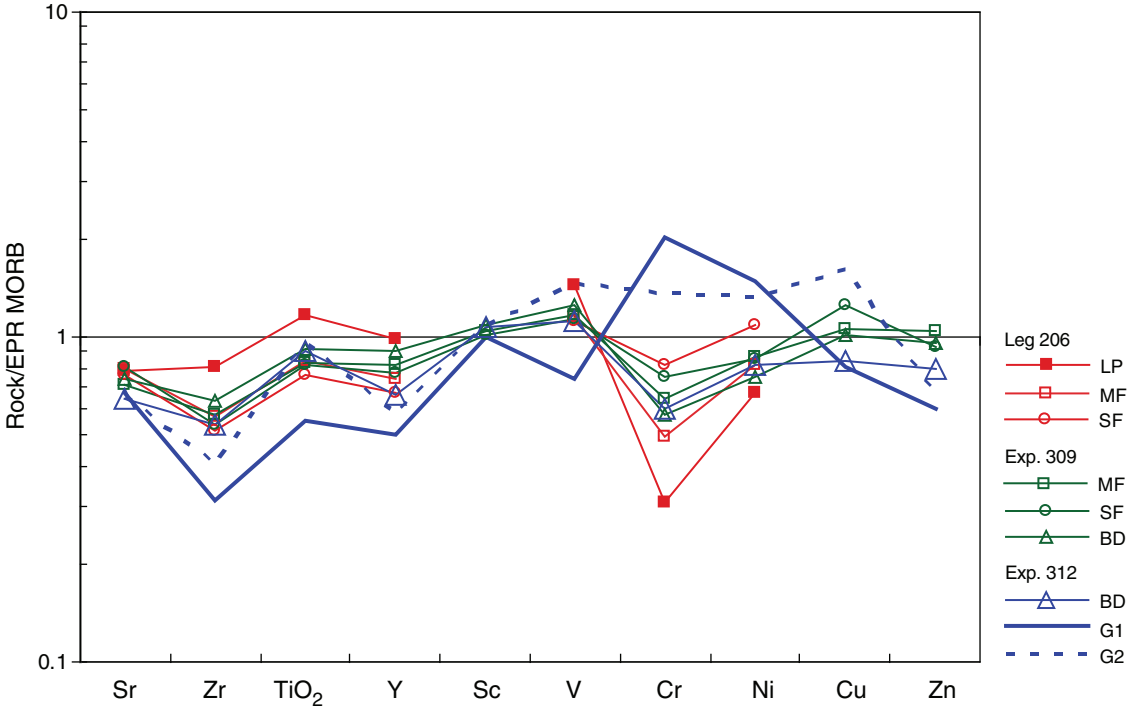

Figure F16. A. Predicted lithostratigraphy of the Site 1256 crust based on geological observations from the Oman ophiolite. **B.** Field photograph showing the intrusive contact of gabbro with sheeted dikes at the sheeted dike–gabbro transition (Aswad, Sumail massif). **C.** Field photograph of varitextured gabbros from a few meters below the dike–gabbro transition (Wadi Gideah, Wadi Tayin Massif). **D.** Field photograph of subvertically foliated cumulate gabbros from the upper gabbro section (Aswad, Sumail Massif). **E.** Field photograph of Moho-parallel modally layered cumulate gabbros (Samrah, Sumail Massif); layers are ~30 to 60 cm thick.

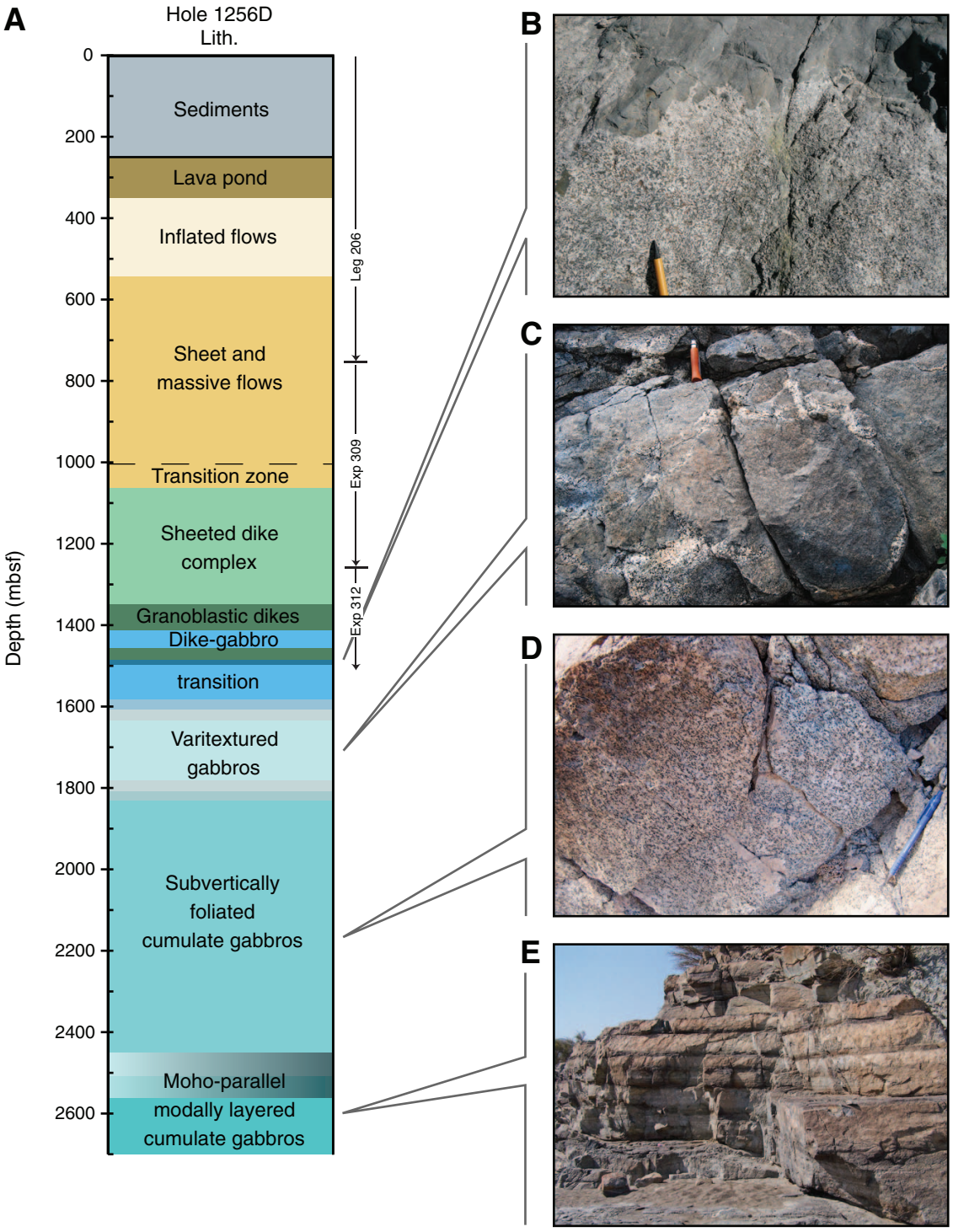

Figure F17. Schematic drawings of crustal accretion models (modified from Korenaga and Kelemen, 1998). Black arrows show the movement of the solid lower crust; blue arrows show the dominant zones where hydrothermal circulation will remove latent and sensible heat; red arrows show the movement of magma—this is unknown in all models. **A.** Gabbro glacier ductile flow model (e.g., Henstock et al., 1993; Phipps Morgan and Chen, 1993; Quick and Denlinger, 1993). Ductile flow down and outward from a high-level axial magma chamber constructs the lower crust. **B.** Hybrid model of ductile flow with sill intrusions (e.g., Boudier et al., 1996). **C.** "Sheeted" or "stacked" sill model of in situ formation of the lower crust by on-axis sill intrusions (e.g., Bédard et al., 1988; Kelemen and Aharonov, 1998; Kelemen et al., 1997; MacLeod and Yoauancq, 2000). **D.** Schematic relative variations in the general trends of latent heat release, bulk Mg#, strain rate, cooling rate, hydrothermal fluid flux, fluid temperature, and intensity of high-temperature (HT) alteration with depth predicted by end-member "gabbro glacier" (with mainly conductive cooling of the lower crust) and "sheeted sill" (with convective cooling of the lower crust) models of crustal accretion (original figure by R. Coggon).

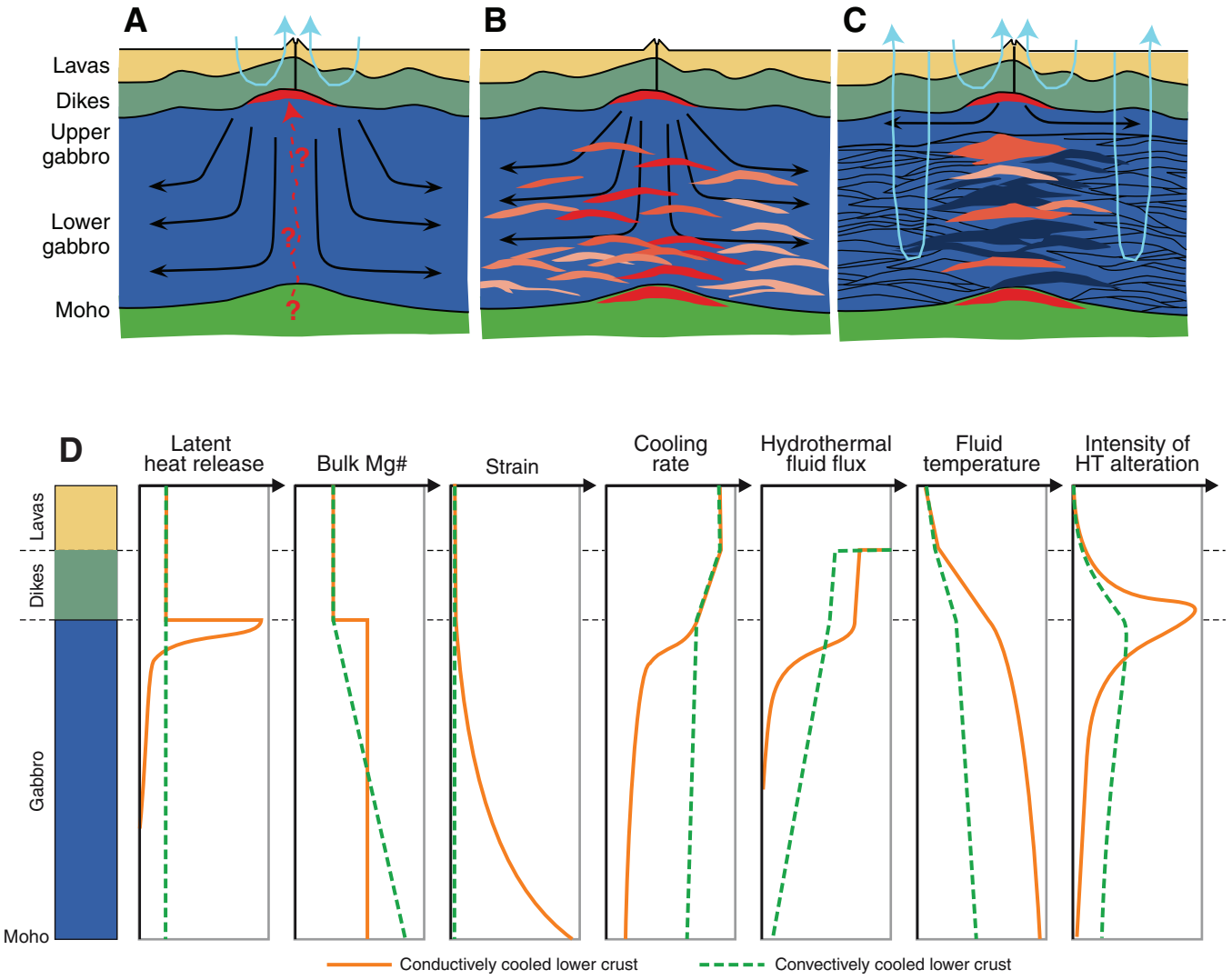

Figure F18. Average core recovery and rate of penetration for drilling in Hole 1256D during Leg 206 and Expedition 309/312. Note the improvement in both parameters in gabbroic rocks back to near average rates for the entire hole (~36% recovery; 1.2 m/h penetration rate). Recovery was very low and penetration rate excruciatingly slow in the granoblastic dikes. ROP = rate of penetration.

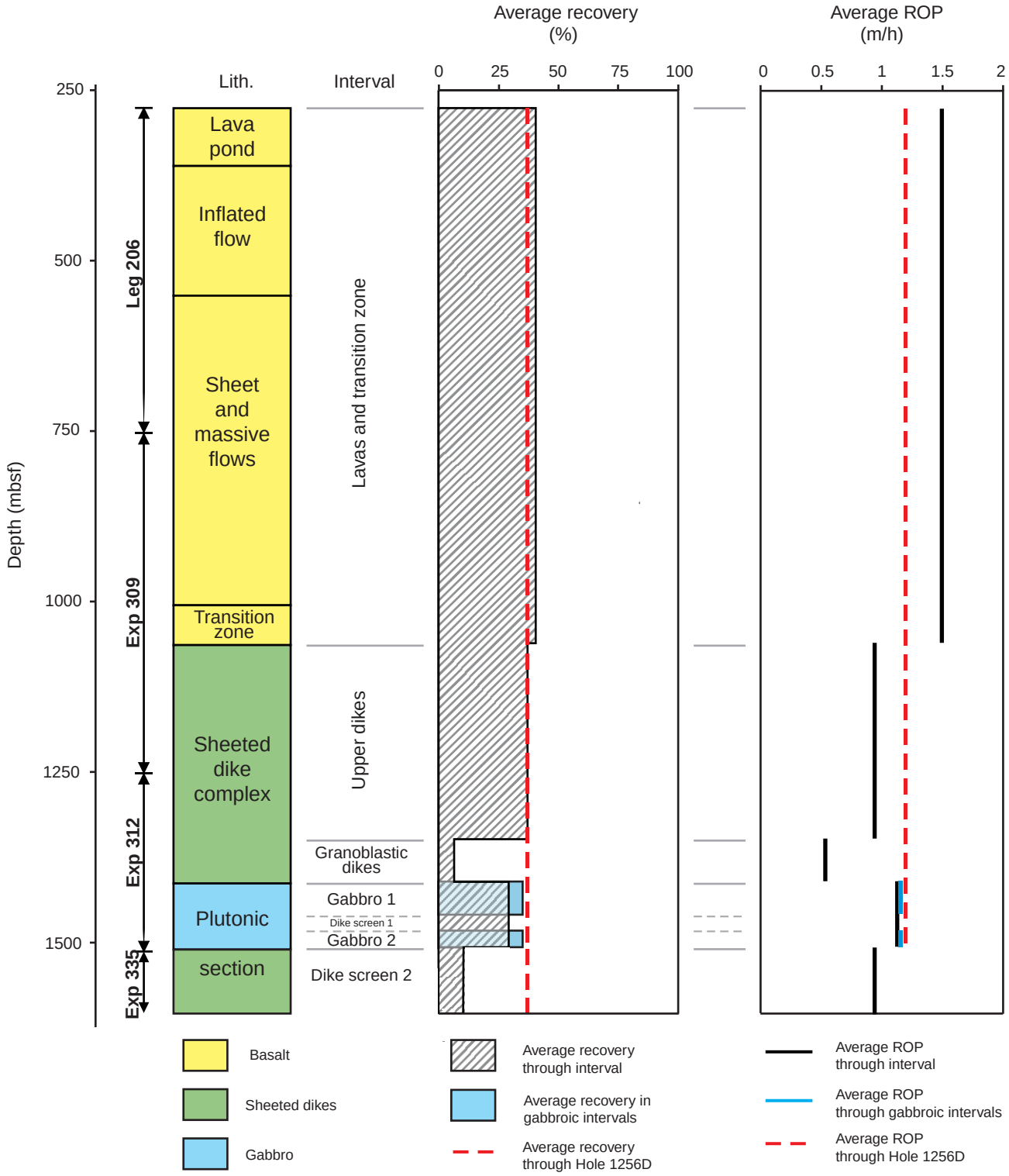

Figure F19. Photographs of various coring, drilling, fishing, and milling tools used during Expedition 335, illustrating some of the multiple operation events reported in **"Operations."** **A.** Smith 9⅞ inch F9 tricone bit used for Run 1 to work the obstruction between 920 and 925 mbsf; teeth were not worn, and much of the work was on the outside faces. **B.** Reed 9⅞ inch tricone bit (IADC Type 517) used for Run 2. Note the more aggressive cutting structure of this bit compared to the first one. Again, after working the obstructed interval between 920 and 923 mbsf, the cones underwent very little damage, except for a couple of missing teeth. **C.** After Runs 3–5, dedicated to working further and cementing the interval between 882 and 922 mbsf, this 9⅞ inch Atlas HP61 tricone bit was used during Run 6 to drill through cement and again work the obstructed interval at 922–923 mbsf. It returned in good condition with no appreciable shirttail wear, with all teeth intact and exhibiting very little wear. **D.** One of the two external junk baskets (EXJBs) run together with the tricone of E during Run 6; the two EXJBs returned basalt fine-grained cuttings and pebbles. (Continued on next 10 pages.)

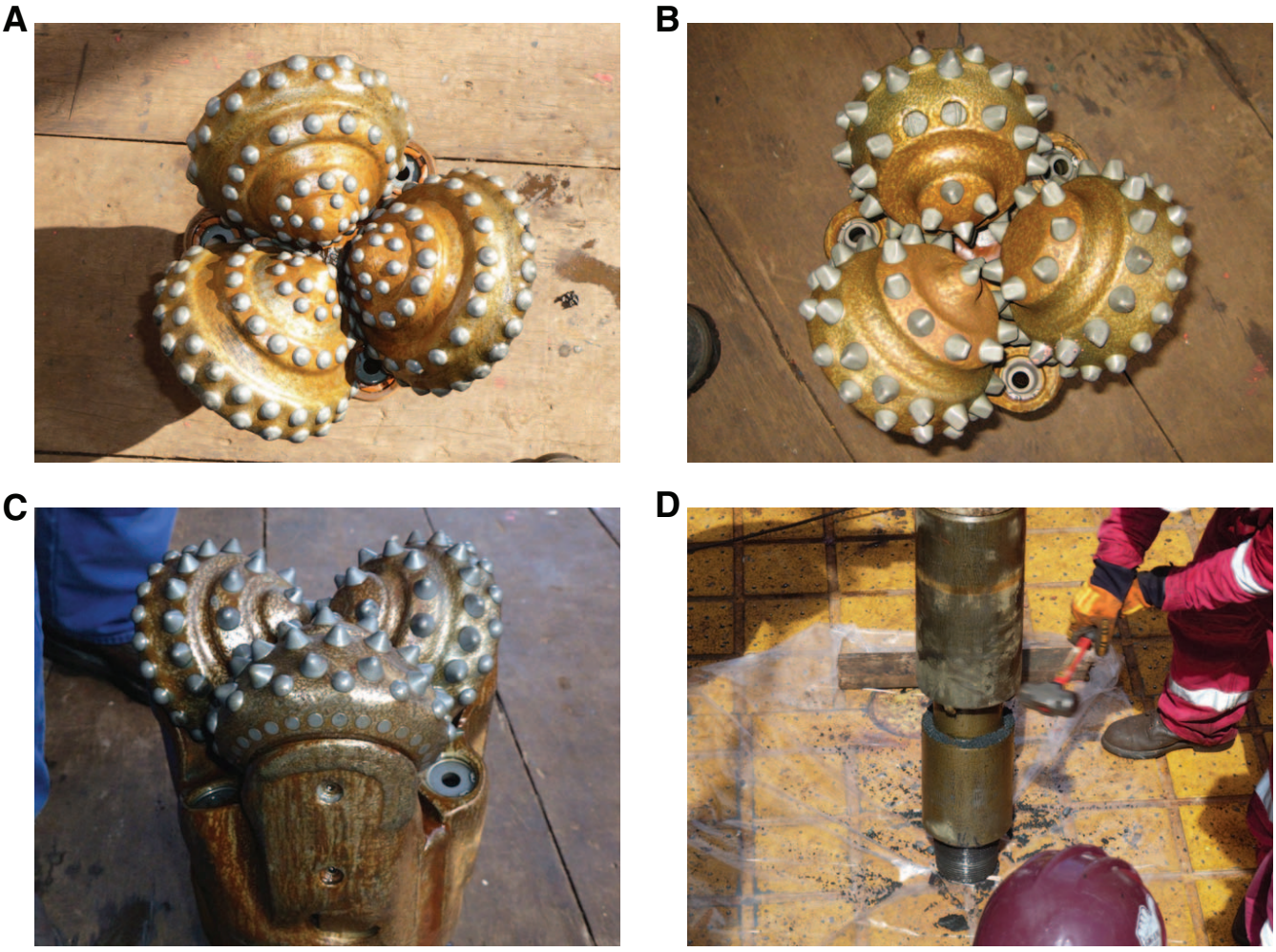

Figure F19 (continued). E. Smith 9⅞ inch tricone bit used for Run 7 to successfully clear the obstructed interval at 922–923 mbsf and work several ledges before reaching the bottom of the hole on the morning of 1 May. The bit was slightly out of gauge after 32.8 h of use. **F.** The worn core catcher used during Run 9, the first coring run of Expedition 335. As drilling continued for ~10 h with a destroyed bit (G, H), the core catcher was in contact with metal/junk and/or rocks; it is ~1 cm shorter than the new core catcher on the right. **G, H.** Remains of the Ulterra C9 RCB coring bit used during Run 9. The bit was probably used for ~10 h after it disintegrated, which resulted in this spectacularly abraded and sculptured bit ("Stumpy"), something never seen before by the drillers. (Continued on next page.)

Figure F19 (continued). I. The 9 inch Bowen fishing magnet used for Run 10. **J.** The fishing magnet could not be deployed all the way to the bottom of the hole, as increased pump pressure indicated loss of circulation at ~1434 mbsf. When back on the rig floor, 4 m of fine-grained cuttings were found inside the bit sub and the two junk baskets. This marked the beginning of a series of fishing runs, which eventually cleared the hole of a massive amount of fine-grained sandlike cuttings. **K.** The fishing magnet recovered a limited amount of small-sized metallic debris mixed with fine basaltic grains. **L.** One of the external junk baskets used for Run 11 in conjunction with an Atlas 9⅞ inch HP61 tricone bit. (Continued on next page.)

I

J

K

L

Figure F19 (continued). M. The junk baskets used for Run 11 recovered fine-grained cuttings to large pieces of rock, mostly granoblastic basalt, and some small gabbro chips. **N.** Bowen 9.75 inch reverse circulation junk basket (RCJB) used for Runs 12 and 13. Once reverse circulation is activated (S), water flows outside the tool through the jets visible in N and returns upward through the center of the tool, where a large junk catcher retains the fished material (O). **O.** Bottom of the Bowen RCJB, showing its hard-facing structure and the junk catcher spring fingers inside. **P.** The entire BHA used for Run 12, up to the top drill collar, returned completely filled with several hundreds of kilograms of fine-grained cuttings. (Continued on next page.)

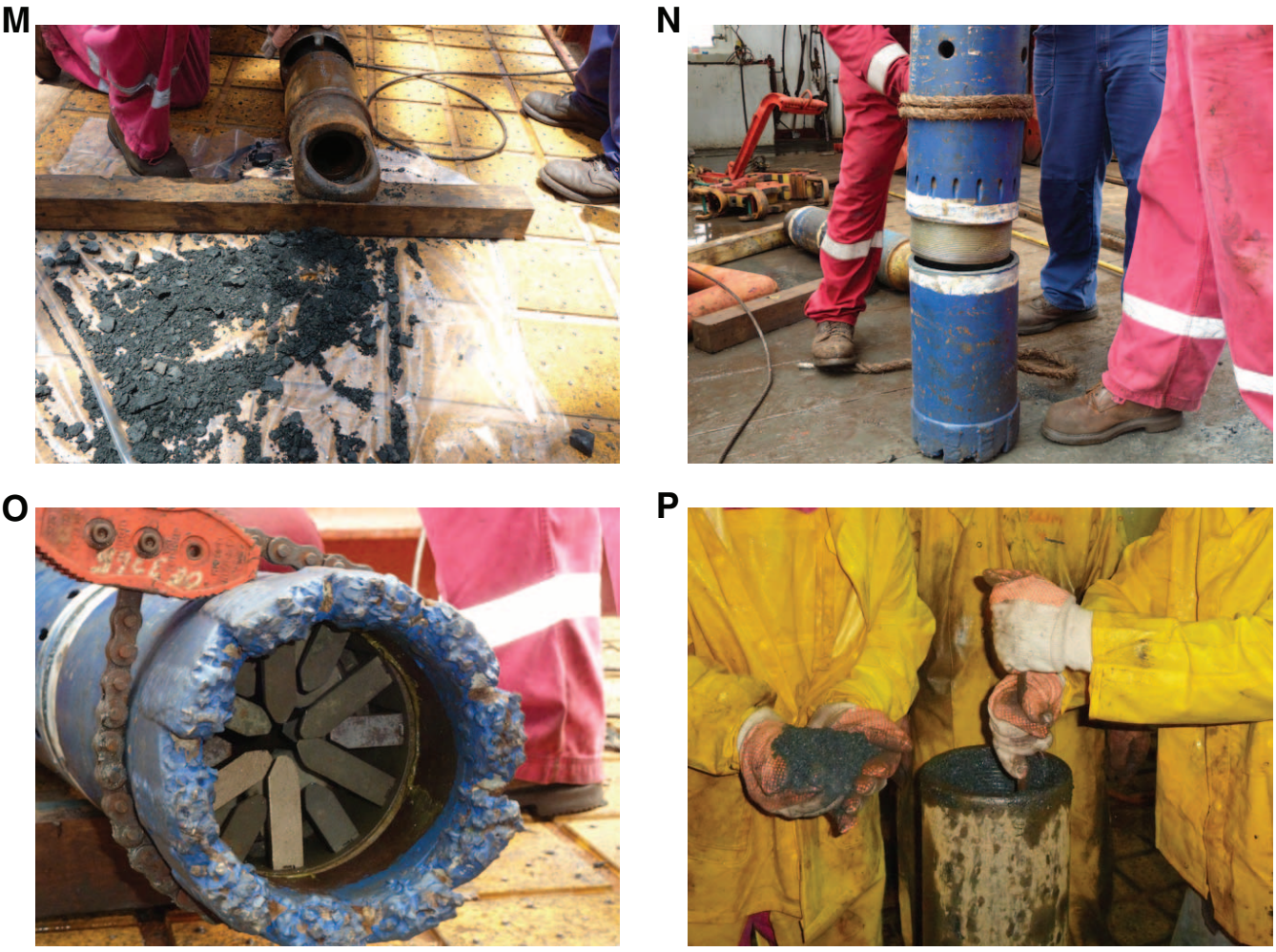

Figure F19 (continued). Q, R. The RCJB returned from Run 12 completely filled with packed cuttings and ~20 kg of rock samples, mostly granoblastic basalt. Note the heavily worn hard-facing structure of the tool after going through ~2.5 m of fill at the bottom of the hole. **S.** Top of the Bowen RCJB, showing the stainless steel ball dropped from the rig floor to activate reverse circulation by plugging the central throat and diverging fluid flow to the jets that are visible on the outside face of the tool in N. **T.** The second RCJB run (13) also returned a BHA packed by fine-grained cuttings and granoblastic basalt pebbles and large cobbles. (Continued on next page.)

Q

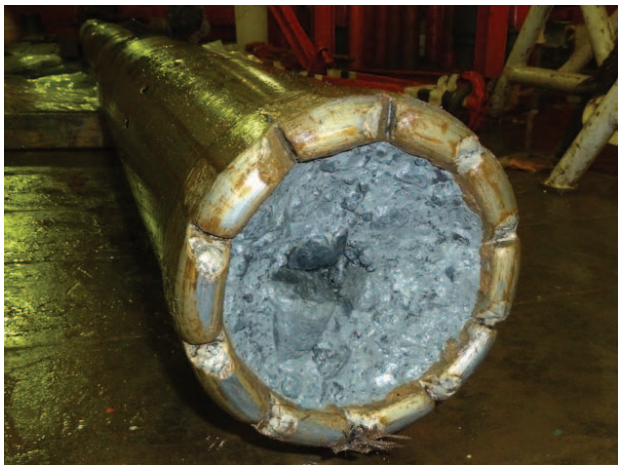

R

S

T

Figure F19 (continued). U. Bottom of the Homco 9.75 inch flow-through junk basket (FTJB) used for Run 14. **V.** The FTJB (Run 14) returned to the rig floor with a completely worn hard-facing structure, all fingers (but one) of the lowermost row of the junk catcher missing, and two large cobbles of granoblastic basalt. **W.** The Smith hard formation 9⅞ inch 7JS tricone bit used in Run 15 to work the lowermost 2–3 m of the hole returned to the rig floor with cone bearings still tight and no worn teeth. The bit was severely under gauge (0.4 inches) with some shirttail wear and minor junk damage on its body (Y), indicating that the lowermost portion of the hole was under gauge. **X.** EXJB used during Run 15, showing significant damage on the edge of one of its pockets. (Continued on next page.)

Figure F19 (continued). Y. Under gauge and worn Smith tricone bit used for Run 15 (W). **Z, AA.** 9⅞ inch Smith FH3VPS tricone bit ("mean motherf… Bruce Willis" tricone) used for Run 16. This more armored bit (compare with the previous one in Y) was more efficient to ream and clean the undergauge bottom of the hole. It returned in gauge to the rig floor, and six large teeth were missing. **BB.** Heavily worn and undergauge 9⅝ inch flat-bottomed milling tool used for Run 17. This tool worked at the bottom of the hole for 12 h; its final (terminal) state indicates the very abrasive nature of metal debris and/or rocks at the bottom of the hole and an undergauge lowermost portion (tens of centimeters) of the hole. Note for comparison the hard-facing structure of the next milling tool (DD) on the right side of the picture. (Continued on next page.)

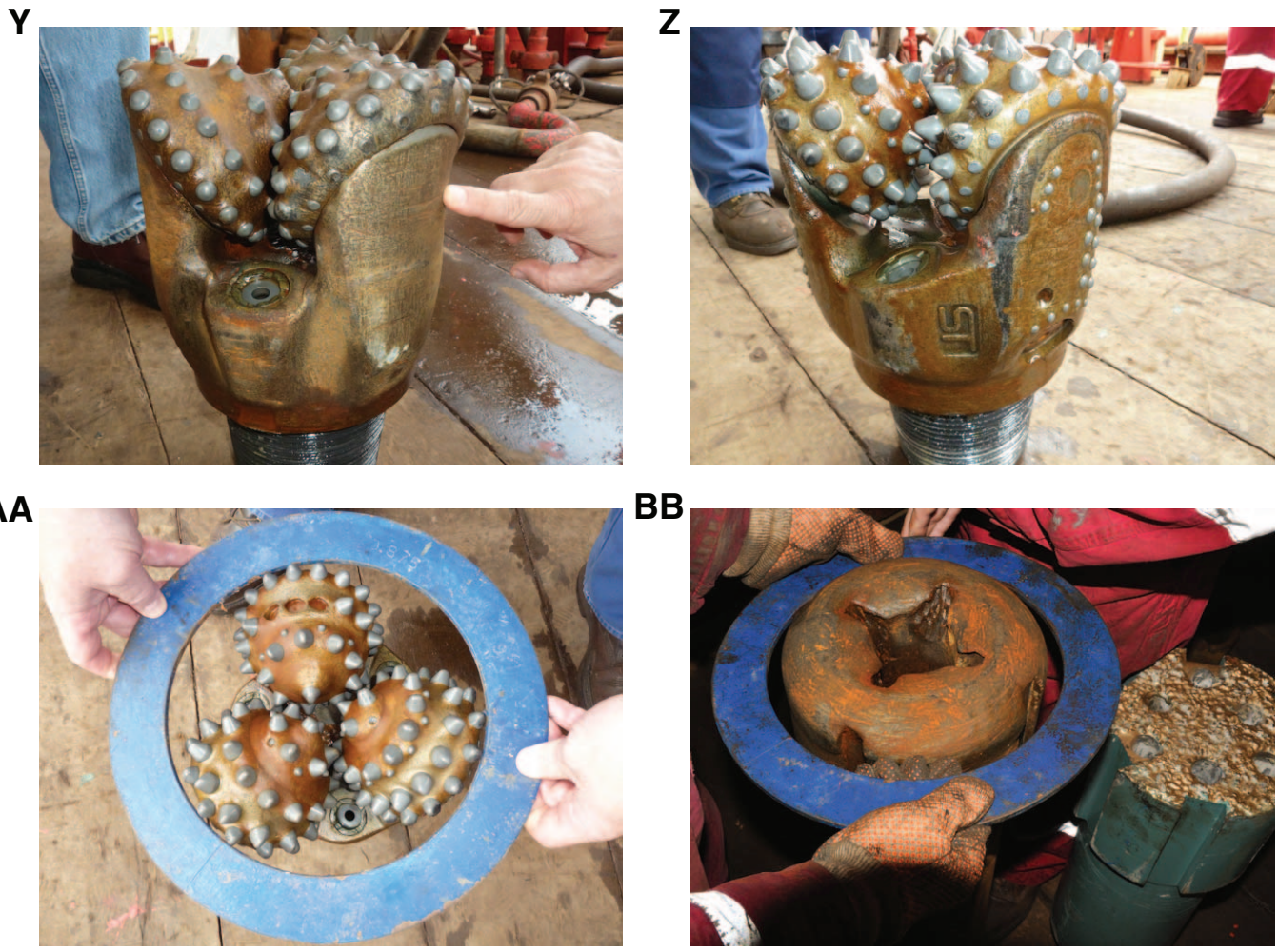

Figure F19 (continued). CC. Damaged bit sub junk basket (BSJB) used for Run 17, probably caused by granoblastic basalt angular blocks falling down the borehole walls while milling at the bottom. **DD.** 9 inch flat-bottomed milling tool used for Run 18. Note the hard-facing structure of the bottom of the tool. **EE.** The BSJB used for Run 18 returned with a damaged pocket, probably due to rock(s) detached from the borehole wall (CC). **FF.** 9 inch flat-bottomed milling tool used for Run 18, after working 6 h at the bottom of the hole. The abrasive surface (note the difference with DD) was eroded away and some external junk damage noted on the side of the tool and the crossover sub directly above the milling tool. (Continued on next page.)

CC

DD

EE

FF

Figure F19 (continued). GG. Bottom of the Bowen RCJB used for Runs 19 through 21. Note the spring fingers of the catching structure inside the tool. **HH.** The RCJB was deployed in Runs 19 through 21 with two EXJBs and one BSJB. This picture shows the junk basket tower being assembled on the rig floor. **II.** The RCJB on its return to the rig floor after Run 19 recovered four large cobbles of granoblastic basalt and rock pebbles. **JJ.** Jets on the outside of the RCJB, just above the tool bit. These grooves in the metallic body of the tool were formed by high-pressure water flow when reverse circulation was activated at the bottom of the hole (compare with the new tool in N). The picture was taken at the end of Run 20 (i.e., after a total of four runs for this tool). (Continued on next page.)

GG

HH

II

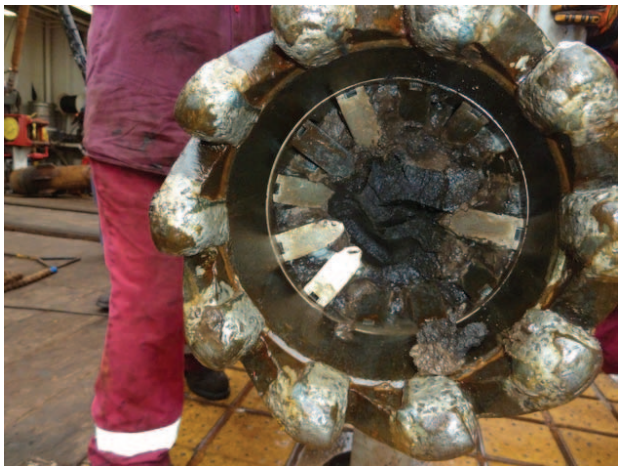

JJ

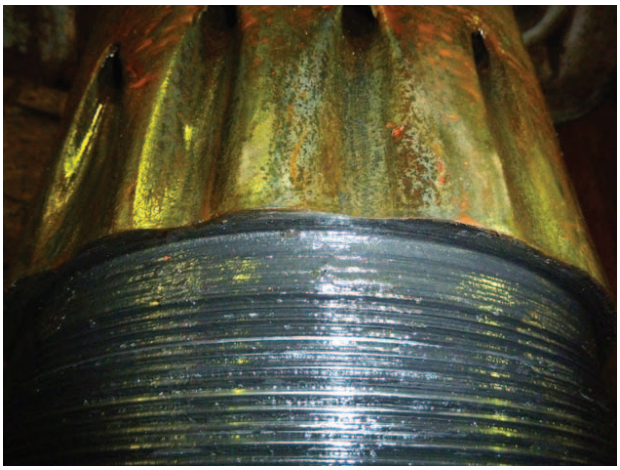

Figure F19 (continued). KK. Bowen fishing magnet tool, at the end of Run 22, with very little metal debris, although the tool tagged the bottom of the hole. **LL.** Damaged bowsprings of the upper centralizer of the logging tools after running the first (triple combo) logging run (Run 23). **MM.** The bowsprings were replaced by new, slightly thicker ones, which caused the FMS-sonic tool to be stuck in the logging BHA at the start of the second logging run. This picture shows the bowsprings stuck in the landing saver sub during the recovery of the tool. **NN.** Ulterra RCB C-9 bit used for the last run of Expedition 335 (24), for coring and then cementing the lowermost 10 m of the hole and the interval between 910 and 940 mbsf. (Continued on next page.)

KK

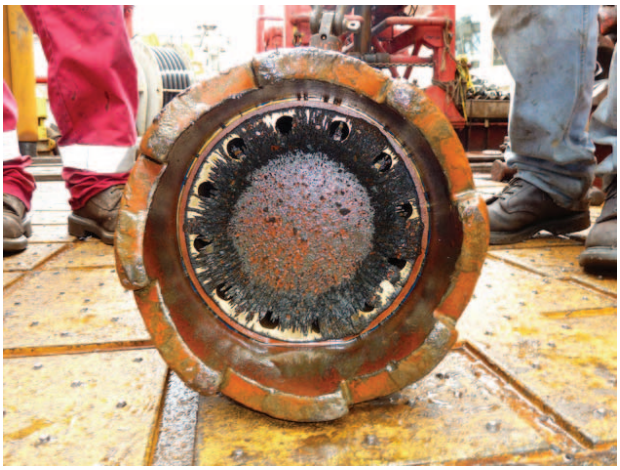

LL

MM

NN

Figure F19 (continued). OO. The C9 bit used for Run 24 (NN) returned to the rig floor in relatively good condition and nearly in gauge. It cored for ~2.5 h. **PP.** Worn outward faces of the cones, one missing tooth, and a small crack that started to propagate in the welding of the cone leg (see bottom right, close to the jet). **QQ.** Small marks on the outward facing structure of the Run 24 C9 bit, likely caused by hard, abrasive granoblastic basalt. Note the difference with the next picture. **RR.** For comparison with QQ, this picture shows the partly broken bit from Expedition 312 (missing cones), heavily damaged and cut by metal junk.

OO

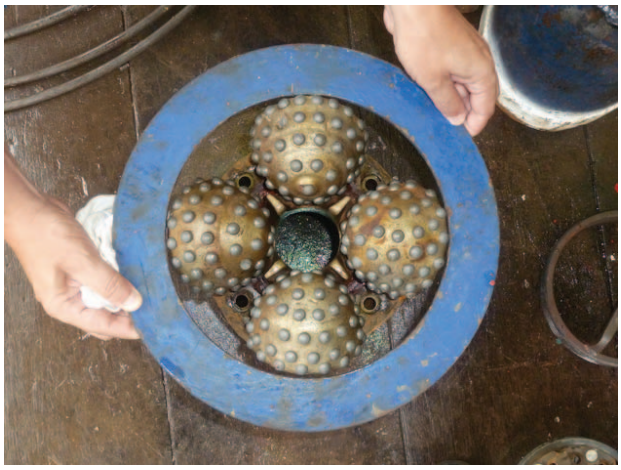

PP

QQ

RR

Figure F20. Simplified stratigraphic column of Hole 1256D at the end of Expedition 312 showing the caliper, *P*-wave velocity, and resistivity logs. Note the large out-of-gauge interval from 920 to 930 mbsf.

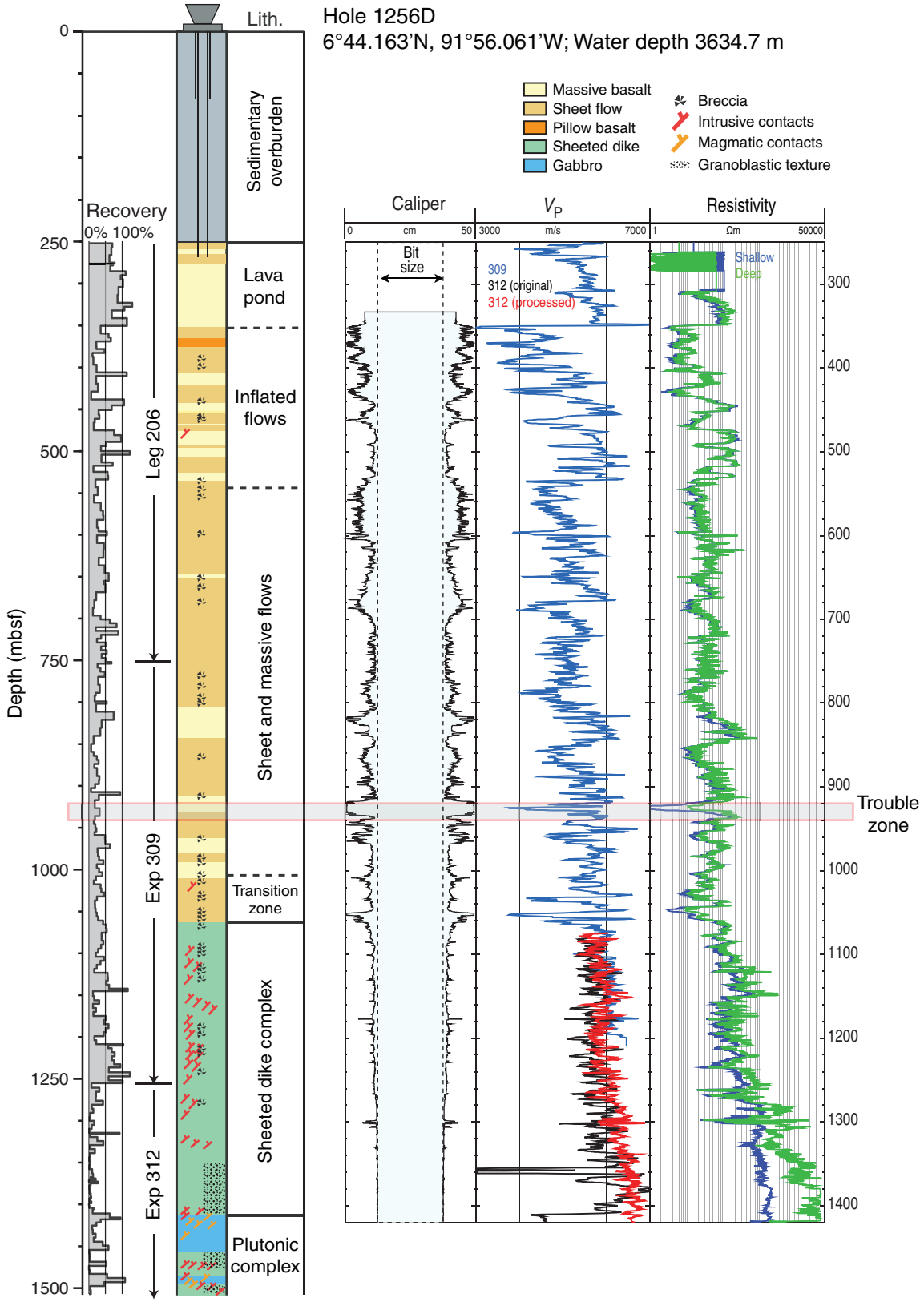

Figure F21. Perspective diagram of Hole 1256D showing the deviation of the hole against a background of the simplified crustal stratigraphy to ~1400 mbsf. The hole trajectory color and diameter is proportional to the caliper. Hole 1256D deviates with a near pure westerly trend with the hole at the granoblastic dike/Gabbro 1 boundary 60 m to the west of the reentry cone (directly below the ship's bell when on a westerly heading).

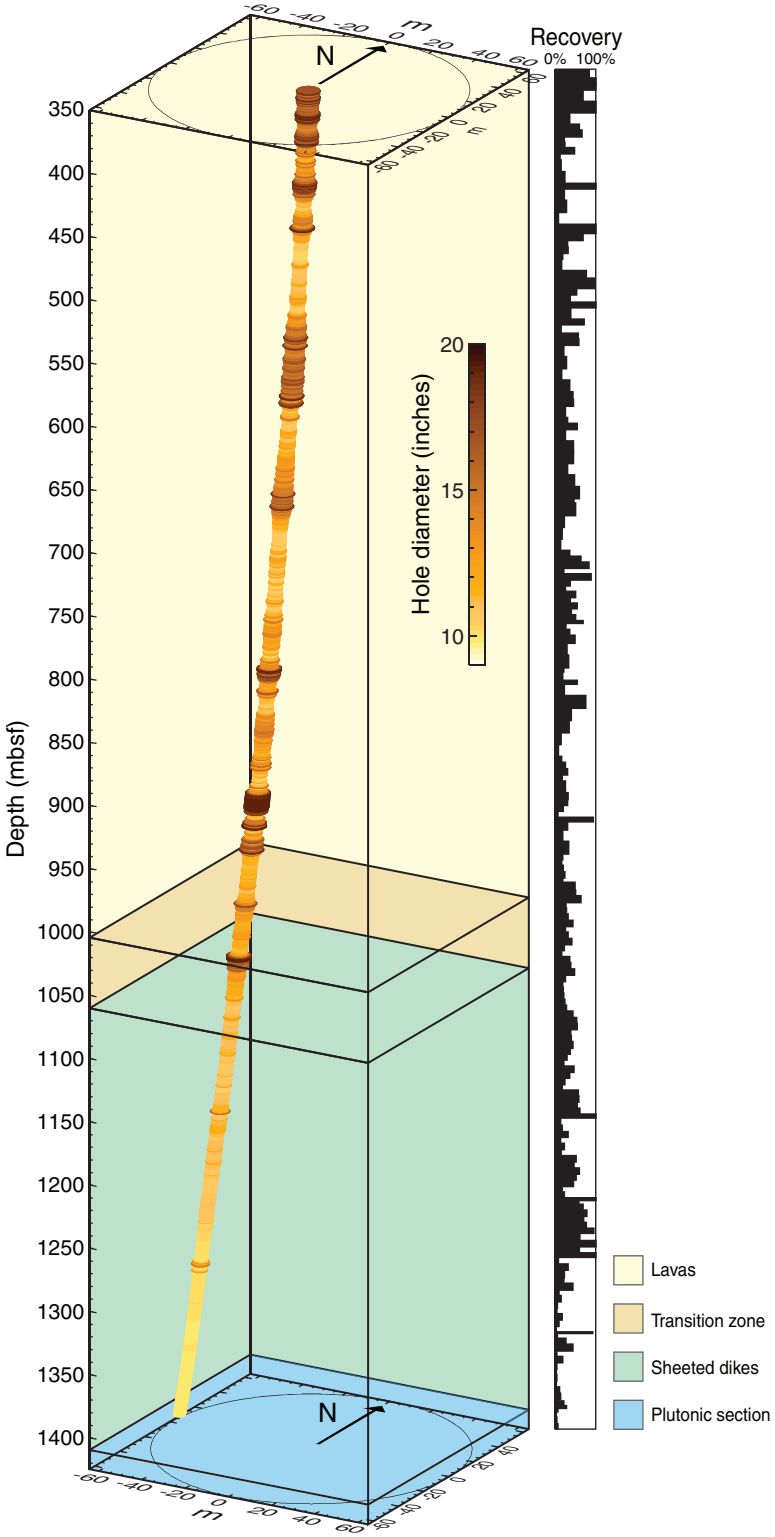

Figure F22. Caliper logs between 900 and 1000 mbsf recorded by the Ultrasonic Borehole Imager (UBI), Formation MicroScanner (FMS), and Hostile Environment Litho-Density Sonde (HLDS) tools during Expedition 309 and by the HLDS tool during Expeditions 309/312 and 335. Comparison of the Expedition 335 and 312 caliper logs shows that cementing has improved the interval from ~930 to 970 but widely out-of-gauge hole persists above that.

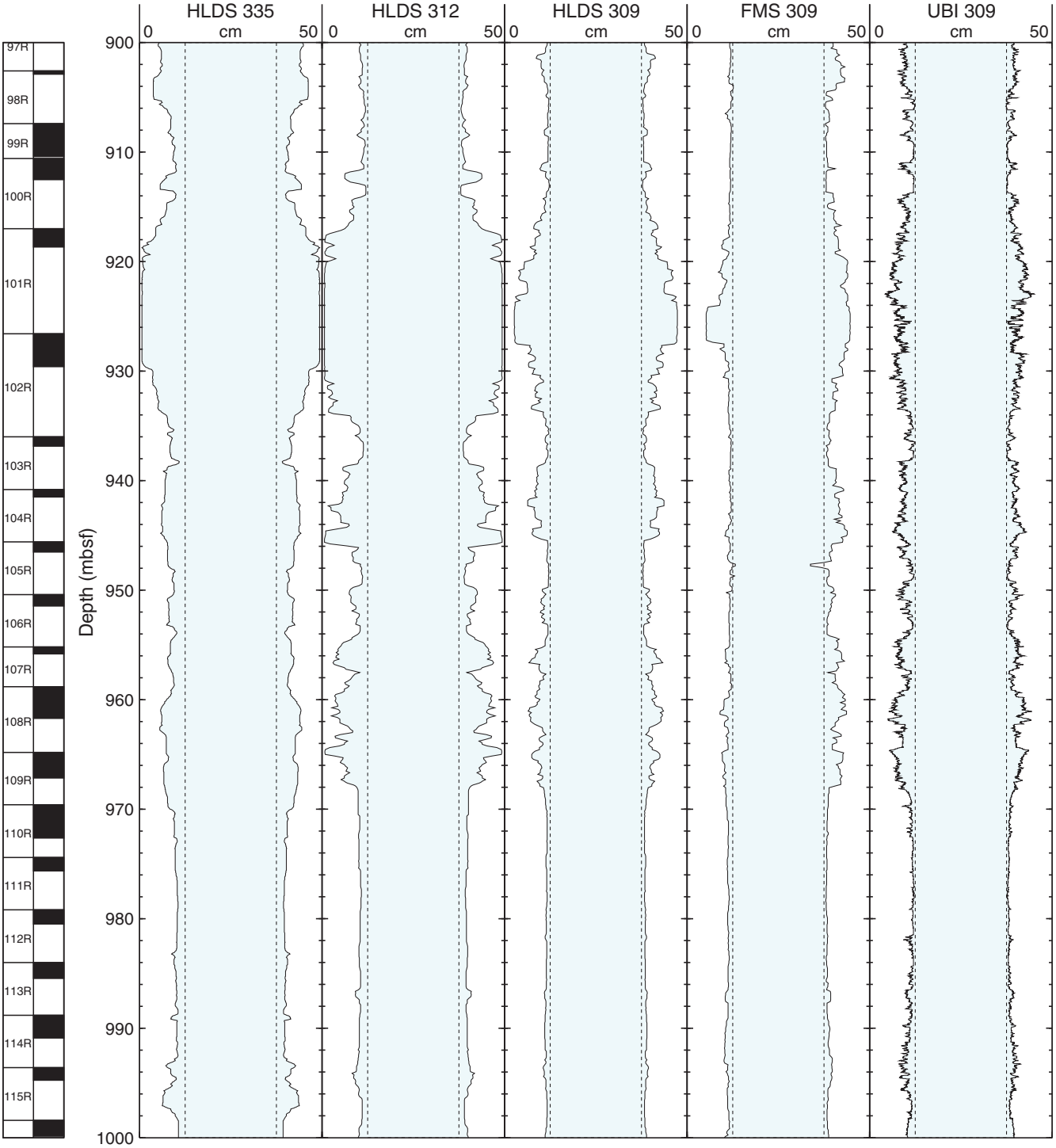

Figure F23. Geological and wireline observations of the problematic zone between 910 and 970 mbsf in Hole 1256D. **A.** Penetration rate and recovery, along with core and unit numbers. **B.** Caliper log from the end of Expedition 312. The zone from 920 to 930 mbsf is strongly out of gauge (>20 inches; i.e., larger than the diameter of the caliper tool, as indicated by the dashed curves). There is no clear relationship between the trouble zone, lava flow type, core recovery, or penetration rate. **C.** Caliper log from the end of Expedition 335. The intervals cemented during Expedition 335 are indicated on the right side. Comparison of Expedition 335 and 312 caliper logs shows that cementing has improved the interval from ~930 to 970 but widely out-of-gauge hole persists above that. **D.** Wireline temperature measurements show a strong negative inflection at ~920–940 mbsf, indicating the return of cold drilling fluids from the formation following the cessation of drilling operations. EDTCB = enhanced digital telemetry cartridge, MTT = Modular Temperature Tool, TAP = Temperature/Acceleration/Pressure tool. (Figure shown on next page.)

Figure F23 (continued). (Caption shown on previous page.)

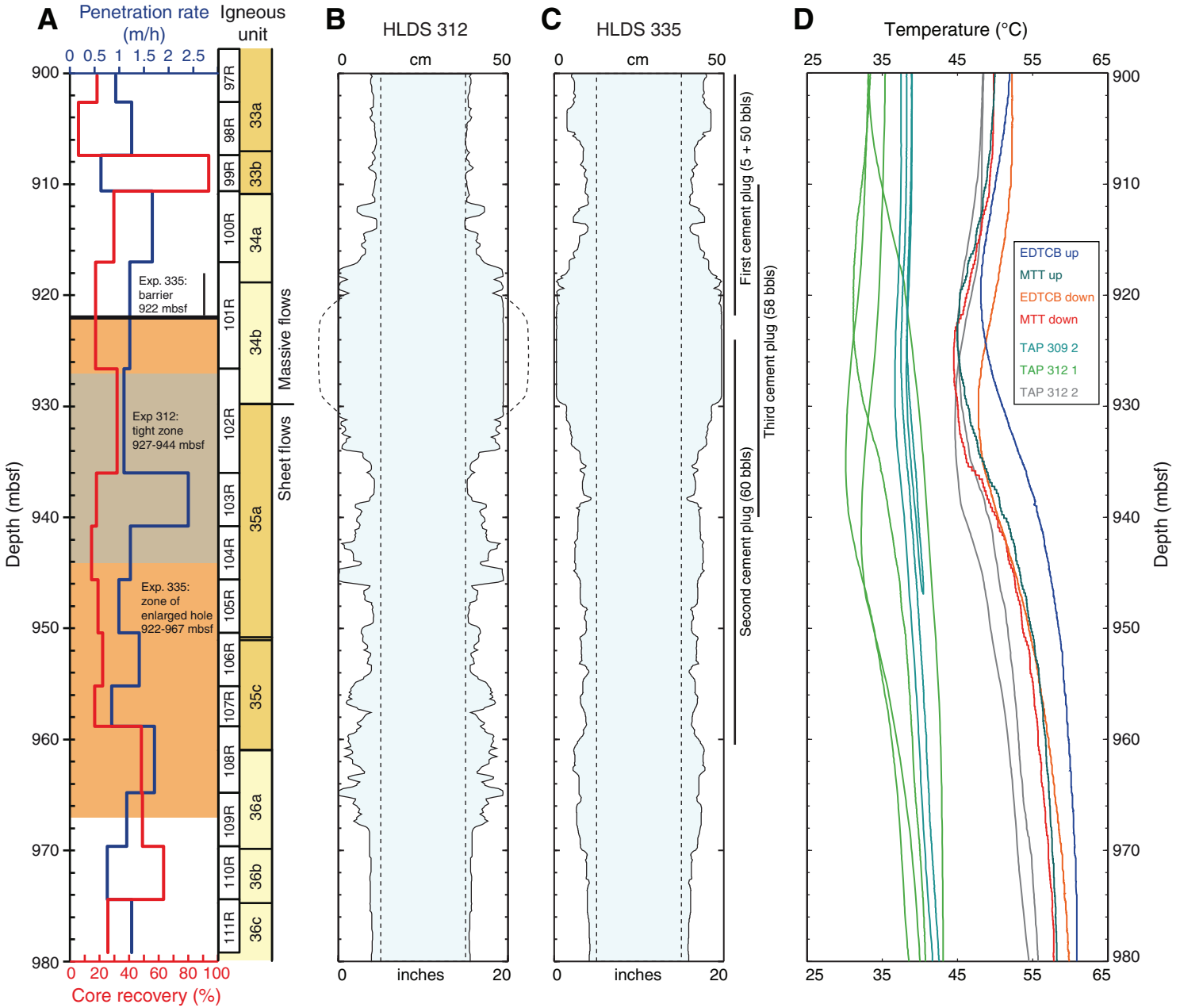

Figure F24. Sketch of a possible cause for the obstruction at 922 mbsf (not to scale; the deviation of the BHA is strongly exaggerated). Yellow slabs represent more massive units in fractured flows.

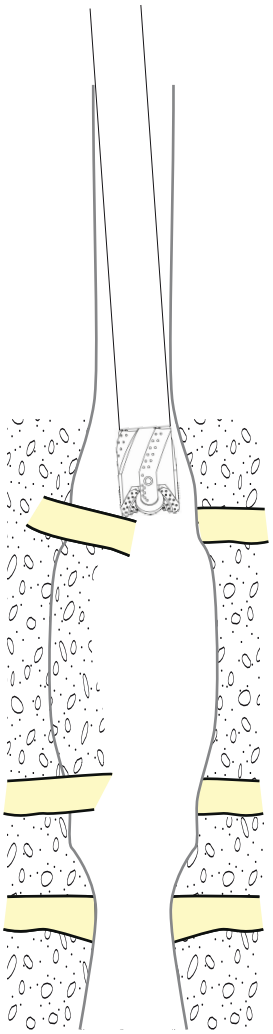

Figure F25. Plot showing the progressive deepening of Hole 1256D over four scientific ocean drilling cruises and showing the division of time on site into casing, coring, downhole logging, and hole remediation activities.

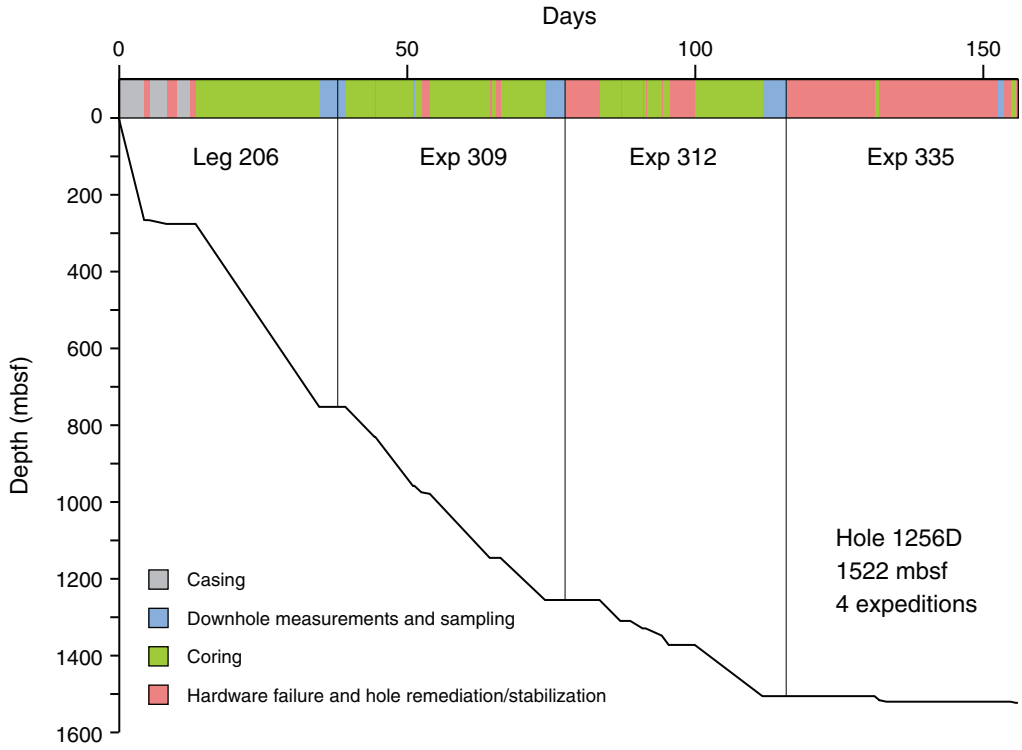

Figure F26. Stratigraphic column for Hole 1256D at the end of Expedition 335, showing the major and minor lithologic divisions of the upper oceanic crust.

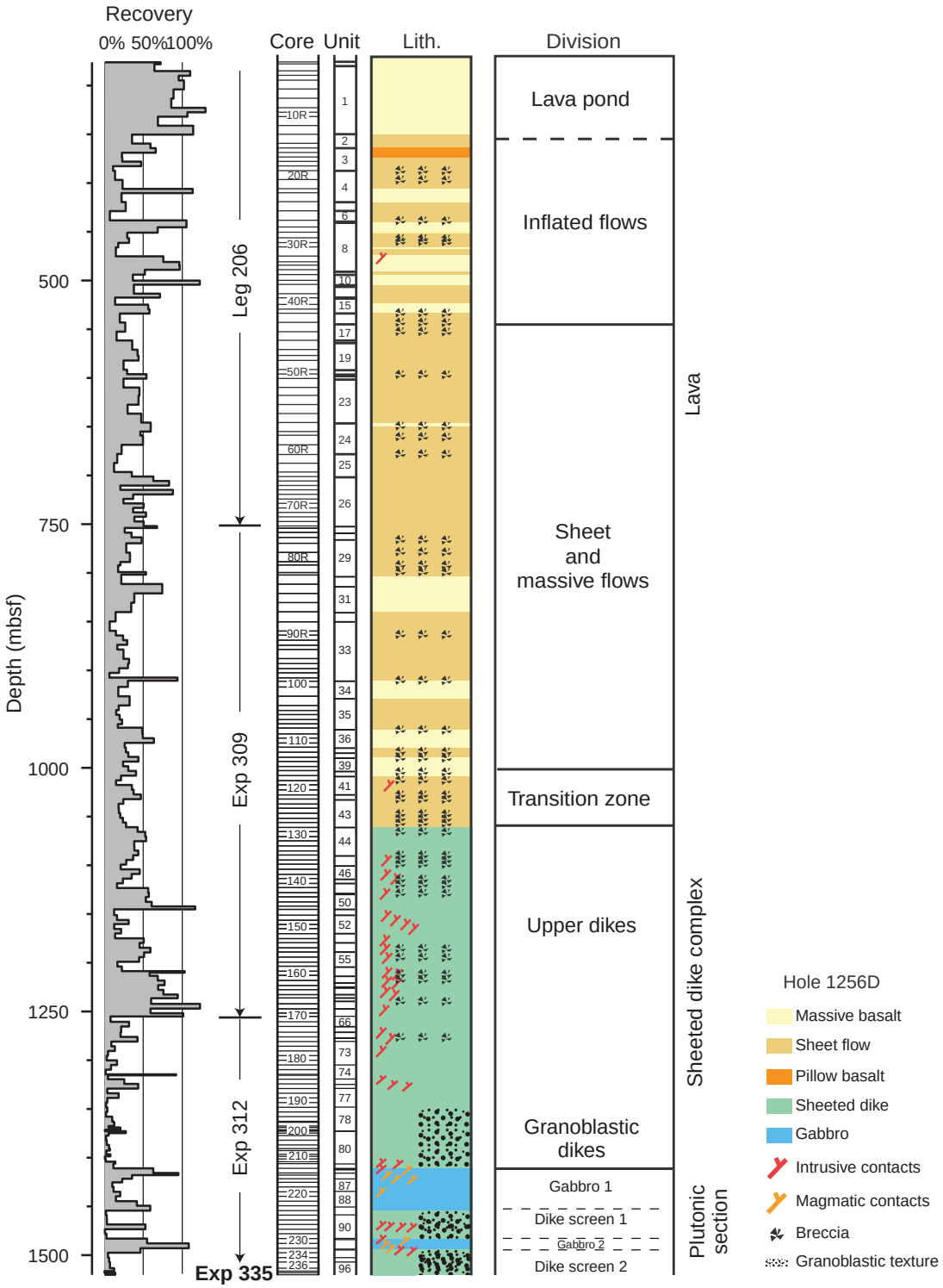

Figure F27. Photomicrograph in plain polarized light of almost completely recrystallized basalt (granoblastic texture), showing a relict plagioclase microphenocryst and an orthopyroxene vein (Sample 335-1256D-236R-1, Piece 7 [Thin Section 5]). Opx = orthopyroxene.

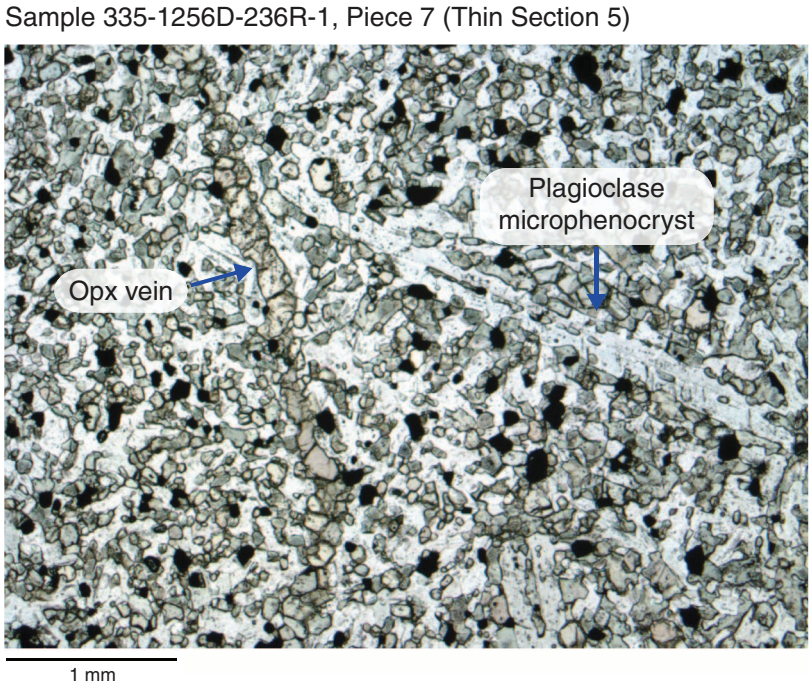

Figure F28. Overview of the lithostratigaphy of the upper crust–lower crust transition recovered in Hole 1256D.

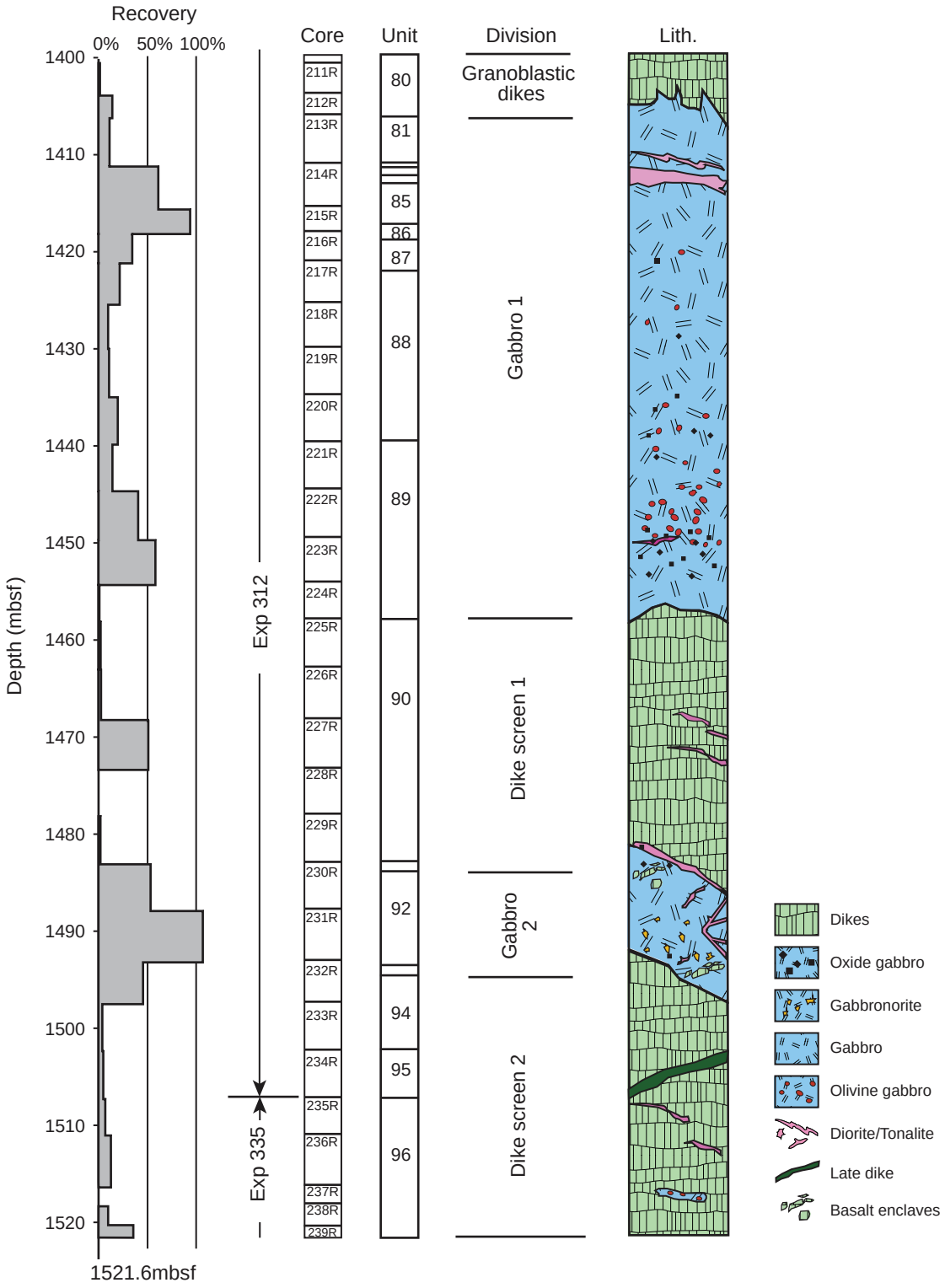

Figure F29. A. Close-up photograph illustrating the occurrence of a diorite dikelet crosscutting granoblastic basalt (Sample 335-1256D-Run19-RCJB-Rock C). **B.** Overview of a diorite patch in a fine-grained granoblastic aphyric basalt (cross-polarized light) (Sample 335-1256D-Run11-EXJB [Thin Section 13]). An offshoot of the diorite crosscuts the granoblastic basalt, demonstrating that the diorite is intrusive. (Continued on next page.)

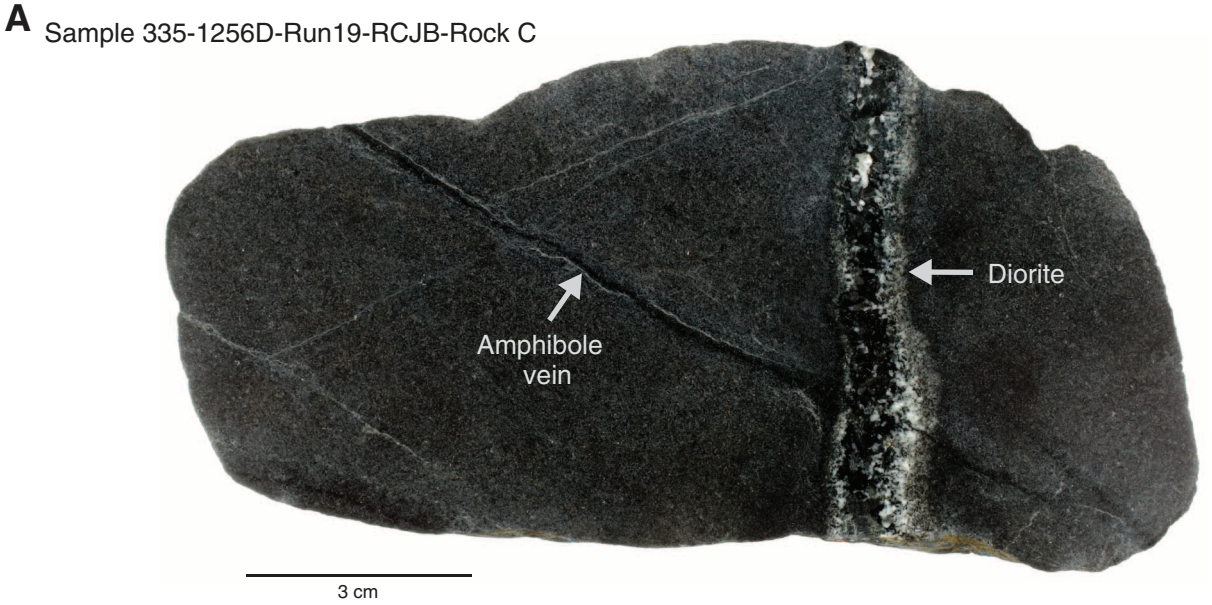

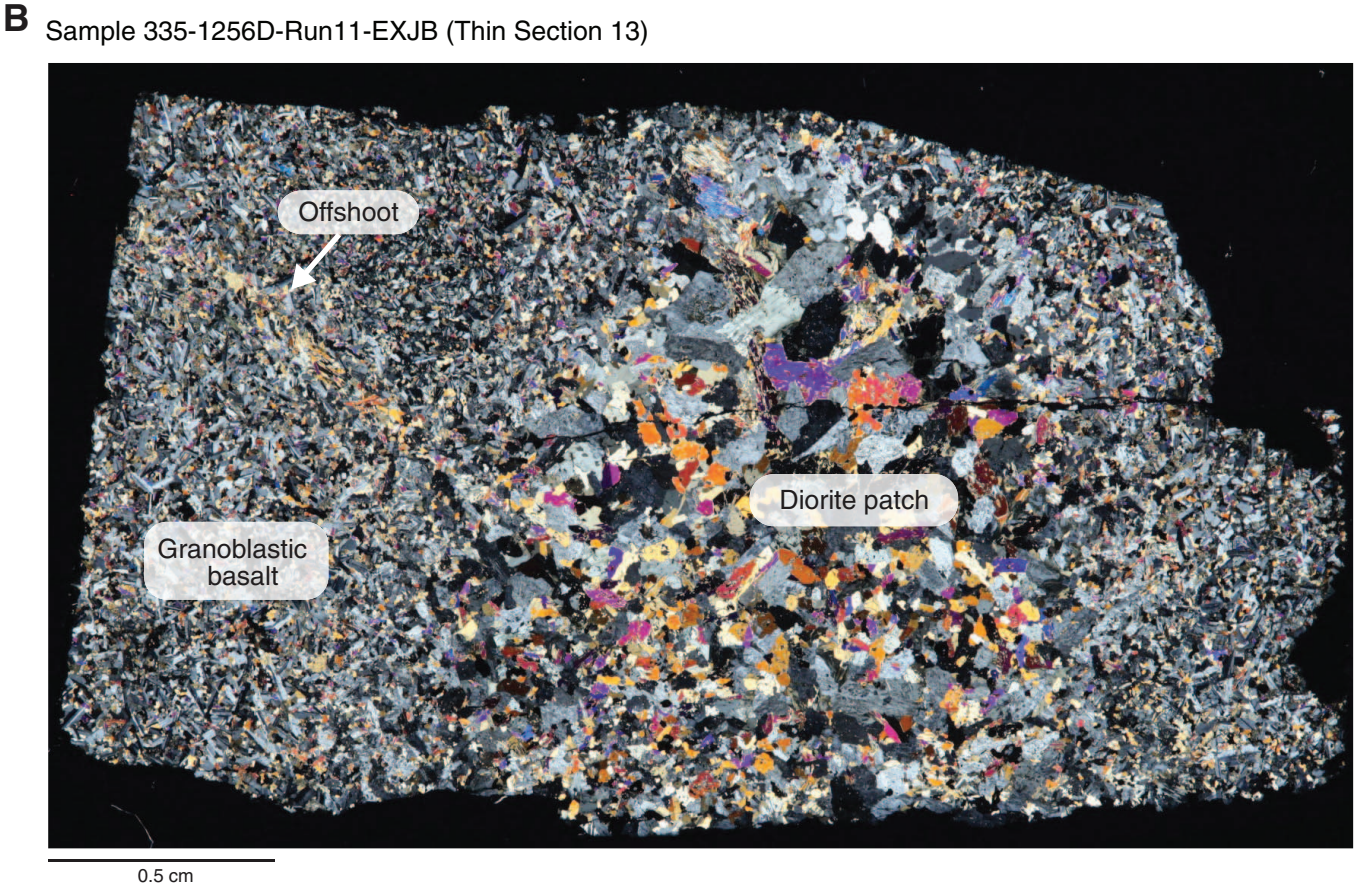

Figure F29 (continued). C. Close-up photograph of orthopyroxene-bearing olivine gabbro (Sample 335-1256D-Run20-RCJB-Rock C).

Figure F30. Sketch of a hypothetical outcrop in a future Site 1256 ophiolite of the dike–gabbro transition zone showing the contact relationships observed in the cores and junk basket rocks recovered during Expedition 335. **A.** Diorite dikelet, comprised predominantly of primary igneous amphibole and plagioclase, crosscutting granoblastic basalt (Sample 335-1256D-Run19-RCJB-Rock C). **B.** Fine-grained dike chilled against coarser grained dike (Sample 335-1256D-Run12-RCJB-Rock S). The entire sample is recrystallized to granoblastic assemblages of plagioclase, orthopyroxene, clinopyroxene, magnetite, and ilmenite. Later fine postcontact-metamorphic hydrothermal amphibole veins (not shown) cut across the contact and both dikes. **C.** Chilled and brecciated dike margin recrystallized to granoblastic assemblages (Sample 335-1256D-Run14-EXJB-Foliated). Angular clasts consist of granoblastic plagioclase with minor orthopyroxene, clinopyroxene, ilmenite, and magnetite and are recrystallized from chilled dike margin breccia protolith. Clast matrix is orthopyroxene rich with minor clinopyroxene, plagioclase, and oxides and is recrystallized from hydrothermal minerals (amphibole and chlorite) that veined and cemented the breccia protolith. **D.** Subophitic texture in gabbro (Sample 335-1256D-Run11-EXJB [Thin Section 12]). **E.** Diorite vein crosscutting a conjugate set of metamorphic orthopyroxene veins (Sample 335-1256D-Run19-RCJB-Rock B). **F.** Postcontact-metamorphic hydrothermal hornblende vein cutting granoblastic basalt (Sample 335-1256D-238R-1, 2–4 cm, Piece 1). **G.** Granoblastic basalt with a diorite patch (Sample 335-1256D-Run11-EXJB-Rock [Thin Section 13]). **H.** Granoblastic orthopyroxene vein, recrystallized from precursor hydrothermal vein, in granoblastic dike (Sample 335-1256D-238R-1, 2–4 cm, Piece 1). Orthopyroxene vein is cut by small postcontact-metamorphic hydrothermal amphibole vein. **I.** Postcontact-metamorphic hydrothermal amphibole vein cutting granoblastic basalt, with 1 mm wide amphibole-rich alteration halo where pyroxenes are replaced by amphibole (Sample 335-1256D-Run12-RCJB-Rock B). (Figure shown on next page.)

Figure F30 (continued). (Caption shown on previous page.)

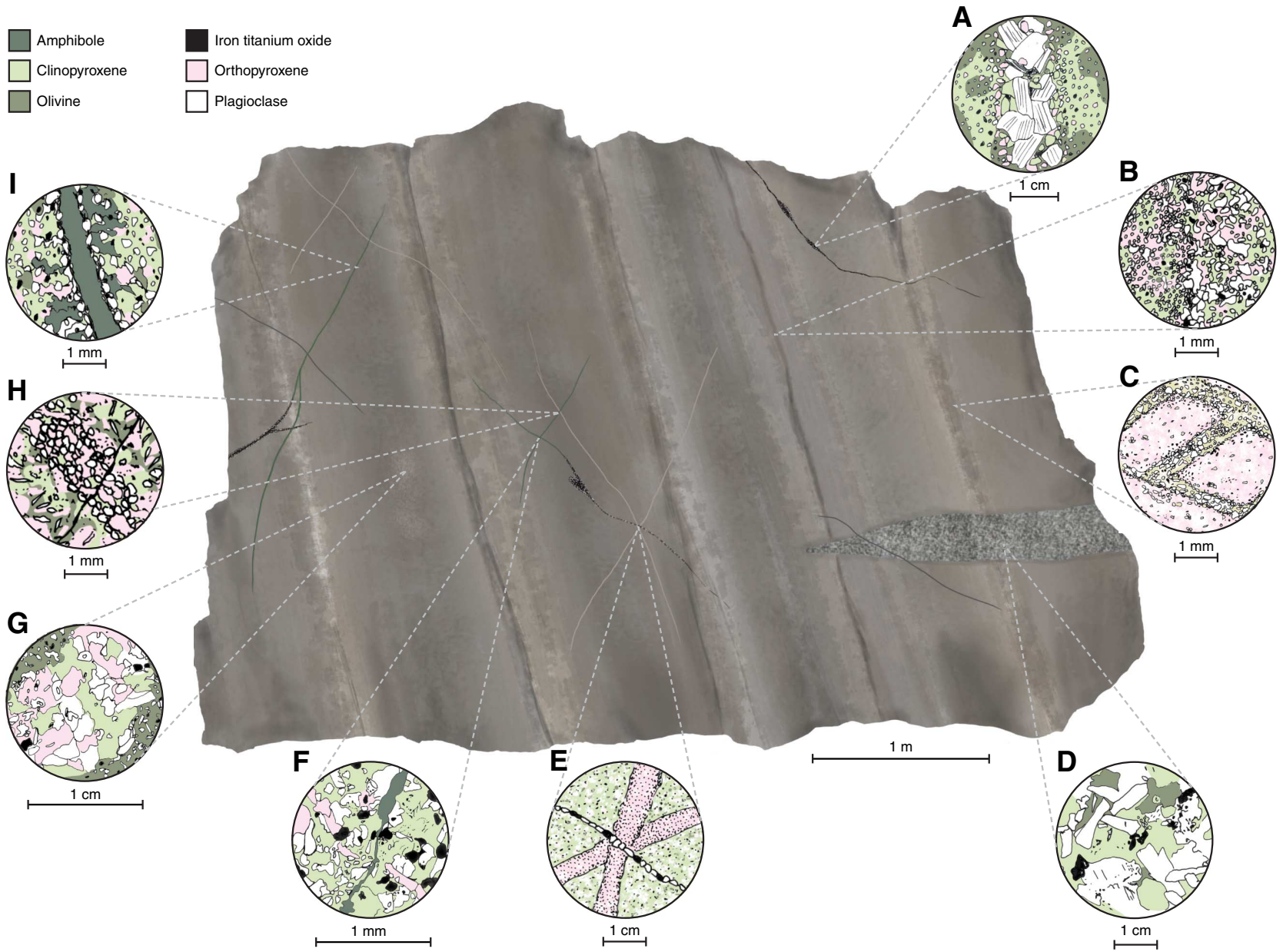

Figure F31. Depth profiles for the lower part of Hole 1256D for Mg#, Zr, Zr/Y (mass ratio), Zn, and Cu. Rock samples retrieved from junk basket (JB) runs to the bottom of the hole (BOH) are plotted in the bottom boxes. C = cored.

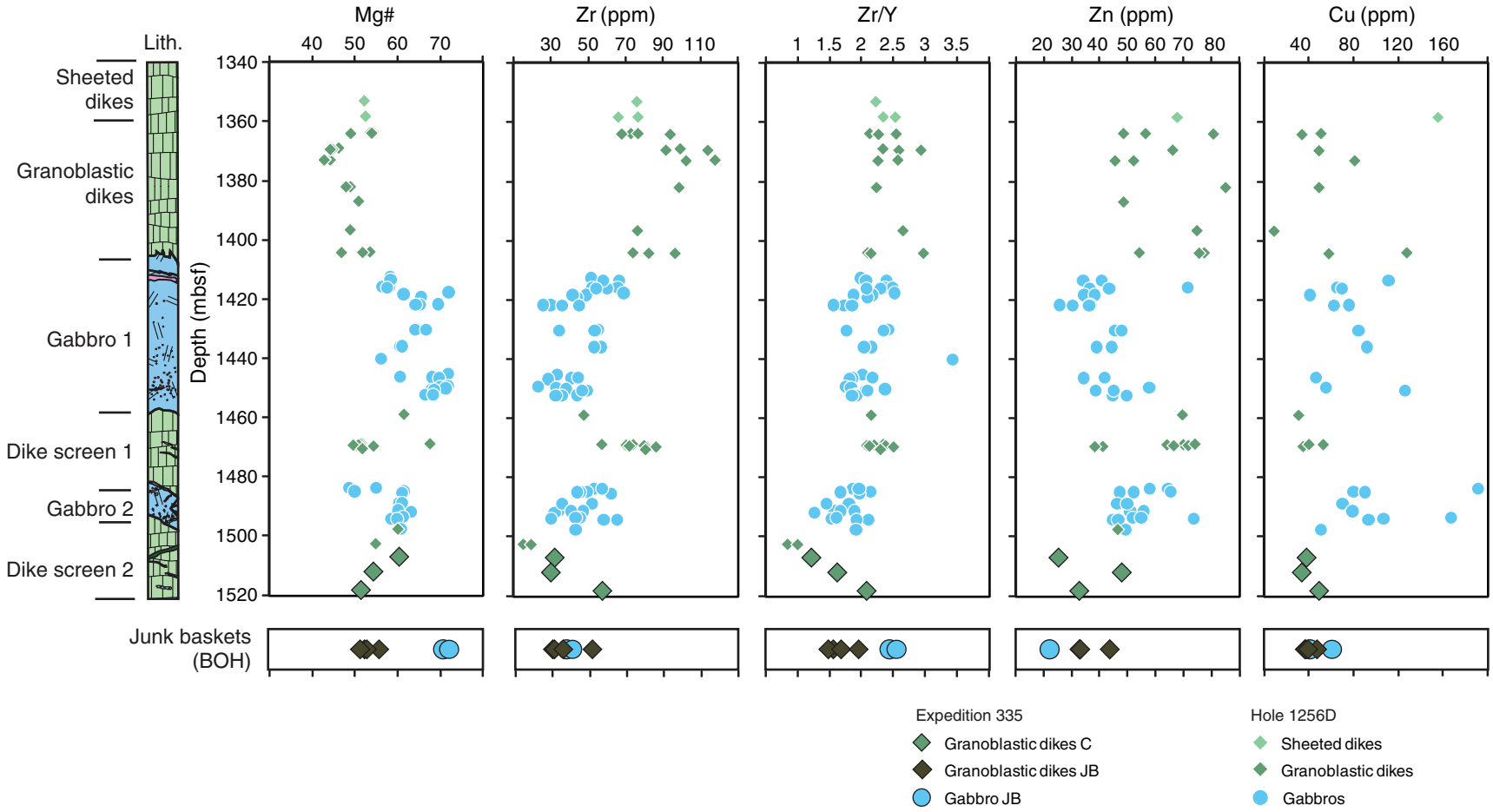

Figure F32. Photographs summarizing sequence of major alteration and metamorphic features in Expedition 335 cores and rocks. Intrusive dike contact in A represents original crustal construction processes. The darker gray, very fine grained dike at left in A is chilled against the lighter gray fine-grained dike at right (red line highlights contact). The lower sheeted dike complex was hydrothermally altered and subsequently intruded by gabbros and more evolved rocks, as exemplified in C, where diorite intrudes into a fine-grained dike (red dashed line). The host sheeted dikes were contact metamorphosed to granoblastic assemblages at this stage, as illustrated by the recrystallized dike contact in B. Former hydrothermal veins were recrystallized into granoblastic veins as in E, where a light gray vein of granoblastic plagioclase + orthopyroxene cuts diagonally across the sample. Two granoblastic orthopyroxene veins are also shown in B (subvertical at center and right). Following crystallization of the intrusive rocks and cooling, hydrothermal fluids penetrated and altered the rocks, cutting across all earlier features (intrusive igneous contacts and contact metamorphic effects in A–E). Red boxes in A, C, and E are localizations of the close-ups shown in B, D, and F, respectively. **A, B.** Fine amphibole veins (arrows) that cut across igneous/dike contact (Sample 335-1256D-Run12-RCJB-Rock S [Thin Section 26]). **C.** Fine amphibole veins (arrows) and thicker amphibole vein with amphibole-rich alteration halo (Sample 335-1256D-Run12-RCJB-Rock B [Thin Section 21]). **D.** Close-up (from C) of amphibole replacing pyroxenes along vein. **E, F.** Evolving hydrothermal activity, with dark greenish actinolite vein cutting across earlier light brown amphibole vein (Sample 335-1256D-238R-1, Piece 1 [Thin Section 6]). (Figure shown on next page.)

Figure F32 (continued). (Caption shown on previous page.)

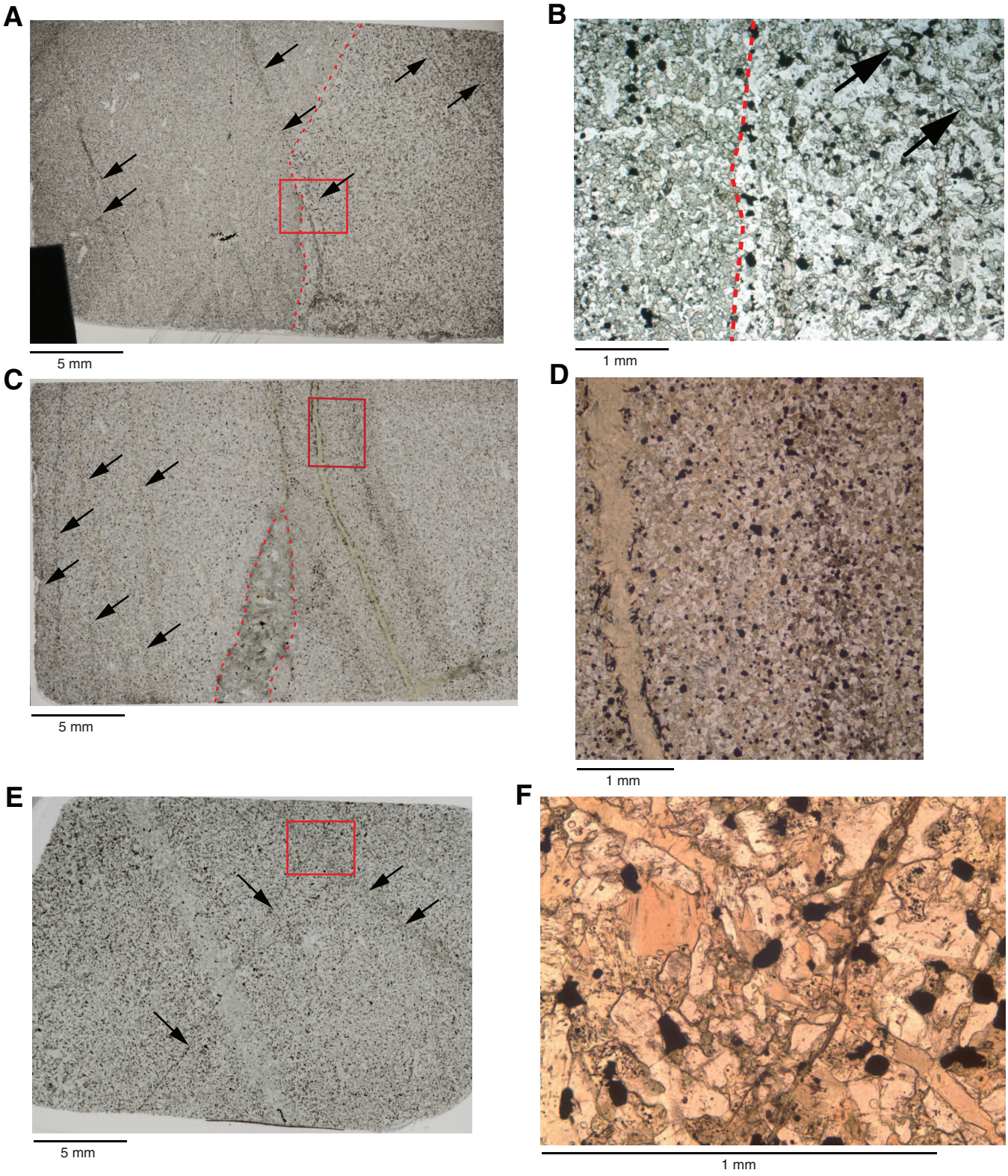

Figure F33. Thermal demagnetization of discrete Sample 335(312)-1256D-231R-1W, 115 cm, from Gabbro 2, showing a clear two-component remanence structure (excluding the initial drilling-induced component). A negative inclination component that unblocks between 200° and 500°C and a positive inclination component that unblocks between 500° and 580°C are antipodal, indicating remanence acquisition during different geomagnetic polarity periods. Solid circles = projection onto the horizontal plane, open circles = projection onto either the vertical north–south or east-west planes.

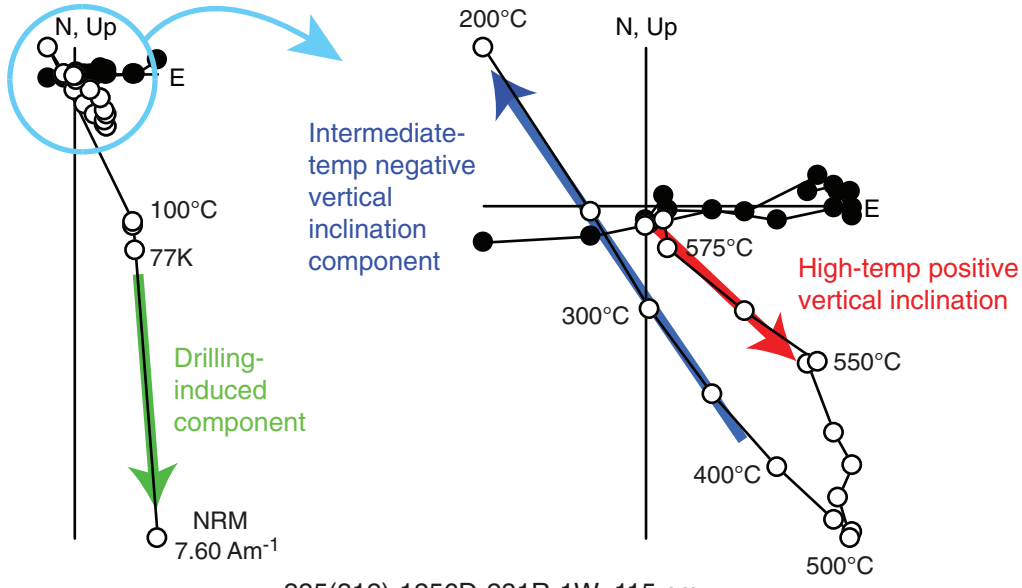

Figure F34. Anisotropy of low-field magnetic susceptibility (AMS) data from discrete samples from Hole 1256D (from top of Gabbro 1 downward). **A.** Data in the azimuthally unoriented IODP core reference frame, showing a random distribution. **B.** Data after restoration of ChRM declinations to a common north, resulting in a coherent fabric. **C.** Samples with prolate AMS fabrics, which have a pronounced north–south orientation of maximum principal axes (magnetic lineation).

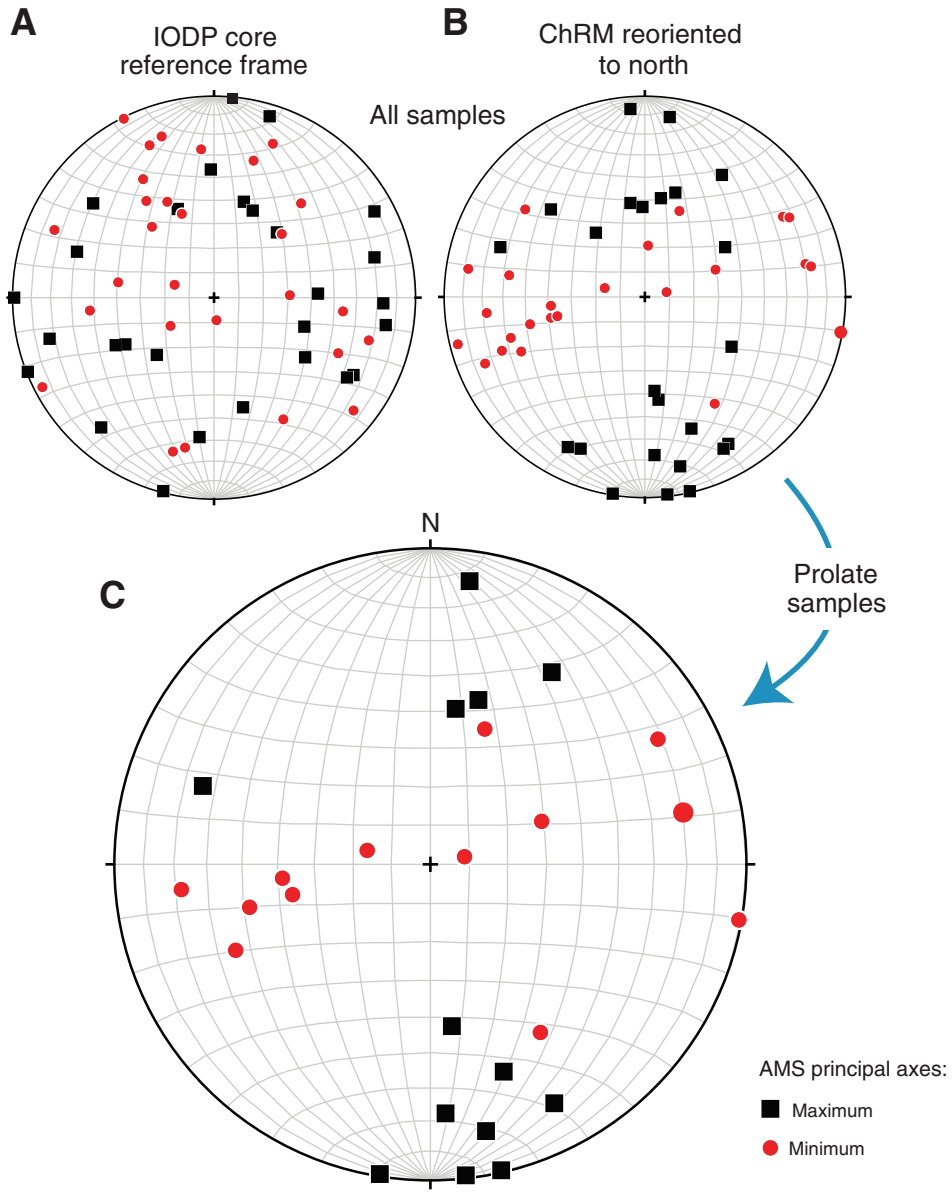

Figure F35. Downhole summary of Expedition 335(312) archive section half and Expedition 335 whole-round sections measured by the Whole-Round Multisensor Logger (WRMSL), Section Half Multisensor Logger (SHMSL), and Natural Gamma Radiation Logger (NGRL). Pale symbols show the raw data; points with strong colors are the results after eliminating data for gaps between pieces.

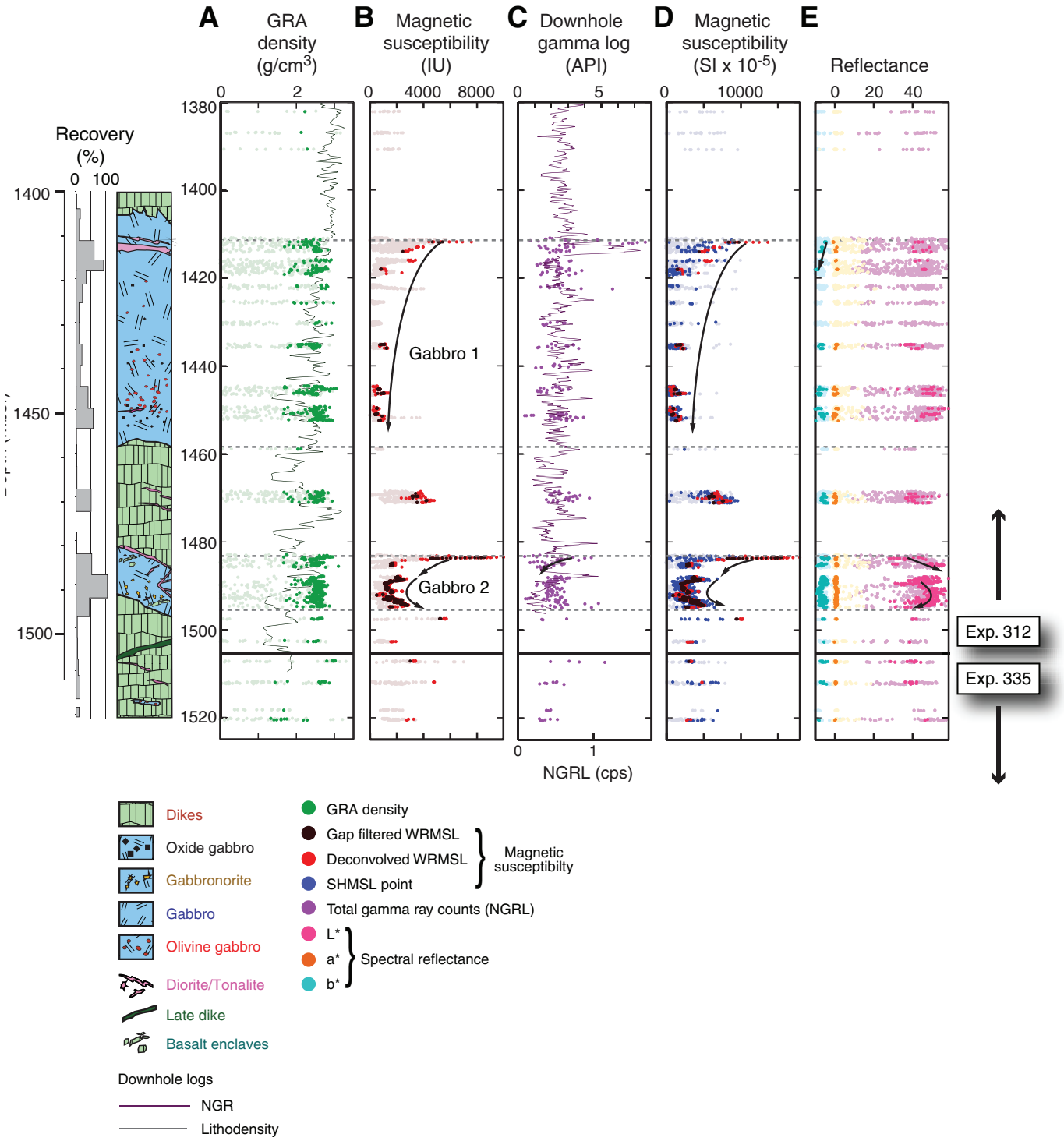

Figure F36. *P*-wave velocity for discrete samples from Expeditions 312 and 335. Solid diamonds are revised velocities for gabbro samples from core measured onboard during Expedition 335, whereas colored solid circles are measurements from noncore samples plotted at the depth from which they were recovered. Colors indicate the measurement direction in the standard IODP core reference frame where red, green, and blue are the *x*-, *y*-, and *z*-directions respectively. For noncore samples, directions were assigned with respect to the cut faces. Expedition 335 samples were submerged in seawater during measurement and are deemed to be more representative of in situ conditions than measurements made during Expedition 312 (solid black circles). Open circles represent shore-based measurements from Violay et al. (2010). The downhole sonic log (Guérin et al., 2008) is also shown for comparison.

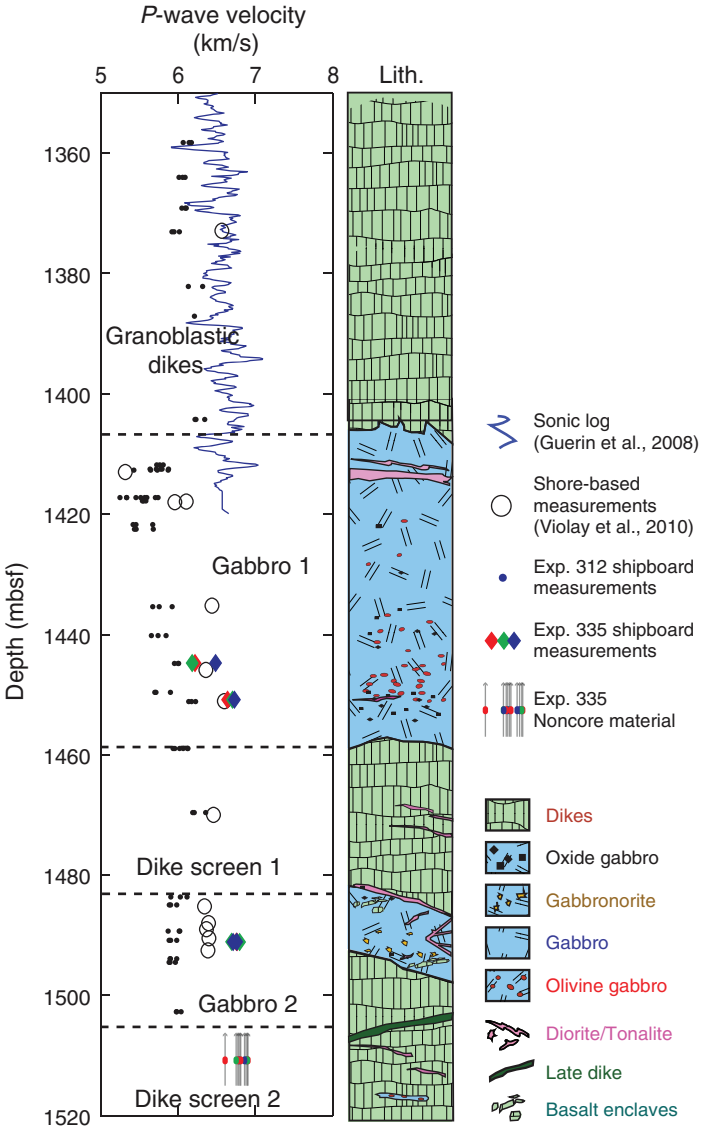

Figure F37. Summary of downhole logs recorded during Expedition 335 in Hole 1256D. Hole size was measured by the caliper of the HLDS density sonde. Lithostratigraphy is based on observations made during Expedition 309/312 and on refinements made during Expedition 335 below 1400 mbsf (see **"Igneous petrology"**). MAD = moisture and density measurements on discrete samples, EDTCB = enhanced digital telemetry cartridge, MTT = modular temperature tool.

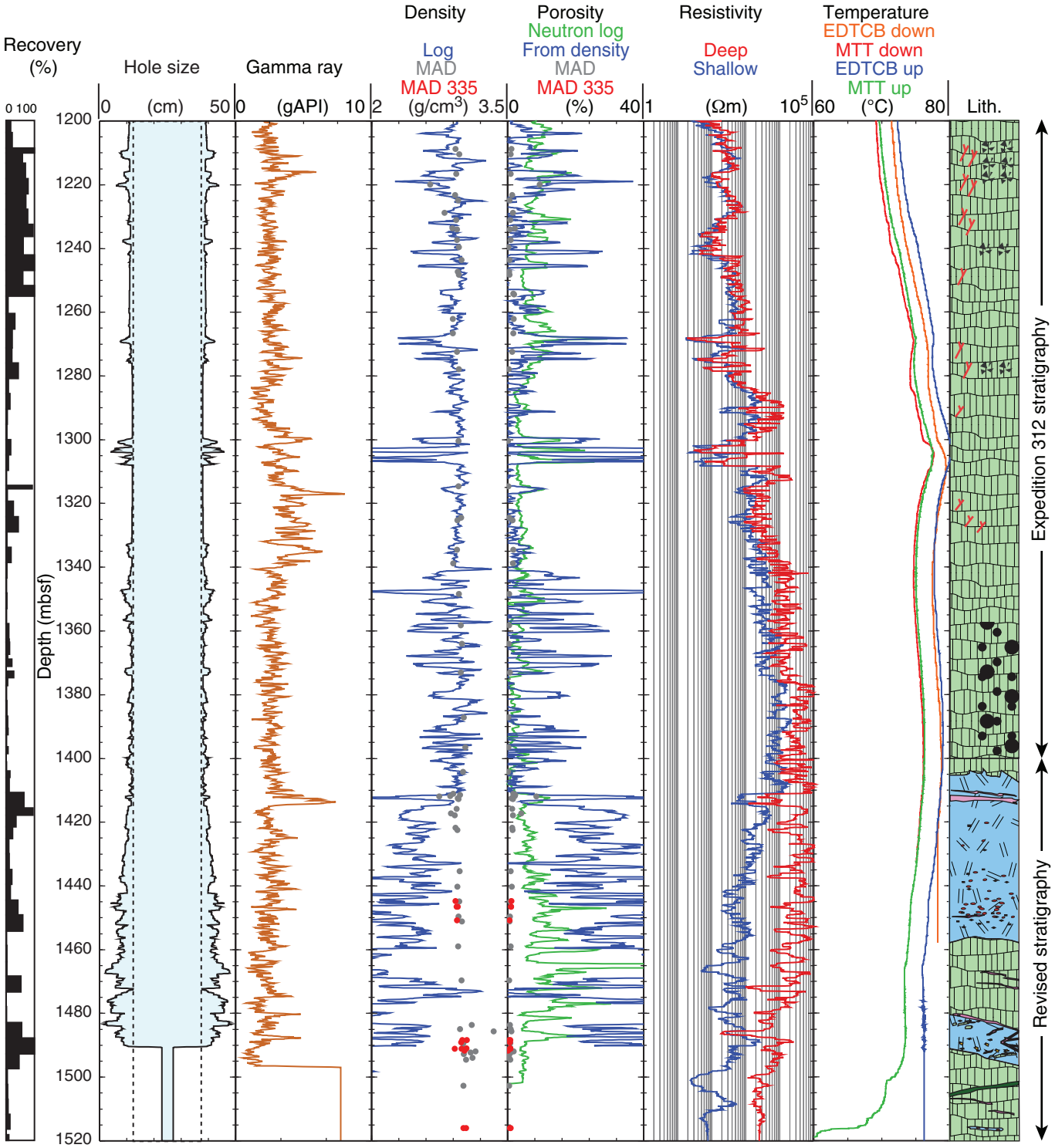

Figure F38. Comparison of hole size between 880 and 980 mbsf, measured by the caliper of the HLDS density sonde at the end of Expeditions 312 and 335. This part of the hole was cemented during Expedition 335 (see Fig. F23).

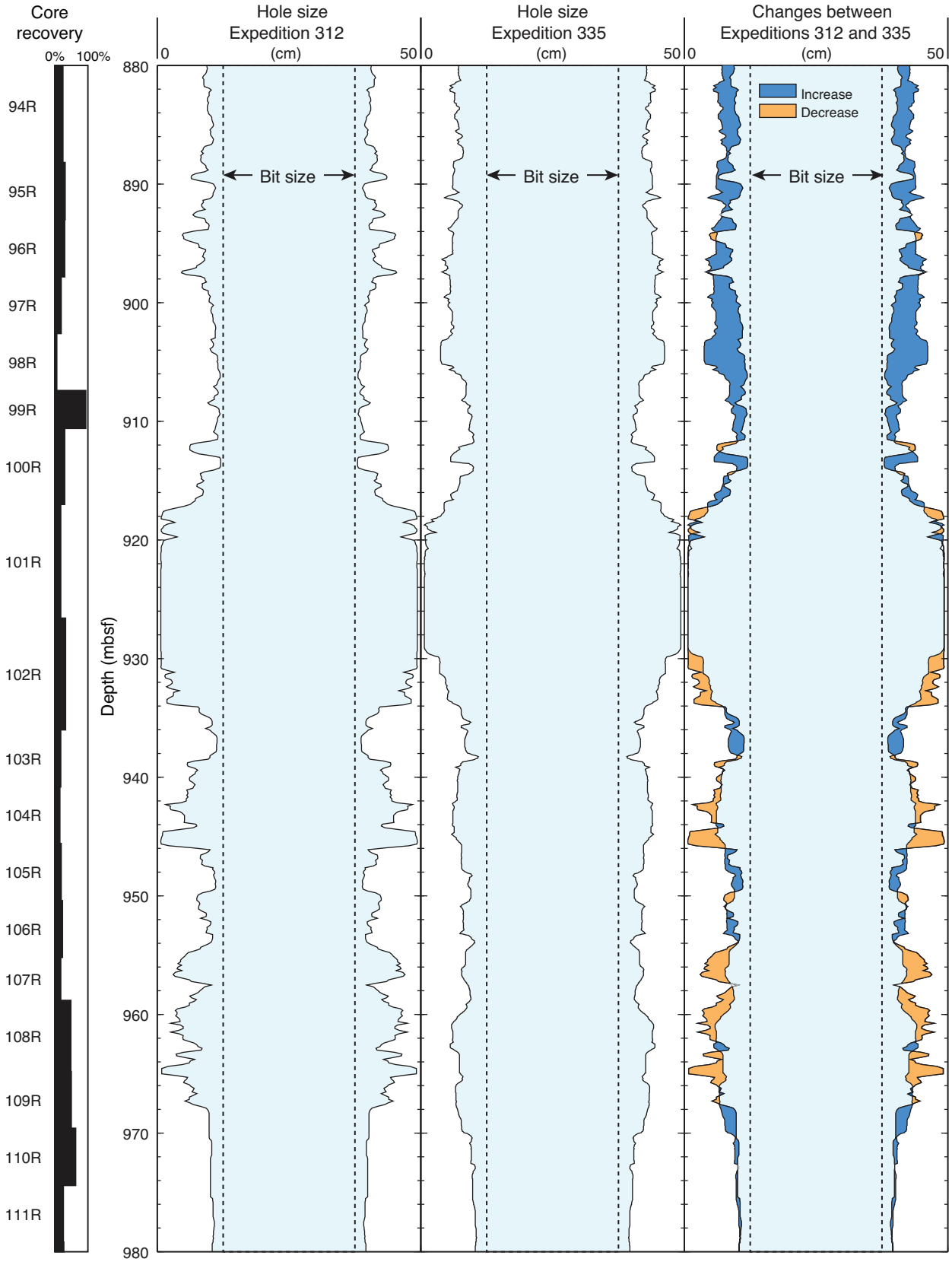

Figure F39. Temperature logs recorded during Expedition 335 compared with previous temperature logs in Hole 1256D. Lithostratigraphy is based on observations made during Expedition 309/312. MAD = moisture and density, EDTCB = enhanced digital telemetry cartridge, MTT = modular temperature tool, TAP = Temperature/Acceleration/Pressure tool. See Figure F26 for key to lithology column.